Journal of the
OPTICAL SOCIETY
of AMERICA

VOLUME 40, NUMBER 12 DECEMBER, 1950

Editorial

Physics Today

IN 1931, the Optical Society of America joined with the American Physical Society, the Acoustical Society of America, the Society of Rheology, and the American Association of Physics Teachers in founding the American Institute of Physics to carry on for these societies "those of their functions which, for economy or for effectiveness, could be accomplished better in cooperation than separately." The objectives of this combination were twofold:

(a) to provide *operative* services on a joint basis for greater economy and efficiency, and

(b) to provide *promotional* services for a better unity among functional interests of physicists in non-technical activities.

The first of these functions has been largely effected through the publication of journals for the founder societies in a common format. The societies themselves retained complete control of editorial policy, but the editorial mechanics and all the other details associated with printing and distributing a journal have been handled by the Institute. The societies have reimbursed the Institute for all the actual expenses involved, and have in addition paid a proportional share of the American Institute of Physics overhead.

In this combination for business economy and efficiency it was expected and assumed by the Optical Society, and in all probability by all other member societies, that this service would be operated on a full cost charge to the member society for editorial services, printing, subscription handling, backnumber sale, advertising sale, reprint sale, or other business services, with no profit to the Institute over and above a full repayment for the cost of the work involved and the proper overhead for the Institute building and operation.

To provide financial support for the second function of the Institute——promotional service in behalf of physics——annual contributions are made by each member society amounting to approximately 15 percent of the dues collected from individual members. This contribution was intended to cover other activities of the American Institute of Physics that have no relation to the publication of journals and member society business operations. These promotional activities include maintenance of a placement service, provision of legal advice, and other similar services.

It was decided during the discussion that preceded the foundation of the American Institute of Physics in 1931 that there was a need for some sort of common-interest "house-organ," to be sent, as a partial return for the assessment contribution, to every member of the American Institute of Physics. The Optical Society had started publishing *The Review of Scientific Instruments* in 1922, at first in combination with its own journal and later as a separate publication which all Optical Society of America members were entitled to receive free of charge. Of all the journals published by the founder societies, *The Review of Scientific Instruments* seemed to have the greatest number of common-interest features, and it was proposed that it become the "house-organ" of the American Institute of Physics. The Optical Society allowed the Institute to take over the publication of *The Review of Scientific Instruments*, and all its advertising revenue, with the understanding that every member of every founder society would receive a free subscription. At the same time, the member societies agreed not to carry competitive advertising in their own journals; the concentration of advertising in the "all Institute" journal, with its wide distribution, would carry much of the cost of this journal. Profits, if they should develop, would be spread as a publication subsidy to reduce publication costs to the other society publications.

After a trial, the American Institute of Physics discontinued the free distribution of *The Review of Scientific Instruments* to members of founder societies and placed it on an "individual choice" subscription basis. For one year thereafter, the Optical Society bought a block subscription for its own membership; but was unable to continue this practice in subsequent years.

In 1946 the American Institute of Physics constitution was revised to broaden the character of the Institute, and while provision was made for "associate membership" for individuals who were not members of the founder societies, a form of management was retained which insured that the Institute would continue as primarily a federation of member societies rather than individual members acting independently of the founder societies.

Part and parcel of the reorganization of the American Institute of Physics was the resurrection of the plan to publish a "house-organ." To effect the proposed "house-organ" journal, *Physics Today* was initiated in 1948 and was sent to all "member society" members without extra fee. There was some difficulty in the budgeting and balancing of costs which by the end of 1949 had incurred such a deficit that *Physics Today* could no longer be provided without a payment above the dues assessment paid by members of the founder or member societies to the Institute and it was announced that in 1950 individual subscriptions would be necessary.

To those of us who felt that it was essential that there be a mutual "house-organ" to help mold and direct a common enthusiasm and support for the broad field of physics, this abandonment of full Institute coverage seemed a step backwards and hence the Optical Society Board of Directors upon the suggestion of Dean Harrison supported a proposition that the society take a block subscription for the entire society. We made this more inclusive within the Institute by agreeing to this "block subscription" only if two other Institute member societies would also agree to similar subscriptions. It was felt that, if a guaranteed

subscription return could be provided in 1950, some reorganization could be effected in this year which would provide a balanced budget and still permit a complete distribution to the entire Institute of Physics as was the original intention.

The Institute membership and its house-organ journal should be as inseparable as the technical membership and journal subscription of the individual founder societies. To be effective the Institute must reach *all* of its members with its medium for exchange of news-and-views in physics. The Optical Society of America has twice committed the society funds in support of an Institute house-organ and has evidenced greater interest in the success of a promotional physics medium than has been shown by most of the other founder societies. The salvation of *Physics Today*, if it is to survive, must be based on providing a new magazine primarily for physicists and operating within its assigned budget, which should be nearly balanced through application of a portion of the assessment dues and a reasonable amount of advertising. Another year of life has been indicated for *Physics Today* and it would seem that this time it must justify its existence or fold up. We regret exceedingly that it will not in this year be sent to all Institute members or even to all Optical Society members.

We can only urge the members of the Optical Society to exercise their "individual choice" in the direction of a separate subscription during 1951 with the hope that in this next year we can make *Physics Today* indispensable to physicists, and that the members of other societies will jointly support, directly and through their representatives on the Institute Board of Governors, a reestablishment of *Physics Today* as a part of each Institute member's return for his investment in the Institute. *Physics Today* needs not only individual financial support during this year of experimentation but friendly help and constructive suggestions.

For the second time in as many decades we have completed in the Institute a cycle in the "house-organ" evolution, involving first a magazine sent to all Institute members; then a block subscription by the Optical Society for its members in an effort to sustain full circulation, which was not well supported by other founder societies; and finally the withdrawal of the journal to the "individual choice" subscription basis. There are slight differences in the two cycles; for example, in the first cycle the Optical Society could not afford to continue subscriptions, whereas in the recent cycle the executive committee of the Institute decided to refuse block subscriptions from the founder societies in line with the "individual choice" policy.

We do not feel that either the Institute, or *Physics Today* (as the "house-organ" of the Institute), "has now been well introduced and that it should now be a matter of individual choice whether or not to receive the magazine" or to contribute to the Institute support.

The Editor of the *Journal of the Optical Society* is a member of an "emergency group" that has been enlisted in the attempt to establish *Physics Today* on a sound basis. Your Editor has carefully informed himself concerning the attitudes and policies of the Boards of the Optical Society of America that existed during the nineteen years of affiliation with the American Institute of Physics, and is urging that the character of *Physics Today* be shifted in the direction of emphasizing the house-organ features that will make *Physics Today* a news-and-views magazine for all of physics. He believes that within the next year *Physics Today* can become indispensable to physicists, that it can again be sent to all members of the American Institute of Physics family, and that, if it is not then completely self-supporting, any deficit should be made up from the annual contribution that the founder societies make to the American Institute of Physics even if this involves the curtailment of some less essential American Institute of Physics services or an assessment increase.

Support for *Physics Today* must not only be financial but in suggestions, contributions of material, and criticism if it is to be changed to a more representative promotional medium in physics.

Your Editor hopes that the individual members of the Optical Society, as well as all founder society members, will support these efforts by subscribing to *Physics Today* for 1951 on an individual basis.

Annual Subject Index

A Technical Journal index, to be of greatest utility, should effect a reasonable compromise between too few and too many subdivisions of knowledge. The subdivisions and indexed items should be alphabetically arranged in accordance with the subject, rather than alphabetical according to the first word of the title or by page number. The previous indexes of the *Journal of the Optical Society of America* have been arranged according to broad subjects (from 30 to 40 subject titles) with the articles classified under one or more of these headings and arranged within these headings in an alphabetical order in accordance with the full title of the paper. Such an index was satisfactory when the *Journal* had a much smaller number of papers but with the larger number of papers it has become increasingly more difficult to scan the titles, which under some headings have occupied more than a full page of alphabetized titles where the alphabetical key or first word of title may be "on, some, further, new, direct, rapid, etc."

The subject index this year is an experiment, upon which the editor would appreciate comments, suggestions, or criticism. It is expected that work on a cumulative index of the *Journal* will be inaugurated in the near future to cover the last 15 and possibly the complete 40 volumes of issue of this *Journal* and that the style and format of the cumulative index would follow the pattern of this year's annual index, subject to such suggestions as may be obtained from readers after examination of the present index.

Briefly, in this year's index *subjects*, not words, have been indexed. The *content* of each paper (and abstract of papers presented at meetings) and not merely the title of the paper has been the basis of selection of subjects to be indexed. Alphabetical arrangement has been according to subject without regard to prepositions such as, "of," "in," etc., which may precede the subject for a euphonious purpose.

A further explanation of the index precedes the index in this number of the *Journal*. Readers are requested to transmit to the editor their suggestions with regard to annual or cumulative indexes.

High Precision Measurements with Simple Equipment*

A. C. S. VAN HEEL
Technical University, Delft, Holland

(Received June 5, 1950)

The precision of alignment attainable with a single slit, a double slit and cross wires, placed respectively at the three points to be aligned, can be about at least 0.17 in., provided use is made of pointings on transition colors in the interference pattern. Practical uses of this method are described, including technical measurements and laboratory experiments of very high precision. Among the last is a spherometer for large radii, that is also an absolute flatness tester with a precision of about $\lambda/100$. The method can be expanded to other types of measurement, when instead of a double slit a grating of coarse structure is substituted. Alignment in two directions simultaneously can also be achieved by a modification of the diffracting screen.

1. INTRODUCTION

THE main difficulty of aligning three points to a straight line[1,2] is the impossibility of seeing them distinctly at the same time. On receding along this line in order to facilitate focusing by enlarging the distance of all the three points, the precision is diminished by reason of the enlargement of the mean distance. If one tries an improvement by magnifying with a telescope, the depth of focus diminishes when the telescope is given a larger aperture or is better corrected.

In practice, sighting (arranging three openings in such a way that a "light-ray" passes through them) gives a low precision and furthermore has the disadvantage of a nearly discontinuous passing from darkness to light, when the stops with the openings are being shifted, resulting in an uncertainty as to which way a stop has to be moved when no light is observed.

Bonnaffé[3] has obtained more precise results, but he needed nearly complete darkness during his experiments, and the resulting precision depends rather strongly on luminosity and training.

We recommend the following arrangement (Fig. 1). The first of the three points is realized by a single slit S, illuminated by a condensed filament lamp of 6 v and 15 to 25 watts, provided eventually with a simple condensing lens. At a distance c_1 the screen D is placed, containing two parallel slits, each of which is parallel to S. The center of S represents the first point, the center of the double slit represents the second point. The third point to be aligned is the point of intersection of the cross wires W, situated at a distance c_2 from D, and observed either with the naked eye or with an eyepiece.

With this classical arrangement (the interference experiment of Young or Fresnel) an interference pattern is formed at any sufficiently large distance c_2. (At *very* large distances we get the interference patterns of the Fraunhofer class.) The center is white, bordered at both sides by dark colored bands, these being brown to reddish purple at the inner side and blueish purple to blue at the outside. Farther away more bands are visible, which are vaguer and need not be considered.

The transition of reddish purple to blueish purple is particularly suitable. By making use of the color sense of the eye it is possible to make precise determinations.

The center of the interference pattern, formed by the diffracted light of two slits, is found either by recording both the right and the left color transitions, or only one of these and to apply afterwards a correction to center, which for many practical applications is easily made with sufficient precision. When only displacements are being observed, the observation of one transition is sufficient.

For distances c_1 and c_2 from 3 to 50 meters the following dimensions appeared to be suitable: height of the slits 0.5 to 4 cm, breadth of S (which slit assures a sufficient degree of coherence of the light falling on the double slit) 0.25 to 0.5 mm, breadth of each of the slits of the double slit about 0.5 mm, distance between the centers of the two slits 2 to 3 mm.

To align in two dimensions S and D are rotated by 90° about the line of sight or the slit is replaced by circular holes. Alignment in two dimensions can also be obtained by means of *one* determination by making use of other forms of the diffracting opening, e.g., a circular hole surrounded by a concentric circular slit; the slit S must be replaced by a small hole and the double slit by a circular hole surrounded by a concentric slit. In the example given the interference pattern consists of concentric colored circles, allowing alignment by means of an eye piece provided with a plate with a number of blackened concentric circles. We found by observations that the precision of alignment is the same as with two straight slits for observation in one direction.

For the case of the straight double slit, we were surprised to find that the precision of aiming on one of the color transitions is better than 1 in. (without

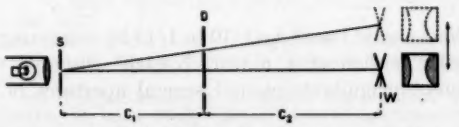

FIG. 1. Alignment set-up.

* Based on an invited paper presented at the annual meeting of the Optical Society of America at Buffalo, October 28, 1949.
[1] A. C. S. van Heel, J. Opt. Soc. Am. 36, 242 (1946).
[2] A. C. S. van Heel, App. Sci. Research B 1, 306 (1949).
[3] J. Bonnaffé, Rev. d'optique 9, 17 (1930).

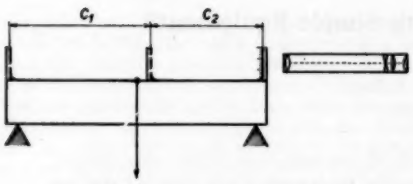

FIG. 2. Measurement sag of loaded bar.

magnification). Many of our experiments were achieved with a Ramsden eye piece with magnification of 5, giving a precision of 0.06 in.

In a given case we had $c_1=c_2=35$ m, the distance between the "minima" (between the two transitions) being about 8 mm, and the precision of aiming of 0.02 mm.

If the double slit is on a mirror, which need not have larger dimensions than 4×4 mm^2, its rotations can be observed to within 0.03 in. This corresponds to a displacement of the reflected image of 3 microns at a scale distance of 10 meters.

In an experiment to record a setting, a parallel beam was used, obtained by a narrow slit and an objective lens of 60 cm focal length (diameter 6 cm) of very good quality, before which a straight double slit was placed. The distance between the slits was 2.75 mm. The width of each 0.5 mm. The aberrations of the lens were negligible. The light source was a super high pressure mercury arc. At a distance of 37 m an Ektachrome film recorded the interference pattern. The time of exposure was 1 minute.

The distance between the two symmetrically located color transitions of one of the exposures was measured. The result was 22.407 mm with a mean error of 0.011 mm. On an other exposure the same distance was measured to 22.418 mm with a mean error of 0.007 mm.

Thus it appears that not only a precision better than 0.01 mm is obtainable on such films (it is to be remembered that above data pertain to differences of settings), but that this precision compares well with the visual measurements, as 0.01 mm at a distance 37 m is 0.06 in.

It was found that observers with weak color discrimination get results of comparable precision.

2. COMPARISON WITH PRECISION OBTAINED WITH TELESCOPE

Our precision compares favorably with those of other methods. The angular aiming precision is defined by $\alpha=k\rho$, in which ρ is the angular resolution and k a fraction dependent on the conditions of the experiment (magnification of the telescope, illumination, contrast, etc.).

Wadsworth[4] found $k=1/10$ to $1/15$ by measuring the angular motion of a mirror. Noetzli[5] observed with different magnifications and several apertures of the object glass. Under favorable circumstances he could obtain $k=1/38$ (and even $1/58$ with large magnification). Tilton[6] also reaches $k=1/40$ when the conditions are favorable.

So taking $b=0.4$ cm in order to compare with the over-all breadth of the double slit, we have $\alpha=35$ in., and with $k=1/58$, $\alpha=0.6$ in.

Not to put too fine a point to it we may conclude that our results, obtained without optical parts (the weak eye piece excepted), are several times better. Of course it will depend on the circumstances which method is to be preferred.

3. INFLUENCE OF DISTANCE; SMALL DISTANCES

A discussion of the dependence of the precision of pointing and of the luminosity on the distances c_1 and c_2, ont the distance h between the centers of the two slits, and on the width q of the primary slit is given in reference 2. For distances larger than some meters the linear precision of aiming δ, the angular precision of alignment ϵ, and the brightness E are practically constant, provided q and h are suitably chosen (for E, this is only the case if the magnification of the interference pattern is produced by a cylindrical lens).

For smaller distances this does not obtain: q soon would become too small, and the magnification would have to be increased unduly to make the pattern well observable.

Still a considerable linear precision can be obtained with these simple means even when the distance c_1+c_2 is small.

A practical example may elucidate this point. The sag of a small rectangular bar of 5 to 6 cm length when resting on two points and loaded in the center may be determined in this way (Fig. 2). Three glass plates are mounted on the bar; the distances c_1 and c_2 are 25 mm. The first plate is silvered and has a horizontal scratch of about 0.025-mm width; the second also is silvered and has two parallel horizontal scratches of about 0.04-mm width, about 0.25 mm apart. The third plate has a scale with horizontal division scratches.

When the first slit is illuminated the well-known interference pattern is observed in the plane of the scale by means of a microscope (magnification 100). The distance between one of the color transitions to one of the scale divisions is measured by the micrometer eye piece of the microscope.

In this manner the changes of the position of the bar when a load is applied are of no influence, thus the difficulties of zero-point changes, occurring when mirrors are used, are eliminated.

The distance between scale and objective of the microscope is sufficient (4 mm or more) to allow a glass window to be inserted, in case the apparatus must be kept at a constant temperature. The position of the microscope is of no consequence as long as the scale

[4] F. L. O. Wadsworth, Phil. Mag. 44, 83 (1897).
[5] A. Noetzli, Zeits. f. Instrumentenk 35, 65, 89 (1915).
[6] L. W. Tilton, Bur. Stand. J. Research 6, 58 (1931).

divisions are seen in focus. The plates and window need not be of utmost planeless or parallellity as only differences in the position of the pattern are of interest. The bending of the bar occasions a slight tilt of the outermost plates, which can be neglected or corrected for.

The only difficulty arises from the fact that the image with the narrow slits and large magnification is of low brightness, unless a direct current carbon arc is used as a light source. Otherwise the determination of the points of color transition is too difficult. Especially it is observed that the eye is rapidly fatigued, giving bad observation results.

When well adjusted this arrangement allows a precision of at least one micron in the plane of the scale, corresponding to 0.5 micron at the midpoint. It is to be noted, that with a well-calibrated scale the range can be several millimeters.†

A microscope with cylindrical lenses giving the magnification 100 only in a vertical direction would have been better, as the magnification in a horizontal direction is of no use and only diminishes the brightness of the image.

4. SEVERAL SLITS

If we replace the double slit in Fig. 1 by a series of slits, we get again very interesting diffraction phenomena, which consist of colored line patterns. The period of these coarse gratings can (for measurements at distances over 1 meter) with advantage be chosen between 0.5 and 2 mm. They can be made in many ways with the required degree of precision (period constant to within a few microns).

We made use of samples of modern metallic sieves. These are made by a galvanoplastic process out of photographic reproductions of standard patterns. The mean positions of the *rows* of centers of the (round or rectangular or otherwise formed) holes appear to be equidistant to about 1 micron. When we use a slit as a light-source and a sieve as diffracting screen, we get the effect of rows of holes, as if they were slits, and this integration of rows secures the required precision, even though each hole separately does not yield it.

We also tried autotype gratings on glass, but these are at a disadvantage, because even the smallest deviations from flatness of the glass plates and the deviation from exact squaring on to the line of observation have to be taken into account. Utmost precision cannot be obtained in this way, even if the grating is of a perfect periodicity. On the other hand, the method of observation to be described allows investigation of these errors.

It appeared that by the use of sieves the direction of "light-rays" could be ascertained with a precision, which probably cannot be attained by other means.

† This arrangement was set up at Tufts College, Medford, Massachusetts, at the request of S. S. Ballard and tested by L. S. Combes and the author in November, 1949; the experiments were repeated later at Delft.

5. ELEMENTARY THEORY

An insight into the formation of the patterns can be got by means of the elementary theory of diffraction. We expected this to be a sufficient approximation for our purpose; see, e.g., Rayleigh[7] and Savornin.[8]

A linear light source O (Fig. 3) illuminates a screen at A at a distance a. The illumination on a screen B at a distance b is to be studied. The screen at A is provided with one or more slits, perpendicular to the plane of Fig. 3. When b is very small the transitions of illumination in the plane at B are very abrupt. With increasing values of b these transitions are more and more influenced by diffraction.

The path difference $PB-AB=e=(a+b)s^2/2ab$, where s is the length of arc AP. With $\frac{1}{2}\pi v^2=2\pi e/\lambda$ we have for the intensity I the value C^2+S^2, the integration being extended over the open parts of the diffracting screen. Evidently $v=s\sqrt{\{2(a+b)/ab\lambda\}}$.

The data given by Jahnke-Emde[6] have been extended considerably by the Mathematical Centrum at Amsterdam, which has obliged us with tables with v ranging up to 20 by steps of 0.01, giving the values of C and S to the sixth decimal place.[9]

A difficulty remains *viz.* the color of the diffraction phenomenon. One ought to make the calculations for many wave-lengths, for different gratings and for several distances. Even then the superposition of the (incoherent) patterns for the different wave-lengths is precarious (eye sensibility for the different wave-lengths, spectral light distribution of the light source, etc.).

Between the region immediately after the screen (the region of the "geometrical shadow") and the far away region (the "Fraunhofer region") the Fresnel region shows patterns, whose forms change considerably with the distance from the diffracting screen.

The principal maxima are accompanied by additional maxima and the pattern can become very complex. With a grating as diffracting screen, the principle maxima show lateral shifts at periodical distances as shown in a schematic way by Fig. 4. This well-known fact, described, e.g., by Zernike,[10] makes it difficult to ascribe a maximum to one of the slits.

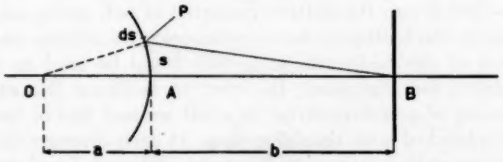

FIG. 3. Diffraction at screen.

[7] Lord Rayleigh, "Wave theory of light," Scient. Pap. III, p. 127 (1888, 1902).

[8] J. Savornin, "Étude théorique de la diffraction par une fente," "La théorie des images optiques," Colloques Internationaux, Paris, 1949.

[9] A. van Wijngaarden and W. L. Scheen, Verhand. Kon. Akad. Amsterdam, **19**, no. 4 (1949). (Report R 49 Computation Dept. Math. Centre, Amsterdam.)

[10] F. Zernike, Ned. Tijdschr. v. Natuurkunde **9**, 357 (1942).

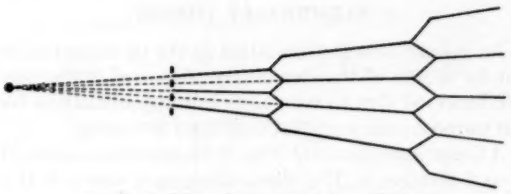

FIG. 4. Position of maxima (schematically).

In the range, however, between the screen and the first forking there is no difficulty about this point. Here another problem remains: the loci of the principle maxima are not straight. As long as the deviations from straightness are slight and known these loci may be used as if they were "light-rays." We will revert to this point in the next paragraph.

That the best experimental results with gratings or sieves were obtained when $a=b$, has not yet been accounted for by this simple theory; nor could we predict the dimensions of the double slit, which would give the best results. These were found experimentally.

The two-dimensional case (round hole, several symmetrically placed round holes, circular hole surrounded by concentric slit, etc.) is more complicated, though of considerable importance from the practical point of view in alignment in two directions simultaneously. No calculations for these cases have been made, but they have been studied experimentally.

6. DEVIATIONS OF "LIGHT-RAYS" AS GIVEN BY THE COLORED PATTERNS OF SIEVES

As diffraction plays a part, accounting also for the non-straightness of the loci of the maxima, the wavelength has influence on the pattern, and so it is understandable that colors are shown even in the region before the first forkings. The colors provide us with a simple method of alignment. The deviation from straightness has been determined experimentally.

In a given case we used a grating (sieve) with a spacing of 0.6427 mm, standing at a distance a of 2 to 3 meters from the slit. At distances b of 2 to 3 m behind the sieve a colored pattern was observed with an eye piece mounted on a scale. For $a=2484.0$ mm and $b=2545.5$ mm the pattern consisted of red, green, and nearly black stripes. Each of the color transitions and each of the midpoints of a color could be used as a subject for alignment. In order to facilitate the assigning of a certain stripe to a slit we had two of the slits blocked with moulding wax. At each distance the corresponding stripes had a color different from the other stripes. In the case given they were blue. The loci of these differently colored stripes, when the observing distance b was changed, were straight lines with a good approximation. The deviation δ from straightness is small and with given a and given distance np between the blocked slits (here n is an integer) seems to obey the law:

$$\delta=\alpha b^2,$$

where α is a constant depending on a and np. The deviation is, in the case studied, towards the central line.

7. PRACTICAL CASES; GRATINGS AND DOUBLE SLITS

For $n=11$, which means a distance between the blocked slits of 7.0697 mm $\alpha=0.00617.10^{-6}$, when b is measured in millimeters, the observed distance between the differently colored stripes at $b=2545.5$ mm was 14.273 mm$\pm$0.006 mm. If the loci should have been straight this distance would have been 7.0697 (2484.0 +2545.5)/2484=14.314 mm, the correction from observed to theoretical distance being +0.040 mm.

In an other case with $a=2130.0$ mm and 10 $p=6.437$ mm we found $\alpha=0.00465.10^{-6}$. The dependence on a and np has still to be investigated.

It follows that with the corrections given, the method gives good results. When utmost precision is desired, the blocked slits can be unblocked and all color transitions of all the stripes can be used.

A surprisingly large assortment of colored patterns can be realized by varying the distance of observation, the period of the grating, and the width of the slits.

Even with *two slits* a rich variety of aspects is to be seen by changing their dimensions. For measuring purposes a proportion of 1 to 2.25 of the slit width and the distance between the centers of the slits appeared to be a practical value. In view of the applications it is important that accurate squaring on to the line of sight is not essential.

With double slits it appeared that the center of the pattern is easily found, further that a set of three screens, each with a double slit of different dimensions suffices to serve distances from 1 to 60 meters.

The two-dimensional case allowed a precision of 0.1 in., when the openings in the screen (circular hole surrounded by a concentric slit) had been manufactured with high precision, the magnification of the eye piece being again five.

For lower precision the two-dimensional case can be solved by a sieve with round holes arranged in a honeycomb pattern. All holes are to be filled up except a central hole with three adjacent holes, lying in three directions, which make angles of 120° with one another. This gives a beautiful colored pattern with well-defined center, yielding a precision of 1 in. As here no rows of holes are used, but the effect of singular holes, the precision is appreciably less by reason of the imperfections of the sieve.

8. OTHER WAYS OF OBSERVATION OF THE STRUCTURE OF A BEAM OF LIGHT

At very large observing distances the diffraction phenomena enter into the Fraunhofer class, where nearly all sensibility to lateral displacement of the diffracting screen has disappeared. At very small distances from the diffracting screen the phenomena are described by the geometrical shadow, which does not

yield any angular precision because of the smallness of the distance. Between these two regions the interesting range of the Fresnel class exists, which is too much neglected for the practical applications.

Of the many ways in which the structure of a beam can be analyzed we only will choose that of Ronchi[11] and Lenouvel[12] to compare with ours. Here a fine grating, which is placed in the neighborhood of the image point (either "intrafocal" or "extrafocal") of the system, whose aberrations are to be tested. Thus the "light-rays" are first formed into a pencil, converging to the image point. The shadow pattern is very complicated on account of diffraction and must be analyzed by means of theoretical considerations in order to yield the path of the individual rays. In the method described above each part of the wave front has the opportunity to show in a direct way its individual properties. The advantage gained in precision and simplicity, however, results in a loss of luminosity.

When the pencil is not exactly a parallel one, the conclusions are much the same. Here the deviations from homocentricity are observed.

9. PRACTICAL APPLICATIONS

The many possibilities of application of double slit and sieve have not been fully investigated. Our results are given under several headings, in a classification which is somewhat artificial.

I. Small Angles

(a) With double slit and without lenses of mirrors small angles can be measured to within 1 in.

(b) By addition of an eye piece with a magnification of five 0.1 in. is easily attained. A direct application is the angle comparator. The advantage of the absence of lenses and mirrors, entailing the use of large distances, can be sacrificed in order to realise a compact apparatus. The pencil before the diffracting screen can be made parallel by a collimating lens of good quality, while after the screen a good telescope can be placed. The telescope is not focused for infinity, but for an object distance of say 5 to 15 meters.

For the observation of small rotations by means of a mirror, this must be blackened with the exception of two parallel strips. If desired the observation is made with an autocollimating telescope, which is not focused for infinity.

Precision refractometry with a liquid prism (which may be provided with compensating prisms, filled with standard liquid, to obtain direct vision) can be done in a similar way. When light of the interference pattern is falling on one or two photoelectric cells, the refractometer can be made registering, or regulating (e.g. for the regulation of the mixing proportions of a liquid during a process). It may be of importance that the diameter of the light pencil need not be more than 4 mm in order to give a precision of 0.1 in. or less.

(c) Extremely small variations of angle can be measured by means of a sieve, which has many more features for pointing. Thus it is feasable to measure the velocity of light to within 10 percent with a revolving cube, rotated at 13,000 revolutions per minute, some plane mirrors and one spherical mirror of 18-cm diameter and 250-cm radius, the whole length of the optical path between cube and spherical mirror being twice this amount of 250 cm.

II. Measurement of Angles up to 5°

The magnitude of the field of view of the eye piece limits the applicability of double-slit method to angles less than 0.5 or 1 degree. Still it is possible to extend the range, as described below, while retaining the advantages of the method.

We constructed an immersion refractometer for lenses after Fabry and Arnulf[13] (Fig. 5). Light from a slit S (helium, hydrogen, mercury or sodium) is collimated by an excentric parabolical mirror M, passes through a trough with parallel walls, is reflected by a plane mirror N, again passes the trough, and is converged by M at a small distance above S. The slit image is observed with an eyepiece with cross wires E. In the trough the light passes first the lens L to be tested and a prism P, whose refracting angle as well as refractive index are well known.

A mixture of two liquids, as benzene and carbon disulfide, is poured in the trough after observing the best focusing position of E and the correct position of N in order to bisect the slit image by the cross wires. The difference of index between liquid and prism produces a deviation δ and the difference of index between liquid and lens gives a convergence or divergence of the pencil at the eyepiece. By focusing E (or E and S together) by a change of position m along the line of sight and by rotating N *simultaneously* until at the same moment the slit image is sharp and bisected an observation at a

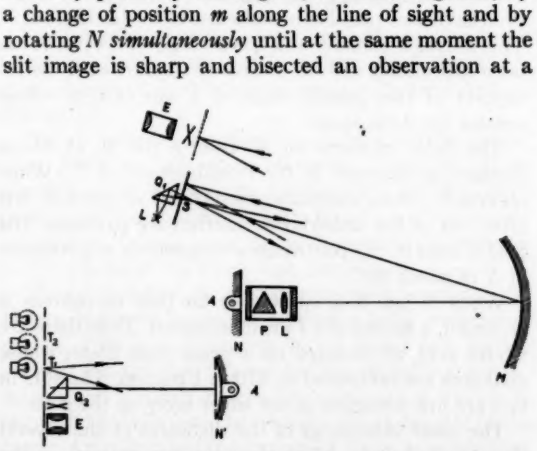

FIG. 5. Immersion refractometer for lenses and measurements of angles up to 5°.

[11] V. Ronchi, Rev. d'optique 5, 441 (1926).
[12] L. Lenouvel, Rev. d'optique 3, 211, 315 (1924).
[13] C. Fabry, J. de phys. et rad. 8, 11 (1919).

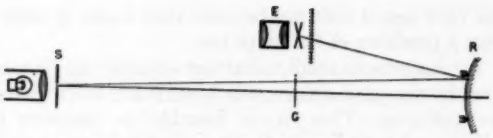

FIG. 6. Absolute spherometer for large radii and flatness tester.

given (but unknown) well-agitated mixture is made. Making three of these observations the graph δ against m gives readily the deviation corresponding to the mixture for which m should have been zero, i.e., for the mixture of the same index as the lens. From this value of the deviation the index is calculated from the known data of the prism. The advantage of the simultaneous observations is well known and of primary importance.

Without going into further particulars (obviation of secondary spectrum by the use of the parabolical mirror, autocollimation, possibility to mount slit and eyepiece on one block in such a way that the influence of slight transverse deviations from the line of sight are compensated), we will only describe the determination of the position of the mirror N.

By a suitable choice of a not too large number of prisms P it appears possible to cover the whole range of indices, provided the deviations can be measured from $-2.5°$ to $+2.5°$. In order to reach the fifth decimal place the precision must be of the order of 2 in., that is to say the position of the mirror must be known over a range of 5° to within 2 in.

Reservation of a precision goniometer, for this purpose only, did not seem tolerable, so we sought and found a much cheaper solution by means of the double-slit method.

On the same axis as N an auxiliary mirror N' (shown in Fig. 5 separately; the axis on which N turns in the upper part of the figure is the same as that on which N' turns in the lower part) has been mounted; it might even have been possible to make use of the backside of N. This mirror is concave and has a radius of 53 cm. It has been aluminized and afterwards blackened with the exception of two parallel slits of 5 mm width, whose centers are 2 cm apart.

The light, received on N' from a slit T_1 at 53-cm distance, is focussed in the neighborhood of T_1. When observed with an auxiliary prism Q and an eyepiece E it gives one of the well-known interference patterns. The field of view of this contrivance corresponds to a rotation of N of about 0.6°.

When N has been rotated so far that no pattern is observed, a second slit T_2 is illuminated. Thus there are twelve slits, all situated on a plane glass plate, whose distances are calibrated to within 1 micron. The slits in fact are fine scratches in the silver layer on the glass.

The small differences of the distances of the several slits to the mirror N' is of minor importance, as the observation with all mirrors is made either within or out of focus. Always a beautiful interference pattern is observed with a clearly defined center.

Beside its cheapness this arrangement has the important advantage of invariability after calibration of the set up. Excentricity and variations of this do not interfere with the results as with a goniometer.

If observation took place as with a stellar interferometer and the observation methods of Michelson[14] and Cotton,[15] a large magnification should have been necessary in order to make the very fine interference lines observable, thus preventing the use of light in the room. Furthermore the differences of the distances between mirror and the several slits should be prohibitive.

How such an arrangement can be made use of for other purposes will be clear without further explanation.

III. Deviations from Flatness; Spherometry

Flatness of a surface can easily be controlled and the deviations measured by using it as a mirror. Light from a distant slit reflected by the surface is studied by means of a sieve. From the known distances, the period of the sieve of grating and the observed distances of the colored diffraction lines the form of the surface is to be derived. When desired the long distances can be obviated by means of collimating lenses, which however introduce the possibility of aberrations.

Here as with all the methods described the precision can be lowered at will for preliminary measurements, or rapid over-all readings on bad surfaces, by simply interchanging the grating with a coarser one. The transformation of extreme precision to very coarse is made very easily indeed.

As an example we will describe a spherometer for direct use in the optical workshop for convex and concave surfaces with radii upwards of 60 cm, as well as for the absolute determination of deviations from flatness of flats with utmost precision (Fig. 6).

Slit S (width some tenths of a mm) is illuminated by a small autocar lamp. At a distance $a=2130.0$ mm the grating G is situated; at a distance $b=1015.4$ mm further a contact ring R is placed, against which the surface to be tested is lightly pressed. The diameter of this surface must be at least 25 mm (this is practically always the case with the interference gauges as otherwise reduction of precision ensues). The light reflected by the surface is observed by means of an eyepiece E, whose position is observed to 0.005 mm over a range of several centimeters. The eyepiece is focused on a plane at a distance $b_2=1001.5$ mm from R.

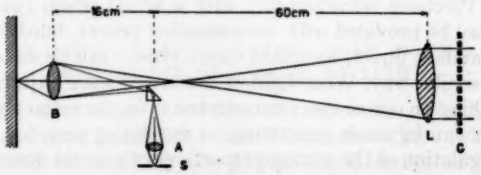

FIG. 7. Autocollimation arrangement.

[14] A. A. Michelson, Astrophys. J. 47, 283 (1918).
[15] A. Cotton, Physica 1, 274 (1921).

The grating (a sieve) has a period of 0.6437 mm. Two rows of holes, whose distance is 6.437 mm, are blocked. Thus no disturbance either from the limits of the grating or from the surface, or from the blocked rows mutually is to be feared, as special investigations revealed.

The distances between slit and grating, between grating and surface, and between surface and cross wires of the eyepiece are known to 0.2 mm.

Within each period of the diffraction pattern four good aligning characteristics can be observed.

Technical and preliminary measurements can be made by means of the diffraction lines corresponding to the blocked rows. A more precise determination makes use of all the characteristics (colors and color transitions) of all rows.

Measurements in the plane of the diffraction fringes are made with a precision of 0.005 mm without much difficulty. This corresponds to a sagitta of the reflecting surface of 0.012 micron. This is equivalent to 1/24 fringe in an interferometer or interference gauge.

For higher precision four characteristics of twenty lines can be observed, which brings us below 1/200 fringe. The correction mentioned above in paragraph 7 has to be applied with $b=2b_1+b_2$. We were glad to find that with such simple means the flatness can be measured up to a radius of 30 km, the more as no more than one cm² of the surface is needed.

Up till now we only considered flat surfaces. But also for spherometry the contrivance is very suitable. For, when the surface is convex, the reflected pencil is divergent, when concave, convergent. Only the distance of the diffraction lines corresponding to the blocked rows has to be measured. The same precision as with flat surfaces can be reached.

With respects to the measurements with interference guages or contact spherometers a special advantage is that the surface to be tested needs only be pressed gently to the (plastic) ring R, thus scratching is minimized.

IV. Measurement of Small Displacements in the Line of Observation

It follows from the above data about the precision that can be attained in the determination of small deviations of a wave front, that the position of a reflecting surface can be ascertained with a great precision. Figure 7 gives a sketch of an autocollimation arrangement for this purpose. S is the primary slit, A and B are microscope object glasses, L and G a telescope object glass and a sieve. Having no observations available we will not dwell on this application. We can only deduce from a precision of $\lambda/100$, as found for other cases, that it must be possible to ascertain the position of a reflecting surface, lying at a distance of, say, 2 meters to within one wave-length, while at the same time the rotational orientation is found to a fraction of a second.

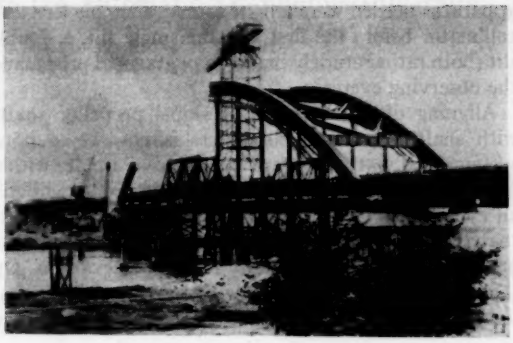

FIG. 8. Iron bridge at Hedel (1947).

V. Measurement of Aberrations and Defects of Homogeneity

By placing the primary slit at the focus of the system to be tested and a sieve in the emerging parallel pencil, deviations of parallelity and thus aberrations of the system can be measured at a precision within say $\lambda/100$. This is effectuated with a very simple and cheap apparatus, as the measurements have to be made to 0.01 mm only, while the results are such that it would be difficult to obtain them with this accuracy by any other method or apparatus, which is certainly much more delicate and costly.

As an example we can cite the case of a photographic lens with an aperture of $\frac{1}{10}$ and a focal length of 60 cm, whose axial aberrations have been determined to a small fraction of a wave-length.

VI. Some Technical Applications

For the sake of completeness we will mention some technical applications that have been made by us. A more elaborate description of these is to be found in reference 2.

The reconstruction of an iron bridge of 124 meters span width on the river Meuse at Hedel has been accelerated by four months by determining the relative positions of the component parts by means of the double slit method, thereby creating the opportunity of working at two places at the same time (see Fig. 8).

The amplitude of the churchtower in the center of the Hague could be measured while the bells were being pealed. This was of interest as the tower had several vertical fissures, one of these having a length of twenty meters and a width of 2 cm or more, and it was questioned if the bells could be pealed without damage to the tower. Amplitudes of 0.3 mm and 1.7 mm at a height of 33 and 53 meters were measured when the bells were in phase. The observation was completed in one afternoon of preparation and one night of measurement. The only

apparatus needed were a light source, a simple lens as a collimator before the first slit, the single slit, a double slit (both rather crudely made), a pentagonal prism, and the observing eyepiece.

Aligning of the bearings of ships' propellor shafts with shaft lengths to 60 meters is now being done systematically at a shipyard by means of a plate with a circular hole surrounded by a concentric circular slit and an eyepiece as described above. Here again it appears that the high precision does not impair in the least the practicability and the rapidity of the observations. On the contrary the advantage with respect to the usual sighting method is marked, as the direction and the amount of the deviations are seen immediately, while with the common sighting method much time is lost by "groping in the dark."

At the National Airtransport Laboratory at Amsterdam the double-slit method has been applied to the rapid and precise determination of the focal length of collimating lenses and also for the transportation of a North-South line to another place.

In the above we have endeavored to show, that new opportunities are available of precise optical measurements with simple, even primitive contrivements, when one is either forced in this direction by circumstances or drawn to it by its attractive features.

PSA Journal—Section B—Photographic Science and Technique

The above title is the new designation which has just been adopted for the Photographic Science and Technique quarterly Technical Supplement to the PSA Journal which is published by the Photographic Society of America. This technical quarterly contains technical material of general interest to most readers of the *Journal of the Optical Society of America*. The June 1950 quarterly, for example, includes articles on deep sea underwater photography, copying black-and-white prints, colored lighting for colored separations, photo-micrography of nuclear tracks, gold treatment of photographic silver halide emulsions, the meaning of absolute opening, and American Standards for photography. The August number of this technical supplement has articles on the photography and study of underwater missiles at the Naval Ordnance Test Station, stablization processing of films and papers, electron microscopy of an estron fiber surface, the description and theory of a spectrosensitometer and a discussion of washing techniques in photographic processing. These articles are presented in a technical form which might be discouraging for the average amateur photographer but are equally acceptable for the technically trained reader in optics and photography.

Society for Applied Spectroscopy

The tentative program for meetings of the Society for Applied Spectroscopy for the first half of 1951 has been announced and is as follows:

January 9, "Quantitative Chemical Analysis by X-Ray Absorption Spectroscopy"—Harold K. Hughes, Socony Vacuum Laboratories.
February 6, Contributed papers by members of the Society for Applied Spectroscopy.
March 6, "Microspectroscopy"—John R. Loofbourow, Massachusetts Institute of Technology.
April 3, "Spectrochemical Methods in Ferrous Metallurgy"—J. T. Rozsa, National Spectrographic Laboratories.
May 1, "Structure of Steroids by Infra-Red Spectrometry"—R. Norman Jones, National Research Council of Canada; "Applications of Spectrochemical Data in Cancer Research"—Konrad Dobriner, Sloan Kettering Institute for Cancer Research.

The meetings, which are open to all interested persons, are held at Socony-Vacuum Training Center, 63 Park Row, New York City and begin at 8:00 P.M. The annual meeting of the society will be held May 25–26 and details of the program will be announced.

Atlas of Raman Spectra

Abstracts of technical papers appearing in other Journals are not usually carried in this Journal; however, the recent paper by W. G. Braun, D. F. Spooner, and M. R. Fenske on "Raman Spectra of Hydrocarbons and Oxygenated Compounds" [Anal. Chem. **22**, 1074 (1950)] merits individual attention. In this 40-page paper, 119 different compounds have been studied and their spectra presented in graphical and tabular form. In combination with some 172 compounds previously reported [Fenske, Braun, Wiegand, Quiggle, McCormick, and Rank, Anal. Chem. **19**, 700 (1947)], Dr. Fenske and his co-workers have now presented Raman spectra data on 291 compounds in a convenient reference form. The data are presented in tabular form with respect to wave-number shift, scattering coefficient and depolarization factor; and in a graphical form on a linear wave-length scale with wave-number scale indicated on the same abscissa.

An Illuminant-Converting Filter for Use with the Automatic Tristimulus Integrator

H. R. DAVIDSON, I. H. GODLOVE, J. M. LAMBERT, AND G. J. WRIGHT
Central Research Laboratory, General Aniline and Film Corporation, Easton, Pennsylvania
(Received August 7, 1950)

If a suitable filter is placed in the sample beam of the recording spectrophotometer, the automatic tristimulus integrator may be used for calculations based on illuminants other than Illuminant C without a change in the cams. Instructions for making a filter for use in calculating tristimulus values based on an illuminant approximating Illuminant A are given.

TRISTIMULUS specifications of color are used for two different purposes, for standardization or description of specific colors, and for description of color differences or color tolerances. In the first use, highly accurate computations of tristimulus data are required, but in the second case, precision, or reproducibility, is far more important than accuracy. ICI Illuminant C is generally used in this country for specifications of both types, and for this reason the automatic Tristimulus Integrator[1] was designed for calculations based on Illuminant C.

Although specification of color difference is generally given in terms of Illuminant C, it is often desirable to specify the same difference in another illuminant. Two specific uses for specification in two illuminants are detection of metameric matches and detection of undesirable color changes with change in illuminant. Both of these, and most other applications of specification under two illuminants, require a high degree of precision rather than accuracy since they involve specification of color difference. To satisfy this requirement of two illuminant specification, therefore, the automatic Tristimulus Integrator should be capable of calculating precise values for some illuminant other than Illuminant C, but these calculations need not be highly accurate.

Unfortunately, there is no simple change which can be made in the integrator to permit calculations on more than one illuminant. The cams can be changed, of course, but this is impractical because of the time required for making this change and recalibrating. It is possible, however, to alter the spectrophotometric curve of the sample in such a manner that the tristimulus values obtained will be for some illuminant other than the one for which the integrator was designed.

Let us consider the case in which we wish to change from Illuminant C to Illuminant A. The following equations for the X tristimulus value may be written:

$$X_C = \int E_C \bar{x} R d\lambda; \tag{1}$$

$$X_A = \int E_A \bar{x} R d\lambda. \tag{2}$$

Standard notation[2] is used and the subscripts A and C stand for Illuminant A and Illuminant C values, respectively. Similar equations may be written for the Y and Z tristimulus values. Let a function w be defined as follows:

$$w = E_A / E_C. \tag{3}$$

Since both E_A and E_C are functions of wave-length (λ), w will also be a function of wave-length. We may now substitute Eq. (3) in Eq. (1), and obtain

$$X_A = \int w E_C \bar{x} R d\lambda = \int E_C \bar{x} (wR) d\lambda. \tag{4}$$

It will be apparent that if the value wR rather than R is transmitted to the automatic integrator, X_A rather than X_c will be calculated. This may be accomplished simply by placing a filter with a transmission w in the sample beam of the spectrophotometer. The spectrophotometric curve plotted will then be wR rather than R. The transmittance of this filter must be w and may be calculated from the standard values for Illuminants C and A.[3]

The function w, however, cannot be used in this particular case. Values for Illuminant A are about three

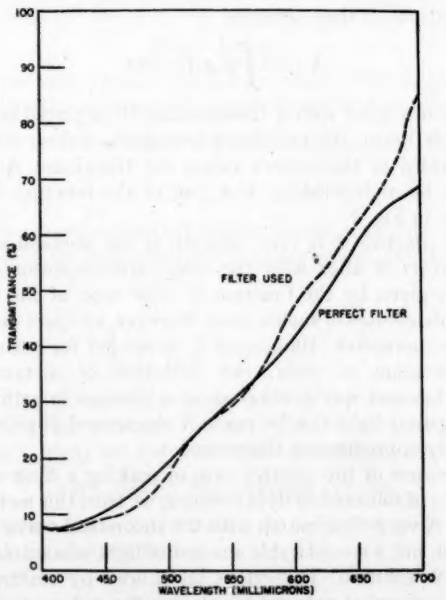

FIG. 1. Spectral transmission characteristics of conversion filters.

[1] H. R. Davidson and L. W. Imm, J. Opt. Soc. Am. 39, 942 (1949).

[2] A. C. Hardy, *Handbook of Colorimetry* (Technology Press, Cambridge, Massachusetts, 1936).

[3] See reference 2, Table V.

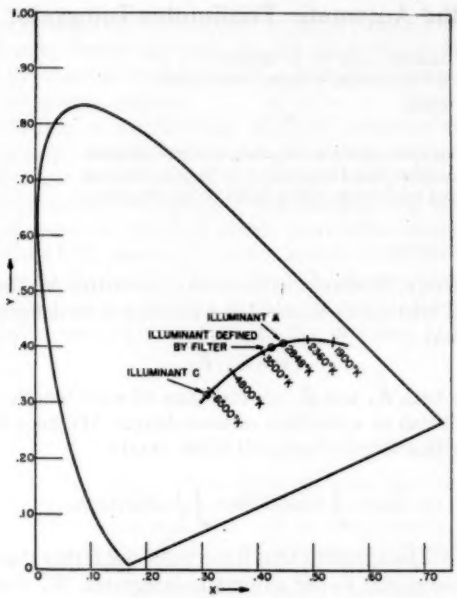

FIG. 2. Position of illuminants in chromaticity diagram.

times as large as values for Illuminant C at 700 mμ. This means that w at 700 mμ is about 3 and the filter would have to transmit about three times as much light as falls upon it. In order to overcome this difficulty, a new function W may be defined in such a manner that it is always less than 1.

$$W = E_A/3E_c. \tag{5}$$

Equation (2) then becomes

$$X_A = 3\int E_c\bar{x}(WR)d\lambda. \tag{6}$$

Now if a filter with a transmission W is placed in the sample beam, the calculated tristimulus values will be one-third of the correct values for Illuminant A and must be multiplied by 3. A plot of the function W is given in Fig. 1.

In practice it is very difficult, if not impossible, to construct a filter with the exact spectrophotometric curve given by the function W. For most of the contemplated uses of such a filter, however, an exact match is not necessary. Illuminant C is needed for accurate specification of color, but detection of metameric matches and specification of color changes in artificial (tungsten) light can be made if the second illuminant merely approximates Illuminant A.

Because of the relative ease of making a filter consisting of solutions of dyes in water, we tried this method first. A very close match with the theoretical curve was found, but a considerable amount of light was scattered by the solution. The errors introduced by scattering were somewhat reduced by placing the cell containing the solution in the forward part of the sample chamber (i.e., away from the sphere).

A more practical filter, the spectrophotometric curve of which is shown in Fig. 1, was then made by dyeing Cellophane[4] and binding it between two glass plates. The following procedure was used. 0.5 percent solutions of Direct Fast Brown TSL, Fastusol Green LBB and Fastusol Blue LBA were made up. 230 cc of brown, 185 cc of green, and 2 cc of blue were then placed in a beaker with sufficient water to make 500 cc. This solution was heated to 58°, and a 1-gram piece of cellophane (No. 450 PT) was placed in the beaker on a glass frame. The cellophane was held in the dyebath for about one-half hour, then a piece of it was placed between two glass plates to form a filter.

Figure 2 is a chromaticity diagram showing the relative positions of ICI Illuminants A and C and the illuminant defined by the cellophane filter.

Although the filter described does not permit accurate calculations on Illuminant A, it may be considered as permitting accurate calculations on an illuminant defined by the filter itself and approximating Illuminant A. Except for a slight lowering of the sensitivity of the spectrophotometer, it has no effect upon the precision of measurement and calculation. We have found that this provides a cheap and simple means of carrying out almost all of the computations which we wish to make.

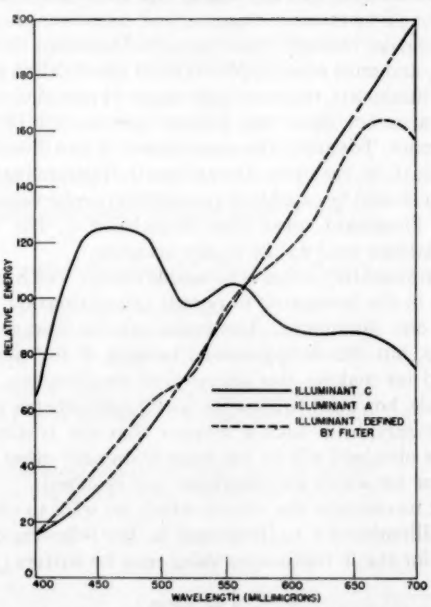

FIG. 3. Relative distribution of energy in various illuminants.

This same method of filter construction can, of course, be used to obtain tristimulus values for any desired illuminant.

Figure 3 is a plot of Illuminants A and C and the illuminant defined by the filter which has been described.

[4] Polarization caused by the Cellophane is corrected on our spectrophotometer by means of a retardation plate. See G. L. Buc and E. I. Sterns, J. Opt. Soc. Am. 35, 458 (1945).

JOURNAL OF THE OPTICAL SOCIETY OF AMERICA VOLUME 40, NUMBER 12 DECEMBER, 1950

Optical Design by a Matrix Method

CLYDE W. HARRIS
Research and Development Division New Mexico School of Mines, Socorro, New Mexico
(Received July 28, 1950)

A symmetrical optical system consists of a series of vertex to vertex intervals separating coaxial refracting or reflecting surfaces of revolution. This paper develops two types of matrices composed of constant elements, one representing intervals and the other surfaces. These matrices are multiplied together in the same order as the corresponding intervals and surfaces occur in the optical system. The resultant product matrix expresses the paraxial, aberrational and chromatic behavior of the system.

Such a formulation may be applied mechanically by unskilled computers, and suggests a passive electrical network analogue to optical systems. The surfaces are not limited to spheres.

INTRODUCTION

THE use of 2×2 matrices to investigate the properties of axially symmetric optical systems has been described before in the literature.[1,2] In the paraxial case the elements of these matrices reduce to constants, and the ordered product of matrices corresponding to separations (intervals) and those representing refracting or reflecting surfaces yields a 2×2 matrix which describes the first-order behavior of the system.

Unfortunately, if third- and higher-order aberration terms are to be included, these matrix elements cease to be constants, and are functions of the vectors on which the matrix operates. Further, investigation of the behavior of the optical system with respect to variations of the wave-length of light demands the differential of the product of these matrices. This requires a tedious summing of a number of matrix sub-products.

A great gain in logical simplicity would be attained if each interval and each surface could be represented by a matrix of constant elements, which would include not only higher order aberration terms, but the chromatic variation introduced by each component.

This may be done. This paper develops the 10×10 interval and surface matrices necessary to express the paraxial, third-order, and chromatic behavior of any composite system. The method of extension to higher order terms is obvious. These matrices are in such a form that subsequent interval or surface matrices operate from the right, exactly as the corresponding elements occur in the system. Such a formulation makes it easy to determine the individual effect of modifying any system parameter, and is ideally adapted to machine computation. The matrix approach immediately suggests a passive electrical network analogue to optical systems, in which the "setting up" and analyzing of a design would be a matter of no more than a few minutes.

THE INTERVAL TRANSFORMATION

Let the unit vector $\mathbf{k}$ define the optical axis of the system. Reference planes are perpendicular to this axis, and may be located at pupils, surface vertices or image planes. The refractive index of the medium is μ, considered positive when the light is progressing to the right. A particular light ray is completely specified by the vector $\mathbf{a}$ in the reference plane giving the point of ray intersection, and the vector $\mathbf{s}$ of length μ directed with the light ray. Necessarily $\mathbf{k}\cdot\mathbf{a}=0$. Finally let z be the interval separating reference planes, positive when the subsequent plane is to the right.

Equate the two vector paths from the origin of the first reference plane to the ray intersection with the second. Then

$$\mathbf{a}+F\mathbf{s}=z\mathbf{k}+\mathbf{a}',$$

where F is an undetermined length factor and primes are applied to subsequent quantities. If this is multiplied through scalarly by $\mathbf{k}$ it is found that $F=z/\mathbf{k}\cdot\mathbf{s}$, and hence

$$\mathbf{a}'=\mathbf{a}+\frac{[\mathbf{s}-\mathbf{k}(\mathbf{k}\cdot\mathbf{s})]}{\mathbf{k}\cdot\mathbf{s}}z.$$

This suggests surrendering $\mathbf{s}$ for the new vector

$$\mathbf{b}\equiv\mathbf{s}-\mathbf{k}(\mathbf{k}\cdot\mathbf{s}).$$

It is the vector projection of $\mathbf{s}$ on either reference plane, so $\mathbf{k}\cdot\mathbf{b}=0$. Squaring the expression for $\mathbf{b}$ shows that

$$\mathbf{k}\cdot\mathbf{s}=\pm(\mu^2-\mathbf{b}^2)^{\frac{1}{2}}=\mu-\mathbf{b}^2/2\mu,$$

so that

$$\mathbf{s}=\mathbf{b}+(\mu-\mathbf{b}^2/2\mu)\mathbf{k} \qquad (1)$$

to the (third) order that we are immediately interested in. Since $\mathbf{s}'=\mathbf{s}$, the interval transfer equations may be written:

$$(\mathbf{a}\ \mathbf{b})\begin{pmatrix}1 & 0\\ z/\mu+z\mathbf{b}^2/2\mu^3 & 1\end{pmatrix}=(\mathbf{a}'\ \mathbf{b}').$$

The 2×2 interval matrix operates on the vectors $(\mathbf{a}\ \mathbf{b})$ defining the incident ray to yield the emergent ray $(\mathbf{a}'\ \mathbf{b}')$, ready for the next element of the system.

THE SHAPE TRANSFORMATIONS

Assume that the refracting or reflecting surface of revolution is specified by

$$z=\tfrac{1}{2}\rho\mathbf{a}^2+\tfrac{1}{8}\rho^3\lambda\mathbf{a}^4 \qquad (2)$$

where z is parallel to $\mathbf{k}$ and ρ is the vertex curvature, positive when convex to the left. Aspherical surfaces are

[1] M. Herzberger, Quart. App. Math. 1, 69 (1943).
[2] T. Smith, "Optics" Encyclopaedia Brittanica 16, 815 (1948).

allowed for by the shape factor λ, which vanishes for a paraboloid of revolution and is unity for a sphere. Since the reference surfaces are always the vertex planes rather than the refractive surfaces, we require the interval transformation from the vertex plane to the surface before refraction, and from the surface back to the vertex plane after refraction. These are obtained by substituting $+z$ and $-z$ from (2) respectively into the interval transformation. They are

$$(\mathbf{a}\ \mathbf{b})\begin{pmatrix} 1 & 0 \\ \pm\rho\mathbf{a}^2/2\mu & 1 \end{pmatrix}=(\mathbf{a}'\ \mathbf{b}').$$

Consider now the meridional plane section of the surface of revolution where $\mathbf{a}\to x$. Then

$$z=\tfrac{1}{2}\rho x^2+\tfrac{1}{8}\rho^3\lambda x^4$$

so that l, the length of the projection of the surface normal (to its axis intersection) onto the axis is, to this order:

$$l=x/(dz/dx)=1/\rho-\tfrac{1}{2}\rho\lambda x^2.$$

The length of the normal between the surface and the axis is

$$f=(l^2+x^2)^{\frac{1}{2}}=1/\rho+\tfrac{1}{2}\rho(1-\lambda)x^2.$$

In three dimensions, if $\mathbf{n}$ is the unit vector surface normal, then

$$\mathbf{a}+f\mathbf{n}=l\mathbf{k}$$

and so

$$\mathbf{n}=[1-\tfrac{1}{2}\rho^2\mathbf{a}^2]\mathbf{k}-[\rho-\tfrac{1}{2}\rho^3(1-\lambda)\mathbf{a}^2]\mathbf{a}. \tag{3}$$

THE REFRACTION TRANSFORMATION

Snell's law of refraction[3] is

$$\mathbf{n}\times\mathbf{s}'=\mathbf{n}\times\mathbf{s},$$

where the cross designates the vector product. Premultiply through vectorially by $\mathbf{n}$ and resolve this vector triple product[3] to obtain

$$\mathbf{n}(\mathbf{n}\cdot\mathbf{s}')-\mathbf{s}'=\mathbf{n}(\mathbf{n}\cdot\mathbf{s})-\mathbf{s}.$$

This may be written

$$\mathbf{s}'=\mathbf{s}+\Gamma\mathbf{n} \tag{4}$$

where

$$\Gamma\equiv\mathbf{n}\cdot\mathbf{s}'-\mathbf{n}\cdot\mathbf{s}.$$

Square (4) to obtain the quadratic

$$\Gamma^2+2\mathbf{s}\cdot\mathbf{n}\Gamma+\mu^2-\mu'^2=0$$

whose solution is

$$\Gamma=-\mathbf{s}\cdot\mathbf{n}+[(\mathbf{s}\cdot\mathbf{n})^2-\mu^2+\mu'^2]^{\frac{1}{2}}.$$

Using (1) and (3), find that

$$\mathbf{s}\cdot\mathbf{n}=\mu-\tfrac{1}{2}\mu\rho^2\mathbf{a}^2-\rho\mathbf{a}\cdot\mathbf{b}-\mathbf{b}^2/2\mu$$

so, after a little manipulation:

$$\Gamma=(\mu'-\mu)+\tfrac{1}{2}\left(\mu-\frac{\mu^2}{\mu'}\right)\rho^2\mathbf{a}^2+\left(1-\frac{\mu}{\mu'}\right)\rho\mathbf{a}\cdot\mathbf{b}+\tfrac{1}{2}\left(\frac{1}{\mu}-\frac{1}{\mu'}\right)\mathbf{b}^2.$$

Multiply (4) through scalarly by $\mathbf{k}$ and use the definition of $\mathbf{b}$ to find that

$$\mathbf{b}'=\mathbf{b}+\Gamma[\mathbf{n}-\mathbf{k}(\mathbf{k}\cdot\mathbf{n})].$$

Using this and the expressions for Γ and $\mathbf{n}$, the refraction transformation becomes

$$\mathbf{a}'=\mathbf{a},$$

$$\mathbf{b}'=-(\mu'-\mu)\rho\left[1+\tfrac{1}{2}\left(\lambda-1+\frac{\mu}{\mu'}\right)\rho^2\mathbf{a}^2+\frac{1}{\mu'}\rho\mathbf{a}\cdot\mathbf{b}+\frac{1}{2\mu\mu'}\mathbf{b}^2\right]\mathbf{a}+\mathbf{b}.$$

The matrix of this transformation is

$$\begin{pmatrix} 1 & -(\mu'-\mu)\rho[1+\tfrac{1}{2}(\lambda-1+\mu/\mu')\rho^2\mathbf{a}^2+(\rho/\mu')\mathbf{a}\cdot\mathbf{b}+(1/2\mu\mu')\mathbf{b}^2 \\ 0 & 1 \end{pmatrix}.$$

The shape, refraction, and inverse shape operators may be multiplied together in that order to yield the surface matrix:

$$\begin{pmatrix} 1+\dfrac{\rho^2\Delta\mu}{2\mu'}\mathbf{a}^2 & -\rho\Delta\mu+\dfrac{\rho^3(\Delta^2\mu-\lambda\mu'\Delta\mu)}{2\mu'}\mathbf{a}^2-\dfrac{\rho^2\Delta\mu}{\mu'}\mathbf{a}\cdot\mathbf{b}-\dfrac{\rho\Delta\mu}{2\mu\mu'}\mathbf{b}^2 \\ \dfrac{\rho\Delta\mu}{2\mu\mu'}\mathbf{a}^2 & 1-\dfrac{\rho^2\Delta\mu}{2\mu}\mathbf{a}^2 \end{pmatrix}$$

where

$$\Delta\mu\equiv\mu'-\mu.$$

CHROMATIC ABERRATION

Suppose that the wave-length associated with the light ray varies. This will, in general, cause a variation in the paraxial matrix elements, so that

$$(\mathbf{a}+\delta\mathbf{a}\ \ \mathbf{b}+\delta\mathbf{b})\begin{pmatrix} A+\delta A & B+\delta B \\ C+\delta C & D+\delta D \end{pmatrix}=(\mathbf{a}'+\delta\mathbf{a}'\ \ \mathbf{b}'+\delta\mathbf{b}')$$

[3] L. Silberstein, *Simplified Method of Tracing Rays Through Any Optical System* (Longmans, Green and Company, London, 1918).

where

$$(\mathbf{a}\ \mathbf{b})\begin{pmatrix} A & B \\ C & D \end{pmatrix} = (\mathbf{a}'\ \mathbf{b}').$$

Ignoring squares of the variations, these may be written in the form

$$(\mathbf{a}\ \mathbf{b}:\delta\mathbf{a}\ \delta\mathbf{b})\left(\begin{array}{cc|cc} A & B & \delta A & \delta B \\ C & D & \delta C & \delta D \\ \hline & & A & B \\ & & C & D \end{array}\right) = (\mathbf{a}'\ \mathbf{b}':\delta\mathbf{a}'\ \delta\mathbf{b}')$$

where zeros are not written. Now $\delta\mu=(\mu-1)/\nu$ where ν is the usual dispersion constant. The paraxial interval matrix including chromatic variation is

$$\left(\begin{array}{cc|c} 1 & & \\ z/\mu & 1 & -z\delta\mu/\mu^2 \\ \hline & & 1 \\ & & z/\mu \quad 1 \end{array}\right).$$

The corresponding surface matrix is

$$\left(\begin{array}{cc|cc} 1 & -\rho\Delta\mu & & -\rho\Delta\delta\mu \\ & 1 & & \\ \hline & & 1 & -\rho\Delta\mu \\ & & & 1 \end{array}\right).$$

THE COMPLETE INTERVAL MATRIX

We must make a final step. Rather than the non-linear transformations of $(\mathbf{a}\ \mathbf{b}:\delta\mathbf{a}\ \delta\mathbf{b})$, consider the linear transformations to be applied to the vector row

$$(\mathbf{a}\ \mathbf{b}:(\mathbf{a}^2)\mathbf{a}\ (\mathbf{a}\cdot\mathbf{b})\mathbf{a}\ (\mathbf{b}^2)\mathbf{a}:(\mathbf{a}^2)\mathbf{b}\ (\mathbf{a}\cdot\mathbf{b})\mathbf{b}\ (\mathbf{b}^2)\mathbf{b}:\delta\mathbf{a}\ \delta\mathbf{b}).$$

The first two vectors comprise the paraxial optics, the next six terms embrace the third-order aberrations, while the last two consider the chromatic variations of the paraxial optics. If we let

$$Z\equiv z/\mu,$$
$$\delta Z\equiv -z\delta\mu/\mu^2=-Z\delta\mu/\mu,$$

the complete interval matrix is found to be:

$$\mathbf{Z}=\left(\begin{array}{ccc|ccc|ccc|c} 1 & & & & & & & & & \\ Z & 1 & & & & & & & & \delta Z \\ \hline & & & 1 & & & & & & \\ & & & 2Z & 1 & & & & & \\ & & & Z^2 & Z & 1 & & & & \\ \hline & & & Z & & & 1 & & & \\ & & & 2Z^2 & Z & & 2Z & 1 & & \\ Z/2\mu^2 & & & Z^3 & Z^2 & Z & Z^2 & Z & 1 & \\ \hline & & & & & & & & & 1 \\ & & & & & & & & & Z \quad 1 \end{array}\right). \tag{5}$$

This includes the entire effect of the interval to the order we are considering. If $z\to 0$ this operator approaches the unit matrix as it properly should.

THE COMPLETE SURFACE MATRIX

The corresponding complete surface matrix is:

$$\mathbf{P}=\left(\begin{array}{cc|ccc|ccc|cc}
1 & -\mathrm{P} & & & & & & & & -\delta P \\
 & 1 & & & & & & & & \\
\hline
\frac{P\rho}{2\mu'} & \frac{1}{2}P\rho\phi & 1 & -P & P^2 & -P & P^2 & -P^3 & & \\
 & -\frac{P\rho}{\mu'} & & 1 & -2P & & -P & 2P^2 & & \\
 & -\frac{P}{2\mu\mu'} & & & 1 & & & -P & & \\
\hline
\frac{P}{2\mu\mu'} & -\frac{P\rho}{2\mu} & & & & 1 & -P & P^2 & & \\
 & & & & & & 1 & -2P & & \\
 & & & & & & & 1 & & \\
\hline
 & & & & & & & & 1 & -P \\
 & & & & & & & & & 1
\end{array}\right). \tag{6}$$

where

$P\equiv\rho\Delta\mu=$ "power" of the surface,
$\delta P\equiv\rho\Delta\delta\mu$,
$\phi\equiv P/\mu'-\rho\lambda$ ($\lambda=1$ for a spherical surface).

If $\rho\to 0$ or the two bounding media become identical, then $P\to 0$ and $\mathbf{P}$ reduces to the unit matrix. If on the other hand the two media are identical at the design wave-length but their dispersions differ ($\Delta\delta\mu\neq 0$), then chromatic variation is introduced and the $-\delta P$ term must accompany the main diagonal of units. According to our early definitions a reflector is introduced by making $\mu'=-\mu$.

AN EXAMPLE OF USE

Suppose that a photographic objective (immersed in air) is under consideration. The matrices $\mathbf{Z}_1, \mathbf{Z}_2, \cdots, \mathbf{Z}_n$ are constructed, corresponding to the interval between the first and second vertex, the second and third, etc. The operators $\mathbf{P}_1, \mathbf{P}_2, \cdots, \mathbf{P}_{n+1}$ representing the first, second, etc., refracting surfaces are also constructed. In addition $\mathbf{Z}_a$ introduces the interval between the entrance pupil and the first vertex, while $\mathbf{Z}_b$ represents the separation of the final vertex and the plate. The matrix $\mathbf{M}$ of the entire system, pupil to plate, is

$$\mathbf{M}=\mathbf{Z}_a\mathbf{P}_1\mathbf{Z}_1\mathbf{P}_2\mathbf{Z}_2\cdots\mathbf{Z}_n\mathbf{P}_{n+1}\mathbf{Z}_b.$$

Let the typical element of $\mathbf{M}$ be M_{ij}. The point of intersection of the emergent ray with the reference plane will be

$$\mathbf{a}'=M_{11}\mathbf{a}+M_{21}\mathbf{b}+M_{31}(\mathbf{a}^2)\mathbf{a}+M_{41}(\mathbf{a}\cdot\mathbf{b})\mathbf{a}+M_{51}(\mathbf{b}^2)\mathbf{a}+M_{61}(\mathbf{a}^2)\mathbf{b}+M_{71}(\mathbf{a}\cdot\mathbf{b})\mathbf{b}+M_{81}(\mathbf{b}^2)\mathbf{b} \tag{7}$$

in terms of the direction and position of the incident ray, while the chromatic variation of the intersection is

$$\delta\mathbf{a}'=M_{19}\mathbf{a}+M_{29}\mathbf{b}. \tag{8}$$

If the plate is located at the paraxial focus then necessarily $M_{11}=0$ and M_{21} is the equivalent focal length. From the definition of $\mathbf{b}$ ideal imagery obtains when

$$\mathbf{a}'=M_{21}\mathbf{b}/(1-\mathbf{b}^2)^{\frac{1}{2}}=M_{21}\mathbf{b}+\tfrac{1}{2}M_{21}(\mathbf{b}^2)\mathbf{b},$$

and hence M_{31} is the spherical aberration coefficient, M_{41} and M_{61} determine the coma, M_{51} and M_{71} together yield the astigmatism and curvature of field, while $M_{81}-\frac{1}{2}M_{21}$ is the distortion coefficient. It will be observed that M_{19} plays a role analogous to M_{11}, and hence measures the chromatic shift of the focal plane whereas M_{29} corresponds to M_{21} and determines the chromatic variation in focal length. The important point is not the names applied to the separate terms, but their effect on the image as expressed by Eqs. (7) and (8).

REMARKS

Larger matrices embracing higher order aberrations and their chromatic variations may readily be constructed in complete analogy to what is presented here. It may be advantageous for fifth and higher order work to use the symmetric scalar variables:

$$u=\mathbf{a}^2,$$
$$v=\mathbf{a}\cdot\mathbf{b},$$
$$w=\mathbf{b}^2$$

and be concerned with the transformation of the row vector:

$$(u\ v\ w{:}u^2\ uv\ uw\ v^2\ vw\ w^2{:}\text{etc.}).$$

Such a matrix involves a 3×3 paraxial sub-matrix, but consolidates the higher order aberration terms.

A Wide-Angle, Underwater Camera Lens*

E. M. THORNDIKE†
Columbia University, New York, New York and Queens College, Flushing, New York
(Received July 11, 1950)

An underwater camera lens covering a half-field of 37.5° is described. The area imaged with this lens is more than seven times that covered with the customary arrangement of a conventional camera lens behind a plane window.

INTRODUCTION

CONCLUSIVE evidence of the utility of underwater photography in biological, engineering, geological, and oceanographic studies and an extensive bibliography on this subject have been given by Ewing, Vine, and Worzel.[1] The need of an underwater camera with a wider field of view than was available prompted Dr. Ewing to suggest that the author design an optical system for a wide-angle camera. A wide field of view is particularly desirable for photography in dirty water as it enables the camera to be placed close to the object being photographed thus reducing the scattering and absorption by the water.

LENS SYSTEMS WITH PLANE WINDOWS

The character of the images formed by plane windows is shown to a sufficiently close approximation for the purpose at hand by considering the light to pass directly from water to air through a plane surface. For infinitely distant objects, the images are also infinitely distant but the light has been refracted at the water-to-air interface thus reducing the field of view and introducing lateral chromatic aberration. A lens with a half-field of 27° in air placed behind a plane window will cover a half-field of only 20° in water. If the reduction of the field were the only difficulty, wide-angle photographic lenses could be used to photograph moderately large fields in water. However, the lateral chromatic aberration introduced by the water-to-air surface precludes the photography of large fields unless color filters are used to limit the region of the spectrum reaching the photographic film. In order to estimate the importance of this effect, consider a 50-mm camera lens behind a plane window. If a resolving power of 20 lines/mm is chosen as the requirement for usable images, it is evident that the lateral chromatic aberration must not be much greater than 1/20 mm. From Table I, this is seen to correspond to an angle of approximately 10°. Thus, one would expect the half-field to be limited to approximately 10°. For objects which are not infinitely far from the camera but which are at distances of 2 m or more, lateral chromatic aberration is still the limiting factor in the production of satisfactory images although spherical aberration, astigmatism, and curvature of the field are now present.

Photographs of a resolving power chart made with a 50-mm lens behind a plane window show that the resolving power for tangential lines drops to 20 lines/mm at approximately 15° from the axis while that for radial lines, which is unaffected by the lateral chromatic aberration, is 40 lines/mm. Visual observations show strong color at this point. These results seem in satisfactory agreement with the predictions given, as the wave-length separation used in the calculation of the chromatic aberration was large. An inspection of underwater photographs confirms the conclusion that the half-field with a plane window is approximately 15°.

The field can be extended in a number of ways: by using color filters to narrow the part of the spectrum reaching the photographic film, by adding a color-correcting lens, or by using a special camera lens designed to correct the color aberration introduced by the window. The loss of light produced by the filters required in the first alternative makes it unattractive. A

TABLE I. Lateral chromatic aberration of a 50-mm camera lens behind a plane surface with water filling the object space.

Angle of incidence in water	Lateral chromatic aberration for *C* and *F* lines
0°	0.00 mm
5	0.03
10	0.06
15	0.09
20	0.14
25	0.22
30	0.36

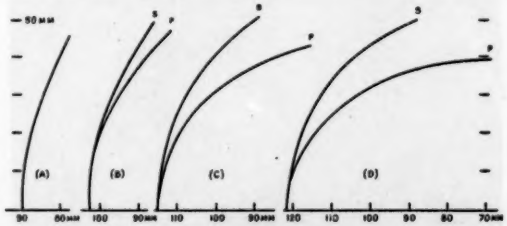

FIG. 1. Positions of images of a distant object formed by a spherical window with radii of 25.4 and 38.1 mm. Abscissas represent distances in front of the aperture stop in millimeters. Ordinates represent distances perpendicular to the axis in millimeters. Tangential images are marked "*P*" and radial images "*S*." The maximum half-field is 30°. The distances of the aperture stop behind the center of curvature of the window surfaces are: (A) 0, (B) 12.7 mm, (C) 25.4 mm, (D) 31.7 mm.

* Lamont Geological Observatory Contribution No. 23, supported by the Navy Department, Bureau of Ships, Contract NObsr-39092.
† Present address, Queens College, Flushing, New York.
[1] M. Ewing, A. Vine, and J. L. Worzel, J. Opt. Soc. Am. 36, 307 (1946).

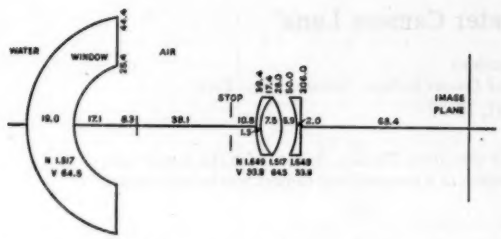

FIG. 2. Wide-angle camera lens. Dimensions are in millimeters.

color-correcting lens of very low power consisting of a plano-convex crown element cemented to a plano-concave flint element has yielded encouraging results, but the greater promise of other solutions caused this one to be abandoned. The third possibility has not been investigated as it seemed wiser to start any new design with a spherical rather than a plane window. This not only gives greater freedom in the optical design but also provides a stronger window for use at great depths.

LENS SYSTEMS WITH SPHERICAL WINDOWS

In studying the complete optical system, it will be convenient to consider the image formed as the light passes from water through the window into air as a first step and then to add the rest of the optical system. The windows considered have concentric inner and outer surfaces. With a stop at the center of curvature of the surfaces, the light rays lie close to the normals to the surfaces and the only serious aberration is curvature of the field. Unfortunately, with windows of reasonable size, this is so great that conventional camera lenses cannot be used to complete the optical system. If the stop is moved back from the center of curvature, astigmatism, curvature, and chromatic aberration for rays at large angles are serious. Figure 1 shows the astigmatism and curvature for a crown glass window with radii of 25.4 and 38.1 mm for various positions of the stop. Clearly a conventional camera lens cannot be used to complete the optical system.

The first attempt at obtaining a satisfactory lens system employed a simple, 10.5-diopter correcting lens to balance the curvature and astigmatism of the window and a 50-mm projection Ektar lens following it. A yellow filter reduced chromatic aberration. At $f/22$,‡ this arrangement gave usable images out to 30° from the axis. The resolving power at 25° was 20 lines/mm for tangential images and 30 lines/mm for radial images.

In the second solution, the astigmatism, curvature, and chromatic aberration of the window are balanced by the corresponding aberrations of a camera lens consisting of a cemented doublet followed by a simple flint lens. Figure 2 shows the arrangement now in use. The diameter of the window is such as to transmit light out to an angle of 37.5° from the axis. With an aperture of $f/11$ this entire field is satisfactorily imaged, the resolving power at 30° being approximately 20 lines/mm. There is considerable distortion in the outer part of the field, but, for most work, this is of little consequence. The area covered with this arrangement is more than seven times that with a plane window. The lens can probably be improved by adjusting radii, refractive indices, and spacings. However, this work is being delayed until more experience shows the properties that are most in need of improvement. The general character of the images can be seen from Figs. 3 and 4. However, the original photographs must be viewed to observe the fine detail which is present.

FIG. 3. Bottom off north shore of Bermuda. Daylight, $f/22$, 4½ ft. off bottom, half-field 37.5°, depth 10 ft.

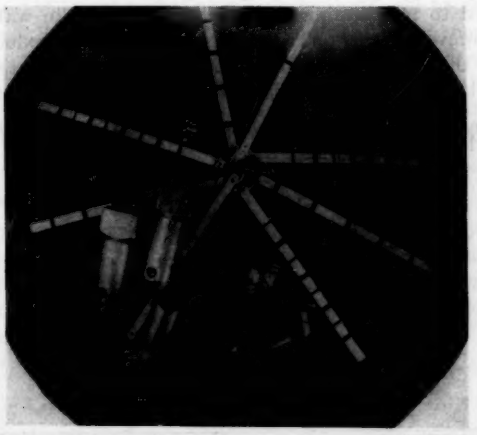

FIG. 4. Bottom of swimming pool. Three No. 5 flash bulbs, $f/11$, 4½ ft. off bottom, half-field 37.5°.

‡ The f/-number is defined as the ratio of the focal length to the diameter of the entrance pupil, both quantities being in the object space. Exposure times are then calculated exactly as with a conventional camera in air.

JOURNAL OF THE OPTICAL SOCIETY OF AMERICA VOLUME 40, NUMBER 12 DECEMBER, 1950

Peripheral Contrast Thresholds of the Human Eye

M. A. BOUMAN
Research Group for Observations of the National Defense, Research Council of the Netherlands, The Hague, Netherlands

(Received July 17, 1950)

Experimental results concerning the behavior of the contrast threshold are given as obtained from about 100,000 responses of the same subject.

The circular test spot of size d between 6.6′ and 8° was projected 7° nasal from the fovea. Green light was used for background and test spot. The stimulus exposure t was varied between 0.02 and 1 second.

So long as d and t are small, the behavior of $\Delta B/B$ agrees with the explanation of de Vries: $\Delta B \sim B^{\frac{1}{2}}$. The dependence of the sensitivity of the eye on B is calculated from the precise shape of the curve for ΔB as a function of B for these combinations of d and t. The result does not contradict direct measurements of the sensitivity.

For combinations of d and t values in which d or t are large, deviations from quanta explanations similar to those published in previous papers on the absolute threshold (J. Opt. Soc. Am. **37**, 908 (1947)) are found.

It appeared that these deviations are due to the fact that ΔB can never decrease below a limiting value depending on B. In a region of the B values studied, this limit for ΔB is proportional to B, so that $\Delta B/B$ is constant for large d and t values in this region.

The duplicity of the retina becomes apparent in the curves representing the sensitivity of the eye as a function of B and in the behavior of the limiting value of ΔB mentioned.

INTRODUCTION

IN continuation of the investigations,[1] concerning the quanta-explanation of the behavior of absolute thresholds values, we have determined the contrast threshold of the human eye under a wide variety of experimental conditions. In this paper we present the data obtained; we compare the results with those of similar investigations and discuss some theoretical explanations.

The typical experimental procedure consisted in projecting a circular test spot, the size and the duration of which were varied, on the center of an illuminated circular background 8° in diameter. When the intensities of both the background and test spot were varied, a large number of such flashes provided the data from which the contrast threshold value as a function of background intensity for the various durations and sizes of the test spot could be determined.

As the results of rather extensive investigations by various authors had been obtained with a view to practical applications so that for them the constant fixation and the artificial pupil were not relevant, we needed the data reported here. For our purpose, namely, the testing of certain theoretical speculations, it was necessary to introduce the precautions of fixing the eye so that the test spot was always projected on the retina 7° nasal from the fovea, and of using a constant artificial pupil in order to eliminate variations in retinal illuminations by the change of the natural size of the pupil. These conditions are similar to those in our previous work.

The spectral distribution of the radiant energy incident on the eye was determined by means of a combination of filters with a half-width value of about 450A and with a maximum transmission at about 5300A.

In all about a hundred thousand flashes of the test spot were observed and are discussed in the present article.

[1] H. A. van der Velden, Physica **11**, 179 (1944); Ophthalmologica **111**, 321 (1946).

THE EXPERIMENTAL ARRANGEMENT

Figure 1 shows the schematical arrangement of our experiments. The light of the tungsten ribbon filament lamp II, placed in the focus of lens L_1, is projected via the planeparallel glass plate M and lens L_2 on the artificial pupil p. The light of the lamp I is focused via lens L_3 in the plane of the rotating disk R, passes the glass plate M, and is focused via L_2 in p. The interchangeable diaphragm D is focused by the lens L_3 in the plane of L_2. The visual angle of the test spot is determined by the size of this diaphragm. The observer sees the plane of lens L_2 homogeneously illuminated by the lamp II and at the same time sees the test spot in this plane.

The rotating disk R is driven by a synchronous motor. In this way, a flash of adjustable duration is presented every 4 seconds to the observer. The duration is determined by the angle of an open sector of the disk R.

The image of the filament of the lamp I on the rotating disk never exceeded one-fourth of the size of the open sector because a suitable focal length of L_3

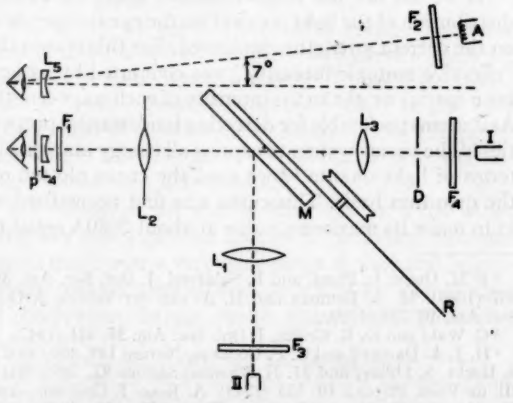

FIG. 1. The experimental arrangement.

and size of the disk R were chosen. In this way, the intensity of the light as a function of time increased at the beginning and dropped at the end of the flashes always approximately instantaneously.

The fixation of the observer's right eye to which our experiments refer is obtained by means of a red fixation lamp A. This lamp is observed with the left eye in such a way that the test spot is seen 7° nasal from the fovea of the right eye. All our previously published peripheral experiments refer also to this retinal spot.

By fixing the red point A, the accommodation of the eyes remains constant under all occurring circumstances. This is important, as thereby the influence of night myopia is eliminated.[2] Indeed, according to recent work of Wald and Griffin,[3] the scotopic eye misses almost completely the power of adaptive accommodation. The more or less fixed state of accommodation in dim light is characteristic for each observer and ranges from the completely relaxed condition to accommodations of 2 to 3 diopters.

As in our experiments the variation of the background intensity covers the regions within which the conditions change from scotopic to photopic, the foveal fixation of the red point was effective in preventing the difficulties arising from the described behavior of the scotopic eye.

The foveal lengths of the lenses L_4 and L_5 were chosen in such a way that the state of accommodation of the eyes, which is determined by focusing the red point A in the fovea of the left eye, brought at the same time the green plane L_2 at infinity for the right eye. We used the data of Wald and Griffin[3] for the difference in refractive power of the eye between the light of the fixation point and of the test spot.

F_2 and F_1 are the filters determining the colors of the fixation point and of the test spot with surrounding field. The intensities of the background and test spot could be varied independently by the interchangeable neutral filters F_3 and F_4 and by the current-strengths of the lamps I and II.

As we did not use monochromatic light, the energy distribution of the light incident on the eye is dependent on the current strengths mentioned. For this reason the "effective scotopic intensity" was computed by assigning a special weight to the intensity of each wave-length. As it seems preferable for detecting fundamental properties of the visual system to express all energy amounts in terms of light quanta,[1,4] we used the curve plotted on the quantum basis. This curve was first normalized so as to make its maximum value at about 5050A equal to unity, after which its ordinates represent the weight mentioned as a function of wave-length.

The transmission of the filters as a function of wave-length had been determined with the photoelectric a.c. amplifier with a.c. galvanometer developed by Milatz.[5]

The lamps I and II were calibrated in accordance with the methods developed and used by Ornstein and co-workers. By means of these methods[6] the current strengths corresponding to temperatures between 1500 and 2800°K were determined.

For these current strengths we computed, in the way mentioned above and using the measured filter, data in the "effective scotopic quantum intensities" incident on the eye and originating from I and II at a relative level. As the weight of the quanta of 5050A was given the value of unity, the resulting quantum numbers refer to this wave-length. When no special information is given we refer to these "effective scotopic quantum intensities." They are indicated by quantum numbers. We computed also along the lines given below the intensities in millilamberts; these are added to the figures.

As in our experiments the intensity of the background covers about 7 logarithmic units, the eye will be for the lower intensity-values in the scotopic state and for the higher in the photopic one. For this reason we also computed the "effective photopic quantum quantum intensities" incident on the eye from the photopic luminosity curve normalized to the value one for 5500A, so that now the quantum numbers refer to 5500A.

For intermediate intensity-values of the background the luminosity curve of the eye does not agree with the scotopic nor with the photopic curve. In order to check our results we computed also the real quantum intensities incident on the eye by giving the weight of unity to the quanta of all wave-lengths.

It appeared that for the particular filter F_1 the three computed quantum intensities are rather insensitive to the shape of the luminosity curve. Indeed, the behavior of these three intensities as functions of the current strengths of the lamps I and II are quite similar. Those referring to the photopic curve are for all current strengths about 20 percent higher than the scotopic values, while for equal weights this percentage is about 40. We give all energies of the experimental data in terms of the quantum intensities based on the scotopic curve. Owing to the facts mentioned above, the resulting error in the absolute values does not exceed 20 percent, even for the highest intensity values of the background, whereas for a fixed background intensity the behavior of the contrast-thresholds is not affected.

For the sake of the practical applications of our data we give the corresponding values also in millilamberts adapted to a constant pupil size of 2 mm. This unit is based on the photopic luminosity curve referring to the energies expressed in ergs. We repeated the calculations mentioned with the erg as unit of energy. It turned out that all conclusions made for the quanta intensities remain valid, the percentages mentioned included. Moreover, the functions representing one of the three computed quantum intensities and one of the corresponding erg intensities, both with the current strength of the lamps I and II are identical except for a constant conversion factor with maximum deviations of 20 percent. We used, therefore, a constant conversion factor for reducing the quantum intensities to millilamberts.

---

[2] J. M. Otero, L. Plaza, and F. Salaverri, J. Opt. Soc. Am. **39**, 167 (1949). M. A. Bouman and H. A. van der Velden, J. Opt. Soc. Am. **40**, 336 (1950).

[3] G. Wald and D. R. Griffin, J. Opt. Soc. Am. **37**, 321 (1947).

[4] H. J. A. Dartnall and C. F. Goodeve, Nature **139**, 409 (1937). S. Hecht, S. Shlaer, and M. H. Pirenne, Science **93**, 585 (1941). Hl. de Vries, Physica **10**, 553 (1943). A. Rose, J. Opt. Soc. Am. **38**, 196 (1948). M. A. Bouman, Thesis, Utrecht, 1949; Soc. Ophthalm. **4**, 23 (1950).

[5] J. M. W. Milatz and L. S. Ornstein, Physica **2**, 355 (1935). J. M. W. Milatz and N. Bloembergen, *ibid.* **11**, 449 (1946).

[6] L. S. Ornstein, D. Vermeulen, and E. F. M. van der Held, J. Opt. Soc. Am. **20**, 573 (1930). L. S. Ornstein, W. J. H. Moll, and H. C. Burger, *Objective Spektralphotometrie* (Sammlung Vieweg, 1932).

THE EXPERIMENTAL RESULTS

The observation of flashes with intensity near the threshold of perception furnishes fluctuating results. Flashes from a constant light source and projected on an illuminated background of constant intensity are not always seen. The region of intensities covered by the fluctuations is rather large. In this region the chance of the flashes being observed takes all values from 0 to 100 percent.[1] We define the contrast threshold by the energy of the flashes for which the chance of being observed is 60 percent. Here we follow van der Velden,[1] who introduced this definition in his investigation concerning the absolute threshold-values.

For each combination of background intensity, visual angle of the test spot, and duration of the flash we determined this contrast threshold by measuring the chance of observation for a few intensities of the test spot, this chance being in the neighborhood of 60 percent and each chance being deduced from 50 flashes. The contrast threshold is found by interpolation between the measured chances. In this way each contrast threshold was determined from 100 to 250 presentations of the test spot.

We found that the slope of the curve representing the chance of observation around the 60 percent value as a function of the intensity of the flash depends on the background intensity as well as on the visual angle of the test spot and the flash-time.[1,7] In agreement with the results of the papers mentioned, the slope becomes steeper with increasing flash-time and increasing visual angle of the test spot for the lower background intensities, while for a fixed combination of duration and visual angle the slope becomes steeper with the background intensity so long as this intensity is low. A suitable measure for this slope can be the relative increase of the intensity of the flash for a change of the chance from 20 to 90 percent. For the steepest slopes we found that the intensity corresponding to a chance of 90 percent was about 1.5 times higher than that belonging to a chance of 20 percent. For the other limit of the slopes obtained this factor was about 4.

For intensities of the background beyond $\bar{N}=10^2$ quanta, no systematical differences between the slopes were found, as for these intensities they all corresponded approximately to the 1.5 value.

Figures 2–9 show the contrast thresholds for various flash-times t, visual angles d, and background intensities B.

DISCUSSION

Without speculating on the theoretical explanation, we give in this section some rules for the behavior of the contrast thresholds deduced from Figs. 2–9. A comparison with the results of other authors on this subject is omitted.

From the curves as a function of the visual angle d of the test spot (Figs. 6–9), it is seen that Ricco's law holds for all flash-times used for d values less than about 15 minutes. Indeed, these slopes almost agree with the relation $\Delta B \times d^2 = \text{constant}$. It follows further from Figs. 6–9 that, for visual angles beyond Ricco's region, Piper's law $\Delta B \times d = \text{constant}$ for the lower intensities changes into $\Delta B = \text{constant}$ for the higher. The way in which this change occurs is highly dependent on t. In general, with increasing intensity and increasing t the region of d values within which $\Delta B \times d = \text{constant}$ decreases, while the d value from which on $\Delta B = \text{constant}$ diminishes.

From the curves as a function of the flash-time t (Figs. 2–5), it appeared that Bunsen's law, $\Delta B \times t = \text{constant}$, is approximately valid so long as d does not exceed about 20′ for t values up to 0.1 seconds. For greater values of the visual angle the relation $\Delta B \times t = \text{constant}$ holds only for the lower intensities within the region of t values mentioned. Furthermore, for flash-times beyond Bunsen's region for the lower intensities and small visual angles ($d<50'$) $\Delta B \times t^{\frac{1}{2}} = \text{constant}$ changes into $\Delta B = \text{constant}$ for the higher intensities. With increasing intensity and increasing d, the region of t values within which $\Delta B \times t^{\frac{1}{2}} = \text{constant}$ decreases, while the t value from which on $\Delta B = \text{constant}$ diminishes.

Concerning the function giving the contrast threshold in dependence on the background intensity for the various combinations of d and t, we observe that the shape of the curve representing this function on a logarithmic scale of B and $\Delta B/B$ does not depend on d or t, so long as neither of them lies outside Ricco's and Bunsen's region. Figure 10 shows this shape. Neglecting small deviations we have, $\Delta B = \text{constant}$ for the lower intensities and $\Delta B \sim B^{\frac{1}{2}}$ for the higher intensities.

It can, moreover, be deduced from Figs. 2–9 that the contrast threshold can never become smaller than a certain limit dependent on the background intensity. Indeed, in the regions of d and t of the curves within which $\Delta B = \text{constant}$, the value of $\Delta B/B$ does not depend on t or d.

In Fig. 11 we present the curve giving this lower limit of $\Delta B/B$ as a function of B. This curve divides the scale of the background intensity B into three parts: for the lower intensities, the lower limit of $\Delta B/B$ is independent of B and equal to about 0.5; for the higher intensities, $\Delta B \sim B^{\frac{1}{2}}$; and for the region near the absolute thresholds, $\Delta B = \text{constant}$.

We compared our results with those of a few other extensive investigations. Blackwell[8] published measurements made over a very wide range of sizes and brightnesses, using a time of 6 seconds and an infinite time of observation. Lamar, Hecht, Shlaer, and Hendley[9,10]

[7] M. A. Bouman and H. A. van der Velden, J. Opt. Soc. Am. **37**, 908 (1947).

[8] H. R. Blackwell, J. Opt. Soc. Am. **36**, 624 (1946).

[9] E. S. Lamar, S. Hecht, S. Shlaer, and C. D. Hendley, J. Opt. Soc. Am. **37**, 531 (1947).

[10] E. S. Lamar, S. Hecht, S. Shlaer, and C. D. Hendley, J. Opt. Soc. Am. **38**, 741 (1948).

studied the relevant range of sizes and shapes at high brightness only. Hendley[11] undertook a study to obtain a more comprehensive view of the relation between size, contrast, and brightness. None of the authors mentioned studied the influence of the flash-time extensively. The constant fixation of the eye was also omitted.

The results of all these studies contradict our conclusion about the dependence on background intensity, flash-time, and size of the test spot of the slope of the curve representing the probability of observation as a function of the intensity of the flash. They found that the slope of this curve does not depend materially on the parameters mentioned: for an increase of the probability from 20 to 90 percent, a fixed increase of the intensity of 2–2.5 times is necessary.

For Blackwell's results, Ricco's law is valid up to about 40′ for the lower intensities and to about 4′ for the higher ones. The same is true for Hendley's work. Without using a constant fixation of the eye there is with increasing intensity a change from rod vision to foveal cone vision. The differences from our present results are, no doubt, due to this fact. The main features of our curves giving $\Delta B/B$ as a function of B shown in Figs. 12–15 agree with those of Blackwell's and Hendley's results.

THEORETICAL OBSERVATIONS

After the publication of the papers by de Vries,[4,12] Rose,[4] and van der Velden,[13] there is in our opinion no reason to start from the photo-chemical aspect of vision for the explanation of the behavior of the contrast threshold.

Hecht's photo-chemical theory[14] of the intensity discrimination neglects the discontinuity of light. From the papers mentioned it appears that it is just this physical aspect which is of great importance.

Van der Velden[1] described the behavior of the absolute threshold-values with the aid of the two-quanta explanation. Summarizing the results of his investigation, he found that for the occurrence of a light perception by the rod system the absorption of two quanta one after the other within a time τ and within a distance D of each other is sufficient. The distance D determines the region of d values within which Ricco's law is valid, and the time τ the region of t values within which Bunsen's law holds. The chief support of this theory is the fact that the law of Piper agrees with it, and that an experimental check on the dependence of the absolute threshold on the time of observation led also to the two-quanta explanation. Indeed, according to this theory the threshold intensity is proportional to t^{-1} when $t > \tau$, which is in agreement with the experiments.

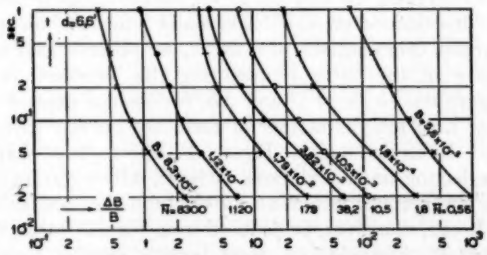

FIG. 2.

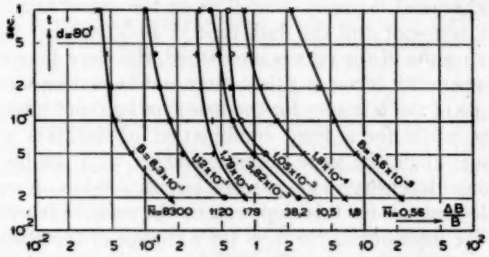

FIG. 4.

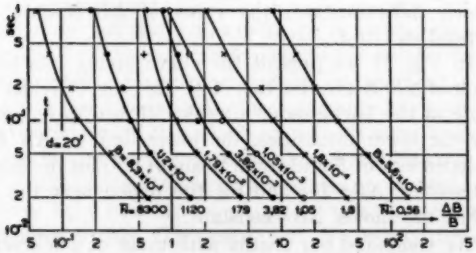

FIG. 3.

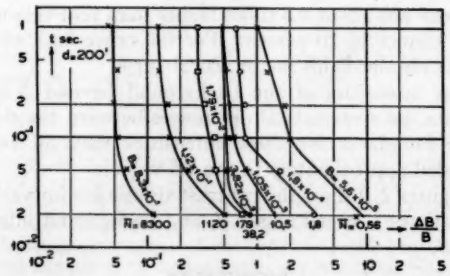

FIG. 5.

FIGS. 2–5. The contrast threshold $\Delta B/B$ as a function of the flash-time t for various visual angles of the test spot and various background intensities B or $\bar{N}$. B is the brightness in millilambert of a surface corresponding to the illumination of the retina when the pupil has the constant diameter of 2 mm. $\bar{N}$ is the average number of effective scotopic quanta incident in the eye per second and per square area subtending a visual angle of 10^{-3} radians.

[11] C. D. Hendley, J. Gen. Physiol. **31**, 433 (1948).
[12] Hl. de Vries, Experientia **4**, 205 (1948).
[13] H. A. van der Velden, Nederland Tijdschr. Natuurk. **15**, 145 (1949).
[14] S. Hecht, *Handbook of General Experimental Psychology* (Clark University Press, Worcester, 1934), p. 704. S. Hecht, J. Gen. Physiol. **18**, 767 (1935).

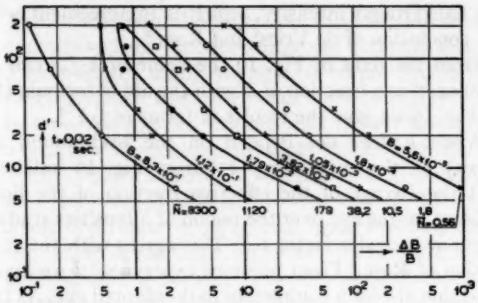

FIG. 6.

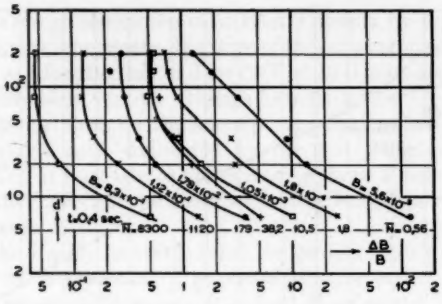

FIG. 8.

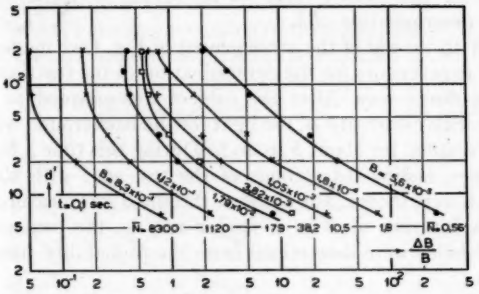

FIG. 7.

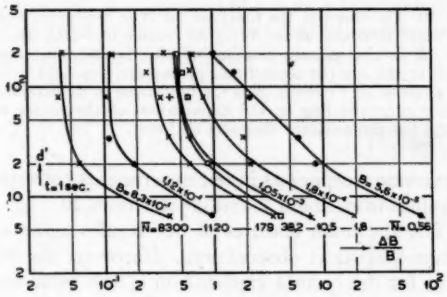

FIG. 9.

FIGS. 6–9. The contrast threshold $\Delta B/B$ as a function of the visual angle d of the test spot for various flash-times and background intensities, B or $\bar{N}$. B is the brightness in millilambert of a surface corresponding to the illumination of the retina when the pupil has the constant diameter of 2 mm. $\bar{N}$ is the average number of effective scotopic quanta incident in the eye per second and per square area subtending a visual angle of 10^{-3} radians.

When part of the retina is illuminated for a certain time with an intensity just near the threshold, a light perception will occur when, owing to the statistical fluctuations in place and time, two quanta happen to be absorbed within a time τ and a distance D somewhere in the retina.

So long as the intensities of our measurements on the contrast threshold B are less than or near the absolute threshold intensity, ΔB will be independent of B and will agree with the value for $B=0$, i.e., the absolute threshold value. Indeed, for these B values the seeing of contrast by the occurrence of a light perception arising from the test spot is completely or nearly independent of the actual absorptions of quanta from the background at this place of the retina obeying the two-quanta conditions. For this reason Piper's law and the relation $\Delta B \times t^{\frac{1}{2}} = \text{constant}$ will be valid for the lower values of B, in agreement with our results.

As Ricco's and Bunsen's laws are based on the capacity of the nerve system of the visual sense to integrate over a certain area of the retina and over a certain time,[15] these laws hold approximately over the whole range of intensities investigated. This is in agreement with our previous study on the brightness impression. We found that for a large range of intensities the brightness of an illuminated surface is determined by the number of absorbed quanta within an area 0 with diameter of about 30′ of the retina and within a time T of about 0.1 second, so far as rod vision 7° nasal from the fovea is concerned.

It is clear that for values of B beyond the threshold, ΔB will be greater than would correspond with the value for $B=0$, so that the number of quanta that must at least be absorbed within a certain area and a certain time for the seeing of contrast will exceed two and will increase with increasing B. Of course, it is highly probable that this area and time agree with 0 and T found in the experiments on the brightness impression.

When under certain conditions at least p quanta must be absorbed within 0 and within T, it can be concluded from mathematical considerations that $\langle \Delta N \rangle \sim t^{-1/p} \cdot d^{-2/p}$ (7) for $t \gg T$ and $d \gg$ diameter of 0, in which $\langle \Delta N \rangle$ is the total number of quanta of the flash incident on the eye under these conditions. According to this formula, the slopes of the curves representing $\langle \Delta N \rangle$ as a function of d or t become steeper for increasing p in agreement with the behavior of the slopes of the curves of Figs. 2–9. Moreover, the steepness of the curve representing the probability of the realization of contrast as a function of ΔB increases with increasing B.

[15] M. A. Bouman and H. A. van der Velden, J. Opt. Soc. Am. 38, 231 (1948).

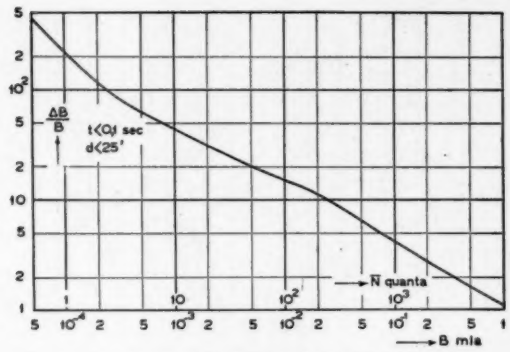

FIG. 10. The shape of the function $\Delta B/B$ in dependence of the background intensity B or N for all values of $t<0{,}1$ sec. and $d<25'$. $\bar{N}$ is the average number of effective scotopic quanta incident in the eye per second and per square area subtending a visual angle of 10^{-3} radians. B is the brightness in millilambert of a surface corresponding to the illumination of the retina when the pupil has the constant diameter of 2 mm.

The extreme steepnesses in our experiments correspond to p values from about 2 and greater than 20.

So far, the main features of our results agree with quantum-statistical observations. However, the chief support for the quanta explanation of the behavior of the contrast threshold is the agreement of our results with the theory of de Vries[4] for this visual function. If, namely, the test spot and the background are projected on a recipient unit 0 of the retina, then according to this theory, contrast will be seen, if the average number of quanta absorbed during the averaging time T of the visual sense organ increases more than it corresponds to the average of the statistical fluctuations in the number of quanta absorbed in an area 0 and the time T:

$$f\langle\Delta N\rangle > [f\bar{N} + (f\bar{N} + f\langle\Delta N\rangle)]^{\frac{1}{2}}$$

or

$$f\langle\Delta N\rangle = k[2f\bar{N} + f\langle\Delta N\rangle]^{\frac{1}{2}}, \qquad (1)$$

where $\bar{N}$ is the average number of quanta incident on the eye from the background, $\langle\Delta N\rangle$ is this number from the test spot, f is the effective fraction of the quanta incident on the eye, and k is the efficiency ratio of the sense organ.

Rose[4] used a simpler formula which includes the main idea of this theory. Of course, this theory will only hold so long as the background intensity exceeds the range within which the behavior of $\Delta B/B$ is determined by the absolute threshold values where ΔB does not depend on B.

When we first neglect the possible variations of f and k for the various background intensities, we have according to formula (1) $\Delta B/B \sim B^{-\frac{1}{2}}$. Indeed, the general slope of the curve of Fig. 10 agrees with this law, except for the very lowest intensities for the reason mentioned above, so that, provided the contrast threshold indeed behaves according to this quanta explanation, the parameter $k \cdot f^{-\frac{1}{2}}$ is only slightly dependent on the background intensity, which is in agreement with the conclusion of de Vries[4] and Rose.[4]

From the data of Fig. 10 the value of $k \cdot f^{-\frac{1}{2}}$ can be computed as a function of B with the aid of formula (1). In Fig. 16 we give the results in terms of $f \cdot k^{-2}$.

When k does not depend on the background intensity B, the curve for $f \cdot k^{-2}$ from Fig. 16 indicates that the change of the effective fraction of the light incident on the eye over the region of intensities studied does not exceed a factor 6.5. This agrees with the conclusion of Rose.[4] From previous experiments[7] we know the value of f for a completely dark-adapted eye. As the present results were obtained by the same subject, we can use this same f value for the lowest intensities for the determination of k.

With the aid of the arrangement of Fig. 1 we made a few experiments for the determination of the fraction f in a direct way. After the subject was adapted to a particular intensity B, the light for the background was interrupted for about 5 seconds. During this time a few flashes, lasting 0.1 seconds of the test spot with size of 34′ were shown. The absolute threshold was measured as a function of B in a similar way as the contrast thresholds were determined from the probability function.

Of course, the spot of the retina investigated was again 7° nasal from the fovea. We only maintain that from these experiments an indication can be obtained as to the dependence of f on the intensity B. Indeed, during the 5 seconds of interruption the sensitivity of the eye will not be completely constant, but may change in a way dependent on B.

In Fig. 16 we present the results from the preliminary experiments. It seems probable that k is not dependent on B, as the shapes of the functions giving the dependences of f and $f \cdot k^{-2}$ on the intensity B might possibly be similar. In that case, k has the value 3.3. Rose[4] considered the value 5. Of course, this value of k may depend on the part of the retina studied.

One is inclined to assume that for B values higher than $N = 10^2$ the cone system becomes active, which is

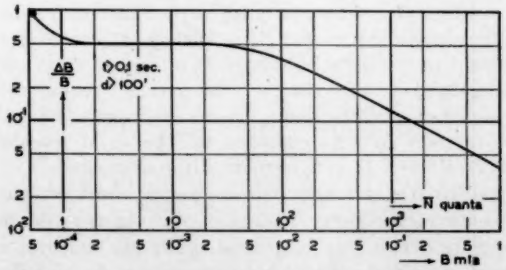

FIG. 11. The minimum obtainable value for $\Delta B/B$ as a function of the background intensity B or $\bar{N}$. $\bar{N}$ is the average number of effective scotopic quanta incident in the eye per second and per square area subtending a visual angle of 10^{-3} radians. B is the brightness in millilambert of a surface corresponding to the illumination of the retina when the pupil has the constant diameter of 2 mm.

in agreement with the fact that the visual sensation changes here from colorless to green, corresponding to the wave-length used. Anyhow, it seems that k does not change much when the cones come into play.

In a previous paper[7] dealing with the explanation of the behavior of absolute threshold values with the aid of the two-quanta theory of van der Velden, deviations from theory were mentioned for the case of the simultaneous occurrence of large test spots and long flash-times. These deviations are neither of a physical nor of a photo-chemical nature. From the present results it appears that so long as t does not exceed 0.1 second and $d25'$ the results are satisfactorily explained by de Vries' theory (formula 1).

When, however, according to these data for $d<0$ and $t<T$ at a fixed intensity B for the realizing of contrast, an average absorption of at least p quanta by the test stimulus is necessary, the slope of the curve representing ΔB as a function of t or d for $t \gg T$ or $d \gg 0$ must approximately obey van der Velden's formula $\Delta B \propto t^{-1/p} \cdot d^{-2/p}$, assuming that, on the average, at least in one of the recipient units subtended by the test stimulus and during at least one of the averaging times T belonging to the flash-time, an absorption of at least p quanta is necessary.

We already mentioned that the general feature of the curves is such that p increases with increasing B, as we expected. However, at a fixed B value the theory predicts independence of p on d or t, so that the slopes of the curves as a function of t or as a function of d for $t \ll T$ or $d \ll 0$ must be constant and in correspondence with the same p value. From the experimental curves

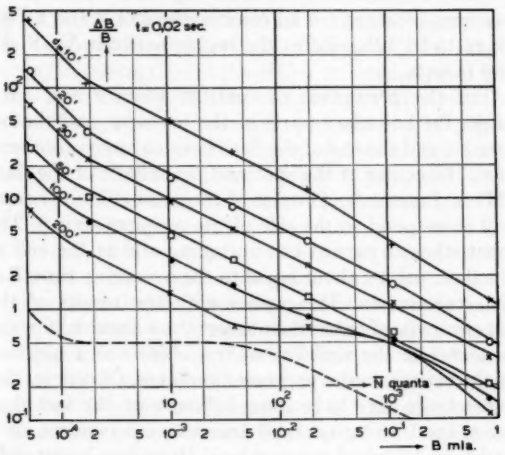

FIG. 12.

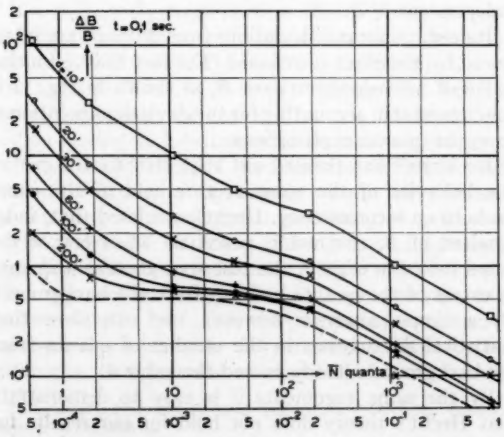

FIG. 13.

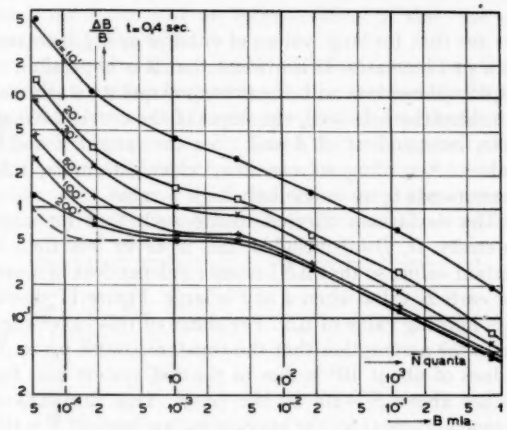

FIG. 14.

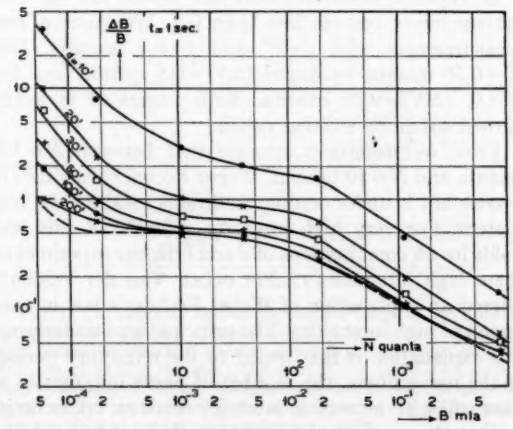

FIG. 15.

FIGS. 12–15. The contrast threshold $\Delta B/B$ as a function of the background intensity B or $\bar{N}$ for various flash-times and visual angles of the test spot. B is the brightness in millilambert of a surface corresponding to the illumination of the retina when the pupil has the constant diameter of 2 mm. $\bar{N}$ is the average number of effective scotopic quanta incident in the eye per second and per square area subtending a visual angle of 10^{-3} radians. The dotted curve represents the minimum obtainable value for $\Delta B/B$.

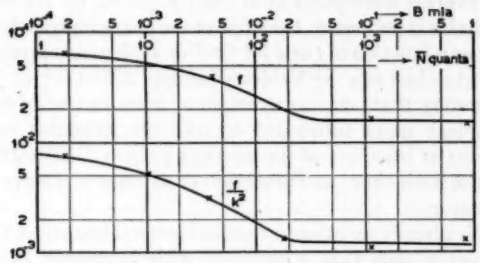

FIG. 16. The value $f \cdot k^{-2}$ computed from the contrast threshold data as a function of B or $\bar{N}$ and the value f from direct adaptation measurements. f is the effective fraction of the light energy incident in the eye, k is the efficiency factor for the perception of contrast. B is the brightness in millilambert of a surface corresponding to the illumination of the retina when the pupil has the constant diameter of 2 mm. $\bar{N}$ is the average number of effective scotopic quanta incident in the eye per second and per square area subtending a visual angle of 10^{-3} radians.

we see that for large values of either d or t, p increases as d or t increases. It is evident that it is impossible to explain these data with the presented quanta statistical considerations. Indeed, the slopes of the curves become even independent of d and t for the largest d and t values. According to van der Velden's formula, this corresponds to an indefinitely high p value.

The deviations referred to are such that for each intensity B, $B=0$ included, ΔB is never less than a certain value, so that ΔB becomes independent of d or t for each B value when d or t is large. Figure 11 shows this limiting value of ΔB. The shape of this curve suggests the assumption that the constant course up to $\bar{N}$ values of about 10^2 is due to the rod system and for values above $\bar{N}=10^2$ to the cones. This furnishes a second argument for the hypothesis that beyond $\bar{N}=10^2$ the cones come into play.

It appears, therefore, that $\Delta B/B$ can for the rod system never become less than 0.5. We made a few measurements with $d=8°$ and $t=0.4$ seconds. For $\bar{N}=0.56$ quanta we found $\langle \Delta N \rangle = 0.6$ quanta and for $\bar{N}=0$, $\langle \Delta N \rangle = 0.25$ quanta. Both values of B again turned out to be limiting values.

From our results it appears that between $\bar{N}=1.8$ quanta and $\bar{N}=10$ quanta, Weber Fechner's law $\Delta B/B$ = constant is under certain conditions valid for the rod system. For very high intensity values[8, 11, 16] this law holds for all combinations of d and t. In our experiments these high intensities do not occur. Van der Velden[13] offered an explanation of Weber Fechner's law in this region of high intensities. The principal idea underlying this explanation is that owing to the refractory period of the nerve fibers, the number of nerve impulses in a fiber will with increasing intensity reach an upper limit so that the number of impulses is then no longer proportional to B. Indeed, this number can never exceed $1/\gamma$ per second when γ is the refractory period.

Each recipient unit 0 of the retina has at least one nerve fiber connecting it with the brain. This unit will certainly not be greater than 30′ for the rod system 7° nasal from the fovea, from which it follows that the number of impulses per fiber per second will certainly not exceed 3.5 to 350 in the region of B in which Weber Fechner's law in our data is valid. In this calculation we have assumed f to be 10 percent. The upper limit $1/\gamma$ of the number of impulses in a fiber is about 500, considerably higher than the possible numbers occurring in the region of B concerned.

For this reason the constancy of $\Delta B/B$ under the conditions mentioned must follow from quite another cause than that active in the case of the highest intensities B. Moreover, for these highest B values $\Delta B/B$ becomes constant for all combinations of d and t, contrary to its behavior in the region between $\bar{N}=8$ and 100 quanta.

For the perception of contrast when d and t are large, the boundary parts of the test spot and the beginning and the end of the flash become more prominent than the center of the spot and the middle of the flash (M. A. Bouman[4]). The size of the most efficient border will correspond to the size of the recipient unit 0. The most efficient part at the beginning and at the end of the flash will be about equal to the averaging time T of the sense organ. This agrees with the results of the experiments of several authors[9, 11] as regards the dependence of the visibility of test objects as a function of the ratio between perimeter and area. Of course, this dependence may have some influence on the fact that for a fixed intensity $B\Delta B$ becomes independent of d and t for higher d and t values. However, it certainly cannot account for the limiting value of $\Delta B/B$ being independent of B.

Indeed, no serious deviations from $\Delta B \sim B^{\frac{1}{2}}$ are introduced by the effect mentioned. The fact that a limiting value of ΔB belongs to each B, as shown in Fig. 11 is fundamental in accounting for the deviations mentioned from the quanta explanations.

De Vries[17] has pointed out that Hecht's theory[10] of the behavior of the contrast threshold of the cones leads to an inconsistency. Hecht postulated that, independent of B, contrast is perceived when one of the cones near the edge of the test spot absorbs 4 quanta in excess of the quanta arriving from the background. By a simple analysis, however, one can show that statistical fluctuations in the number of quanta from the background already exceed the value 4.

By the same arguments it is easy to demonstrate that Hecht's theory does not hold for our results for rod or cone vision.

[16] J. Steinhardt, J. Gen. Physiol. **20**, 185 (1937).

[17] Hl. de Vries, J.O.S.A. **39**, 201 (1949).

JOURNAL OF THE OPTICAL SOCIETY OF AMERICA VOLUME 40, NUMBER 12 DECEMBER, 1950

Tritanopia with Abnormally Heavy Ocular Pigmentation

DEANE B. JUDD,* LORENZO PLAZA,† AND DEAN FARNSWORTH‡
National Bureau of Standards, Washington, D. C., and U. S. Naval Medical Research Laboratory, New London, Connecticut

(Received August 30, 1950)

The chromaticity confusions characteristic of tritanopia may be represented on the (x, y)-chromaticity diagram by a family of straight lines intersecting at a copunctal point near the shortwave extreme of the spectrum locus. A case of congenital tritanopia is reported that departs from typical tritanopia, first by having a luminosity function abnormally curtailed on the shortwave end, second by having chromaticity confusions among object colors describable by straight lines on the (x, y)-plot intersecting in an area surrounding the spectrum locus at 460 mμ instead of near the shortwave extreme, and third by confusing incandescent lamp light at a color temperature of 2900°K with the spectrum at 586 mμ instead of the typical tritanopic value of 579 mμ. It has been found that all three of these disagreements with typical tritanopia are to be expected from a tritanope possessing normal macular pigmentation combined with an ocular pigment five times normal. We believe, therefore, that this case of atypical tritanopia departs from typical tritanopia because of abnormally heavy ocular pigmentation.

I. INTRODUCTION

TRITANOPIA is a form of abnormal vision frequently encountered in diseases of the retina such as inflammation of the retina or separation of the retina from contact with the choroid coat. The inflamed or detached portion of the retina yields color perceptions of red and bluish green or mixtures thereof,[1] but is incapable of distinguishing between gray and what appears to the healthy part of the eye either as greenish yellow or as bluish purple. The tritanopic area of the retina can yield an exact match for any part of the spectrum (and indeed any color whatever) from a mixture in suitable proportions of the extreme long-wave end of the spectrum (red) with a part of the spectrum near 470 mμ (blue). Tritanopia is therefore said to be a dichromatic form of vision; that is, the color matches set up by means of a tritanopic retinal area can be expressed as a function of two variables. This distinguishes it from normal vision, said to be trichromatic since it requires three variables.

If a sufficiently large portion (say 2° subtense) of a healthy retina, however, be used to distinguish the colors of two sufficiently bright fields (luminance of, say, 1 millilambert or more), it is very rare that tritanopic mistakes are made. The one observer in a million having such retinas with no previous history of retinal disease is called a congenital tritanope, and congenital tritanopes are eagerly sought after because by studying their color matches and perceptions we ought to be able to obtain more precise information regarding tritanopia than in any other way. A case of what appeared to be congenital tritanopia was reported by one of us[2] in 1943. It is the purpose of this paper to compare this case with the accepted view of typical tritanopia, to report the results of our calculations on the influence of variations in pigmentation of the eye media on color matches made by a tritanope, and from these results to give an interpretation of this case of congenital tritanopia.

Interest in tritanopia has increased in recent years because of rediscovery of the fact announced by König in 1894[3] that when the normal eye is used to detect the difference between small colored spots by central fixation it makes tritanopic mistakes, and is, in fact, tritanopic.[4] We now know that the normal eye tends to make tritanopic errors whenever it is used to compare

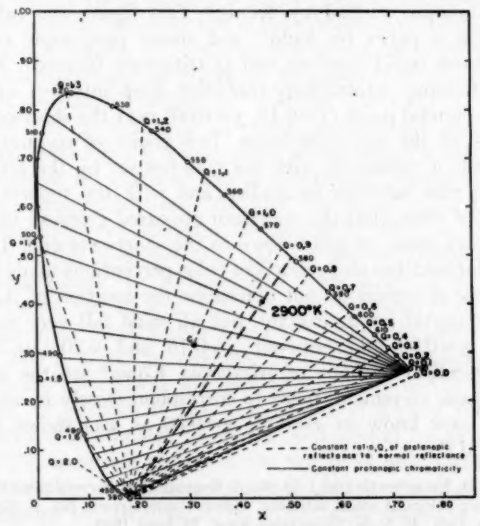

FIG. 1. Chromaticity confusions (dotted lines) of the classical tritanope on the (x, y)-chromaticity diagram (see reference 10). Note that the classical tritanope sees the spectrum at about 567 mμ as having the same chromaticity as standard source C (representative of average daylight), and that he sees the spectrum at about 579 mμ as having the same chromaticity as an incandescent lamp at a color temperature of 2900°K.

* Physicist, Photometry and Colorimetry Section, National Bureau of Standards.
† Physicist, Institute of Optics, Madrid.
‡ Lt. Cdr., Medical Research Laboratory, U. S. N. Submarine Base, New London, Connecticut.

[1] H. Köllner, *Die Störungen des Farbensinnes* (Karger, Berlin, 1912).

[2] D. Farnsworth, J. Opt. Soc. Am. 33, 350 (1943).

[3] A. König, *Ueber den menschlichen Sehpurpur und seine Bedeutung für das Sehen* (Sitz. Akad. Wiss. Berlin, June, 1894), p. 577; also *Gesammelte Abhandlungen* (Leipzig, Barth, 1903), p. 338.

[4] E. N. Willmer and W. D. Wright, Nature 156, 119 (1945).

TABLE I.

		Tritanomalous Figure	Tritanomalous Background
Normal	Figure	5 *GY* 7/6	7.5 *Y* 6/6
		5 *GY* 6/4	7.5 *Y* 7/6
	Background	7.5 *PB* 7/6	2.5 *P* 7/6
		7.5 *PB* 6/6	5 *P* 6/4

the colors of two fields either too dimly lit or too small to be correctly seen.[5–7]

II. CLASSICAL TRITANOPIA

The accepted view of tritanopia is based largely upon measurements and reports by nine pathological cases studied by König.[8] He found that color matches between various parts of the spectrum and a two-part mixture of spectrum lights (apparently 480 with 650 mμ) was set by these tritanopes in such a way that they would find matched any metameric pair set by an observer of normal vision. On this account tritanopia is called a reduction form of normal vision, and we can show the chromaticity confusions characteristic of tritanopia on the same chromaticity diagram used for normal vision. Figure 1 shows (dotted lines) on the (x, y)-chromaticity diagram of the standard ICI coordinate system for colorimetry[9] the chromaticity confusions characteristic of the nine cases of acquired tritanopia studied by König.[8] This figure was taken from a paper by Judd[10] and shows protanopic confusions (solid lines) as well as tritanopic (dotted). The tritanopic chromaticity-confusion lines intersect at a co-punctal point (x=0.18, y=0.00) near the shortwave end of the spectrum locus. This choice of co-punctal point is consistent with the matches set by the six of the nine subjects so studied and with the reports of all of them that the spectrum appeared greenish blue, bluish green, or green down to the shortwave end. The color matches and reports of color perceptions made by these observers do not determine the location of their co-punctal points exactly, but all must fall very near to y=0.00 and between x=0.16 and 0.20. In his theoretical account of tritanopia König[8] set the tritanopic co-punctal point to correspond closely to what we now know as x=0.18, y=0.00 as was shown by Judd.[10]

Subsequent studies of acquired tritanopia have confirmed the observations by König's observers.[11–15] Some of them,[11–13] show only one neutral point in the spectrum which falls in the neighborhood of 570 mμ, the longwave portion appearing red; the shortwave, bluish green. This corresponds to the location of the copunctal point at x=0.18, y=0.00; note on Fig. 1 that the dotted line passing through the point representing illuminant C (close to average daylight chromaticity) intersects the spectrum locus at only one point, that corresponding to about 567 mμ. Other studies[14,15] show

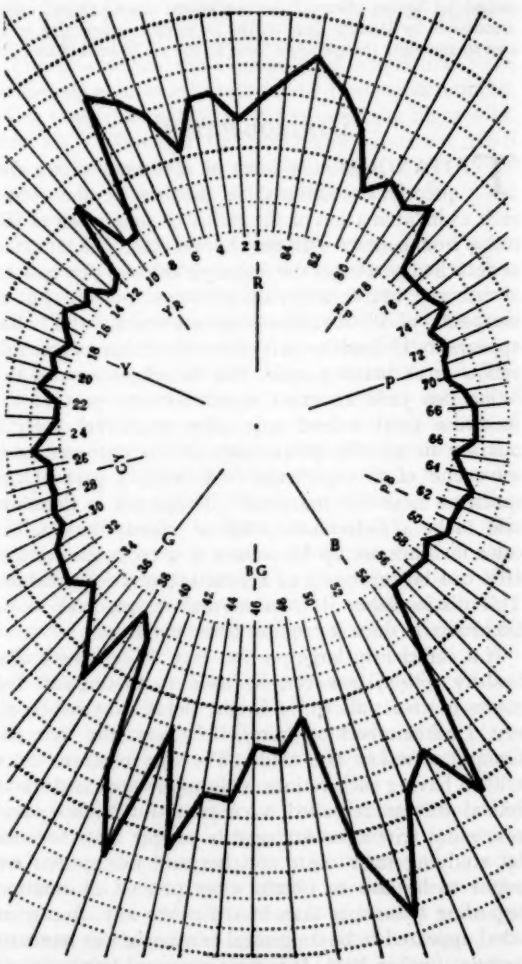

FIG. 2. Score made by Mr. V. on F-M 100-hue test, average of four trials, shown on the Farnsworth profile diagram. (See reference 28.) Mr. V's ability to distinguish hues in the yellow to green and purple to blue ranges is about equal to that of the normal eye, but he cannot distinguish yellowish reds from purplish reds, nor greens from blues.

[5] D. Farnsworth and J. D. Reed, Retention of discriminable hue of ten colors at small subtense, Color Vision Report No. 7, Med. Res. Lab., U. S. N. Submarine Base, 20 April 1944.

[6] H. Hartridge, Phil. Trans. Roy. Soc., London (B) **232**, 535 (1947); Nature **155**, 391, 657 (1945).

[7] W. E. K. Middleton, J. Opt. Soc. Am. **39**, 582 (1949).

[8] A. König, Ueber "Blaublindheit," Sitz. Akad. Wiss. Berlin, p. 718 (July 8, 1897); also *Gesammelte Abhandlungen*, p. 396 (Barth, Leipzig, 1903).

[9] Commission international de l'Éclairage, Proceedings of the 8th Session, Cambridge, England, 19–29 (September, 1931). A. C. Hardy, *Handbook of Colorimetry* (Technology Press, Cambridge, Massachusetts, 1936). D. B. Judd, J. Opt. Soc. Am. **23**, 359 (1933).

[10] D. B. Judd, J. Research Nat. Bureau of Stand. **33**, 407 (1944); *RP*1618; also J. Opt. Soc. Am. **35**, 199 (1945).

[11] H. Köllner, Zeits. f. Augenheilk. **19**, Ergänzungsheft (1908).

[12] H. Köllner, Zeits. f. Augenheilk. **17**, 234 (1907).

[13] H. Köllner, Zeits. Sinnesphysiol. **42**, 281 (1907).

[14] Collin and W. A. Nagel, Zeits. Sinnesphysiol. **41**, 74 (1907).

[15] H. Piper, Zeits. Psychol. **38**, 153 (1905).

a second neutral point or region in the neighborhood of 430 mμ. This corresponds to location of the copunctal point at $x=0.165$, $y=0.000$, as is possible also for one of König's nine tritanopes. Willmer and Wright[4] likewise found an indication of such a neutral region for small fields in the normal fovea, and Pitt[16] considers this to be typical of tritanopia though the cases cited[8] by him in support of the view showed only the neutral point near 570 mμ. G. E. Müller[17] in his detailed analysis of the various types of color blindness recognizes the fact that individual cases of tritanopia may show either a neutral region near 430 mμ or no second neutral point at all, and suggests explanations for these individual differences in terms of his stage theory of color vision. It has been shown by Judd[18] that the Müller theory evaluated according to modern data on additive color mixture[9] accords best with a tritanopic co-punctal point at $x=0.165$, $y=0.000$.

There are also observers[19–26] having dichromatic vision and ability to distinguish red from green who are further characterized by confusion of yellow colors with blue. These observers have two neutral points in the spectrum, one in the neighborhood of 582 mμ, the other in the neighborhood of 470 mμ. Some students of colorblindness class these observers as tritanopes,[27] but Müller[17] has proposed a new name for them—tertartanopes. Because of the paucity of cases on record, because of the rather large individual differences between cases, and because of the fact that the ability to distinguish red from green is usually far below normal, there is doubt what the exact characteristics of this class are, and indeed doubt whether it is useful to have this class at all.

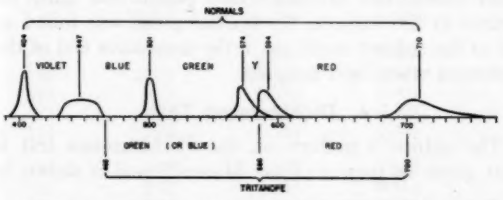

FIG. 3. Division of the spectrum according to hue by the normal eye (violet, blue, green, yellow, red) compared to that by Mr. V's tritanopic eye (green, red). The division points are subject to individual variation. Those for the normal eye are indicated here by approximate distribution curves derived from settings of 141 observers with normal color vision.

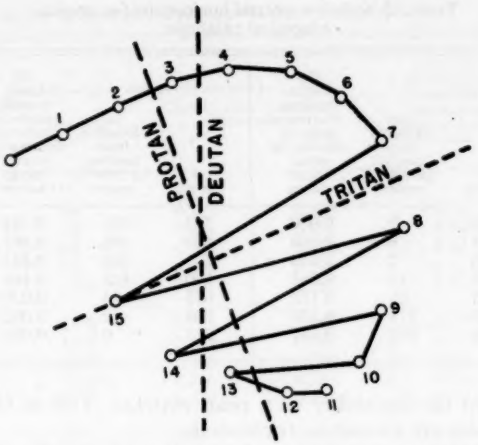

FIG. 4. Sequence of colors found by Mr. V. on the dichotomous test (see reference 28). The normal eye sees these colors (various Munsell hues at value 5/, chroma /4) in serial order (0 to 15). The kinds of confusion made by the three types of dichromat and the corresponding anomalous trichromat are indicated by dotted lines (protan, deutan, tritan).

It may be concluded that the classic view of tritanopia derived from pathological cases is that it is a reduction form of vision whose chromaticity confusions therefore may be derived from the chromaticity diagram of the standard ICI colorimetric coordinate system. These confusions are indicated by a family of straight lines co-punctal either at $x=0.18$, $y=0.00$, or at $x=0.165$, $y=0.000$, or at some intermediate point. Thus, from Fig. 1 it is seen that a retinal region rendered tritanopic by inflammation or detachment should find the spectrum between 567 and 568 mμ to have the chromaticity of standard illuminant C, that is, this part of the spectrum that appears normally greenish yellow cannot be distinguished from daylight by a tritanopic retinal area. Similarly, the yellowish color of a gas-filled incandescent lamp at a color temperature of 2900°K would be confused by a classical tritanope with the color of the spectrum at about 578 to 579 mμ. And, in general, if two color chips of known chromaticity coordinates (x, y) are represented by points on the same line of any of the family of lines passing through the copunctal point, we would expect a classical tritanope to find them to be of the same chromaticity.

III. DESCRIPTION OF A CASE OF ATYPICAL CONGENITAL TRITANOPIA

The subject of this report, Mr. V., was the father of two children, sons, one deuteranomalous and the other protanomalous. Examination of the two sons revealed only traits which are characteristic in these types. Their mother has normal color vision. The family traditions contain but one item of evidence related to color facility in the ancestry; the mother of the subject was

[16] F. H. G. Pitt, Proc. Roy. Soc. (B) **132**, 101 (1944).
[17] G. E. Müller, *Darstellung und Erklärung der verschiedenen Typen der Farbenblindheit* (Göttingen, Vandenhoeck, & Ruprecht, 1924), p. 51.
[18] D. B. Judd, J. Research Nat. Bureau of Stand. **42**, 1 (1949); *RP*1946.
[19] S. Alrutz, Psyke **10**, 1, 130 (1915).
[20] E. Hering, Pflügers Arch. f. d. ges. Physiol. **57**, 308 (1894).
[21] G. Hermann, *Ein Beitrag zur Casuistik der Farbenblindheit*, Inaug. Diss. (Dorpat, 1882).
[22] D. B. Judd, J. Opt. Soc. Am. **33**, 294 (1943).
[23] F. Richardson, Psych. Bull. **8**, 55 (1911).
[24] F. Richardson-Robertson, Amer. J. Psych. **34**, 157 (1923).
[25] E. Uhry, *Beitrag zur Casuistik der Blau-Gelbblindheit*, Diss. (Strassburg, 1894).
[26] M. von Vintschgau, Pflügers Arch. f. d. ges. Physiol. **57**, 191 (1894).
[27] G. F. Göthlin, Acta Ophthal. **21**, 88 (1943).

TABLE II. Relative spectral luminosities for atypical congenital tritanope.

λ in mμ	(a) Relative luminosities for 2900°K source	(b) Luminosities relative to unity at 580 mμ for equal-energy source	λ in mμ	(a) Relative luminosities for 2900°K source	(b) Luminosities relative to unity at 580 mμ for equal-energy source
400	0	0.000	575	691	0.994
425	0	0.000	600	636	0.807
450	2	0.010	625	385	0.423
475	12	0.043	650	165	0.161
500	66	0.173	675	33	0.030
525	175	0.370	700	2	0.002
550	396	0.687	725	0	0.000

noted for her ability as a pearl matcher. Two of his cousins are anomalous trichromats.

The congenital nature of his tritanopia is affirmed by incidents from his history as a jeweler. At the age of 21 while apprenticed to a clockmaker he could find no difference between the green and blue enamel tiles which he had been assigned to set alternately in the minute positions on a clock face. In later life his children remember being called in from play to help him distinguish emeralds from sapphires.

The subject has had no severe illnesses or accidents in his lifetime and carried on his work as a jeweler and watch repairer up to the age of 66. Regular examinations (one son is an optometrist) revealed no ocular abnormalities up to the time of our last test sessions. His lenses became cataractous two years later. Tests were made at ages of 61, 63, and 66.

1. Tests on Polychromatic Plates

The subject gave normal responses on all Ishihara, Rabkin, and American Optical Company Plates. He made no errors on a replica of the Royal Canadian Navy Lantern or the 1940 Edition of the Inter-Society Color Council Color Aptitude Test. Indeed, his performance on all tests for the detection of red-green blindness was above average.

His responses to the 1929 Stilling plates intended to detect tritanomaly were ambiguous (as they are for many normals) and indicate that the colors in these and the Rabkin tritanomalous plates were ineffectively chosen for detecting color deficiency of this subject's type. However, a polychromatic plate of the reversible figure type was constructed based on an apparent co-punctal point at 460 mμ which was effective. Two other plates, based on apparent co-punctal points at 400 and at 475, were not effective. The Munsell designations of the colors used in the successful plate are given in Table I.

2. F-M 100-Hue Test

The average of four examinations made in 1942 and 1943 with the Farnsworth-Munsell 100-Hue Test[28] is shown in Fig. 2. It indicates near-normal color discrimination between red and blue-green through neutral (medians of the error scores are at 1 and 46), between yellow and green and between purple-blue and red-purple. Confusions are indicated between greens and blues, between red-purples and yellow-reds, and between greenish yellow, neutral and bluish purple.

3. Spectral Settings

Spectral divisions were made with a high intensity projection spectroscope which used a 1000-watt projection lamp as the source and was burned at approximatley 2900°K. A spectrum was projected on a white screen along which a pointer could be moved; the transilluminated background had a luminance of 8 foot-lamberts, of the same color temperature as the source; spectral luminance at 570 mμ was about 12-foot-lamberts. Observers were asked to "set the needle at points between the colors." Figure 3 shows the averages and approximate distributions of settings made by 141 normal observers in comparison with the settings made by the subject. All spectral stimuli below 585 mμ were called "blue" by the subject (or, "blue or green- some people say one thing and some the other") and all above 588 mμ were called "red or reddish." The 586-mμ region matched the background color. The shortest wave-length at which the subject was certain of chromatic color by this method was at about 465 mμ. Special observing conditions with a dark surround gave an absolute limit of sensation at 447 or 450 mμ. This is the point at which the average normal divides blue from violet. The brilliant violet region was quite invisible to the subject. No neutral point was found as far as the subject could see in the shortwave end of the spectrum when light adapted.

4. Dichotomous Test

The subject's pattern on the Dichotomous test is that given on page 6 of the Manual[29] and is shown in

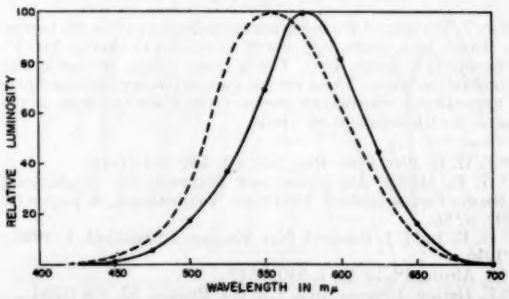

FIG. 5. Comparison of Mr. V's relative spectral luminosity function (solid curve) with that of the standard observer (dotted curve). Mr. V finds the brightest part of the equal-energy spectrum at about 580 mμ instead of the usual 555 mμ, and the spectrum seen by him is considerably cut off on the short-wave end compared to that seen by an observer with normal vision.

[28] D. Farnsworth, J. Opt. Soc. Am. 33, 568 (1943).

[29] Dean Farnsworth, *Manual of the Farnsworth Dichotomous Test for Color Blindness* (The Psychological Corporation, New York, 1947).

TABLE III. Munsell chips found by atypical congenital tritanope to have identical chromaticities in daylight.

Greenish yellow chip				Purplish chip of closest chromaticity				
Munsell production number	Munsell hue	Chromaticity coordinates (illuminant C) x	y	Munsell production number	Munsell hue	Chromaticity coordinates (illuminant C) x	y	x-intercept of the straight line connecting the points representing the two chromaticities
				Color matches found in 1943				
143	7G	0.277	0.364	162	6B	0.243	0.276	0.14
142	6G	0.280	0.370	163	7B	0.244	0.274	0.14
142	6G	0.280	0.370	164	8B	0.244	0.272	0.14
141	5G	0.283	0.373	165	9B	0.248	0.272	0.15
136	10GY	0.315	0.398	169	3PB	0.257	0.265	0.14
134	8GY	0.326	0.407	169	3PB	0.257	0.265	0.13
132	6GY	0.340	0.413	170	4PB	0.259	0.262	0.12
131	5GY	0.343	0.411	173	7PB	0.266	0.259	0.14
129	3GY	0.361	0.425	173	7PB	0.266	0.259	0.12
126	10Y	0.380	0.425	176	10PB	0.279	0.261	0.12
123	7Y	0.401	0.431	178	2P	0.289	0.266	0.11
122	6Y	0.406	0.431	179	3P	0.295	0.269	0.11
121	5Y	0.411	0.434	180	4P	0.296	0.267	0.11
118	2Y	0.425	0.425	184	8P	0.316	0.273	0.12
117	1Y	0.426	0.421	185	9P	0.321	0.275	0.12
116	10YR	0.427	0.413	188	2RP	0.334	0.282	0.13
115	9YR	0.429	0.407	187	1RP	0.330	0.278	0.12
114	8YR	0.431	0.401	185	9P	0.321	0.275	0.08
111	5YR	0.423	0.382	190	4RP	0.350	0.290	0.12
110	4YR	0.428	0.376	192	6RP	0.354	0.291	0.10
107	1YR	0.418	0.357	194	8RP	0.363	0.295	0.10
								Mean 0.12
								PE Mean 0.0025
				Color matches found in 1945				
141	5G	0.283	0.373	165	9B	0.248	0.272	0.15
140	4G	0.290	0.383	164	8B	0.244	0.272	0.13
139	3G	0.297	0.386	164	8B	0.244	0.272	0.12
137	1G	0.308	0.393	163	7B	0.244	0.274	0.10
137	1G	0.308	0.393	164	8B	0.244	0.272	0.10
137	1G	0.308	0.393	165	9B	0.248	0.272	0.11
136	10GY	0.315	0.398	165	9B	0.248	0.272	0.10
134	8GY	0.326	0.407	167	1PB	0.252	0.267	0.11
133	7GY	0.333	0.409	168	2PB	0.254	0.266	0.11
133	7GY	0.333	0.409	169	3PB	0.257	0.265	0.12
132	6GY	0.340	0.413	170	4PB	0.259	0.262	0.12
131	5GY	0.343	0.411	170	4PB	0.259	0.262	0.11
131	5GY	0.343	0.411	171	5PB	0.263	0.265	0.12
129	3GY	0.361	0.425	172	6PB	0.265	0.263	0.11
129	3GY	0.361	0.425	173	7PB	0.266	0.259	0.12
127	1GY	0.373	0.428	174	8PB	0.271	0.261	0.11
126	10Y	0.380	0.425	175	9PB	0.277	0.263	0.11
126	10Y	0.380	0.425	176	10PB	0.279	0.261	0.12
124	8Y	0.394	0.427	177	1P	0.286	0.268	0.10
123	7Y	0.401	0.431	178	2P	0.289	0.266	0.11
121	5Y	0.411	0.434	179	3P	0.295	0.269	0.10
119	3Y	0.422	0.428	181	5P	0.302	0.271	0.10
119	3Y	0.422	0.428	182	6P	0.309	0.274	0.11
116	10YR	0.427	0.413	183	7P	0.313	0.271	0.10
116	10YR	0.427	0.413	184	8P	0.316	0.273	0.10
116	10YR	0.427	0.413	185	9P	0.321	0.275	0.11
115	9YR	0.429	0.407	186	10P	0.323	0.275	0.10
114	8YR	0.431	0.401	187	1RP	0.330	0.278	0.10
113	7YR	0.429	0.392	187	1RP	0.330	0.278	0.09
113	7YR	0.429	0.392	188	2RP	0.334	0.282	0.09
112	6YR	0.427	0.386	189	3RP	0.340	0.285	0.09
								Mean 0.11
								PE Mean 0.0015

Fig. 4 on a projective transformation of the ICI chromaticity diagram.

The serial order, 14, 9, 10, 13, 12, 11, produces a pattern somewhat counterclockwise of what would be expected from classical tritanopia[10] if no allowance were made for such individually variable factors as ocular pigmentation.

5. Luminosity Function

The subject's luminosity data were taken in 1948. By using the same instrument, the luminance of a test patch of the source was equated to those of stimuli of selected wave-lengths from 400 to 725 mμ. The surround of the test patches was black, room illumination dim. The patches were small, each subtending 1° by 1.5° visual angle. Variable instrument errors could have amounted to as much as 3 mμ, and no corrections were applied for possible variations of transmittance of the spectroscope with wave-length. Luminance reduction was accomplished by the use of Wratten filters which are accurate to about five percent of their densities. Values were obtained by hetero-chromatic matching. When the data are examined these sources of possible error should be remembered.

Table II gives the average of four readings for relative luminance per unit wave-length in column (*a*), calculated for an equal-energy source and adjusted to unity at the maximum value in column (*b*). The latter figures are plotted in Fig. 5 in comparison with the standard luminosity curve.

Regardless of uncertainties in the data there were three unequivocal results outside the range of experimental error, (a) a decided depression of the short-wave side of the curve was found, (b) the luminosity peak shifted about 20 mμ in the long-wave direction compared to the standard luminosity curve and (c) a perfect chromatic match was obtained for the background near the peak of the curve. This latter was repeatedly verified; the subject was very sensitive to a 2-mμ change in either side of the 586-mμ region, always recognizing one as bluish, the other as reddish.

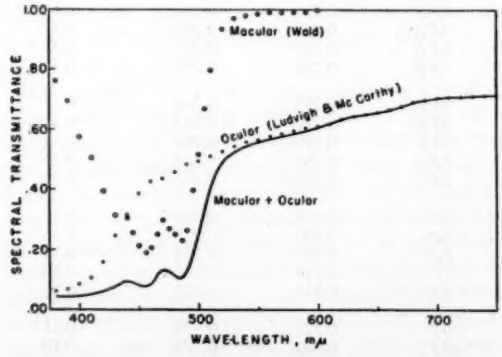

FIG. 6. Spectral transmittance of the ocular media (cornea, lens, humours) according to Ludvigh and McCarthy (see reference 31) (dots), and spectral internal transmittance of the macula lutea (circles) according to Wald. (See reference 30.) The curve shows the product of these two spectral transmittances and for the normal eye is our best estimate of the ratio of the radiant flux incident upon the fovea to that incident on the cornea so as to pass through the pupil from a source at the fixation point.

6. Contiguous Matches

Matches were made with circular disks of Munsell papers under Macbeth daylight lamps approximating illuminant *C*, with color temperatures averaging about 6400°K. The visual angle subtended by each disk was approximately 3°. One of the matching disks could be tilted to the incident light until a brightness match was obtained. Many sets of Munsell papers were used, embracing both high and low chromas at several value levels and all gave comparable results. However, the 100-hue series gave the most reliable data because the small color interval between steps supplied an almost continuous hue series against which to match; see Table III.

When the matching chromaticities from the 5/5 series were plotted on (x, y) diagrams and the points connected by straight lines the extensions intersected closely, in 1943 near $x=0.180$, $y=0.100$ and in 1945 near $x=0.155$, $y=0.075$. Other sets of matches gave similar results but with more scatter of the intersections.

Although these reports by Mr. V. correspond in an approximate way to typical acquired tritanopia, they differ from classical tritanopia in three respects. In the first place, plot of the pairs of points specified as near chromaticity matches in Table III and connection of the members of each pair by a straight line on the (x, y)-chromaticity diagram fail to yield a family of straight lines intersecting at a point intermediate be-

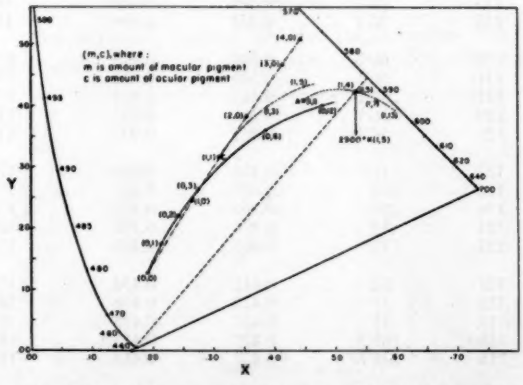

FIG. 7. Changes in chromaticity produced by various multiples of the normal macular and normal ocular pigmentation. The point (0, 0) corresponds to the chromaticity of standard source *C* viewed by a pigment-free but otherwise normal eye. The point (1, 1) corresponds to source *C* for the standard observer; the point *A* (1, 1) corresponds to source *A* for the standard observer. Note from the dotted straight line that the classical tritanope with normal macular pigment and 5 times normal ocular pigmentation would find an incandescent lamp at a color temperature of 2900°K to have the same chromaticity as the spectrum at 586 mμ.

tween $x=0.165$, $y=0.000$ and $x=0.18$ and $y=0.00$. Instead the x-intercepts average 0.12 for the 1943 matches (see last column, Table III) and 0.11 for the 1945 matches. In the second place the part of the spectrum having the same chromaticity as a tungsten-filament lamp of color temperature 2900°K is not between 578 and 579 mμ, but is at 586 mμ. And in the third place, Mr. V. could not see the spectrum at the short-wave end much below 450 mμ; but an area of the retina rendered tritanopic by disease has a luminosity function not significantly different from normal and in the usual spectroscope will easily serve to detect light of wave-length less than 420 mμ. It is concluded, therefore, that Mr. V., if tritanopic at all, must be classed as atypically tritanopic. Furthermore, there is an indication from the x-intercepts (odds 50 to 1 against a pure chance explanation), that Mr. V's color-vision system changed in a two-year interval still further from classical tritanopia.

IV. INFLUENCE OF OCULAR PIGMENTATION ON TRITANOPIC CONFUSIONS

The first two ways in which Mr. V's reports depart from classical tritanopia suggest that his eye media have more than the usual yellow pigmentation. His failure to respond to the short-wave end of the spectrum might be expected because of absorption of an abnormally high proportion of such energy by a heavy pigmentation of the ocular media. Furthermore, the chromaticity of an incandescent lamp at a color temperature of 2900°K, represented for the ICI standard observer at $x=0.444$, $y=0.406$, would for a heavily pigmented eye be shifted toward the long-wave end of the spectrum and might be representable by a point falling on the line connecting the tritanopic co-punctal point with that representing 586 mμ as found by Mr. V. However, the changes in the chromaticity confusions between object colors caused by making the classical tritanope view them through an amber filter, such as one corresponding to some multiple of the normal pigmentation of the eye media, are complicated. They cannot be determined precisely unless the spectral transmittances of the amber filter, and the spectral reflectances of the objects viewed are both known.

There are two principal pigments in the ocular media. One of these is a melanin type pigment that gathers gradually in the normal crystalline lens as the subject grows older. The other is the macular pigment suffusing the retina in a central spot subtending 3 or 4° identified by Wald with a high degree of probability as xanthophyll.[30] Figure 6 shows (circles) the spectral internal transmittance of the macular pigment according to Wald, and it also shows (dots) the spectral transmittance of the refractive media of the eye according to the measurements of Ludvigh and McCarthy for an average age of 21.5 years.[31] Even at this comparatively low age the absorption of light by the refractive media of the eye is due chiefly to the pigmentation of the crystalline lens. The solid curve on Fig. 6 is the product of the spectral internal transmittance of the macular pigment by the spectral transmittance of the refractive media of the eye, and it represents the spectral transmittance of the macular and ocular pigments combined.

Figure 7 shows on the (x, y)-chromaticity diagram of the standard ICI system the chromaticity changes

TABLE IV. Chromaticity coordinates of 18 of the Munsell 5/5 papers illuminated by standard illuminant *C* and viewed through an amber filter equivalent to 5 times the normal pigmentation of the refractive media of the eye (see Fig. 6).

Munsell production number	Nominal Munsell hue	Chromaticity coordinates (Illuminant *C* combined with 5 times normal lens pigment) x	y
110	4*YR*	0.532	0.418
114	8*YR*	0.524	0.432
117	1*Y*	0.513	0.447
121	5*Y*	0.497	0.462
126	10*Y*	0.474	0.469
130	4*GY*	0.451	0.479
136	10*GY*	0.422	0.476
138	2*G*	0.410	0.477
141	5*G*	0.398	0.468
164	8*B*	0.375	0.422
166	10*B*	0.385	0.419
169	3*PB*	0.397	0.415
172	6*PB*	0.409	0.415
175	9*PB*	0.428	0.409
180	4*P*	0.454	0.403
183	7*P*	0.473	0.400
188	2*RP*	0.493	0.398
193	7*RP*	0.513	0.393

TABLE V. Standard relative luminosity function, $\bar{y}_\lambda$, for equal-energy spectrum adjusted to accord with ocular pigmentation 6 times that found by Ludvigh and McCarthy for young normally pigmented eyes.

Wave-length in mμ λ	Standard relative luminosity (*ICI* obs.) $\bar{y}_\lambda$	Spectral transmittance of normal ocular media T_λ	Relative spectral luminosity: Standard eye with 6 times normal ocular pigment $T_\lambda{}^6\bar{y}_\lambda/(T_\lambda{}^6\bar{y}_\lambda)_{max}$	Relative spectral luminosity: Observed for Mr. V (From Table II)
400	0.0004	0.086	0.000	0.000
425	0.0073	0.204	0.000	0.000
450	0.0380	0.388	0.005	0.010
475	0.1126	0.448	0.031	0.043
500	0.3230	0.495	0.150	0.173
525	0.7932	0.534	0.533	0.370
550	0.9950	0.566	0.889	0.687
575	0.9154	0.588	0.994	0.994
600	0.6310	0.610	0.820	0.807
625	0.3210	0.636	0.515	0.423
650	0.1070	0.657	0.203	0.161
675	0.0232	0.683	0.053	0.030
700	0.0041	0.705	0.011	0.002

[30] G. Wald, Science **101**, 653 (June 29, 1945).

[31] E. Ludvigh and E. F. McCarthy, Arch. Ophthal. **20**, 37 (July, 1938).

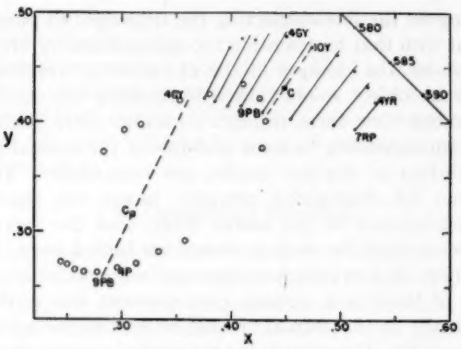

FIG. 8. Effect of increasing ocular pigmentation by a factor of 5. The chromaticities of certain of the Munsell papers (value 5/, chroma /5) illuminated by standard source C are shown on the (x, y)-chromaticity diagram both for direct observation by the standard observer (circles), and for observation through a filter having 4 times the yellowish pigmentation of the normal ocular media (dots). The straight lines coursing among these points are drawn so as to pass through the co-punctal point (x=0.165, y=0.000) of the classical tritanope. Note that interposition of the yellow filter causes different pairs of Munsell papers to be confused by the classical tritanope; for example, the pair *9PB-4GY* is changed nearly to *9PB-10Y*.

produced by viewing standard illuminant C (representative of average daylight) through various multiples of the normal amounts of macular and ocular pigmentation represented in Fig. 6. The chromaticity coordinates of these points have been computed by a routine method (summation over wave-length intervals of 10 mμ). The usual location of the point representing illuminant C (x=0.3101, y=0.3163) is considered to correspond to the normal amount both of macular and of ocular pigmentation. It is identified by the pigment notation (1, 1). The chromaticity corresponding to removal of both these amounts is notated (0, 0); this corresponds to the pigment-free or albino eye. The chromaticity corresponding to the normal amount of macular pigment and zero amount of ocular pigment is notated (1, 0). And, in general, the notation is (m, c), where m is the multiple of the normal macular pigment to which the computations apply, and c is the multiple of the normal ocular pigment.

It will be noted from Fig. 7 that the chromaticity changes corresponding to increasing the amount of macular pigment change the long-wave tritanopic neutral point only slightly. This may be seen from the fact that the line connecting them is nearly parallel to the straight lines passing through the tritanopic copunctal point shown on Fig. 7 as x=0.165, y=0.000. The chromaticity changes corresponding to increase in the amount of lens pigment, however, are such as to increase considerably the long-wave tritanopic neutral point. This may be seen from the curvature of the solid line on Fig. 7. These chromaticity differences between the influence of the macular and ocular pigments arise, of course, from their differing spectral characteristics (see Fig. 6). Oddly enough, the influence of the normal amount of macular pigment is closely the same as the influence of three times the normal amount of ocular pigment, but thereafter there is an increasing divergence between the two loci; compare the solid line on Fig. 7 with the dot-dash line. We cannot look for an explanation of the abnormally high wave-length of Mr. V's neutral point (586 mμ for 2900°K instead of 578 mμ) in terms of abnormally heavy macular pigment. A plausible explanation could rest on abnormally heavy lens pigment, since it is believed that the greatest change in pigmentation with age occurs in the lens and Mr. V's age was over 60 when first tested.

The dotted line on Fig. 7 passing through the point representing standard illuminant A (x=0.4476, y=0.4075) shows the results of similar computations with normal macular pigmentation for increasing amounts of ocular pigment. It is seen that at five times normal ocular pigment, the classical tritanope would expect to find illuminant A (color temperature of 2854°K) identical in chromaticity to the spectrum at about 586.5 mμ, and a lamp at a color temperature of 2900°K would correspond to 586 mμ; see point x close to the intersection of the curved dotted line with the straight dotted line passing through the co-punctal point and the spectrum locus at 586 mμ. We have, therefore, sought an explanation of Mr. V's atypical chromaticity matches between the various Munsell chips in terms of classical tritanopia modified by five times the normal ocular pigment of a young eye.

The chromaticities of the Munsell papers of value 5/ and chroma /5, used for testing Mr. V. have already been published for standard illuminant C by Granville,

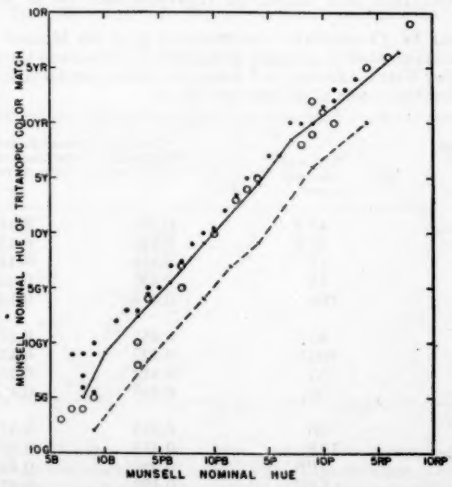

FIG. 9. Comparison of Mr. V's chromaticity matches (circles and dots) with those of the classical tritanope (dotted line) and with those of the classical tritanope having 5 times normal ocular pigmentation (solid line). Note that Mr. V's 1943 observations (circles) correspond to the classical tritanope with about 5 times normal ocular pigmentation, and his 1945 observations correspond to about 6 times normal ocular pigmentation.

Nickerson and Foss;[32] see their Table III. The chromaticities of 18 of the same papers have been computed for illuminant C combined with 5 times normal lens pigment by 10 mμ summation from unpublished spectral reflectances of those papers supplied to us through the courtesy of Granville, Nickerson and Foss. Table IV gives these chromaticity coordinates (x, y).

Figure 8 compares the chromaticities of 18 of these Munsell papers of value 5/ and chroma /5 both for illuminant C (circles) and for illuminant C screened through 5 times the normal lens pigment (dots). The influence of interposing a filter of five times the normal lens pigment (spectral transmittances shown in Fig. 6) on the chromaticity of illuminant C is shown by comparing the location of the open square with that of the solid square. This is the same comparison shown on Fig. 7 between the notations (1,1) and (1,5). The chromaticity points of the Munsell papers all undergo fairly similar shifts except that the points representing blue and purple colors shift somewhat more than the others. The result is that the Munsell 5/5 locus is not only shifted toward the reddish yellow but shortened in the blue-yellow direction and rotated slightly counterclockwise. Because of this rotation straight lines through the copunctal point ($x=0.165$, $y=0.000$) connect different pairs of Munsell papers; see straight lines drawn on Fig. 8. For example, the dotted lines on Fig. 8 indicate that a classical tritanope should find the paper of nominal Munsell hue $9PB$ nearly the same chromaticity as $4GY$ if they are both illuminated by illuminant C, but if the classical tritanope views them through an amber filter corresponding to five times the normal lens pigment he would instead find $9PB$ closely similar to $10Y$.

V. COMPARISON OF ATYPICAL TRITANOPE WITH A HEAVILY PIGMENTED CLASSICAL TRITANOPE

Table V gives values for the standard luminosity curve for an equal-energy spectrum and for the same values adjusted to six times the absorbance of normal ocular pigment which corresponds to the prediction for Mr. V's eyes at the time his luminosity curve was taken in 1948. Comparison of these predicted values with those in Table II found by actual observation shows good agreement.

Mr. V. found that a lamp of color temperature 2900°K had the same chromaticity as the spectrum at 586 mμ. Since we found the multiple of normal lens pigment to be 5 by this criterion, in this respect there is perfect agreement between the actual and theoretical observer.

The pairs of Munsell 5/5 papers that yield equivalence for the theoretical observer can be read with an uncertainty of less than one Munsell hue step from the straight lines drawn on Fig. 8 so as to pass through the tritanopic copunctal point ($x=0.165$, $y=0.000$). These can be compared conveniently with the chromaticity matches found by Mr. V. by plotting for each pair of papers the Munsell nominal hue of the paper found to match against the Munsell nominal hue of the first paper of the pair; see Fig. 9. The circles represent the pairs found by Mr. V. in 1943; the dots, those found in 1945, both taken from Table III. The chromaticity equivalences for the theoretical observer (classical tritanope with five times the normal lens pigment) are shown by the solid line, and those for the classical tritanope with normal macular and lens pigment are shown by the dotted line. It is seen that the chromaticity matches found among the Munsell 5/5 papers by Mr. V. do depart significantly from those of the classical tritanope with normal pigment, but that the 1943 matches are closely what would be expected from a classical tritanope with five times the normal lens pigment. In other words if lines were drawn on Fig. 8 to indicate Mr. V's chromaticity confusions the x-intercepts based on the circles would average 0.12 as shown in Table III but the x-intercepts based on the theoretical removal of 5 times normal lens pigment (dashed line) would average close to 0.165 in agreement with classical tritanopia. The 1945 matches, as was seen from the x-intercepts in Table III, depart from the classical tritanope even more than the 1943 matches, and apparently (from Fig. 9) correspond closely to what would be expected of the classical tritanope with six times normal lens pigment.

It is our interpretation, therefore, that our congenital tritanope is atypical almost wholly because of an abnormally heavy pigmentation of the lens. We would classify Mr. V. as a case of tritanopia with abnormally heavy ocular pigmentation.

VI. DISCUSSION

It is worth pointing out that although we have used the tritanopic co-punctal point ($x=0.165$, $y=0.000$) required by the Müller theory of vision[17,18] as the basis for this analysis, the case could have been analysed with equal success on the basis of the tritanopic co-punctal point indicated by König's observations on nine cases of acquired tritanopia.[8] This basis would have resulted in finding somewhat more than five times normal lens pigment for the 1943 measurements by Mr. V., and somewhat more than six times normal lens pigment for the 1945 measurements. Therefore, we cannot decide between these two theoretical evaluations of the co-punctal point from our study of Mr. V. To yield an improved determination of the co-punctal point characteristic of tritanopia will require the reports of tritanopes whose ocular media are normally transparent.

[32] W. C. Granville, D. Nickerson, and C. E. Foss, J. Opt. Soc. Am. 33, 376 (1943).

JOURNAL OF THE OPTICAL SOCIETY OF AMERICA VOLUME 40, NUMBER 12 DECEMBER, 1950

Three-Line Method of Obtaining Characteristic Curves for Heterochromous Photometry

MILTON GREEN
Signal Corps Engineering Laboratories, Fort Monmouth, New Jersey
(Received April 12, 1950)

By employing three homologous spectrum lines, two in one wave-length range, and a third in the second wave-length range, it is possible to construct the two characteristic curves for heterochromous photometry. Spectra containing the three lines are recorded, at several levels of density, on the photographic emulsion to be calibrated. This provides data for a homochromous and a heterochromous preliminary curve. Calibration curves are constructed in the usual manner from these two preliminary curves.

INTRODUCTION

THE internal standard method of quantitative spectrochemical analysis requires the determination of the intensity ratio of two spectrum lines, namely, the ratio of the intensity of the analysis line to the intensity of the internal standard line. Often the logarithm of the intensity ratio may be employed instead of the intensity ratio itself. If the two lines differ very little in wave-length only a local calibration of the photographic emulsion is necessary. However, when the two lines, the relative intensities of which are to be determined, lie in different regions of the spectrum, the problem is slightly more complicated. In some cases this problem can be solved by choosing a type of photographic emulsion for which the gammas of the two wave-length regions are approximately the same. Polychrome and SAII films and plates satisfy this condition to some degree, in that their gammas vary very little over fairly long ranges of wave-length. However, at the present time not all problems in heterochromous photometry can be solved by this method. Furthermore, many spectrographers are willing to sacrifice the near uniformity in the gamma of some types of emulsions in favor of other desirable properties which are not found in SAII or polychrome emulsions, but which are found in such emulsions as that of SAI films and plates.

EXISTING METHODS

Several methods for heterochromous photometry have appeared in the literature.[1,2] Existing methods are based on the local (homochromous) calibrations, plotted in the usual manner (density *versus* $\log_{10}I$) for the two wave-length regions involved. The two curves are plotted on the same sheet of graph paper and they can cross at any arbitrary point but the relative positions must be maintained when referring to analytical curves derived from them. In so far as heterochromous photographic-photometry is concerned, these methods will give correct results provided the "calibration-intensity-ratios"* (hereafter referred to as C.I.R.) are accurately known so that on the calibration curves, intensities are actually plotted to the base 10 or some common logarithmic base. C.I.R.'s are generally accurately known in the step-sector, inverse square law and constant intensity light source methods, but these methods have certain disadvantages[3] as compared to the two-line[3] and the two-step weakener methods. However, in the latter two methods the spectrographer does not always know the exact value of the C.I.R., and in some laboratories calibration curves are constructed in which its value is never used. They accomplish this by plotting the calibration curve with $\log_F I$ as abscissa (instead of $\log_{10}I$), where F is the C.I.R.; and by plotting the analytical curve with $\log_F R$ as abscissa, where R is the intensity ratio of the analysis to the internal standard line. Thus, the spectrographer can employ the two-line or two-step weakener method for homochromous photometry without knowing the value of the C.I.R. But this is not necessarily true for heterochromous photometry. The reason is that both calibration curves will generally not have a common logarithmic base.† In the three-line method this difficulty is obviated in that three homologous lines are employed and the calibration is made in terms of the logarithm whose base is the intensity ratio of the homochromous homologous pair.

THE THREE LINES

Restrictions on the three lines employed are:

1. They must be homologous.
2. The three-lines must consist of a homochromous and a heterochromous pair of lines, one line being common to both pairs.
3. The homochromous pair must satisfy the same conditions as are required in the two-line method[3] of homochromous photometry.
4. For some exposure of their photographed spectra the transmittances of the heterochromous pair should be

[1] G. H. Dieke, "Progress report on a study of standard methods for spectrographic analysis," No. W-128-26-28 (October, 1944).
[2] R. A. Burdett and L. C. Jones, J. Anal. Chem. **19**, 238 (1947).
* Calibration-intensity-ratio is defined as the fixed or constant intensity ratio provided by the calibration method, such as, the intensity ratio of the homologous pair of lines employed in the two-line method, the step-ratio of a two-step weakener; the ratio of the openings between two successive steps of a logarithmic sector, etc.

[3] J. R. Churchill, Ind. Eng. Chem. Anal. Ed. **16**, 653 (1944).
† Use of the two-step filter method will fulfil this condition (provide a common C.I.R. and hence a common logarithmic base for both calibration curves) if it is neutral for the wave-lengths involved. There are commercially available two-step weakers which are approximately neutral over a considerable wave-length range. These are of monel or aluminum evaporated on quartz.

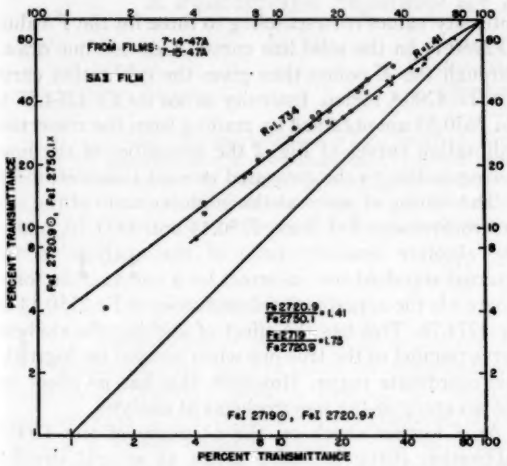

FIG. 1. Preliminary curves in 2700A region. Two sets of homologous lines are employed because the data of one set was not sufficient to cover the entire density range desired.

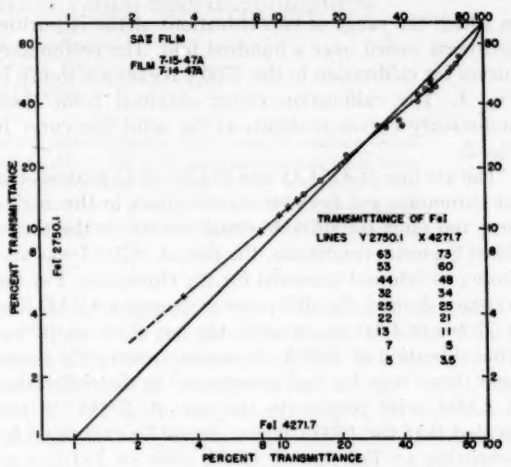

FIG. 3. Heterochromous preliminary curve for 2700A and 4200A wave-length region. FeI 2750.14 and FeI 4271.76 are employed as homologous pair. It is assumed that the intensity ratio of this line pair is one. Transmittance values for which the heterochromous pair have equal intensities are tabulated at right and are taken from the curve.

the same, preferably between five- and sixty-percent transmittance.

THE METHOD

The three-line method for obtaining the characteristic curves for the two different spectral regions can best be demonstrated by the following example:

Some time ago the author was called upon to analyze quantitatively for impurities in a solution of zinc chloride and ammonium chloride used in the fabrication of dry cell batteries. The impurities found in the solution were calcium, cadmium, chromium, copper, iron, magnesium and nickel. The arc spectrum zinc line at 2670.53A was employed as the internal standard for the analysis of the above mentioned impurity elements. The spectra of both standard solutions and unknown were photographed on SAII film which was calibrated by the two-line method in the 2700–2800 wave-length region employing as line pair, the FeI lines at 2720.90 and 2750.14 for which the intensity ratio is approximately 1.41. The line pair 2719.02 and 2720.90 was used to supplement the line pair 2720.90 and 2750.14 in establishing the final calibration curve because the data of the first set was insufficient to cover the entire density range desired. The gradation in density for this purpose was obtained from the spectra of the standard solutions

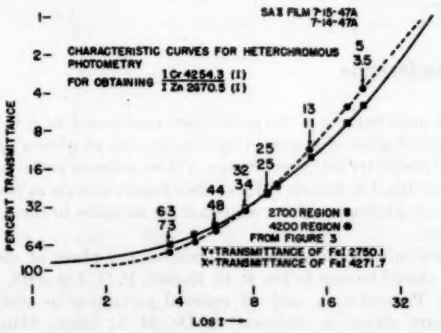

FIG. 2. Characteristic calibration curves for 2700A and 4200A wave-length regions arranged for heterochromous photometry. The paired numbers are transmittance values for which spectral lines at 2700A and 4200A have equal intensity and hence the same abscissa. The upper number of each pair corresponds to the 2700A region and the lower to the 4200A region. These numbers are derived from the heterochromous preliminary curve shown in Fig. 3. This data permits the construction of the characteristic curve for the wave-length region at 4200A.

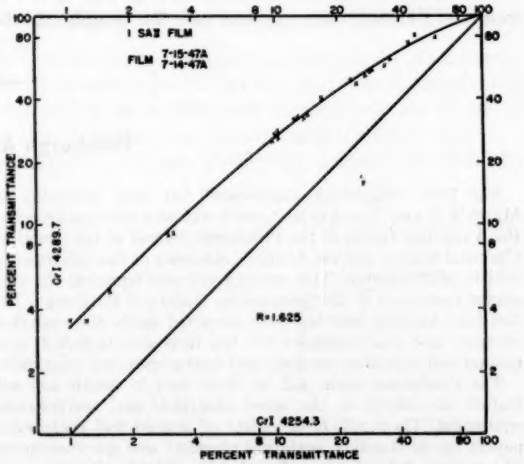

FIG. 4. Preliminary curve 4200A region. Used to check the accuracy of the characteristic curve of the 4200A region derived from the heterochromous preliminary curve of Fig. 3. All points of this preliminary curve give an approximate intensity ratio of 1.62 when measured from the dotted curve of Fig. 2, thus, indicating good agreement.

in which the range of concentrations of the impurities had been varied over a hundred fold. The preliminary curves for calibration in the 2700A region are shown in Fig. 1. The calibration curve obtained from these preliminary curves is shown as the solid line curve in Fig. 2.

The arc line at 4254.35 was employed as analysis line for chromium and because the zinc lines in this region were too faint for suitable densitometry at the established exposure conditions, the line at 2670.53 was also chosen as internal standard for the chromium. For the accuracy desired, the difference in gamma for SAII film at 2700 and 4200 necessitated the use of an additional film calibration at 4200A. To assure consistency (same logarithmic base for log$I$ coordinate) in the calibration at 4200A with respect to the one at 2700A, it was decided that the 4200A region should be calibrated by comparing an FeI line at 4200A with an FeI line at 2700A, that is, a pair of FeI lines were selected for which the intensity ratio was considered to be constant for all arc-excited exposures. The lines selected (the heterochromous pair) were the arc lines of iron at 2750.14 and 4271.76. The purpose of the heterochromous preliminary curve, Fig. 3, is to determine more accurately the corresponding percent transmittances of the two lines (exposure time remaining constant) for different levels of intensity. The calibration curve at 4200A, which is shown as the dotted line in Fig. 2, is established in the following manner. The intensity ratio of the two heterochromous lines is assumed to be unity and the percent transmittance values of FeI 4271.76 corresponding to various percent transmittance values of FeI 2750.14 are read from Fig. 3. The pairs of values thus obtained are listed as the X and Y values respectively in the table on Fig. 3. Referring now to Fig. 2, the X values (T4271.7) are plotted on the graph at the intensity values corresponding to those for the Y values (T2750.1) on the solid line curve. A dotted line drawn through the X points then gives the calibration curve for the 4200A region. Intensity ratios for Cr 4254.35 to Zn 2670.53 are obtained by reading from the respective calibration curves of Fig. 2 the intensities of the lines corresponding to the measured percent transmittances.

The setting of unity as the intensity ratio of the two heterochromous FeI lines, 2750.14 and 4271.76, makes the absolute intensity ratio of the analysis to the internal standard line incorrect by a constant factor r, where r is the actual ratio of intensities of Fe 2750.14 to Fe 4271.76. This has the effect of shifting the analysis curve parallel to the true one when plotted on logarithmic coordinate paper. However, this has *no* effect on the accuracy of the spectrochemical analysis.

As a further check on the accuracy of the 4200A calibration curve intensity ratios at several density levels of the two CrI lines at 4254.35A and 4289.72A were determined from the curve, the spectra of the standard solutions again providing the gradation in density. The intensity ratios thus obtained were found to be approximately equal in value namely 1.62. (See Fig. 4.)

CONCLUSIONS

A method is described for heterochromous photometry which eliminates the need for auxiliary calibration equipment such as a step-sector, step-weakener, optical wedge or constant intensity light source. This method retains for heterochromous photometry the advantages that the two-line[3] method has over others in homochromous photometry. The method can be extended to as many wave-lengths regions as desired by employing an additional heterochromous homologous line for each additional wave-length range.

Pittsburgh Annual Conference

The 1951 "Pittsburgh Conference" has been scheduled for March 5, 6, and 7; and as last year it will be a joint conference of the Analytical Group of the Pittsburgh Section of the American Chemical Society and the Annual Conference of the Spectroscopy Society of Pittsburgh. This meeting will also represent the 10th annual conference of the Spectroscopy Society of Pittsburgh. The first joint meeting, held last year, attracted nearly 800 analytical chemists and spectroscopists for the three-day technical symposium and exposition of analytical instruments and equipment.

The Conference again will be three days in length and will feature an exhibit of the latest analytical and spectroscopic equipment. There will be a variety of invited and contributed papers by outstanding analytical chemists and spectroscopists. The program is being planned so that it will be possible to attend those papers of similar interest with a minimum of conflicts resulting from concurrent sessions.

The main purpose of this preliminary announcement is to invite the contribution of papers. Contributions on all phases of analytical chemistry and spectroscopy will be welcome and contributors are urged to submit titles of their papers as soon as possible. Later on, abstracts will be requested for inclusion in the printed program.

Contributions and communications on any phase of spectroscopy should be sent to Dr. R. G. Russell, P. O. Box 2038, Pittsburgh, Pennsylvania, and all material pertaining to analytical chemistry should be addressed to Dr. M. L. Moss, Aluminum Research Laboratories, New Kensington, Pennsylvania. Papers involving both spectroscopic and analytical interest or on other subjects may be sent to either address. Only papers submitted to Dr. Moss or papers pertaining to non-spectroscopic analytical chemistry will require A. C. S. publication clearance.

A Photometric Separator for Precision Visual Spectrophotometry

J. TERRIEN AND F. DESVIGNES
Institut d'Optique, Paris, France
(Received July 14, 1950)

The photometric separator here described, illuminated by monochromatic light, enables accurate visual measurements of the transmission factors of parallel plates to be made. The geometrical design has been developed to eliminate systematic errors. The scale of densities depends upon Talbot law. Within the uncertainties of visual settings, the results of measurements are in very good accordance with those obtained from the best available photoelectric methods. Improvements are possible with a larger monochromator.

INTRODUCTION

THE determination of transmission factors for monochromatic light of plates having planes and non-diffusing parallel faces is one of the simplest measurements in spectrophotometry. However, it still remains a rather delicate problem, and experiment shows that an accurate and exact result requires rigorous precautions.

The Institut d'Optique uses for this purpose a visual instrument called the "photometric separator." Preceded by a monochromator, it constitutes a spectrophotometer particularly well-adapted to this kind of measurement. This apparatus, of a design suggested by P. Fleury, has been developed after a long study on a prototype; it now gives excellent results, and it is the purpose of this note to describe it.

GENERAL PRINCIPLES

1. Luminosity and Geometrical Definition of the Beams

When using an instrument for visual photometry in which the photometric balance is controlled by observation of a Lummer prism, it is necessary to obtain the brightest possible field of view in order to extend the usable spectral range to the extremities of the visible spectrum, where the luminosity factor becomes small. This condition involves the elimination of any diffusing screen; an image of the light source (in the actual case, an image of the exit slit of the monochromator) must be focused on the observer's eye pupil. It is essential that the uncontrolled movements of the eye (which may restrict the light beam emerging from the instrument) should alter the luminance of both comparison fields equally.

The light source associated with the monochromator must be very intense, and it is desirable to use occasionally a source such as the mercury arc which is of high intensity but unsteady; then the ratio of both comparison surfaces must remain constant when the distribution of intensity in the light source changes.

In order to fulfill these conditions, both beams (each of which illuminates one of the fields of the Lummer cube) must originate by division of the same beam; we use for this purpose an oblique semitransparent plate. It is also essential that the cube, in recombining the partial beams, should superpose them in position and direction exactly as before separation.

The following description explains the geometrical conditions which result from these circumstances, and how these conditions were fulfilled.

2. Quality of the Photometric Comparison Surfaces

The accuracy of visual matching in the photometric field depends largely upon the sharpness of the dividing line, which must disappear in the condition of photometric balance. One cannot easily achieve this in a photometer without a diffusing screen. This difficulty

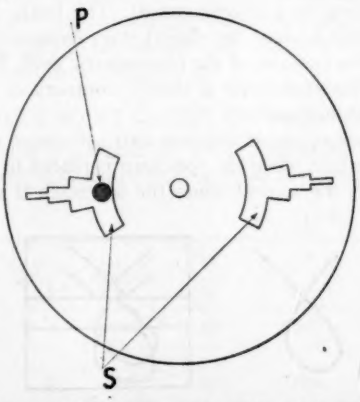

FIG. 1. Shape of the openings of the Talbot disk. The densities are determined by geometric measurements; their values are approximately in the proportions of 0.5−1.0−1.5−2.0.

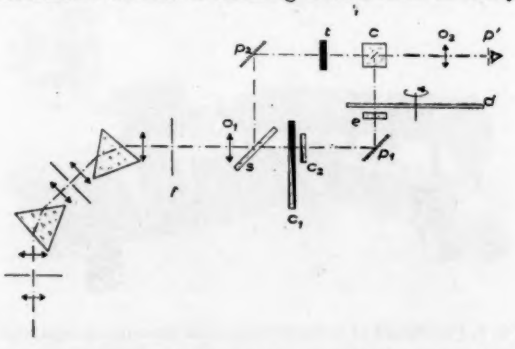

FIG. 2. Schematic diagram of the spectrophotometric scheme, including monochromator. Mirror P_1 reflects measuring beam and P_2 reflects comparison beam.

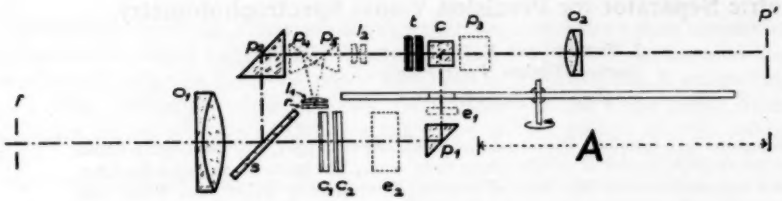

FIG. 3. Scale drawing of photometric separator. Part "A" is actually folded perpendicular to plane of drawing by prism P_3.

arises from large angle diffraction phenomena; even for a good cube, with surfaces limited by a very sharp line, it is necessary to adjust the direction of the entrance slit constituting the light source (a vertical one in the actual case) to be perpendicular to the direction of the dividing line (which must then be horizontal). This condition alone is not sufficient; the image of the slit, which is focused on the eye pupil, must be definitely longer than the diameter of this pupil. A separate study[1] has indicated the smallest dimensions which are possible.

3. Necessity of Short Beams

The insertion of plane-parallel specimens, or of the various neutral absorbing glass plates, into the light paths must not alter the main geometrical adjustments; this involves placing the specimen into a beam where the images of the pupils are infinitely distant, but this leads to a geometrical difficulty. Since the entrance slit must be long enough to limit the diffraction effects of the Lummer cube, the parallel beams issuing from the extreme points include an appreciable angle, and the length of these beams must be reduced in order to avoid the possibility of restriction by the optical elements which receive them. This imposes a very compact mounting on the design.

All the above considerations are quite general and would be valid for most visual photometers without a diffusing screen. In applying them to other instruments the results have proven equally applicable.

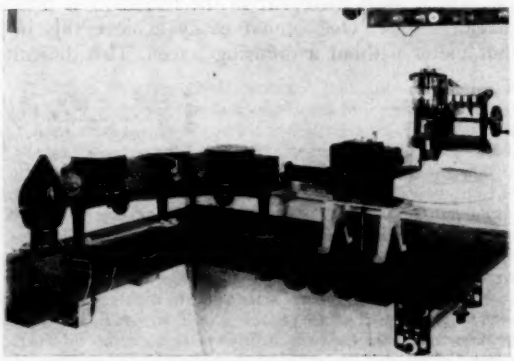

FIG. 4. Photograph of monochromator and photometric separator.

[1] J. Terrien and F. Desvignes, J. de phys. et rad., [8] **10**, 6 (1946).

4. Methods for Producing Controlled Illumination

Since the eye can appreciate only equality of luminance, one must choose a method for controlling illumination so that the luminance of one of the comparison fields can be varied in known ratios. This variation must be continuous in order to allow a suitable adjustment around the balance position, this condition being necessary for achieving precision in the visual photometric matching.

The Talbot disk, geometrically calibrated, is a very convenient means of control. Its transmission factor is strictly independent of wave-length, and it was chosen in preference to any other system. As Fig. 1 shows, this disk presents several openings, whose shapes are parts of sectors. The angles of these sectors are respectively proportional to the numbers 1, 3, 10, and 30; the disk and its motor may be moved together in order to bring the sector of any desired aperture into the light beam. Thus a known density is interposed which can be varied in steps enabling a rough photometric balance to be made at first. Continuous variation and final photometric matching are obtained by means of a "neutral" glass wedge; but, since no glass is perfectly neutral, the wedge is only used for interpolation between two fixed densities of the rotating disk.

5. Photometric Procedure

It was found important to place in the same beam both the specimen, of unknown optical density, and the system of Talbot disc and wedge used for controlling the illumination to a known extent. The beam from the latter, which may be called the measuring beam, illuminates one-half of the photometric field. The other half is illuminated by a steady comparison beam of constant luminance.

The measurement requires two successive equalizations: the first when the specimen is placed in the light path, and the second when the specimen is removed.

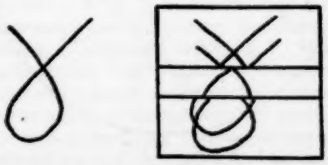

FIG. 5. Appearance of object (left) as seen in photometer (right). Center strip from measuring beam and upper and lower segments from comparison beam.

The variation of the known densities is equal to the density of the specimen. This is the classical substitution method, which is complicated, as explained later, by the interpolation process with the photometric wedge.

APPARATUS

The principle of the apparatus is indicated in Fig. 2 and the following description.

The exit slit f of a double monochromator is used as entrance pupil of the separator. The objective O_1 produces an image of this slit f focused at infinity and the parallel beam thus obtained is divided into two parts by the plane-parallel glass plates s. The transmitted part (measuring beam) passes successively through the movable photometric wedge c_1 with its fixed compensation wedge c_2, the specimen e and the rotating disk d before reaching the Lummer cube c. The reflected part (comparison beam) passes through fixed densities t, made of neutral glass, before reaching the cube c. The cube is observed by means of an eye-piece, whose lens O_2 gives an image f' of the slit on the exit pupil p'. The mirrors P_1 and P_2 give the desired orientations to the divided beams.

The actual scheme corresponds to that described above, but, in addition (Fig. 3), it comprises:

(a) a reading device, for observing in the cube c an image of the divided rule r, supported by the mounting of the movable wedge c_1, and an image of a fixed line (a wire supported by the mounting of the fixed compensation wedge c_2); this afocal device consists of a field lens l_1, an objective l_2 and two prisms p_4 and p_5; the group l_2, p_4, and p_5 may be moved vertically by means of a pedal-operated cable.

(b) a prism p_3 for deflecting the beam emerging from the cube so as to leave room for the disk.

Figure 4 shows on the left the double monochromator, and on the right the photometric separator. On top of the latter can be seen the rods which enable the neutral glass plates to be inserted in the comparison beam; underneath is the cable which brings the reading device into position when actuated by means of a pedal; above and to the right is the Talbot disk with the supporting slide fastened to the wall.

ADJUSTMENT OF THE PHOTOMETER

The complete adjustment of the instrument consists in combining both emerging beams so that they occupy the same relative positions as when entering, and is performed by means of the following operations.

1. Direct into the cube the beams issuing from the same part of the collimator. For this, place in the conjugate plane of the cube (which, in the instrument described, is located about 20 cm in front of the slit f) a rather thin object, with an irregular outline (for instance a rigid wire shaped as shown to the left of Fig. 5), and observe, in the ocular, the images in the cube. The beam transmitted by the plate s gives one image only; the beams reflected by the plate s at the two faces give two images. The best adjustment is obtained when the image of the wire given by the transmitted beam is placed between the two images given by the reflected beams (Fig. 5). To fulfill this condition, the prism p_1 is moved, in order to prevent alteration of the adjustment of the reading system.

2. Bring to coincidence both images f' of the slit f on the exit pupil p'. In order to maintain former adjustment, the Lummer cube only is moved during this operation.

REQUIREMENTS FOR THE SPECIMENS

The specimens must be plane-parallel plates, made of homogeneous and non-diffusing substances. The best accuracy is obtained when the following conditions are satisfied:

1. Condition of optical quality: any ray passing through the plate must not be deviated by more than $5 \cdot 10^{-4}$ radian, whatever the cause of the deviation (lack of flatness, parallelism, or homogeneity).

2. Condition of photometric quality: relative variation of optical density tolerable in the whole sample, caused by lack of parallelism or homogeneity, should not exceed $3 \cdot 10^{-3}$.

METHOD OF MEASUREMENTS

1. Nomenclature

Total optical density placed in the measuring beam $= K$ constant.
Density of the wedge corresponding to the zero of its scale $= C_0$ constant.
Reading on the scale of the wedge $= L$ known variable.
Slope of the wedge (ratio of the variations of density C of the wedge to the variations of readings L) $= \Delta C/\Delta L$ unknown constant.

TABLE I. Measurements and calculations.

λ mμ	$\delta\lambda$ mμ	$N°$	Densities $N°$	D	L	X	$\frac{D_2-D_1}{L_1-L_2}$	$\frac{\Delta C}{\Delta L}$	L_1-L_2	$\frac{\Delta C}{\Delta L}(L_1-L_2)$	D_1-D_2	X
		1	1+3	1.506	6.70	0		+0.1027				
660	12	2	1+3	1.002	11.60	0	$\frac{-0.504}{4.90}$		−3.53	−0.363	+1.506	1.143
		3	1+3	0	10.23	X						

Density of the disk $= D$ known variable.
Density of the sample $= X$ unknown.

2. Measurements and Calculations

The sector disk is previously calibrated by measuring the angles of aperture α and applying the Talbot law:

$$D = \log_{10} \frac{2\pi}{\alpha}.$$

The wedge is used to interpolate between two densities of the disk. One has then to make three equalizations schematically represented by three equations such as the following:

	Disk	Wedge	Sample	
without sample	$K = D_1 + C_0 + L_1(\Delta C/\Delta L) + 0;$			(1)
without sample	$K = D_2 + C_0 + L_2(\Delta C/\Delta L) + 0;$			(2)
with sample	$K = D_3 + C_0 + L_3(\Delta C/\Delta L) + X.$			(3)

(1) and (2) give by difference:

$$\Delta C/\Delta L = (D_2 - D_1)/(L_1 - L_2). \quad (4)$$

Combining (1), (3), and (4); we get:

$$X = D_1 - D_3 + (L_1 - L_3)(\Delta C/\Delta L). \quad (5)$$

As an example, measurements and calculations can be found in Table I.

One can make other equalizations with various fixed densities; this allows a check of the constancy of the slope $\Delta C/\Delta L$ of the wedge, this constancy being assumed for the interpolation.

After many measurements, one can draw the diagram of the slope plotted against the wave-length λ. Two photometric equalizations are then sufficient, instead of three for the measurement of a density.

ACCURACY

The optical densities of the four openings of the Talbot disk are known, from measurements of the angles by a goniometer, with an accuracy of ± 0.0005. There is no reason to think that the Talbot law is not valid to this accuracy. Thus the accuracy is mainly limited by the sensitivity of visual matching. This sensitivity with the apparatus described above is of the order of 0.005 in density for an average of 5 equalizations.

A complete investigation shows that the uncertainty in the density of a sample is about twice as much, i.e., 0.01.

One can expect to obtain a very good accuracy in the results. In fact, the principle itself seems to be irreproachable, and the optical and mechanical equipments have been carefully studied in order to avoid systematic errors.

A valuable check is furnished by the comparison of a transmission curve determined on this instrument with a curve obtained by means of a quite different spectrophotometer (Fig. 6). This second spectrophotetomer consisted of a large double monochromator, designed and made at the Institut d'Optique,[2] which was illuminated by a steady source, and was associated with a photoelectric amplifier having a linear response.[3] Any difference between the curves greater that the expected uncertainty must be due to a systematic error in one or both methods. The agreement shown, though not a positive proof of the elimination of all systematic errors, is a valuable argument however for the accuracy of the results. It will be seen that, between 440 and 700 mμ, the greatest difference in density is 0.02, which is compatible with the uncertainty of both methods, and therefore that the agreement is established on the average to within 0.01 in density.

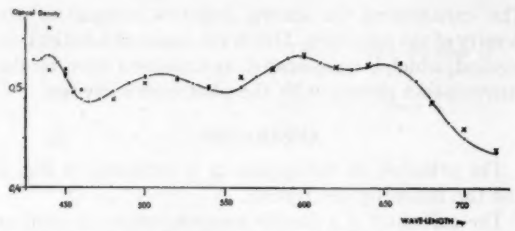

FIG. 6. Comparison of the results obtained visually with the photometric separator (—×—) and by photoelectric means (— · —).

CONCLUSION

This apparatus has been in use for more than four years and has proved very valuable because it is considered to be practically free from systematic errors. In fact, use of the Talbot law is acknowledged to be one of the best means of reducing in a known ratio the luminance of a photometric field; in the best standardizing laboratories, the final check of all spectrophotometers is often made against neutral filters which are measured by visual methods involving use of the Talbot law.

We should, however, like to increase the present rather low sensitivity for the following reasons: 1. the illuminated area of the eye pupil is small, and it is known that, in these conditions, the differential contrast sensitivity of the eye is lowered, and 2. the angle subtended by the illuminated field is small; a larger field would yield more sensitivity, and it would then be possible to accomodate a contrast pattern.

In order to make the increases desired, the geometrical size of the bundle of rays from the monochromator should be larger, i.e.: larger prisms and larger dispersion are required. The present photometric separator has been designed to fit an available monochromator. When a larger instrument becomes available, it will be possible to build another separator, which will enable a much better sensitivity to be obtained whilst preserving the same qualities of faithfulness.

[2] J. Terrien and F. Desvignes, Rev. d'optique **27**, 451 (1948).
[3] J. Terrien and F. Desvignes, Mesures **13**, 411 (1948).

JOURNAL OF THE OPTICAL SOCIETY OF AMERICA VOLUME 40, NUMBER 12 DECEMBER, 1950

A Step-Sector for the Astigmatic Spectrograph

RALPH E. THIERS
Pratt Trace Analysis Laboratory, School of Chemistry, University of Virginia, Charlottesville, Virginia
(Received September 21, 1950)

A step sector is described which can be used with astigmatic spectrographs to give results in every way as good as those obtained with conventional sectors and stigmatic instruments. In its action it may be described as a cross between a focal plane shutter and a band saw, as it consists of a continuous band of opaque film with a succession of stepped openings cut from its center. This film is passed at high speed in front of the focal curve next to the sensitive emulsion, then around a return path which is not in the optical path of the instrument. Added versatility is achieved by the inclusion of adjustable vertical and horizontal masks.

THE step sector is probably one of the most universally used accessories to the spectrograph. It provides the most convenient method of emulsion calibration, a method which, in spite of some controversy, has been proven to be perfectly valid provided that the proper precautions are taken.[1,2] It is also an exceedingly useful tool to the spectrochemical analyst because it widens the range of exposures that can be used. The reason for this is the fact that in one sectored photograph, exposures ranging over a ratio up to 1 to 50 or more appear for each line, and it is therefore very likely that a portion of each line can be found with the proper blackening for photometric readings. This has two beneficial effects. It decreases to a negligible sum the number of times a useless under or overexposed photograph is produced because of error or lack of familiarity with a sample. It also widens the range of any spectrochemical method because the exposure difference between different steps is known, and hence the ratio of the exposures of two lines can be obtained, even though it be greater than the latitude of the emulsion, since the lines can be measured in different steps wherever the blackness of each line is most suitable for measurement.

The common design of a logarithmic or step sector is a disk cut to the desired shape and rotated rapidly in front of the spectrograph slit. This technique of course is possible only when a line at the focus is a stigmatic image of the spectrograph slit. Several very useful spectrograph mountings are not stigmatic and for this reason preclude the use of a disc sector at the slit. Concave gratings in the Eagle, Rowland, or Paschen-Runge mounting are the commonest examples. Sirks[3] showed that an aperture such as a sector could be placed in the optical path before the slit on a line tangent to the Rowland circle at the focus. This technique has found application to the above mountings, but it is sometimes limited in the wave-length range which can be covered.

With the Eagle and Paschen-Runge mountings long lines are obtained with a very uniform central portion which is ideal for the use of intensity reducing devices placed just in front of the focus. This, however, is complicated by the fact that the focus is a cylindrical surface rather than a plane; hence weakeners, such as step filters or wedges, can cover only a short wave-length range and consequently are not very useful.

Hasler and Lindhurst[4] proposed an ingenious logarithmic weakener for placement near the focus. It was made up of a half-cylindrical rod which rotated about its long axis in front of the film in the Applied Research Laboratories' grating spectrograph. The sector covered a length of 13 in. and was said to be superior to the ordinary logarithmic sector because the space between two points of equal density was measured, thus eliminating any base-line and essentially averaging two results.

The author felt very keenly the need for a step sector for use on the ARL 2-meter Paschen-Runge mounted spectrograph with which the Pratt laboratory is equipped. A step sector has been designed, built and tested which gives excellent results over the whole photographed range and which requires no optical adjustment for wave-length. This device is analogous in its action to the focal plane shutter of a camera except that its action is continuous. The material from which it is made is a band of 35-mm film of the type called "jet leader," customarily found as the outer wrapping of a roll of daylight loading film. A piece of this black film has its ends spliced together to form a loop and from the center of the film small shapes are cut, through which light can pass. These shapes correspond to the cut away portion of the disk step sector (Fig. 1). This film is then mounted and caused to rotate like a band saw in such a way that it passes in front of and very close to, the film of the spectrograph. It then completes its loop through a path which is not in the optical plane of the instrument. The shapes which are cut out of the film are shown in Fig. 1 and it is obvious that a succession of these cut away portions passing in front of a spectrographic line will allow different portions of that line to pass through the sector film and reach the photographic film for different fractions of the total exposure time. These shapes are die cut and the ratio between successively longer exposure times is 1:1.5. In order to give a greater contrast between adjacent steps, consecutive steps are

[1] J. H. Webb, J. Opt. Soc. Am. **23**, 157, 316 (1933).
[2] W. C. Pierce and N. H. Nachtrieb, Ind. Eng. Chem., Anal. Ed. **13**, 774 (1941).
[3] Sirks, Astronomy and Astrophysics **13**, 763 (1894).
[4] M. F. Hasler and R. W. Lindhurst, Rev. Sci. Inst. **7**, 137 (1936).

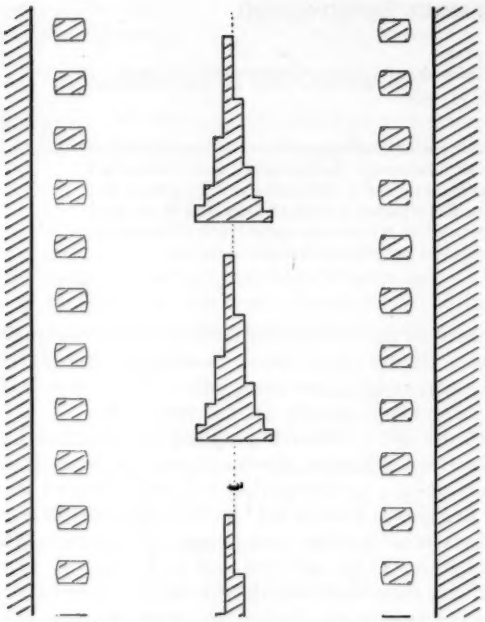

FIG. 1. Piece of sector film.

placed on alternate sides of the center line of the sector shape. Thus the weakest or number one step is at one edge of the shape. The next strongest or number two step is at the opposite edge and the number three step is adjacent to number one. This gives the added advantage that by masking off one-half of the steps a four-step sector may be obtained with a factor between the steps of 2.25. These small cut-out shapes are placed as close together as the strength of the film will allow and are carefully cut so that they follow one another exactly, thereby giving a sharp boundary between the steps. Figures 3 and 4 show sectored iron spectra.

Reference to Fig. 2, a diagram of the apparatus, will show its mechanism. Notable points in the diagram and a discussion of them follows.

1. Sensitive emulsion	This is the 35-mm film on which the spectral lines are to be photographed.
2. Sector film	This is the continuous band which passes in front of the focal curve about $\frac{1}{2}$ cm from the sensitive film. This film has in it the sector shapes which are die cut from its center and pass any given line at rates up to 3500 per minute.
3. Horizontal mask	This is formed by a piece of jet leader film from which no hole has been cut, which is placed in the slot directly in front of the sectored film. The length of this mask can be adjusted to allow the use of whatever horizontal portion of the sectored area is desired.
4. Vertical masks	The vertical masks are thin brass strips which can be raised or lowered so as to cover any desired portion of the sectored area, and they allow any number of adjacent strips to be used in any desired portion of the sectored area.
5. Slot for horizontal mask	The horizontal mask is inserted through this slot and is held in a guide adjacent and parallel to the sector film.
6. Driving sprockets	These two sprockets, one vertical and the other horizontal, are directly connected by bevel gears. The vertical one pulls the film around the curve while the horizontal one pushes it on its return journey through the wide, straight guide below the base plate.
7. Drive shaft	This is connected to a small variable speed motor mounted on the camera yoke inside the spectrograph.
8. Return path of sector film	Since the film is being pushed the return slot is merely a pair of brass strips which act as guides. While this has been quite satisfactory with perfect film, occasional difficulty has arisen from film with flaws in it. These might not have arisen if the horizontal sprocket had been placed at the other end of the apparatus so that it pulled the film. This complicates the gear system, however.

Note also the loops where the film enters and leaves the optical path and the idlers which assist in guiding it. These put no appreciable strain on the film.

The whole unit can be inserted in, or removed from, the ARL camera in a very short time and is quite as convenient as its disk counterpart.

This design is very satisfactory in its operation but through its use several improvements have suggested themselves. Since film finally wears out it would be advantageous to design the instrument with the possibility of slipping in a band of film already spliced. On the present model it is necessary to thread the film through the sprockets and then to splice it when in place. Depending on the amount of use a film receives, it may last from as little as a month to almost indefinitely.

This sector has been in use in the Pratt Trace Analysis Laboratory for six months and has given uniformly

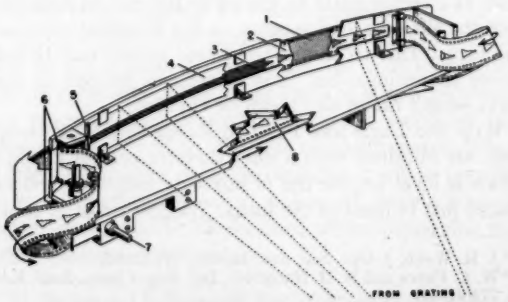

FIG. 2. Focal-curve step sector.

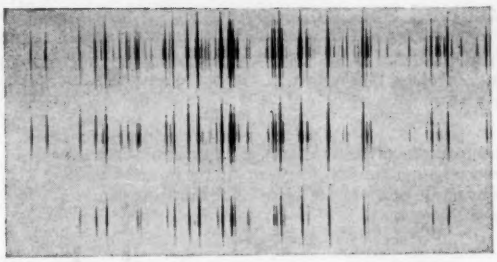

FIG. 3. Stepped iron spectra (8 steps).

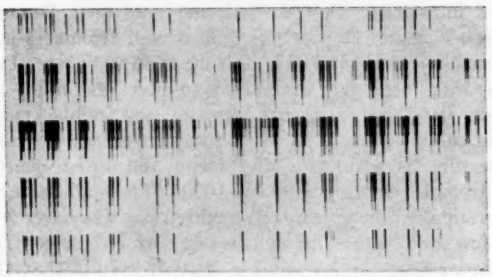

FIG. 4. Stepped iron spectra (Steps 1, 3, 5, 7, and 8).

satisfactory results. The calibration curves obtained from it compare very favorably with other methods of calibration and it has very markedly improved the usefulness of the ARL spectrograph to this laboratory.

In order to obtain a long enough uniform portion of the spectral line the external optics of the ARL spectrograph were changed to the cylindrical lens arrangement of G. Hansen.[5] In this case the arrangement has a spherical quartz lens 4.1 cm in diameter with a focal length of 7.0 cm at 11 cm from the arc (mounted in the hole in the casing of the arc-spark stand). This lens produces a twice magnified image of the source at a position 33 cm from the source. A diaphragm may be used at this position to cut out any undesired portions of the arc. The ARL intensity control stand is mounted so that this image appears on it on the side nearest the arc and any diaphragms are mounted in the place of the original condensing lens. A cylindrical quartz lens 1 cm wide and 3 cm high, curved in its 1 cm dimension with a focal length of 6.7 cm produces on the slit a twice magnified image of the above image. This results in a four times magnified image of the source being focussed on the slit as a vertical line, wide enough so that wandering of the source may be tolerated. This lens is mounted 10 cm from the image, (or 43 cm from the arc) and 20 cm from the slit. A cylindrical quartz lens 1 cm wide and 3 cm high, curved in its long or vertical dimension, is placed at the slit. The flat side of this lens is placed against the slit cover, separated from it by a thin polyethylene gasket, and held in place by the ring provided. This lens replaces the quartz dust cover originally provided with the instrument, and the dust cover is used between the arc and the first lens as a protection for the lens. The slit lens casts on the grating a twelve times magnified image of the arc. All of the lenses involved are large enough so that the grating is entirely filled with light.

Using the lens system described, it has been found that this device gives all of the advantages of a slit step-sector and combines these with the great uniformity of line achieved with the astigmatic instrument. Calibration curves have been obtained which agree with those from other methods. Since the sector has both vertical and horizontal masks, and will allow spectra of any length up to its maximum, and any number of steps to be photographed, and since it can be placed in the spectrograph or removed with very little effort, it has vastly increased the versatility of the ARL instrument.

This therefore, from the viewpoint of the spectrochemical analyst, eliminates astigmatism's biggest handicap.

[5] G. Hansen, Zeits. f. Physik **29**, 356 (1924).

An Apparatus for Time-Resolved Spectroscopy

G. GORDON AND W. M. CADY*
U. S. Naval Ordnance Test Station, Inyokern, California
(Received August 2, 1950)

An apparatus is described for making time-resolved spectrograms of single sparks or other short-time sources of light. Our adaptation of a conventional quartz spectrograph provides for sweeping the image of a selected region of the light source along the length of the slit by means of a rotating mirror. The time base can be made as short as 10 μsec. and time resolution of events in the source as brief as 0.5 μsec.

CONVENTIONAL methods of spectroscopy afford information on the time integral of the light intensity as a function of wave-length. Commonly no time variation in the source can be deduced. This limitation is particularly apparent if the source is a single spark or exploding wire, for which the duration is often less than a few microseconds. In order to observe the changes suffered by the spectrum of such a source during a single flash, at least two courses have been reported. In one, a Kerr cell[1] or other fast-acting shutter may be installed in the light path of the spectrograph; in the other, there may be brought about a relative motion of the spectrum and the photographic emulsion. In the latter case it is possible to move the image of the slit with respect to the photographic emulsion[2] or to move the emulsion with respect to the image of the slit,[3] during the life of the spark. In the spectrogram which results, each spectrum line is endowed with a time sense, as in Fig. 1. The time-resolved spectrogram may be considered as a chart on which the blackening of the emulsion is a function of the wave-length as abscissa and of the time as ordinate. In the apparatus described, the image is moved with respect to the photographic plate by means of a rotating mirror. Although the description is concerned mainly with the optical system, certain ancillary equipment will be mentioned.

The essential apparatus and optical parts for time-resolution are shown in Fig. 2. A pressure-control chamber housing the source is shown in outline. A slot or other small aperture just after the source selects a region of the source for spectral examination and provides time resolution of events. It is oriented so that its image is horizontal, i.e., across the slit of the spectrograph (Bausch and Lomb, Medium Quartz). As the mirror rotates, the image of the slot moves downward along the length of the slit. Since the magnification in the optical train from source to slit is 1.3, a typical slot width of 1.0 mm illuminates a 1.3-mm segment on the slit. The ratio of the slot width to the slit length is about 1:14.

The mirror is made of an octagonal piece of type 410 stainless steel. Opposite faces are parallel and each face is 1 in. square. The mirror is mounted on a Dumore Type-*V* mandrel which is belt driven from a ½-h.p. variable-speed motor at speeds up to 36,000 r.p.m. Two opposite faces are aluminized to give maximum reflectivity; the six faces not optically used are blackened. The condensing lens, of 14-in. focal length and 0.875-in. aperture, is a doublet of fluorite and fused quartz, achromatic between 2400 and 4000A. The manufacturer has supplied the spectrograph with a positive cover lens a few millimeters before the slit, which images the achromat on the collimating lens. It results that the latter is uniformly filled with light during the entire travel of the image of the slot along the slit of the spectrograph. A verification of this condition is afforded by the uniformity of the blackening of the emulsion in the time direction when the mirror is rotated uniformly during the exposure of a constant light source.

A reticle, consisting of a silica flat on which horizontal lines have been ruled at 2-mm intervals, is mounted immediately before the slit. These lines appear on the spectrogram as narrow unexposed streaks, of which nine are occasionally visible (Fig. 1). They resemble the blemishes sometimes caused by dust in the slit of any stigmatic spectrograph. Their purpose is to serve as time markers. When the mirror is rotating at 34,380 r.p.m., the time markers are 1 μsec. apart on the plate at all wave-lengths.

Three pieces of auxiliary equipment play important roles. One of these is the photoelectric trigger.[4] Light from a projection lamp is reflected from the rotating mirror at the face *P* (Fig. 2) and focused upon a 931A photo-tube which thus receives a brief flash of light. The light path is so designed that the photo-tube is illuminated just as the image of the aperture at the source first falls on the upper end of the slit. The amplified output from the photo-tube, controlled by a manually operated switch, is fed to the grid of a hydrogen thyratron in the circuit of the light source. The uncertainty of timing is found to be probably no greater than 0.5 μsec. By this means it is assured that the source is triggered at such an instant as will permit the utilization of the entire slit length in recording the history of events in the source.

The tachometer for the mirror speed is another

* Now with North American Aviation, Downey, California.

[1] J. W. Beams, Jr., and F. L. Brown, J. Opt. Soc. Am. **11**, 11 (1925); E. O. Lawrence and F. G. Dunnington, Phys. Rev. **35**, 396 (1930).

[2] S. Smith, Astrophys. J. **61**, 186 (1925); J. W. Beams, Jr., Phys. Rev. **33**, 1086 (1929); J. A. Anderson and S. Smith, Astrophys. J. **64**, 295 (1926).

[3] T. Futagami, Science Papers of Physical and Chemical Research **31**, 671 (1929).

[4] F. R. Marshall and A. M. Zarem, Rev. Sci. Inst. **19**, 816 (1948).

auxiliary device. Unamplified pulses from the photoelectric trigger, two per revolution of the rotating mirror, are fed to a pulse modifier, an adapted Eccles-Jordan circuit. The pulse modifier halves the pulse

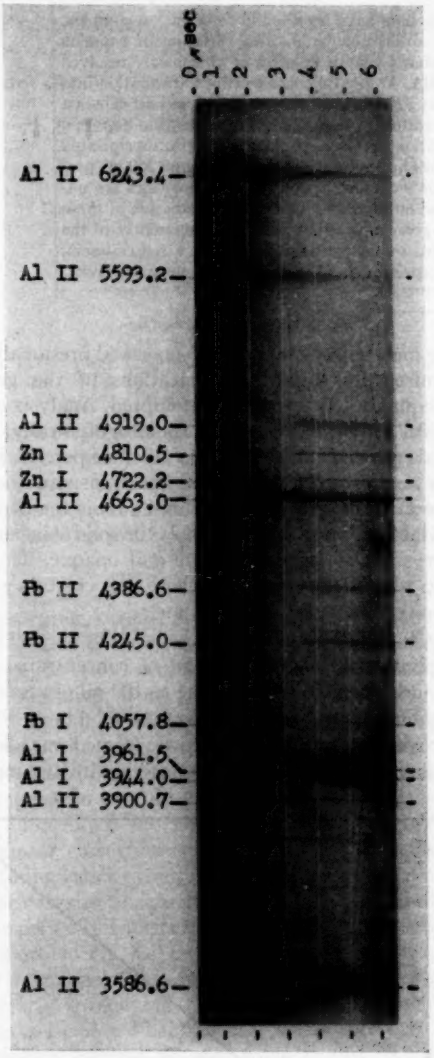

FIG. 1. Time-resolved spectrogram of an exploded aluminum wire. The impurity lines arise from the material of the clamps.

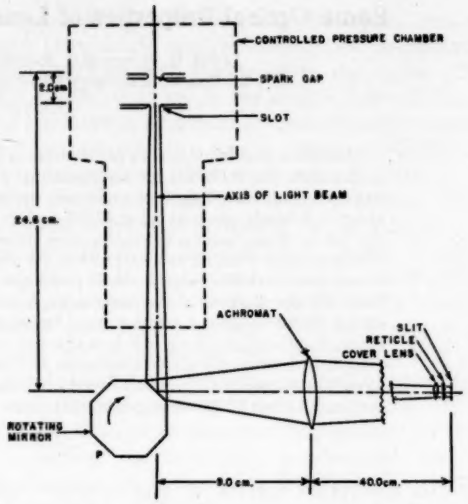

FIG. 2. The light source and optical train.

frequency and changes the wave form from a sharp pulse to a square wave. The output is fed to a Hewlett-Packard frequency meter, on which the frequency of rotation can be read directly.

Finally, photometry is facilitated[5] by a spectrogram of a single spark on each plate, using an appropriately altered arrangement of the condensing lenses and no rotating mirror. This exposure is made with a biprism placed just after the Cornu prism. Actually, two such calibration exposures are made on each plate: the slit width used for one of them is greater than that used for the other; points on the calibration curve may thus be distributed more advantageously.

The apparatus here described has proven adequate for the observation of time-resolved spectra of sparks and exploding wires, where the energy derives from a 5-μf condenser charged to 6000 v. The exposure from a single flash is bright enough to allow good photometry at intervals as close as 0.5 μsec., which is the time resolution of the apparatus.

We would like to acknowledge the cooperation of D. G. Marlow in setting up the Eccles-Jordan circuit, and frequent consultations with F. R. Marshall. The work reported above was supported in part by the ONR.

[5] W. M. Cady and G. Gordon, J. Opt. Soc. Am. 39, 368 (1949).

Some Optical Properties of Lead-Activated Sodium Chloride Phosphors

JAMES H. SCHULMAN, ROBERT J. GINTHER, AND CLIFFORD C. KLICK
Crystal Branch, Metallurgy Division, Naval Research Laboratory, Washington, D. C.
(Received August 3, 1950)

Absorption and luminescence phenomena in NaCl:Pb phosphors have been found to be rather complex. Melt-grown NaCl:Pb has an asymmetrical, 2730A-peaked absorption band. The variation of emission spectrum with wave-length of excitation within this band shows that it consists of two poorly resolved absorption bands, one peaking at 2730A and the other at 2900A. At low Pb concentrations, irradiation into the first of these causes a near-ultraviolet emission peaking at 3200A; irradiation into the second causes a visible emission peaking at about 4500A. At high Pb concentrations, irradiation into the first band gives a second near-ultraviolet emission band peaking at 3850A in addition to the one peaking at 3200A. Precipitated NaCl:Pb shows all the above phenomena, and in addition, has an excitation band peaking at 2600A, producing simultaneously a 3300A-peaked emission and a visible emission. The NaCl:Pb phosphors are unstable, deteriorating after a few days at room temperature and more rapidly at 130°. *X*-irradiation of these phosphors destroys the above absorption and emissions, and gives a print-out effect due apparently to the formation of colloidal Pb. The x-rayed material can be excited by near ultraviolet to give a red emission, peaking at about 6100A. Some suggestions concerning the interpretation of the above phenomena are given.

THE absorption spectra of lead-activated alkali halide phosphors have been extensively investigated.[1,2,3] The emission spectra of these phosphors, on the other hand, appear to have received little attention.[4] Both of the foregoing properties have furthermore been investigated only on melt-grown alkali halides, and no data exist on the properties of lead-activated alkali halide phosphors prepared from aqueous solution. We report in this paper our observations on the absorption, excitation, and emission spectra, and of the stability with time and heat treatment of NaCl:Pb phosphors prepared by crystallization from the melt and by precipitation from solution. The action of *X*-irradiation on some of the above properties has likewise been examined and some new effects have been found.

PREPARATION OF MATERIALS

Single crystals of NaCl:Pb were grown from melts of "c.p." NaCl and $PbCl_2$ using the Kyropoulos technique,[5] the crystals being slowly cooled to room temperature in the Kyropoulos furnace. Figure 1, in which the lead concentration of the crystal is plotted against the lead concentration of the melt, shows that the former is about 0.2 the latter at low lead concentration, decreasing to about 0.08 at the higher lead concentration. A similar result was obtained by Koch[6] with KBr:Pb. It may be seen from the data that there is some variation of lead concentration within a given crystal boule. This is to be expected since the lead concentration in the melt may vary during the time of growth of the crystal due both to volatilization of $PbCl_2$ from the melt and to the effect of fractionation. The first influence would tend to lower the lead content of the melt with time, while the second effect would tend to increase the lead content of the melt with time. Both effects could presumably be minimized by suitable modifications of the growth technique, but this was not attempted. Analysis of the crystals for lead was done polarographically. The crystals grown from the 0.5 and 1.0 mole percent $PbCl_2$ melts were completely colorless and transparent at the temperature of growth. On cooling to room temperature colloidal $PbCl_2$ precipitated out of the solid solution and the crystals became milk-white and opaque. This occurred to a slight extent also with the crystals grown from a 0.1 mole percent $PbCl_2$ melt.

NaCl:Pb was obtained from solution by the following precipitation procedure: 250 ml of concentrated HCl were added rapidly with stirring to 100 ml of a solution containing 5.0 g NaCl and various weights of $PbCl_2$. The coarse precipitate which slowly formed was allowed to stand at least one hour in contact with the mother

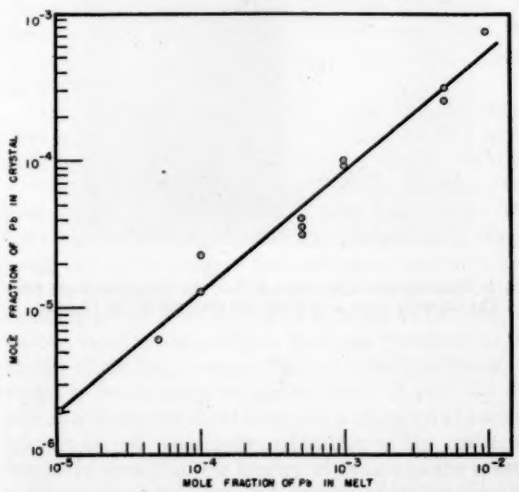

FIG. 1. Composition of melt-grown crystals of NaCl:Pb *vs.* composition of melt.

[1] R. Hilsch, Zeits. f. Physik **44**, 860 (1927).
[2] M. Forro, Zeits. f. Physik **56**, 534 (1929).
[3] H. Lorenz, Zeits. f. Physik **46**, 558 (1928).
[4] M. Kato, Sci. Pap. Physchem. Res. Tokyo **41**, 113 (1943).
[5] S. Kyropoulos, Zeits. f. anorg. allgem. Chemie **154**, 308 (1926).
[6] W. Koch, Zeits. f. Physik **57**, 638 (1929).

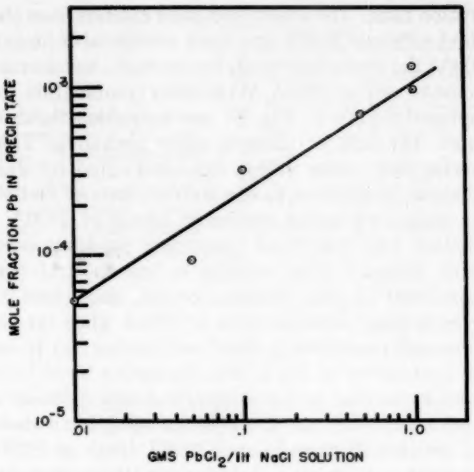

FIG. 2. Composition of precipitated NaCl:Pb *vs.* Pb content of solution.

liquor before it was filtered with suction, washed with acetone on the filter, and allowed to air-dry at room temperature. Figure 2 shows the lead content of the precipitates, determined polarographically, as a function of the lead concentration in the solution.

ABSORPTION SPECTRA

Absorption spectra of the melt-grown single crystals were measured on a Beckman spectrophotometer, and in most cases also with a double monochromator-photomultiplier arrangement. The crystals were placed between the exit slit of the monochromator and the phototube in both methods of measurement, preliminary experiments with the double monochromator arrangement having shown that the error introduced in this way by the fluorescence of the crystals was negligible. Approximate correction was made for the reflection and scattering losses by adjusting the absorption coefficient of each crystal to zero at 4000A, where they are known to be perfectly transparent. Typical absorption spectra are shown in Fig. 3. The 2730A-peaked absorption band characteristic of lead, found by previous investigators, is clearly evident in this figure, rising above what appears to be a "background" absorption, the latter increasing towards shorter wave-lengths. This background absorption is almost certainly the long wave-length part of another characteristic lead absorption band reported by earlier investigators and having its peak near 2000A. Our equipment did not enable us to make reliable measurements below about 2200A, hence we could not study the behavior of this band. As shown in Fig. 3 the 2730A-peaked absorption band is asymmetrical, falling off in intensity more abruptly at the shorter wave-lengths than at the longer wave-lengths. This asymmetry is made more noticeable by plotting the 2730A-peaked band by itself after correction for the "background" (i.e., 2000A-band) absorption, this correction being made roughly by graphical interpolation of the "background" absorption in the region 2500–3200A and subtracting. In one sample (curve 2, Fig. 3) there appeared to be a distinct resolution of the absorption spectrum into two bands peaking at 2730A and 2900A, respectively. The asymmetrical shape of the 2730A absorption band in NaCl:Pb is also clearly discernible in the data of Hilsch[1] and of Arsanjewa.[7]

In order to obtain the absorption spectra of crystals grown from melts containing 0.5 or higher mole percent lead, the milky crystals from these melts were heated to 500–600° and rapidly quenched. Transparent crystals suitable for measurement were obtained in this way. Figure 4 shows the absorption spectrum of one of these crystals (the sample showing indications of resolution of the 2730A band) immediately after quenching, as well as its absorption spectrum after a subsequent one-hour reheating to 130°. It may be noticed that the latter mild heat-treatment produces some changes in the absorption spectrum, the long wave-length side of the band decreasing in intensity somewhat, and the "background" intensity increasing considerably in the region below 2500A. The general aspect of the absorption is, however, not changed by the mild heat-treatment.

Figure 5 shows the dependence of the absorption coefficients for 2730A and 2900A radiation on the lead concentration of the crystal. It may be seen from the figure that the absorption coefficient of the crystals for these two wave-lengths is approximately proportional to the lead content. Comparison of our absorption constant at 2730A with that found by Hilsch for a NaCl:Pb crystal, using his value for lead concentration in the melt, and our calibration curve (Fig. 1) to estimate the concentration of Pb in his crystal, shows good agreement. The absorption coefficients used in Fig. 5 are those directly measured, i.e., they have not been corrected for the absorption due to the long wave-length

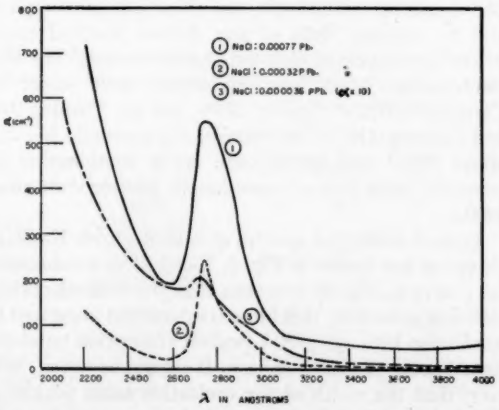

FIG. 3. Absorption spectra of melt-grown NaCl:Pb crystals.

[7] A. Arsanjewa, Zeits. f. Physik **57** 163 (1929).

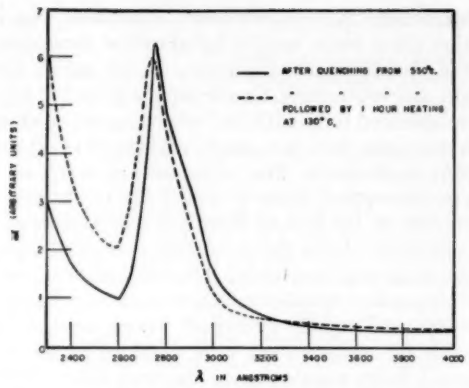

FIG. 4. Effect of 130° heat treatment on absorption spectrum of a melt-grown NaCl:Pb crystal.

extension of the 2000A absorption band. As mentioned above, the measurements on the crystals of high lead content were necessarily made after quenching them from 500–600°; those made on the crystals of lead content below 0.01 mole percent were made on the crystals as grown without further heat-treatment.

Absorption studies of the NaCl:Pb preparations precipitated from solution were not made in the course of the present investigation. That they exhibited a pronounced absorption peak at 2730A was known from earlier work.[8]

EXCITATION SPECTRA

The data of greatest interest were obtained from studies of the excitation spectra of the NaCl:Pb phosphors. The apparatus used in this study consists of a Beckman hydrogen lamp and Beckman monochromator, with automatic wave-length drive, for irradiation of the sample. The sample is viewed by a 1P28 photo-tube, whose output is amplified and recorded. Appropriate filters can be inserted between the sample and the photo-tube to cut out reflected ultraviolet exciting light and to transmit light of any desired spectral region where it is suspected that the phosphor emits. The filter combinations that were employed most were: (a) Corning 9700 and Corning 5840; and (b) Corning 9700 and Corning 3387. Combination (a) transmits between about 3000A and 4000A only, while combination (b) transmits light only of wave-length greater than about 4000A.

Typical excitation spectra of a melt-grown NaCl:Pb phosphor are shown in Fig. 6. Using filter combination (a) (curve a, Fig. 6) it is seen that the near-ultraviolet emission passed by this filter combination is excited by irradiation into the 2730A-peaked absorption band discussed in the previous section. It should be noted, however, that the width of the excitation band peaked at 2730A is smaller than that of the corresponding absorption band. The absorption band extends from about 2600A to about 3100A and has a considerable height at 2900A; the excitation band, by contrast, has decreased almost to zero at 2900A. When filter combination (b) is employed (curve b, Fig. 6) *two* excitation bands are found. The first of these is again peaked at 2730A, showing that some visible light is excited by 2730A radiation in addition to the near-ultraviolet emission. The second excitation maximum occurs at 2900A. Irradiation into this band apparently produces only a visible emission lying entirely in the spectral region transmitted by filter combination (b), since there is no corresponding excitation peak at 2900A when the near-ultraviolet transmitting filter combination (a) is used. The asymmetry of the 2730A absorption band is thus shown to be due to the existence of two different absorption processes, the first corresponding to an absorption between 2600 and about 2950A (peak at 2730A), with an emission lying mainly in the near ultraviolet but with a small amount of visible luminescence also; the second corresponding to an absorption between about 2750 and 3100A (peak at 2900A) with an emission of only visible luminescence.

Investigation of the excitation spectra as a function of lead concentration in the crystal showed that the height of both excitation bands increased at approximately the same rate with increase in lead content. Using the data obtained from the excitation spectra to get the shapes of the two "sub-bands," the absorption spectra of the melt-grown NaCl:Pb preparations are approximately resolvable into two bands as shown in Fig. 7. From this curve the number of "2900A" absorbers is determined to be about 0.4–0.5 of the number of "2730A" absorbers, depending upon whether one takes the areas under the curves or the relative peaks heights as a measure of the number of absorbers. This ratio of "2900A" absorbers

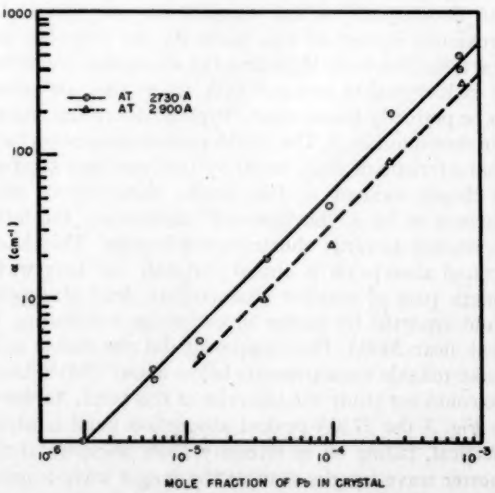

FIG. 5. Absorption coefficients of melt-grown NaCl:Pb crystals *vs.* Pb content.

[8] J. H. Schulman, E. Burstein, L. W. Evans, R. J. Ginther, and M. White, Phys. Rev. 76, 178 (1949).

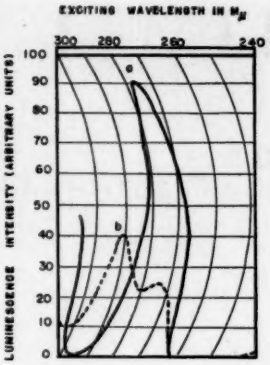

FIG. 6. Excitation spectra of a melt-grown NaCl:Pb crystal. (a) Luminescence viewed through Corning Filters 9700 and 5840. (b) Luminescence viewed through Corning Filters 9700 and 3387.

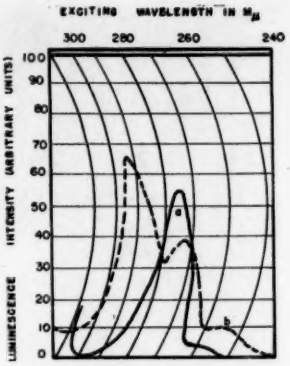

FIG. 8. Excitation spectra of precipitated NaCl:Pb. (a) Luminescence viewed through Corning Filters 9700 and 5840. (b) Luminescence viewed through Corning Filters 9700 and 3387.

to "2730A" absorbers was found to be independent of the lead concentration in the crystal.

Typical excitation spectra of precipitated NaCl:Pb phosphors are shown in Fig. 8. Using filter combination (a) (curve a, Fig. 8) two excitation peaks are observed in the precipitated material, a strong one peaking at 2730A and a weak one peaking at 2600A. With filter combination (b) (curve b, Fig. 8), three excitation maxima appear in the precipitated material, the two mentioned above and a third peaking at 2900A. From the transmission characteristics of the filters used, it can be concluded that the excitations at 2600A and 2730A give rise to luminescence emissions lying both in the near ultraviolet and in the visible, while excitation at 2900A causes excitation only in the visible region, at longer wave-lengths than about 4000A. It appears that the 2730A and 2900A excitation bands found in the precipitated NaCl:Pb are essentially identical with those found in the melt-grown NaCl:Pb. The precipitated phosphors, however, have an additional excitation band at 2600A not found in the preparations from the melt.

Since the position of the 2600A excitation band found in the precipitated phosphors is very close to those of the NaCl:Tl and NaCl:Cu phosphors mentioned in the literature,[1-4] the possibility of ascribing this excitation band to unintentional impurities of thallium and copper was investigated. A study of the excitation spectra of the NaCl:Tl and NaCl:Cu phosphors using different filter combinations, as well as a direct comparison of the emission spectra of these phosphors with that of the precipitated NaCl:Pb phosphor under 2537A excitation (q.v.) showed that neither thallium nor copper was responsible for the 2600A excitation peak found in the latter, and that this is indeed due to lead.

In order to gain some further insight into the nature of the 2600A excitation peak, NaCl:Pb was grown by slow room temperature evaporation of a saturated NaCl solution to which various quantities of saturated lead chloride solution had been added. This excitation band was found (along with the 2730A and 2900A bands) both in large single crystals produced in this way as well as in a polycrystalline crust formed during the evaporation. The 2600A band is thus not connected with the use of HCl in the precipitation procedure, nor with the larger surface area of the polycrystals obtained by this procedure. This experiment did not exclude the possibility that the 2600A band is related to the entrapment of water or mother liquor in a crystal grown from solution. Excitation measurements on a solution of 50 g

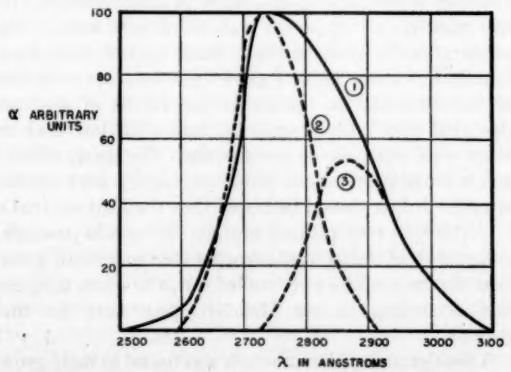

FIG. 7. Relation of excitation bands of melt-grown NaCl:Pb to its absorption band at 2730A. (1) Absorption spectrum. (2) Excitation band for U.V. emission (2730A peak). (3) Excitation band for visible emission (2900A peak).

TABLE I. Effect of aging on brightness of NaCl:Pb precipitate.

		Luminescence intensity in arbitrary units			
		Ppted NaCl:5.3(10⁻⁵)Pb		Ppted NaCl:1.35(10⁻⁴)Pb	
		Fresh ppt.	After 12 days	Fresh ppt.	After 12 days
Filter comb. (a)	2600A excitation peak	5.5	1.0	2.5	0.5
	2730A excitation peak	68.0	26.0	28.0	1.7
Filter comb. (b)	2600A excitation peak	1.0	0.35	1.1	0.25
	2730A excitation peak	4.1	1.7	3.9	0.35
	2900A excitation peak	13.0	2.5	6.6	0.3

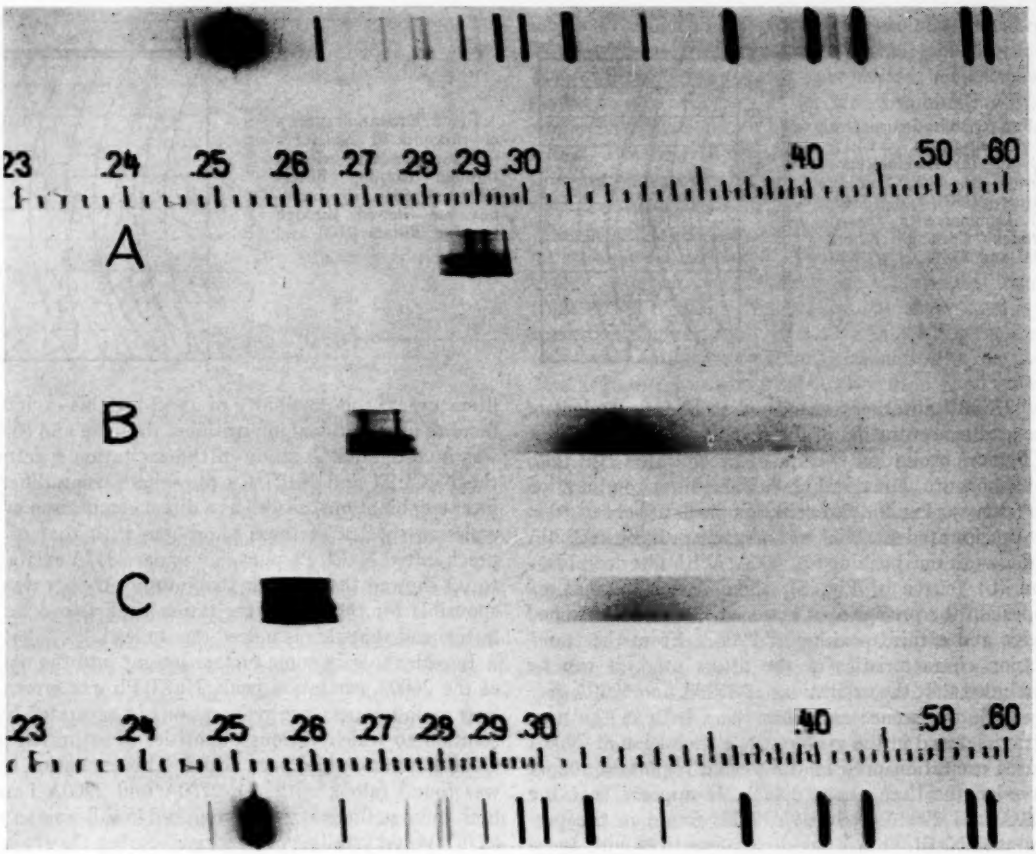

FIG. 9. Emission spectra of precipitated NaCl:Pb as a function of exciting wave-length. (a) 2900A excitation (4500A-peaked emission is weak and is lost in reproduction). (b) 2730A excitation. (c) 2537A excitation.

NaCl plus 1 g $PbCl_2$ per liter did not show any detectable luminescence under irradiation from 2700A–4000A; and although the luminescence of the fused silica cuvette interfered with our observations under shorter wave-length excitation, there appeared to be no response from the solution of these shorter wave-lengths. It thus seems very probable that the entrapment of mother liquor is not responsible for the 2600A excitation. As will be evident from following sections of this paper, the simple test of heating the preparations from aqueous solution to drive off absorbed or entrapped water could not be applied, since heating caused changes in the intensity of all the excitation bands.

STABILITY OF NaCl:Pb PHOSPHORS

Changes with time and heat treatment of both melt-grown and precipitated NaCl:Pb phosphors were discovered and studied by means of the excitation spectra. The first indication that the properties of these phosphors changed with time was obtained on comparison of the excitation spectrum of a NaCl:0.001Pb phosphor, measured two months after it was precipitated, with the excitation spectrum of the material obtained immediately after preparation. While the fresh phosphor had shown very strong excitation peaks originally, after two months its response was extremely feeble. New preparations were accordingly made up and studied as a function of time. Table I shows the decrease with time of the intensity of the excitation bands of two precipitated NaCl:Pb phosphors, one with low and the other with high lead concentration. The aging effect is much more pronounced with the higher lead content sample "*B*." It should be noted that the lead content of 1.35 (10^{-3}) of precipitated sample "*B*" would produce a milky crystal if this were incorporated in a boule grown from the melt and slowly cooled down to room temperature according to our standard procedure for melt growth.

A similar aging phenomenon was found in melt-grown single crystals of NaCl:Pb, particularly in those containing high lead concentrations. These crystals, as already mentioned, were milky and opaque as they came

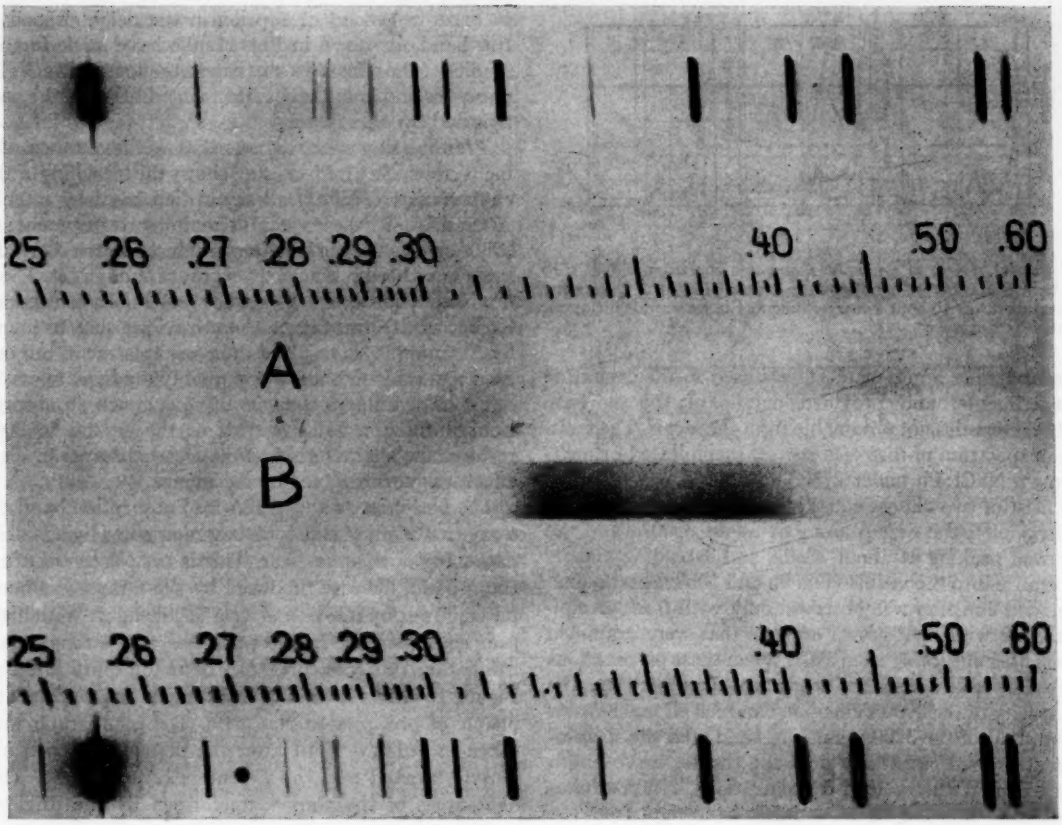

FIG. 10. Emission spectra of melt-grown NaCl:Pb as a function of exciting wave-length. (a) 2900A excitation. (b) 2730A excitation.

out of the Kyropoulos furnace, due to precipitation of colloidal lead chloride. While the milky crystals yielded distinct excitation spectra, much stronger excitation could be observed if they were heated to 500–600° and quenched before measurement. This procedure resulted in perfectly clear and transparent crystals, similar to those obtained directly at lower lead concentrations, and their excitation spectra consisted of very intense peaks at 2730A and 2900A, (curves a and b, Fig. 6). In a matter of a few days, however, the excitation spectrum became comparatively feeble. It is noteworthy that although the luminescence of such quenched crystals decreased to almost negligible values within a few days, *the crystals remained perfectly clear and transparent.* Reheating to 500–600° and quenching restored their luminescence once more, corresponding to curves a and b, Fig. 6. There are indications that a similar aging phenomenon occurs in melt-grown crystals with low lead concentrations, which are clear as they emerge from the Kyropoulos furnace. When these crystals were reheated to 600° and quenched, their response to excitation was increased.

Similar decreases in the luminescence response of both precipitated and melt-grown NaCl:Pb were also found to occur in a very short time on mild heating of the materials, i.e., one hour at 130°. It appeared that the 2730A band survives the heat-treatment better than the 2900A band, and both of these are much more stable towards heat than the 2600A band, which is completely obliterated.

EMISSION SPECTRA

The emission spectra of representative precipitated and melt-grown NaCl:Pb phosphors were investigated by a direct spectrographic technique. In order to eliminate spurious results from scattered light during the exposures, a high pressure mercury lamp enclosed in quartz was used as the light source, and it was monochromatized by a double monochromator. The emission spectra were photographed on Tri-X Panchromatic film using a Gaertner small quartz spectrograph. Exposures with magnesium carbonate plaques in place of the phosphor gave films that were clean except for the reflection of the exciting ultraviolet.

The direct measurements of emission spectra confirmed the inferences previously made on the basis of the

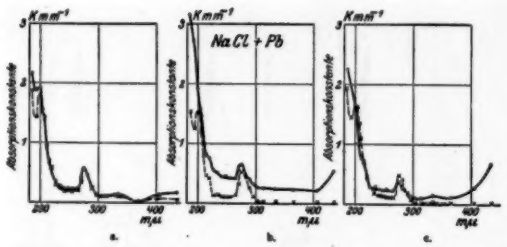

FIG. 11. Effect of x-rays on absorption spectrum of NaCl:Pb (Arsanjewa). (a) 10 minute x-ray treatment. (b) 2 hour x-ray treatment. (c) 10 hour x-ray treatment. Circles = x-rayed crystal; crosses = original crystal.

transmission limits of the filters used in the excitation experiments, and provided details of the emission characteristics not obtainable from the latter. The emission spectrum of *high lead content* precipitated or melt-grown NaCl:Pb under 2730A excitation was found to consist of two almost equally intense bands in the near ultraviolet, the first peaking at about 3200A, and the second peaking at about 3850A and extending a short distance into the visible (Fig. 9b and 10b). This double-banded emission was observed only with *fresh* precipitates or with melt-grown crystals that were examined *soon after quenching* from 500°. When these preparations are allowed to age several days at room temperature, the intensity of the 3900A emission band fell off much faster than that of the 3200A emission band, and the spectrogram showed essentially only the shorter wave-length emission. With *low* lead concentrations, 2730A excitation gave only the 3200A emission band right from the start. At all concentrations of lead, 2900A excitation produced an emission band lying entirely in the visible and peaking at 4500A (Fig. 9a and Fig. 10a) and there was no change with aging other than a decrease in intensity. Since only the precipitated phosphor showed excitation at 2600A, it was the only one examined under this radiation (Fig. 9c). The emission in this case consisted of two bands, one in the near ultraviolet peaking at about 3300A and the other in the visible peaking close to 4500A and apparently identical with the visible emission excited by 2900A.

Our emission results on melt-grown NaCl:Pb are thus similar to those of Kato.[4] However, he reports the emission of all three (3180A, 3850A, and 4530A) bands under 2730A excitation, while our results show that only the first two are emitted under this excitation, the 4500A band being excited only by 2900A. The practical disappearance of the 3850A emission band in our aged preparations is another point in which our data differs from his.

EFFECT OF X-RAYS ON NaCl:Pb

Arsanjewa[7] has found that x-ray irradiation alters the absorption characteristics of NaCl:Pb crystals grown from the melt, causing a decrease in the height of the 2730A absorption band characteristic of lead and an increase in general absorption in the neighborhood of this band, as shown in Fig. 11. We have made further studies of the effect of x-ray irradiation on the NaCl:Pb phosphor and found other effects in addition to the ones reported by Arsanjewa.

Transmission spectrograms that we have taken of a melt-grown NaCl:Pb crystal, shows the bleaching of the characteristic 2730A lead absorption band by intense *X*-irradiation, the crystal remaining transparent at 2730A even after the *F*-centers produced by the *X*-irradiation have been removed by exposure to daylight. There is no indication in our films of the growth of a continuous background absorption in the ultraviolet such as found by Arsanjewa as a result of the x-ray treatment, but our spectrographic method was probably inadequate, without considerable refinement, to detect such an absorption continuum. Mild heating of the crystal to 200° restores the characteristic 2730A lead absorption. This effect was also reported by Arsanjewa.

The bleaching of the 2730A lead absorption band by x-ray treatment of NaCl:Pb is accompanied by a visible darkening of the phosphor. This is best observed after the *F*-band, likewise produced by the x-rays, has been bleached out by irradiation with visible light. With high lead concentration in the phosphor and strong x-ray irradiation this darkening can be made quite intense. Figure 12 shows a "radiograph" made on a (circular) plaque of precipitated NaCl:Pb. The photograph was taken in ordinary light after the plaque had been intensely x-rayed and the *F*-centers bleached out. The light areas of the plaque are formed by the original

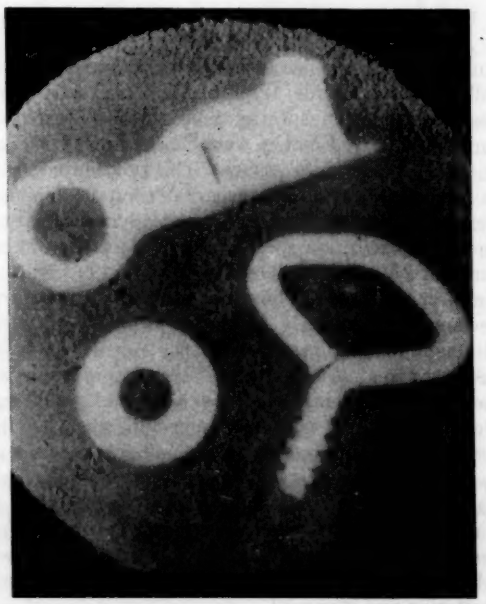

FIG. 12. Radiograph made on NaCl:Pb screen.

phosphor powder which has been protected from the x-ray action by various metallic test objects. The dark grey background is the portion of the plaque which has been exposed to the x-rays. Heating of the x-rayed NaCl:Pb to 200° removes the grey visible discoloration completely, simultaneously restoring the 2730A absorption band.

The decrease in intensity of the 2730A absorption band and the production of the broad visible absorption by *X*-irradiation has obvious consequences on the luminescence emission of NaCl:Pb. It was to be expected that the luminescence response of such an x-rayed phosphor under ultraviolet excitation in the region of the characteristic Pb^{+2} bands should be completely destroyed. Complete destruction of such luminescence was not observed experimentally, but very great reduction in the 2730A excitation band intensity was observed using filter combination (a) (transmitting near ultraviolet luminescence) and an even greater reduction in the height of this peak and the 2900A excitation peak using filter combination (b) (transmitting visible luminescence). It is quite likely that the luminescence under excitation in the 2500–3000A region could have been completely destroyed had we made special efforts to subject the whole crystal volume to a strong enough x-ray dose, by using a thin crystal and irradiating it from both sides. With precipitated NaCl:Pb the 2600A excitation band was likewise seriously diminished by the x-ray treatment.

In addition to the darkening of NaCl:Pb crystals and the killing of the characteristic Pb^{+2} luminescence by *x*-irradiation, there is still another effect observable as a result of this treatment. If the x-rayed NaCl:Pb is examined under light from a "blacklight" lamp (H-4 lamp or 360BL lamp with Corning 5860 filter) a distinct red luminescence is observable. At first, the intensity of the luminescence seems to increase considerably with time under exposure to the "blacklight" lamp, and then to decrease very slowly under continued exposure to this source. The spectral distribution of the emitted luminescence is shown in Fig. 13. An x-rayed NaCl:Pb crystal preserved in the dark for 17 hours after x-raying showed the same effect as a similar crystal exposed to the "blacklight" lamp immediately after x-ray treatment. Moreover, luminescence under "blacklight" excitation was still clearly observable in an x-rayed crystal that had been exposed to strong white light from an incandescent lamp for 17 hours. Measurement of the excitation spectrum was not possible with our present equipment due to the low intensity of the luminescence, hence we do not know if the luminescence is excited by irradiation into the *F*-band, the tail of the general absorption band produced by *X*-irradiation (Arsanjewa), or in some new excitation band distinct from these two.

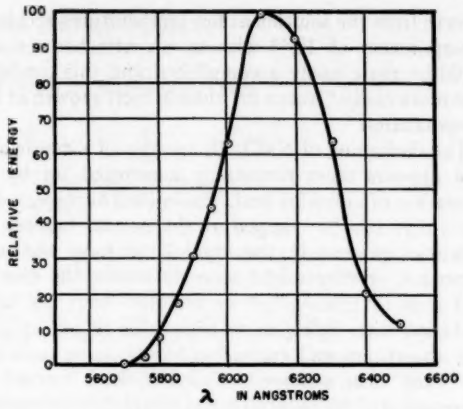

FIG. 13. Emission spectrum of x-rayed NaCl:Pb under 3650A excitation.

DISCUSSION

The absorption, excitation, and emission data are tentatively interpreted in the following manner. The variation of emission spectrum with Pb^{+2} concentration and with time, on exciting at 2730A, indicates that two different centers can give rise to the same excitation band peaking at this wave-length. (Our attempts to subdivide the 2730A band further, by observing the 3200A and 3850A luminescence emissions separately, were unsuccessful.) Since the 3850A emission peak is observed with this excitation only at high Pb^{+2} concentration, we associate this emission band with "pairs" of Pb^{+2} ions, and the 3200A emission band with "singlet" Pb^{+2} ions. The more rapid disappearance of the 3850A emission peak on aging is ascribed to the precipitation of $PbCl_2$ from these high Pb^{+2} bearing materials, aggregation into the new phase being more rapid for those Pb^{+2} ions that are already "paired" with others. The occurrence of the 3200A emission band exclusively at low Pb^{+2} concentrations is consistent with the above interpretation. The 2900A-peaked excitation (and absorption) band we ascribe to an excited state of the "singlet" Pb^{+2} ion different from the state leading to the 3200A emission. This conclusion is supported by the observation that the relative heights of the 2730A and 2900A peaked absorption bands is independent of the lead concentration, i.e., the same asymmetrical shape of the absorption curve is found in all the melt-grown crystals even at very low Pb^{+2} concentrations.

The 2600A excitation band is observed only in precipitated NaCl:Pb and the ultraviolet portion of the emission resulting from such excitation differs somewhat in spectral location from the ultraviolet emission excited by 2730A excitation in the same or in melt-grown material. This excitation band is, moreover, much less stable toward heat than either the 2730A or 2900A excitation bands. It seems fairly certain that this band is due to Pb^{+2} in peculiar configurations assumed only in growth from solution at low temperatures. One possibility is that the 2600A band is due to Pb^{+2} from which a vacancy is dissociated, if we assume the stable configuration is Pb^{+2} ion with an associated vacancy. In

growth from the solution at low temperatures accidental incorporation of Pb^{+2} without an attached vacancy could be more easily accomplished and this configuration more easily "frozen in" than in melt-growth at high temperatures.

The darkening of NaCl:Pb crystals of x-ray irradiation appears most reasonably accounted for by the formation of colloidal lead. Photo-electrons ejected by the x-rays can be trapped at the normal halogen ion vacancies present in the crystals to form the usual *F*-centers, or they might serve to reduce the divalent lead ions to monovalent or metallic lead, the latter oxidation state being more reasonable in our opinion. The absorption and excitation bands characteristic of Pb^{+2} are thus removed. Colloidal lead formed by aggregation of the reduced metal would then give a stain that is more permanent at ordinary temperatures than the *F*-center coloration. The bleaching of the discoloration by heating to 200° and the re-appearance of the characteristic Pb^{+2} absorption band in the clear crystal is due to the re-oxidation of the atomic lead by the holes (neutral Cl) stored in the crystal. On this basis a larger and more stable concentration of positive holes should be produced by *X*-irradiation of an alkali halide crystal containing a cationic impurity capable of chemical reduction than should be produced by irradiation of the pure crystal itself. The increased "general" absorption in the region of 2000–3000A observed by Arsanjewa on *X*-irradiation of KCl:Pb may indeed be due to such positive holes.

The nature of the excitation and emission processes leading to the red luminescence of x-rayed NaCl:Pb is still under investigation, and no discussion of this phenomenon is justified until further data have been obtained. Similar temporary luminescence has been observed with NaCl:Mn,[9] and the x-raying of cadmium-activated[9] and silver-activated[10] alkali halides has been found to produce a permanent response to ultraviolet excitation. In the case of the silver-activated alkali halides the formation of atomic silver has been postulated to be the result of the *X*-irradiation, and the new absorption and emission bands of the x-rayed phosphors have been ascribed to this center.[10]

Our final remarks concern the peculiar change in state of NaCl:Pb crystals, that occurs slowly at room temperature and more rapidly at 130°, and results in a tremendous loss of luminescence response with no major change in absorption spectrum. This effect is shown most markedly by crystals having a very high lead concentration. Such crystals, when grown from the melt, are clear at the temperature of growth but precipitate colloidal lead chloride at some stage during the annealing process to which they are subjected after being pulled out of the melt. The temperature at which precipitation of the lead chloride takes place on such slow cooling is in the neighborhood of 425°. When the precipitated lead chloride is redissolved in the crystals by heating to 500–600° and quenching, they are evidently highly supersaturated with respect to lead chloride. On standing at room temperature, or more rapidly on mild heating, one would therefore expect that this supersaturation condition would tend to relieve itself by precipitation of the excess lead chloride (non-luminescent) leaving the parent crystal with a much lower concentration of dissolved Pb^{+2} corresponding to the solubility of lead at the temperature in question. This solubility is evidently extremely low at room temperature and even at a few hundred degrees above room temperature, so that the resulting crystal is only feebly luminescent. The fact that the highly supersaturated clear crystal does not become turbid when precipitation of the excess lead chloride occurs at room temperature or at 130° probably is due to the very small lead chloride agglomerates that are formed at these low temperatures. On annealing at higher temperatures (*ca.* 425°) the lead chloride crystallites can grow to colloidal size and produce turbidity, while at low temperatures this growth is impossible. From the results of Fesefeldt[11] on the absorption spectrum of thin films of lead chloride, one would not expect to find much change in the absorption spectrum of NaCl:Pb after the precipitation of such small agglomerates of lead chloride, and this is borne out by experiment. It thus appears that investigation of the luminescence of the NaCl:Pb system can yield information concerning solubility and precipitation phenomena in this system not readily obtainable by other physical measurements. This subject is being investigated further in this laboratory, as part of a general program of study of alkali halide phosphors.

ACKNOWLEDGMENTS

We wish to express our appreciation to Mrs. Esther W. Claffy for polarographic analyses of our materials; to Samuel Zerfoss for his observations on the temperature at which the clouding of supersaturated NaCl:Pb takes place; and to Clyde Glover for putting at our disposal the Beckman spectrophotometer used in some of the absorption measurements.

[9] J. H. Schulman, R. J. Ginther, C. C. Klick, and L. W. Evans, Phys. Rev. **76**, 459 (1949).

[10] W. A. Weyl, J. H. Schulman, L. W. Evans, and R. J. Ginther, J. Electrochem. Soc. **95**, 70 (1949).

[11] H. Fesefeldt, Zeits. f. Physik **64**, 741 (1930).

JOURNAL OF THE OPTICAL SOCIETY OF AMERICA VOLUME 40, NUMBER 12 DECEMBER, 1950

Photography of High Altitude Aerial Objects*

C. N. NELSON
Kodak Research Laboratories, Eastman Kodak Company, Rochester, New York

AND

D. H. HAMSHER
Signal Corps Engineering Laboratories, Fort Monmouth, New Jersey

(Received September 29, 1950)

An experimental study of the photography, from the ground, of objects in the upper atmosphere shows that the results are improved by the use of long-focal-length lenses, high contrast film, and color filters chosen with regard to the relative spectral qualities of the object and the sky background. The most difficult problem was the photography of dark gray objects against a blue sky, and for these conditions a blue filter gave best results. For these same conditions, an increase in vertical range (altitude) was found to give a greater decrease in subject contrast than an equal increase in horizontal range. Of lesser difficulty was the photography of bright, white objects against a blue sky; and for these conditions a red filter gave best results. Data were obtained regarding the optimum spectral-reflectance characteristics of targets for special purposes. The required characteristics of the photographic emulsion were the subject of a detailed study. A high contrast, high speed panchromatic film, especially designed for this work, is described. Exposure and processing data for this film are given.

I. INTRODUCTION

IN recent years interest has increased in the problem of photographing objects at altitudes of 15,000 feet and higher from positions on the ground for the purpose of locating accurately the object in space with respect to a coordinate system. While in many cases such photography involves the use of known principles, attempts to meet the requirements of special or difficult conditions have led to several investigations, the results of which should be of benefit to future workers in this field. In particular, the advantage of using long-focal-length camera lenses has been shown, certain photographic emulsion requirements have been determined, color filters have been selected which enhance image contrast, a greater decrease in subject contrast with vertical than with horizontal range has been found to exist, and data regarding the adjustment of the controllable factors to obtain maximum image contrast sensitivity have been collected. The work reported herein was entirely concerned with photography of objects, the outline or details of shape of which were unimportant but the presence and position of which were to be detected. While the photographs were made on 35-mm motion-picture film and in a few cases on 16-mm motion-picture film, the results of the study should be applicable also to still photography of aerial targets under conditions similar to those encountered in this work. Some aspects of this general problem have been treated in the literature by Duntley,[1,2] by Coleman, Morris, Rosenberger, and Walker,[3] and by Coleman and Rosenberger.[4]

The result desired was a photographic image of the target which could be detected simply by viewing the film with the aid of a slow-motion projector or magnifier. The viewers were so made that, when the target image was seen, the film could be stopped in register with a grid of coordinate lines to obtain data on the target position. Stereo analysis was obtained by the use of a pair of films in two widely spaced cameras.

This study was made at the request of the Armed Forces and the National Defense Research Committee. The experimental work was done largely at Fort Monroe, Virginia, and Camp Davis, North Carolina, in collaboration with the Antiaircraft Artillery Board.

II. GENERAL PROBLEM

A difficult condition for obtaining photographs is one in which a dark gray object appears against a clear blue sky background at slant ranges of 5000 to 20,000 yards. The difficulty is further increased when a second object having the characteristic of being brighter than the background must be photographed simultaneously. The object which was darker than the background in the tests to be described was the black or dark gray smoke of an antiaircraft shell exploding at a predetermined position, the diameter of the initial smoke puff being approximately 10 feet. Targets towed by aircraft were also used, which sometimes photographed brighter and sometimes darker than the background. These targets were approximately 2 feet in diameter and 30 feet long. Finally, towed flares and aircraft were also photographed. In addition to blue sky, overcast sky was sometimes used as a background, although for high altitude work, clouds are usually too low to permit photographic techniques to be employed.

The problem was to obtain, on the photographic film, images of the target which had sufficient contrast so that they could be seen readily in a suitable viewer and

* Communication No. 1331 from the Kodak Research Laboratories.

[1] S. Q. Duntley, J. Opt. Soc. Am. 38, 179 (1948).
[2] S. Q. Duntley, J. Opt. Soc. Am. 38, 237 (1948).
[3] H. S. Coleman, F. J. Morris, H. E. Rosenberger, and M. J. Walker, J. Opt. Soc. Am. 39, 515 (1949).
[4] H. S. Coleman and H. E. Rosenberger, J. Opt. Soc. Am. 39, 990 (1949).

located accurately with respect to a set of coordinate lines. The contrast of the final image was evaluated subjectively and was dependent upon the following objective factors:

1. The radiance contrast of the subject.
2. The camera, camera lens, and filter.
3. The exposure.
4. The photographic emulsion and its processing.
5. The viewer.

From the beginning of this work it was apparent that, regardless of the focal length and resolving power of the lenses used, a major difficulty in photographing the aerial objects at the distances required was that the contrast in radiant intensity between the object and the sky background was usually extremely low. Thus, even if lenses having perfect resolution could have been used, the problem would have been a difficult one because of the veiling of the target by the atmosphere and haze. The term "contrast," when applied to the subject, is here used to mean the ratio of the radiance of the lighter area to that of the darker area.

In general, though not always, the spectral-energy distributions for the radiation from the two areas were dissimilar. Consequently, it was important to classify the subject conditions and to determine for each condition what filter was best for isolating the spectral region for which the contrast of the subject was the greatest. The problem of selecting filters was not a simple one, since data were not available on the actual spectral-energy distributions for the particular conditions involved. It was necessary to make numerous tests using a variety of filters for a variety of atmospheric conditions, target distance, and elevation angles, and to select the optimum filters from a study of the photographic results.

The camera images of the targets were, of course, very small. If an object is 10 feet in diameter and is at a distance of 10,000 yards, the calculated image diameter for a 6-inch focal-length lens is 0.05 mm, assuming no lens aberrations or diffraction. The task of finding a low contrast image of this size on the film is not easy, even when considerable magnification is used in viewing the final film. Great care must be taken to keep the film clean during processing and handling; or the image will be confused with dust marks, pressure marks, or any small spots which are introduced. The use of a 12-inch camera lens increases the calculated size to 0.1 mm, and it was suspected from the beginning that the use of even longer-focal-length lenses might be advantageous. There is, of course, some increase in image size due to lens aberrations, to diffraction, and to shimmer of the atmosphere. Moreover, some spreading of the image occurs in the film because of the turbidity of the emulsion. These factors all have the effect of increasing image size at the expense of image contrast. The use of a longer-focal-length lens, on the other hand, was expected to have the advantage of giving a larger image without the corresponding loss in contrast.

Even the combination of the best lens and the best filter cannot give a camera image having a contrast which is higher than that of the subject itself. Some photographic emulsions, on the other hand, are capable of giving an image having higher contrast than that of the subject. It was, therefore, especially important in this work that the proper emulsion be selected and that its processing be properly controlled.

Since many factors entered the problem in a complex manner, it was decided to obtain the required information by experimental rather than theoretical methods. Experiments were carried out under practical field conditions to determine the following:

1. Suitable focal length for the camera lens.
2. Number and types of color filters needed.
3. Classification of the filters according to their use with the different types of targets and backgrounds.
4. Optimum spectral reflectance for the targets, including the requirements imposed by visual tracking of the target with a telescope.
5. Filter factors for various sky conditions.
6. Correct camera exposure in terms of sky luminance, filter factor, and film speed.
7. Optimum emulsion characteristics (speed, spectral sensitivity, contrast, resolving power, and graininess).
8. Film processing requirements.

III. EQUIPMENT AND PROCEDURE

A. The Camera

The photographs were taken with several 35-mm motion-picture cameras specially designed to permit orientation toward all parts of the sky, either to point in predetermined directions or to follow targets towed by airplanes. The required degrees of freedom were obtained by rotation of the camera around a vertical axis with a calibrated worm and gear having a handwheel control and by rotation of a part of the instrument, not including the film mechanism, around a vertical axis in a similar manner. An elbow telescope fitted with cross-hairs and aligned with the optic axis of the camera aided in following moving targets in the sky, and dials giving the azimuth and elevation of the optic axis permitted direction of the camera at the fixed positions. The telescope, camera lens, camera filters,

TABLE I. Filters used in the tests.

Kodak Wratten Filter No.	Color	Wave-length region of useful transmittance
2A	Light yellow	420 mμ to infra-red
5 or 5N5	Yellow	480 mμ in infra-red
15	Yellow	520 mμ to infra-red
23	Orange	570 mμ to infra-red
25	Red	590 mμ to infra-red
29	Red	610 mμ to infra-red
88A	Dark red	720 mμ to far infra-red
39	Blue	320 mμ to 460 mμ
47	Blue	400 mμ to 500 mμ
58	Green	500 mμ to 560 mμ

and a front-surface mirror were mounted on the section which rotated about the horizontal axis. The normal to the reflecting surface of the mirror was at 45 degrees to the optic axis of the camera lens and to the axis for horizontal rotation, so that the film-moving mechanism did not need to rotate about the horizontal axis.

The camera lenses used were 6-inch focal-length, f:2.7, Baltar motion-picture objectives; 12-inch focal-length, f:4.5, achromatic doublets; and 14-inch focal-length, f:6.3, Ektars. Light filters to isolate particular spectral regions could be mounted directly in front of the lens and a graduated iris was mounted at the lens. A rheostat control in the motor circuit permitted varying the camera speed between 10 frames and 20 frames per second. The shutter was a 170-degree rotary sector mounted directly in front of the film.

An internal optical system focused, on the edge of the film, images of the azimuth- and elevation-indicating dials, the camera number, and the dial of a counter which was pulsed at the rate of once per second for use in identifying the photographs after development.

B. Light Filters

The filters employed at various times during the tests transmitted radiation in the spectral regions indicated in Table I.

C. Photographic Emulsions

Various commercial as well as experimental emulsions were used. The spectral sensitivities of most of the emulsions were panchromatic because of the need to make studies throughout the visible spectrum, but sufficient tests were made with emulsions sensitive in the region of 700 to 850 millimicrons to explore the situation in the near infra-red. Other characteristics of the emulsion which were varied were the gradient or slope of the density-*versus*-log-exposure curve, the speed, resolving power, and graininess. The maximum gradient (gamma) of the curve was varied progressively in small increments from 0.7 to 4.0. Emulsion speed ranged from that of high speed motion-picture negative films to that of low speed Microfile type of film. Resolving power varied from 60 to 180 lines per millimeter in terms of laboratory tests using a conventional test object having a contrast of 30 to 1. It was recognized that the resolving-power tests were not necessarily applicable to this problem.

D. Exposure Meters

The exposures for all photographs were computed from readings of photoelectric-type exposure meters obtained by aiming the meter in the same direction as the camera. The computation of exposure was somewhat different from that used in ordinary photography. It was necessary to take into account the color of the portion of the sky used and the differences in filter factors for different sky colors (white and blue). High accuracy in determining exposure was required because of the high contrast and consequent short exposure latitude of most of the films used.

E. Film Viewers

The photographs were observed with two types of viewers. One type provided a magnification of two, three, or five, and the film was viewed through an eyepiece by transmitted light. The other type projected an image of the film onto a ground-glass screen at twelve times magnification.

F. Subjects Photographed

The targets employed in the tests were as follows: aircraft; white, yellow, red, and black cloth sleeves towed by aircraft; magnesium flares towed by aircraft; and dark and light smoke puffs. These targets were photographed against white and blue sky backgrounds when ground haze was slight and when it was appreciable. In general, slant ranges to the target varied from 2000 yards to 30,000 yards, while the altitude of the target varied from 2000 yards to 10,000 yards.

G. General Procedure

Motion-picture photographs of the subject were taken simultaneously with between two and eight cameras, so that the result of a variation in filters, film, etc., would not be affected by changes in the characteristics of the subject. On the other hand, all those studies for which the result might vary as a consequence of a particular characteristic of the subject were repeated numerous times, so that a wide variety of conditions in the subject being photographed were compared before a general conclusion was drawn. Controlled conditions were also maintained as much as possible in such a way that comparisons were affected by the variation of one factor at a time.

After the photographs were made, the film was developed under controlled conditions for the most part, although some was developed purposely by semiskilled personnel under field conditions without their knowledge that a test was in progress.

Finally, relative evaluation of the ease of detecting the target image on the film was made, using several observers and two types of viewers. A grading system of 5 steps or 11 steps was generally employed. This grading process was based on a standard of comparison in some cases and on direct comparison of related photographs in others. The observers graded the photographs completely subjectively. The harmony of the conclusions drawn in extensive series of tests leaves little doubt that no appreciable errors were introduced by these methods. In fact, the nature of the problem and the aim of the project dictated that the evaluation be made by such a subjective method.

The data, including the result of the evaluation of

TABLE II. Data showing the different effects of horizontal and vertical range.

Angle above horizontal (mils)	Horizontal range (yards)	Vertical range (altitude) (yards)	Slant range (yards)	Quality of image of burst	
				No. 39 (blue)	No. 5N5 (yellow)
1087	4464	8103	9251	0	0
625	7428	5240	9080	1	1
930	4158	5391	6800	2–1	1–0
639	4452	3229	5460	3	3–2
305	8582	2647	8980	3–2	2–1–0

the quality of the target image and all pertinent notes, were compiled in tabular form and studied from the point of view of drawing general conclusions which would serve for the selection of the characteristics of film, filter, etc., for future work under a variety of conditions. Variations in prevailing atmospheric conditions with locality and deviations from the prevalent conditions make it impossible to specify from the present data the exact limits of range and altitude for which successful photographs can be obtained for specified targets.

IV. REPORT OF INDIVIDUAL TESTS

A. Effect of Altitude and Range

It is to be expected that the contrast between the target and the sky background would be a function of the distance from the camera to the target. Photographic data accumulated in this study showed, however, that the horizontal and vertical components of this distance are not of equal importance in their effect on contrast. For a dark target on a clear day, subject contrast is decreased considerably more by an increase in vertical range (altitude) than by an equal increase in horizontal range. Thus, if the target is directly overhead, for example, its contrast is lower than if it were at an elevation angle of 45 degrees but at the same distance from the camera.

This distinction between the vertical and horizontal components is minimized when the target is in haze, and becomes negligible in the case of a uniform fog. Of greatest interest in our problem of obtaining photographs at maximum range and altitude is, of course, the case of a clear blue sky; and most of the tests were made under this condition.

A description of one such test, which was typical of several, is as follows:

A series of dark shellbursts were obtained by firing at five specified points in space so distributed that some points were at various altitudes but at the same slant range from the camera, and other points were at various slant ranges but at the same altitude. Several bursts were obtained near each of the specified points. The sky was blue and very little haze was present. Photographs on panchromatic film developed to a gamma of about 1.2 were made with a 6-inch focal-length lens using a Kodak Wratten No. 39 Filter and a Kodak Wratten No. 5N5 Filter. The results are given in Table II, where 0 means that no image of the burst was found, and the numbers 1 to 3 indicate a progressive increase in the quality of the image from poor to good. It is evident that the No. 39 Filter (blue) is superior to the No. 5N5 Filter (yellow) for these conditions.

Figure 1 is a space plot of the results with the No. 39 Filter. This illustrates the great dependence of contrast on altitude and the small dependence on horizontal range. The results show, however, that the horizontal range cannot be extended indefinitely without loss in contrast. If the target were much larger, it is conceivable that the horizontal range could be extended considerably without loss in contrast; but with a 6-inch focal-length lens, the size of the image becomes too small for adequate resolution at slant ranges greater than 8000 yards. Subsequent tests using the 12-inch focal-length lens extended the maximum distance at which constant contrast was obtained for constant altitude, which supports the view that subject contrast and image size should be treated as separate variables and that long-focal-length lenses are advantageous.

It is not intended that an adequate theoretical explanation of the distinction between the vertical and horizontal components of the range with respect to their effect on contrast be given in this paper. It will be sufficient to point out that the effect is a consequence of the relatively high transparency of the atmosphere on a clear day and the finite thickness of the layer. Thus, if a black target were directly overhead and high enough to be at the limit of the atmosphere, the apparent contrast between the target and the background would be zero. Keeping the distance to the target the same but lowering its angle of elevation would bring the target into the atmospheric layer, where it would obscure a portion of the layer contributing to the background luminance and would thus introduce contrast. In this work, visual contrast may be defined as the ratio of the luminance of the background to that of the

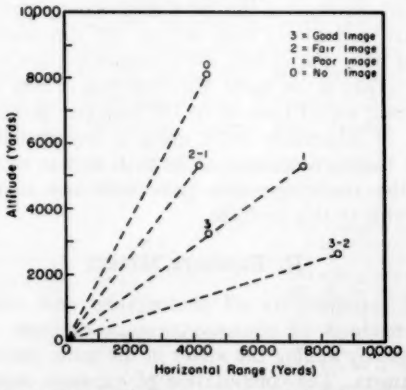

FIG. 1. Relative quality of the photographic images of shellbursts shown as a function of altitude and horizontal range. This shows the great dependence of image quality on altitude and relatively small dependence on horizontal range.

target area. Sunlight scattered by the atmosphere reaches the observer, but part of the scattered light is obscured by the target. It is not the distance to the target which determines contrast but the ratio of that distance to the total distance from the camera to the limit of the atmosphere measured in the direction of the target. This ratio is constant for constant altitude regardless of slant range. Contrast is, of course, not a simple function of this ratio but is complicated by changes in atmospheric composition and density.

For low elevation angles, the contrast is less dependent on this ratio because of the relatively great importance of dust and condensed water vapor in the long path near the ground. The conditions then tend toward those in a uniform fog, where the vertical and horizontal components of the slant range to the target are more nearly of equal importance.

It was important to keep in mind the distinction between the vertical and horizontal components of the range of the target in interpreting the numerous tests made on different occasions over a period of several years. For example, the false conclusion might easily have been drawn that one filter or film was better than another on the basis of tests made on clear days at equal slant ranges but at unequal altitudes. If the altitudes for the tests are not constant, the results are not directly comparable.

B. Lenses

When this work was initiated, only the 6-inch focal-length, *f*:2.7, Baltar motion-picture objective was used. During the progress of the tests, evidence accumulated that 8000 yards represented the maximum slant range at which the target image could be resolved by the lens and film combination used. Since the target could be seen in the visual telescopes at greater ranges, it was suspected that the veiling of the target by atmospheric haze was not the limiting factor, but rather that the size of the target image formed by the camera lens was too small to be resolved by the film or that the resolving power of the lens was insufficient. It was concluded that longer-focal-length lenses should be tried because of the double advantage which they could be expected to provide: (1) greater resolving power because of the greater diameter for any given *f*-value (the *f*-value being dictated by exposure requirements which were the same for any focal-length lens); (2) larger size of the image falling on the film. Comparison tests were, therefore, made in the laboratory using the 6-inch lens and a 12-inch, *f*:4.5, achromatic doublet of a telescopic objective type. This test consisted in photographing gray dots on a uniform white background and comparing the relative quality of the photographic images over a 5-degree and a 2½-degree field, respectively. The size of the dots corresponded to the size of the aerial targets at about 10,000 yards' range. In this test, the 12-inch lens gave results which were definitely superior to those given by the 6-inch lens over the entire field of view of the camera. Comparative field tests of these two lenses and also of a 14-inch focal-length, *f*:6.3, Ektar lens demonstrated that both the 12-inch and 14-inch lenses were superior to the 6-inch lens at long ranges. Moreover, the larger image on the film obtained with the longer-focal-length lenses greatly increased the ease of detectability of the small images at shorter ranges as well as at the longest range. The maximum range at which a detectable image was recorded was 20,000 yards (see Table III) and this was obtained with the 14-inch Ektar lens and a special high contrast film described in the last few sections of this paper.

TABLE III. Effect of change in gamma and spectral region.

Film	Gamma of film	Filter	Maximum slant range (yards)
Panchromatic	1.2	Blue	11,000
Panchromatic	1.2	Red	8,500
Panchromatic	1.2	None	14,000
Infra-red	1.6	Red	7,000
Panchromatic	2.5	Red	20,000
Panchromatic	3.5	None	20,000

It was hoped that even longer-focal-length lenses could be tried, but this was not possible to do within the limited scope of this particular project. It was concluded, however, that long-focal-length lenses are desirable in this work, and it seemed likely that focal lengths of the order of 50 to 100 inches or more may be advantageous if targets having the general size of an airplane are to be photographed at ranges greater than 20,000 yards. Practical limits on focal length would, of course, be set by several factors, one of which would be the difficulty of aiming the camera accurately enough to keep the target within the small field of view imposed by the 35-mm motion-picture film.

Antiflare coatings were tried on the lenses. It was found that such coatings were slightly beneficial in that they increased the contrast of images of dark targets against the sky background in those cases in which the subject contrast was already high. For subjects in which the atmosphere caused the target area to have very nearly the same luminance as the sky, the effect of the lens coating was very small. This result was to be expected, since it is well known from the use of such coatings in ordinary terrestrial photography that the coating increases contrast markedly in the shadow region of the image, but has scarcely any effect on the contrast in the highlight region of the image. Thus, coating of the lenses is recommended in the present work; but only small improvements in image quality should be expected when subject contrast is low.

C. Filters for Dark Gray Targets against Blue Sky

Before a discussion of the spectral effects in photographing targets is begun, it should be pointed out that the gamma of the film is sometimes a function of the wave-length of light. Therefore, this factor was taken

into account in the analysis of the data, and generally the films used had a gamma-characteristic which changed only slightly with wave-length. When blue filters were used, resulting in a slightly lower gamma with normal development, the gamma frequently was raised to that obtained with red light by increasing the development time.

Table II, described in the preceding section, is indicative of the result obtained by a study of the relative merits of a blue and a yellow filter in photographing dark bursts against blue sky. It can be seen that the use of the blue region of the spectrum produced equal or better images at all altitudes and ranges covered by these tests.

Tests of the maximum slant range in photographing an airplane were also conducted. In these tests the airplane was flown at 5000-feet altitude in a direction away from the sun and camera until it disappeared from view just above the horizon. The lens used in this test was a 14-inch focal-length, *f*:6.3, Ektar lens. The sky was blue overhead but gray near the horizon. Table III summarizes the results.

The data of Table III do not necessarily represent the average results at low elevation angles, and the better quality of the image with a blue filter compared to that with a red filter was sometimes found to be reversed. The contrast obtained from these low elevation photographs, involving very long paths through the atmosphere, will depend very much on variations in composition of the atmosphere along the horizontal direction. Also, the presence of distant clouds may not be distinguishable from haze under some conditions, and these would certainly reverse the order of preference of filters. Finally, if the sun is low in the horizon at nearly 180 degrees to the direction of the target, a blue deficiency in the scattered light might be found because of the long path length of the primary sunlight through the atmosphere.

The extent of the tests at low elevation angles and at long ranges has not been sufficient to determine what is the ultimate factor limiting the range. Several factors are involved: the resolving power of lens and film, shimmer due to air currents, and the light-scattering effects described above. It is reasonable to expect that at times, with the equipment being used, each of these factors played a part.

A review of all the tests leads to the conclusion that, other factors being equal, a blue filter produces superior results when photographing a dark target against a blue sky. The exception to this rule might be found at extreme ranges at very low elevation angles when the choice of filter is not critical, since the sky tends to be gray rather than blue and the elimination of the filter is a safe choice. A search of the spectrum by means of a series of filters with progressive change of the short-wave-length cut-off leads to the conclusion that the change in subject contrast with wave-length is gradual; no sharp changes in contrast were observed.

Because of the good results of using a blue filter with a dark target, it is concluded that the proportion of blue light scattered by the upper atmosphere is greater than that scattered by the lower atmosphere. This might be anticipated by the predominance of dust particles and water droplets in the lower atmosphere, which are not so strongly selective in scattering.

D. Filters for White Targets against Blue Sky

The photography of bright, white objects against a blue sky background need not be discussed at length, because it is a much simpler problem than the photography of dark objects against a blue sky. For a spectrally non-selective, white object, the use of a red filter ordinarily gives excellent contrast with a blue sky background, since the red filter has the effect of darkening the blue sky much more than the white object.

Numerous photographs were made of white targets against blue sky with red, yellow, and blue filters. The blue filter gave poor results, while both the yellow and red filters gave good results, although the red filter was noticeably superior to the yellow filter.

It should be noted that any yellow or red objects which have high reflectance for red light will photograph with a red filter as though they were white objects and should be expected to give good results.

Flare targets or self-luminous targets come under the category of targets which would ordinarily be brighter than the blue sky background and would be expected to photograph well with a red filter unless the target emits predominantly blue light. Magnesium flares having candlepowers of 70,000 and 300,000 were towed at slant ranges of 9000 to 12,000 yards from cameras equipped with 12-inch focal-length lenses. Photographs were made with red, yellow, and blue filters against a blue sky background. Both flares photographed very well with the red filter and poorly with the blue filter, while the result with the yellow filter was intermediate. It is believed that successful photographs could have been obtained at much greater ranges with the red filter.

E. Filters for Combination of Dark Gray and White Targets against Blue Sky

In the problem of photographing the black smoke puffs from shellbursts in combination with the magnesium flare target against a blue sky, it was found that the filter which was the best for the smoke was the worst for the flare. Consequently, a compromise was made. A filter transmitting green and blue-green light was used with reasonable success. The use of no filter was nearly as successful. Dark targets at high altitudes have extremely low contrast, while altitude is not a critical factor with a target which is brighter than the blue sky background; and, hence, when a compromise is made, that which lends greater weight to the blue end rather than to the red end of the spectrum results in the best photographs.

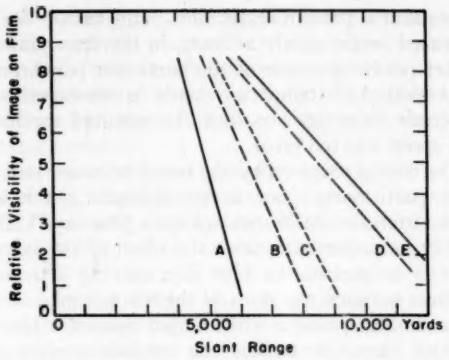

FIG. 2. Relative visibility of photographic images of various cloth targets: A, white; B, yellow; C, red; D, improved yellow; E, black. A blue filter was used over the camera lens in each case

F. Filters for Dark Gray or White Targets against White Sky

While a white target is usually lighter than a blue sky background, it is usually slightly darker than a white sky background and is difficult to photograph under the latter condition, in which it is found that color filters are of little or no help. If the target is colored, the choice of filter to obtain the best result is that which darkens the target more than the background. Except for the case of a white target, excellent photographs were obtained of all sleeve targets. A blue filter was used for the yellow and red targets.

The clouds forming the white background in these tests usually lay beyond the target. In no case were successful photographs made through clouds.

Tests of flare targets against a white sky were not conducted, but it is expected that the flares would be considerably brighter than the background and that satisfactory photographs would be obtained even without the use of filters.

G. Optimum Spectral Reflectance for the Sleeve Targets

The establishment of the blue filter as the best for the photography of the black smoke puffs from shell-bursts gave rise to the related question of the optimum color for the cloth sleeve which is towed by aircraft as the target for the firing. With a white target, the filter which was best for the black smoke was the worst for the target. A black target was tried, since it was expected that it would photograph satisfactorily with the same blue filter which was best for the smoke; but the black target was found to be too difficult to see against the blue sky background with the visual telescopes which were required in aiming the camera. The use of a blue filter in the telescope was of little help because of the large decrease in luminance and the resulting loss in visual acuity.

A white target was relatively easy to see in the visual telescopes, but it did not photograph well with the blue filter required for the black smoke. It was thought that the best solution of the problem might lie in the use of a yellow or a red target. These were tried and were found to photograph with a blue filter nearly as well as the black target and were much easier to see in the telescope than a black target. It was concluded that a yellow target was the best choice, since it photographed with the blue filter as though it were a black object, owing to the high blue absorption of the yellow dye, and was seen in the telescope with nearly as much luminance contrast as a white object against the blue sky, owing to its high reflectance for green and red light, and with more color contrast than a white object.

Figure 2 is a plot of the evaluation of the quality of photographs of various cloth targets towed by aircraft as a function of slant range. The photographs were taken on a clear day, using a blue filter (Wratten No. 39). Under these conditions, the targets photographed darker than the sky. The sun was behind the camera; and, therefore, considerable sunlight was reflected from the targets. It can be seen from the graph that the yellow target represented by line B was not as effective photographically as the black or the red target. This was the result of the particular yellow dye not being as efficient an absorber of blue light as the black dye, as shown by spectrophotometric reflectance curves run on samples of the target material. A different yellow target was then used which gave the results shown by line D in Fig. 2. It had higher blue absorption than the first yellow target, was nearly as effective as the black target photographically, and was much better than the black or the red targets visually. In Fig. 3 are shown the spectrophotometric curves of the two yellow target materials. Curve A applies to the material which was unsuitable, while Curve B applies to the material which gave good results. It should be kept in mind that a yellow target can be made to photograph not only as a dark object but, by the use of a red filter, as a light object. The latter possibility is important when the target is to be photographed simultaneously with a puff of white rather than black smoke from a

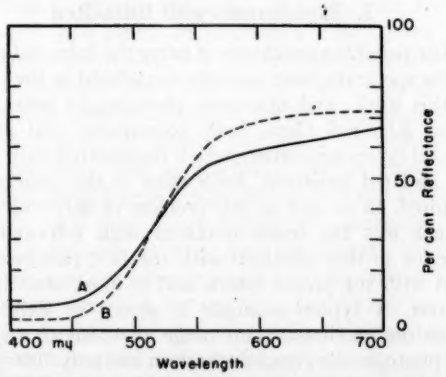

FIG. 3. Spectral-reflectance curve for two yellow targets. Curve A, poor yellow target; Curve B, improved yellow target.

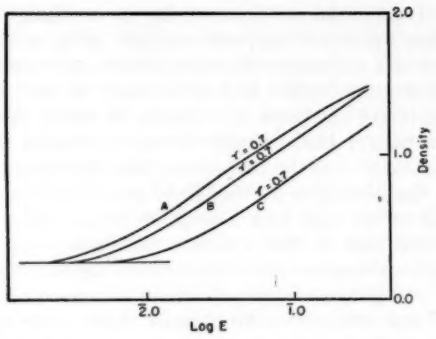

FIG. 4. Density-*versus*-log-exposure curves for typical negative motion-picture films used in the early stages of these tests.

shellburst. A red filter is required for the white smoke; and a black sleeve target would then photograph poorly, since the red filter in effect darkens the blue sky and would lower the contrast between the black target and the sky.

Thus, a suitable yellow target is adaptable to more conditions and will serve more purposes than the black, red, or white targets.

H. Effect of Haze from Condensed Water Vapor

Light scattered by condensed water vapor in the air is less blue, and thus more neutral, than that scattered by air molecules. When an appreciable amount of haze arising from condensed water vapor was present between a dark target and the camera on an otherwise clear day, it decreased the contrast of the image but increased the superiority of the blue filter relative to the red filter. When such haze was present above a dark target on an otherwise clear day, it increased the contrast of the image; and the blue filter was less needed but still of some value. With a light target, the presence of such haze had the effect of decreasing contrast, the red filter being of value but not as much so as with a clear blue sky.

I. Experiments with Infra-Red

The possible advantages of using the infra-red region of the spectrum were carefully considered in the course of this work; and numerous photographs were made using infra-red films, both commercial and experimental types, with filters which transmitted only infra-red and red radiation. Refocusing of the camera was required. In no case in this problem of detecting small images was the result obtained with infra-red film superior to that obtained with the best panchromatic films with the proper filters, and in most cases it was inferior. A typical example is shown in Table III, where the maximum slant range at which an airplane was photographed near the horizon was only 7000 yards with infra-red film, but was 14,000 yards with a low-gamma panchromatic film and 20,000 yards with a high-gamma panchromatic film. The reason for this appeared to lie, partly at least, in the finer grain and higher resolving power of the particular panchromatic films used. An attempt was made to use experimental fine-grain infra-red film, but the required sacrifice in film speed was too great.

The results obtained by the use of infra-red radiation were particularly poor in photographing the black smoke from the shellbursts against a blue sky. This can readily be understood, since the effect of the infra-red filter is to darken the blue sky, leaving little or no contrast between the sky and the black smoke.

In photographing a white target against a blue sky at high elevation angles, the conditions were more favorable for the use of infra-red film; but even in this case it was not as satisfactory as the panchromatic film, the lower resolving power and coarser grain of the infra-red film apparently being the factors responsible.

J. Photographic Emulsion Requirements

1. *Contrast Characteristics*

In the early part of this work, an attempt was made to use a low contrast film because of its wide exposure latitude. Even if the image were invisible or scarcely detectable on this film, the image contrast could be enhanced by printing this film on a second film having high contrast. This method was tried and abandoned because it was found that pseudo-images produced by small particles of dust, dirt, or abrasion were enhanced in contrast along with the image, and it was very difficult to distinguish these from the true image. If the processing and printing could have been done in a commercial establishment of high quality, this method could possibly have been used; but it should be kept in mind that the purpose of this work was to locate the position of the target in space as soon as possible. Consequently, processing was done in the field without benefit of air conditioning and the usual care which the film could have received in a commercial processing station. It was concluded that the film used in the cameras should have high enough contrast so that the resulting negatives could be used directly in the film viewer in locating the target position.

The first tests to determine the optimum photographic emulsion characteristics were made with commercially available 35-mm high speed negative films of the type used in professional motion-picture photography. The density-*versus*-log-exposure curves for typical emulsions of this type, with approximately normal motion-picture processing, are shown in Fig. 4. In the photography of aerial targets, the slope or gradient of the straight-line portion of the D-log$E$ curve is a significant evaluation of the effective contrast of the film, since camera exposures are usually used which place the image on this portion of the curve. The slope of this portion is referred to as "gamma." The gamma of

these films was approximately 0.7 for this processing. These films differed progressively in speed and resolving power, their exposure indices being 32, 64, and 125, and their resolving powers being 100, 95, and 90 lines per millimeter, respectively, according to conventional laboratory tests.

It was soon found that photographs of distant targets made at a gamma of 0.7 were unsatisfactory, the images on the films being very low in contrast and extremely difficult to detect even with careful inspection of the film on a good viewer. The increased resolving power provided by the slowest of these films appeared to be only slightly beneficial; and it seemed likely that the main problem was not that the camera image was too small to be reproduced on these films, but that the camera image was too low in contrast as a result of the veiling of the subject by atmospheric haze. The use of fine-grain developers was found to be of little or no value.

The next step consisted in increasing the contrast of the negatives as much as possible by the use of a high contrast developer, Kodak D-11. This gave a definite improvement in the results. For the motion-picture negative films which were then available, gamma-values of about 1.2 to 1.4 were obtained, depending on the particular film used. This represented approximately the highest gamma which films of this type were capable of attaining; further increase in gamma was not obtained by prolonging the development time. Other high contrast developers, such as Kodak D-19, gave similar results.

This preliminary evidence supported the theoretical conclusion that a high contrast film should be used. It was decided to study systematically the practical effect of progressively increasing the gamma from 1.2 to 4.0 or more. While simple theory indicated that the higher the gamma, the better the result should be, it was expected that the requirement of adequate exposure latitude would place an upper limit on gamma.

Films capable of giving the gamma-values desired for this study were not readily available. The additional requirement that the films be panchromatic to permit the use of various color filters for different subjects made the use of blue-sensitive motion-picture positive films undesirable. Nevertheless, these positive films were tried with a subject (dark target against a blue sky background) which would have required a blue filter if panchromatic films had been used. The desired gammas were readily obtained by suitable choice of development times with Kodak D-16, a developer of the type often used for positive films in motion-picture work. Gamma-values of 1.5, 2.0, 2.5, and 3.0 were obtained with Kodak Motion Picture Positive Film, and 3.0, 3.5, and 4.0 with Kodak Contrast Positive Film. Photographs were made of shellbursts (black smoke) against a blue sky with slant ranges up to 10,000 yards. Four identical motion-picture cameras with 12-inch, *f*:4.5, lenses were used simultaneously to provide a direct comparison of the effects of different gammas for the same burst. Overlap tests were made in extending the comparison to include a greater number of variations in gamma than could be tested simultaneously with only four cameras.

The usual procedure was to start the cameras a few seconds before the burst was expected to occur and stop the cameras a few seconds after the burst occurred. The cameras were usually run at 12 frames per second. A number of bursts were photographed in order to permit the use of a series of different lens aperture settings as a means of obtaining correct exposure.

An inspection of the negatives made in this test led to the following conclusions:

(a) Provided that correct exposure is given, gammas of 2.0 to 4.0 are much superior to gammas of 1.0 to 1.5.

(b) Because of the practical difficulty of predicting the correct exposure with sufficient accuracy, gammas of 3.0 or more are undesirable. Although exposure meters were used, small errors in meter readings, camera settings, and film processing gave undesirably wide variations in negative density when gammas of 3.0 or more were used.

(c) Gammas lying between 2.0 and 2.5 provide the best compromise between the conflicting requirements of adequate exposure latitude and high contrast in the negative to compensate for the low contrast in the subject.

The motion-picture positive films used in this test had the drawback that they gave no record whatever of the azimuth, elevation, and time dials which were imaged by a separate lens on the edge of the film as it passed through the camera. The sensitivity of these blue-sensitive films to the tungsten illumination on the dials was too low, and it was found to be difficult to increase the illumination sufficiently. However, these films provided the desired basic information regarding the optimum gamma.

At the time of these tests, the only commercially available 35-mm panchromatic film capable of giving the desired gamma of 2.0 to 2.5 was Microfile Film. This film was tried, but was found to be much too slow for this work.

Since no 35-mm panchromatic film existed having the desired contrast and speed, the Eastman Kodak Company was asked to produce a film having the desired characteristics; and several experimental emulsions of different speed and contrast were supplied for trial. These were tested under normal field conditions. The conclusion was reached that, while the contrast of these emulsions was satisfactory, they did not have adequate speed for the proper recording of the azimuth, elevation, and time dials in the camera. Moreover, the contemplated use of very long-focal-length cameras with low aperture lenses made it desirable to provide a high speed film even for recording the targets against the sky background. In a subsequent experimental emulsion, a fourfold increase in speed over the previous coatings was obtained without sacrificing the desired contrast. Preliminary field tests indicated that this film

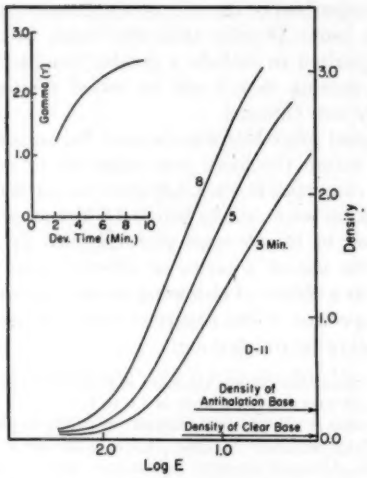

FIG. 5. *D*-log*E* curves for Kodak Linagraph Shellburst Film.

met the requirements satisfactorily. Sufficient quantities were then obtained for trial on a larger scale.

This film was made available in production quantities under the name "S. B. Panchromatic Film," later changed to "Kodak Linagraph Shellburst Film." The term "shellburst" was introduced because of the frequent use of the film with this type of target, although the film was also used successfully with other types of aerial objects.

The *D*-log*E* curves for this film developed in D-11 developer for 3, 5, and 8 minutes at 68°F are shown in Fig. 5. A plot of gamma *versus* development time is shown on the same figure. It can be seen that the desired gamma-values of 2.0 to 2.5 are obtained by using development times of 4.5 to 8 minutes. Essentially the same results are obtained in D-19 with development times of 4 to 7 minutes. Thus, the control of the development time is not critical so far as gamma is concerned; but it is desirable to control development time, agitation, and temperature as a means of maintaining constant film speed to permit accurate determination of correct camera exposure. (See Section IV-g for further details on processing.)

The resolving power of the Linagraph Shellburst Film, expressed in terms of conventional laboratory tests using a test object contrast of 30 to 1, is 120 lines per millimeter. This can be compared with 90 to 100 lines per millimeter for the motion-picture negative films previously used in this work. It should be kept in mind that these resolving-power data are not necessarily applicable in this problem, where the subject to be photographed has very low contrast and a shape quite different from that of the resolving-power test object. However, they serve as a convenient and reasonably significant basis of comparison.

Numerous field tests were made to compare the performance of the Linagraph Shellburst Film with that of the lower contrast motion-picture films formerly used. The results showed unmistakably the advantage in the use of the Linagraph Shellburst Film. Not only were the small images of the target much easier to find on the new film, but the range (distance from camera to target) at which the target was detectable on the film was considerably increased.

Figure 6 shows graphically the relation between the subject contrast, spectral quality of the subject, choice of filter, contrast of the film, and contrast of the final image. The purpose of the graph is to illustrate the advantages which are to be expected from the use of a film having sufficiently high gamma and a filter which is appropriate for the subject. The spectral-energy distribution curves for the blue sky and a distant dark gray target have very little separation in a typical case in this work. The separation is greatest in the blue region, and, consequently, a blue filter is used to give maximum distinction between the image and the background. The ordinate for this graph is the log intensity of the camera image. This ordinate scale becomes the log exposure axis for the adjacent graph, giving the density-*versus*-log-exposure curves for two emulsions having different contrast. In the case of the low contrast film, the $\Delta \log E$ for the image is converted into a ΔD which is frequently too small to be detected on the film. In the case of the high contrast film, the $\Delta \log E$ for the image is converted into a larger ΔD which in most cases can be detected. The increased resolving power of the film, as well as its high contrast, undoubtedly contributes to the ease with which the image is detected.

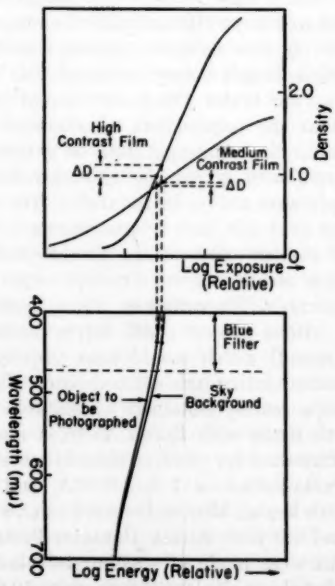

FIG. 6. A filter is chosen which isolates the spectral region where the contrast of the subject is the greatest, and a film is chosen which gives enhanced image contrast.

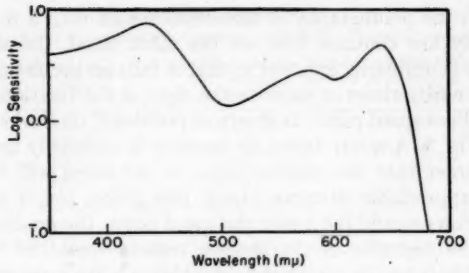

FIG. 7. Spectral-sensitivity curve for Kodak Linagraph Shellburst Film.

2. *The Shape of the Density-versus-Log-Exposure Curve*

The importance of the shape of the *D*-log*E* curve in this work should be mentioned. Not only should the straight-line portion of the curve have a gradient lying between 2.0 and 2.5, but the straight-line portion should be long enough to provide adequate latitude in camera exposure. Since the gradient in most of the toe portion of the curve is too low to be useful in this work, the toe should be short. The straight-line portion should begin at a low density and extend to densities above 2.0, but the shape of the curve above a density of about 2.3 is less important. Practical experience in viewing the film showed that the target image in the viewer is too dark to be seen properly if its density lies in the range of 2.3 to 3.0 or more. This is undoubtedly related to the decrease in visual acuity and contrast sensitivity of the human eye at low luminance levels. The target image is small and is nearly the same density as the image of the sky background, and, consequently, favorable luminance levels in the viewer are required. Increasing the light intensity of the viewer is difficult and impractical, because of the heat and because luminance is then excessive when normally exposed films are viewed. Consequently, an attempt is made in practice to avoid exposures which would give image densities above 2.3, approximately.

Thus, the exposure latitude of the film extends from a point on the toe where the gradient is nearly equal to that of the straight-line portion to a point on the curve where the density is about 2.3. For the Linagraph Shellburst Film, this latitude in exposure (for a gamma of 2.25) is approximately 0.7 in logarithmic units, or 5.0 in arithmetic units. Thus, the maximum tolerance in exposure is slightly more than ± one camera stop, i.e., ±2.

3. *Spectral Sensitivity*

In this work, the photographic emulsion must have sufficient sensitivity throughout the visible region of the spectrum to permit the use of a variety of color filters, the choice of filter depending upon the differences in spectral-energy distribution between the target and the sky background. The filters used most frequently were Kodak Wratten No. 25 (red), Kodak Wratten No. 5 (yellow), and Kodak Wratten No. 39 (blue). To permit the use of such filters, a panchromatic sensitizing was necessary. High sensitivity in the red region of the spectrum was particularly desirable as a means of increasing the speed of the film to the tungsten light used in recording the azimuth, elevation, and time dials in the camera. Consequently, a panchromatic sensitizing which may be classified roughly as Type C, giving high red-sensitivity, was chosen. The spectral sensitivity curve for Kodak Linagraph Shellburst Film is shown in Fig. 7.

As mentioned previously, infra-red-sensitive films (with appropriate filters) were tried extensively in this work, but were always found to be unsatisfactory.

4. *Film Speed*

On days which are sufficiently clear for the photography of distant aerial targets, the luminance of the sky is usually high: 500 to 2000 foot-lamberts during most of the daylight hours. Since the distant target plus atmosphere also has high luminance, it might be concluded that a low speed for the film would be acceptable. There are several reasons, however, why a high speed is desirable, namely:

(a) Rapidly moving objects, such as airplanes or rockets, have optimum contrast against the sky background only if the camera exposure time is short enough to "stop" the motions. At 200 miles per hour, an airplane will fly a distance equal to its own length in approximately 1/10 second. If an exposure time of 1/10 second were used, the luminance difference between the target and the background would, on the average, be only one-half of the luminance difference which would have occurred if the airplane had not moved during the exposure. This assumes that the airplane is moving at right angles to the camera axis. For this case, therefore, exposure times of 1/100 second or less are desirable. This means that high film speed is required to permit the use of color filters and available lens apertures.

(b) Long-focal-length lenses have been shown to be advantageous in this work. A 12-inch lens is to be preferred over a 6-inch lens, other factors being equal; and it is believed that focal lengths as great as 100 inches or more may be advantageous. A high film speed is needed to compensate for the unfavorable relative apertures or *f*-values which ordinarily must be accepted with such long-focal-length lenses.

(c) It is difficult to provide adequate illumination on the azimuth, elevation, and time dials in the interior of the camera, which must be photographed on the edge of the film. The use of high speed film simplifies this problem.

The American Standard Method for Determining Photographic Speed and Exposure Index, Z38.2.1-1947, is intended to apply to terrestrial photography, and the details of the method do not apply to the photography of aerial targets. It is of interest, however, to apply the fractional-gradient speed criterion of the Standard to the *D*-log*E* curve of the Linagraph Shellburst Film in order to obtain a number which can be compared, approximately at least, with the published speeds of more familiar films. In Fig. 8, the fractional-gradient speed point is shown at *S* on Curve A, which is the *D*-log*E* curve for Linagraph Shellburst Film, exposed in an intensity-scale sensitometer to sunlight-

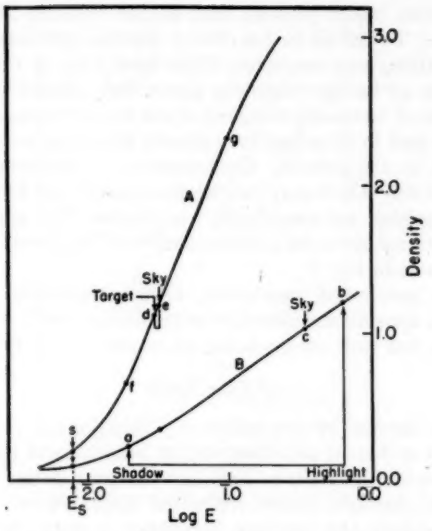

FIG. 8. Graph showing the difference between ordinary landscape photography, where the camera image often occupies a large interval such as "a" to "b" on the *D*-log*E* curve of the film, and aerial target photography, where the image usually occupies a short interval such as "d" to "e." Because of the large difference in the luminance scale of these subjects, the exposure for the sky area differs by approximately ten times in the two cases, even though the two films have the same sensitivity as measured in the toe region of the curve.

quality light for 1/25 of a second and developed to a gamma of 2.5 in D-11. The exposure, E_s at this point is 0.008 meter-candle-second. Speed is defined as $1/E_s$ and is expressed on the American Standard Speed Scale with the prefix 0. Thus, $1/E_s$ for this film is 125, and its fractional-gradient speed may be expressed as 0125. This can be compared with the fractional-gradient speed of 0125 for Kodak Panatomic-X Film, which is a more familiar film to many photographers. While Linagraph Shellburst Film has approximately the same speed as Panatomic-X Film, the latter has lower contrast. Motion-Picture Positive Film, on the other hand, has approximately the same contrast as Linagraph Shellburst Film but only about one-eighth its speed.

In the photography of aerial targets, a camera exposure is ordinarily used which places the image of the sky and the target on the *straight-line* portion of the curve in order that the maximum contrast may be obtained in viewing the negative. In a typical case, the image of the sky may fall at the point, *e*, on Curve A in Fig. 8. There are no deep shadows to be concerned with. Even if the object to be photographed is darker than the sky, it is only slightly darker (because of the atmosphere between the object and the camera) and it falls on the *D*-log*E* curve very near the sky point, as shown at *d* on Curve A. In this work, the exposure used for the sky and the target is approximately five times greater than the exposure at the fractional-gradient speed point, *S*, on the curve.

In the photography of terrestrial scenes with a relatively low contrast film, on the other hand, the sky area is ordinarily exposed so that it falls on the *D*-log*E* curve fifty times or more to the right of the fractional-gradient speed point, as shown at position *C* on Curve B in Fig. 8. A safety factor in exposure is ordinarily used in order that the shadow areas in the scene will fall an appreciable distance above this point, for, if the shadows should fall below the speed point, the gradient in the negative in the shadow regions would be insufficient for the production of a high quality print and the negative would be considered underexposed. In amateur black-and-white photography, a safety factor of two to four times is ordinarily used.

A pertinent point is that, in the photography of aerial targets with Linagraph Shellburst Film, the camera exposure can be reduced to about one-tenth of the exposure normally required in daylight photography of a typical sunlit terrestrial scene using a relatively low contrast film having the same fractional-gradient speed as the Linagraph Shellburst Film. This is a fortunate circumstance and is a consequence of the low contrast of the subject and its high luminance. The low exposure which is used in the photography of aerial targets should, nevertheless, include a safety factor. By reference to Curve A in Fig. 8, it can be seen that maximum gradient occurs between the points, *f* and *g*, which mark the beginning and end of the straight-line portion of the curve. If the image falls below *f*, an undesirable loss in final image quality results. It is recommended that a safety factor of 2 be used in computing the camera exposure, so that, on the average, the exposure of the image is twice the exposure at point *f* in order to allow for errors in measuring the luminance of the sky, in the camera aperture or shutter settings, in film processing, etc.

Practical tests were made, as described in the following section, to determine the relation between sky luminance and optimum camera exposure. Commercially available photoelectric exposure meters were used, and a film rating was determined which would permit the use of exposure meters calibrated in accordance with the American War Standard for Service Model Photographic Exposure Meters (Photoelectric Type) Z52.12-1944.

K. Determination of Correct Camera Exposure

It is important in this work that the camera exposure be determined accurately. Since a high contrast film is used, a slight error in exposure causes a relatively large change in density in the final image. The technique used was to determine the sky luminance by pointing a photoelectric exposure meter at the portion of the sky containing the target and to compute the exposure by means of the calculator dial on the exposure meter.

Practical tests were made to determine the relation

TABLE IV. Exposure data.

Meter reading of sky (c/sq. ft.)	Optimum camera exposure, without filter, at 16 frames per second (1/30 second) Blue sky	White sky
100	*f*:22	*f*:20
200	*f*:32	*f*:28
400	*f*:45	*f*:40
800	...	*f*:57

between sky luminance and optimum camera exposure. A rating for the film was determined which would permit the use of photoelectric exposure meters calibrated in accordance with the American War Standard, for Service Model Photographic Exposure Meters (Photoelectric Type) Z52.12-1944. The calibration formula given in this Standard has recently been included in the American Standard for General-Purpose Photographic Exposure Meters (Photoelectric Type) Z38.2.6-1948.

Table IV summarizes the results of numerous practical tests, the variables being sky luminance, exposure time, and lens aperture (*f*-value). The photographic effectiveness or actinic value of the blue sky was found to be appreciably higher than that of the white sky for the same luminance. For a meter reading of 400 candles per square foot for the blue sky, the optimum camera exposure was 1/30 second at *f*:32 for the Linagraph Shellburst Film developed to a gamma of about 2.25 in D-11. For a white sky giving the same meter reading, the optimum exposure was 1/30 second at *f*:28.

From these data and from the calibration formula given in American Standard Z38.2.6-1948, it can be deduced that the rating to be used for the Kodak Linagraph Shellburst Film on the exposure meter dial is 200 for blue sky and 160 for white sky. This applies, of course, only to exposure meters calibrated in accordance with this American Standard. This also assumes that the "normal arrow" is used on the calculator dial of the meter. The following formula can be used instead of the calculator dial of the meter:

$$t = 1.25f^2/B \times R,$$

where t = exposure time; f = lens aperture or f-number; B = luminance of the sky in candles per square foot; and R = film rating (200 for blue sky and 160 for white sky for the Linagraph Shellburst Film). If a filter is used over the camera lens, the filter factor should be inserted in the denominator of the equation.

The film ratings derived in these tests for use with exposure meters are analogous to the film "exposure indices" which are widely used in terrestrial photography. The conditions of derivation and use in the present work, however, differ so widely from those involved in terrestrial photography that it is not strictly appropriate to refer to the present film ratings as exposure indices.

Photoelectric exposure meters of the type ordinarily used do not actually measure the true visual luminance of the portion of the sky to be photographed. The meters are more blue-sensitive than the normal human eye and their angle of view is greater than that of cameras used in this work. The errors are ordinarily not large, however, and are effectively canceled in the empirical method which is here used for relating the variables. In a particular case, the meter reading on the sky was found to be 12 percent greater than the true luminance. The error due to the wide angle of view was negligible in most cases, since the sky was of nearly uniform luminance over the area involved. Large errors, however, can result if the sun is in the field of view of the meter; and care must be taken to prevent direct sunlight from entering the meter.

The use of a blackened tube over the exposure meter to restrict its field of view to about ±10 degrees is recommended, although this, of course, requires a recalibration of the meter.

Since filters are nearly always used in this work, it was necessary to determine the filter factor for each filter for the blue sky and the white sky conditions, the filter factor being the increase in exposure required because of the filter. Numerous tests were made in order to determine these factors accurately. The results are shown in Table V. These values may differ from those ordinarily published for these filters, since the published values usually apply to sunlight- or tungsten-quality light rather than to white sky or blue sky.

Since there is no separate scale for filter factors on the computer dials of most exposure meters, the method of using the filter factor is to divide the film rating number by the filter factor and use the resulting number on the computer dial as though it were a film rating.

Because of the high contrast of the film and the consequent need for accurate determination of exposure, it is recommended that preliminary tests be made whenever possible in order to establish the optimum exposure for the particular equipment and sky conditions involved. A series of different camera exposures should be made, centering about the estimated value, and a correlation of exposure-meter reading with correct exposure can then be established by inspection of the results obtained on the processed film.

1. *Processing*

Since the image on the film of the distant target is usually very small and difficult to find, it is important

TABLE V. Filter factors.

Kodak Wratten Filter No.	Blue sky	White sky
5	3	2.5
5N5	10	8
15	4	3
25	8	5
29	12	8
39	2	4
47	3	5
58	6	6

TABLE VI. Kodak D-11 Developer.

	Avoirdupois	Metric
Dissolve chemicals in the order given:		
Water, about 125°F (50°C)	64 ounces	500.0 centimeters
Elon	60 grains	1.0 gram
Kodak Sodium Sulfite, desiccated	10 ounces	75.0 grams
Kodak Hydroquinone	1 oz 90 grains	9.0 grams
Kodak Sodium Carbonate, monohydrated	4 ounces	30.0 grams
Kodak Potassium Bromide	290 grains	5.0 grams
Cold water to make	1 gallon	1.0 liter

that the film be developed to a gamma of at least 2.0. A gamma greater than 2.5 is not recommended, however, because of the difficulty of predicting exposures accurately.

The film must be kept clean and free from abrasion and dirt marks. This means that the processing solutions and equipment must be kept clean and the handling of the film must be done with great care.

Kodak D-11 Developer is recommended for use with the Linagraph Shellburst Film. The formula is shown in Table VI.

In the field work which was ordinarily done on this project, the films were developed in 100- or 200-foot lengths using the Stineman Reel and the manipulation technique specified by the U. S. Army Signal Corps. A number of other methods of processing, however, can be used; and the film can, of course, be processed in a commercial processing station.

A development time of 5 minutes in D-11 at 68°F is recommended. The temperature of the processing solution should be as near 68°F as possible. If the developer temperature cannot be kept at 68°F, the development times shown in Table VII for the different temperatures should be used. It should be noted, however, that the control of gamma and film speed is more difficult at the shorter development times which must be used for higher temperatures, and that the higher temperatures should be avoided whenever possible. Kodak D-19 or D-16 Developers can also be used. Development times are approximately the same as for D-11.

After development, the film is rinsed in water for a few seconds and then placed in a hardening bath, such as Kodak Tropical Hardener or Kodak SB-4. The film should remain in the bath for 3 minutes and should be agitated frequently. The film is then fixed for 10 to 20 minutes at 68°F in an acid hardening fixing bath, such as Kodak F-5. While the film is still on the reel, it is washed for 20 to 30 minutes in fresh running water. The surfaces are wiped lightly with clean absorbent cotton well-saturated with water, and wiped again carefully with a clean, well-wrung cotton pad before winding the film on the drying drum or reel. No abrasive particles, such as sand, should be allowed on the cotton because of the importance of avoiding scratches on the film.

V. CONCLUSIONS

1. In the photography of objects in the upper atmosphere from the ground, 12-inch and 14-inch focal-length lenses have been shown to be better than a 6-inch focal-length lens, and it is believed that focal lengths as great as 100 inches or more may be advantageous.

2. For black or dark gray objects against a blue sky, an increase in vertical range has been shown to give a greater decrease in subject contrast than an equal increase in horizontal range. Consequently, tests made of different lenses, films, or filters are not directly comparable unless both horizontal and vertical components of the range are held constant.

3. The most difficult problem was the photography of black or dark gray objects against a blue sky. For these conditions, a blue filter gave the best results.

4. The photography of a bright, white object against a blue sky is less difficult than that of dark objects against a blue sky. A red filter is recommended. A deep yellow filter is nearly as satisfactory in some cases, and it has the property of having higher transmittance than a red filter.

5. Infra-red film was not advantageous in this work. It was especially poor for the photography of dark objects against a blue sky. It was expected to be satisfactory for the photography of white objects against a blue sky, but the tests showed that the high contrast panchromatic material used with a red filter was superior. This result may be attributed to the finer grain and higher resolving power of the particular panchromatic film used.

6. In the photography of antiaircraft shellbursts, where a moving reference target (towed by aircraft) is to be included, the optimum color for the target depends on the relative spectral quality of the smoke and the sky background. For a black or gray puff of smoke against a blue sky, a blue filter is used over the camera lens and the optimum target color is then black, or any color which has a low reflectance for blue light. Thus, a yellow target or a red target is also satisfactory, if it has low reflectance for blue light. For a white puff of smoke against a blue sky, a red filter is used over the camera lens and the optimum target color is white, or any color which has high reflectance for red light. A yellow target dyed with a suitable yellow dye was found to be as satisfactory as a white target. Thus, the yellow target fulfilled the dual purpose of being as

TABLE VII. Recommended development times in D-11.

Temperature (°F)	Development time (minutes)	Temperature (°F)	Development time (minutes)
62	8	70	4½
64	7	72	4
66	6	74	3½
68	5	76	3

satisfactory as the black target when used with the black smoke, and as satisfactory as the white target when used with the white smoke.

7. Black or red targets against a blue sky were found to be very difficult to see in the tracking telescopes. On the other hand, white or yellow targets were relatively easy to see. The yellow target was adaptable to more conditions and served more purposes than the black, white, or red targets, provided that the yellow material chosen has low reflectance to blue light and high reflectance to red light.

8. To obtain photographs of objects at high altitudes near the limit of the earth's atmosphere, the object should be brighter than the blue sky background and a red filter should be used to darken the sky. If the object is illuminated by the sun, a white paint, or a yellow paint having high reflectance in the red region of the spectrum, is usually satisfactory. Contrast can be further increased by making the object self-luminous. Good results were obtained by the use of magnesium flares.

9. The film used in this work should have high contrast and high resolving power. The gradient of the used portion of the density-*versus*-log-exposure curve for the film should lie between 2.0 and 2.5. Gradients higher than 2.5 would be better than a gradient of 2.5, if correct exposure were always obtained; but, because of the short exposure latitude which accompanies the high gradient, the difficulty of obtaining correct exposure then becomes too great in practice. An upper limit of 2.5 is therefore recommended. A high film speed is needed because of the relatively small apertures which are obtained with long-focal-length lenses, because of the need to use short exposure times to "stop" the motion of rapidly moving targets, and because of the difficulty of getting adequate illumination on the azimuth, elevation, and time dials which are ordinarily photographed on the edge of the film.

10. A high contrast, high speed panchromatic film, especially designed for this work, has been shown to give good results. This film is available commercially under the name "Kodak Linagraph Shellburst Film." The characteristics of this film are described in detail in this paper. Exposure and processing data are given.

11. Commercially available photoelectric exposure meters can be used satisfactorily in determining correct exposure in this work. Calibration data are given for the particular conditions involved.

VI. ACKNOWLEDGMENTS

The writers wish to express their thanks to Dr. Loyd A. Jones, of the Eastman Kodak Company, for his helpful guidance in a considerable portion of this work, particularly in the portions dealing with photographic emulsions and light filters.

Special mention should be made of the contribution made by Colonel R. H. Kreuter, under whose personal direction the practical field tests were made by the Antiaircraft Artillery Board at Fort Monroe and Camp Davis. His understanding of the problem and wholehearted cooperation with the writers greatly facilitated this work.

A number of individuals on the Antiaircraft Artillery Board, on the National Defense Research Committee, in the Signal Corps, and in the Eastman Kodak Company assisted materially in this work; and the writers are appreciative of their contributions.

Letters to the Editor

Isotope Shifts in Enhanced Samarium Isotopes

D. D. SMITH AND J. R. MCNALLY, JR.
Oak Ridge National Laboratory, Y-12 Area, Oak Ridge, Tennessee
September 1, 1950

PRELIMINARY isotope shift studies have been made on the first calutron enhanced isotopes of a rare earth element.[1] This element, samarium, is of especial interest because of its reported alpha-activity,[2] its missing Sm^{146} nuclide,[3] its anomalous isotope shifts,[4,5] and uncertain nuclear spin assignments.[5]

We have photographed the spectrum of enhanced samples of Sm^{144} (72.13 isotopic percent *versus* 3.14 percent natural abundance) and of Sm^{154} (92.10 percent *versus* 22.53 percent) in the wave-length region 2200A to 8450A at dispersions of 1.2A/mm to

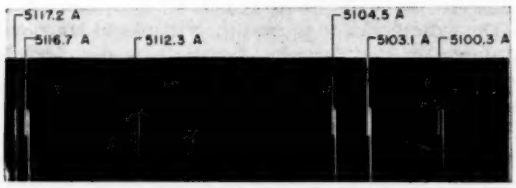

FIG. 1. Spectrum shifts in enhanced samarium samples. Top spectrum Sm^{144}, bottom Sm^{154}.

0.4A/mm. More than 400 shifts have been observed with the Sm^{154} lines to the violet of the Sm^{144} lines in the majority of cases.

Figure 1 illustrates large isotope spectrum displacements at 5100A. No appreciable shift is observed in the line at 5117.2A.

We hope to extend in a more complete report the work of Brix and Kopfermann in the configuration identification of levels from their isotope displacements.

This report is based on work performed under contract for the Atomic Energy Commission by the Isotope Research and Production Division, Oak Ridge National Laboratory, Y-12 Area, Carbide and Carbon Chemicals Division, Union Carbide and Carbon Corporation, Oak Ridge, Tennessee.

[1] C. P. Keim, H. W. Savage, and Boyd S. Weaver, submitted to Phys. Rev.
[2] First reported by G. von Hevesy and M. Pohl, Nature **130**, 846 (1932). Activity variously reported as being due to Sm^{148} by T. R. Wilkins and A. J. Dempster, Phys. Rev. **54**, 315 (1938); to Sm^{152} by A. J. Dempster, Phys. Rev. **75**, 1125 (1948); and to RaD impurity by C. Haenny, M. Najar, and M. Gaillond, Helv. Phys. Acta **22**, 611 (1949).
[3] M. G. Ingraham, D. C. Hess, Jr., and R. J. Hayden, Phys. Rev. **73**, 180 (1948), conclude Sm^{146} is probably <0.002 percent natural abundance.
[4] H. Schueler and T. Schmidt, Z. Physik **92**, 148 (1934); P. Brix, Z. Physik **126**, 431 (1949).
[5] P. Brix and H. Kopfermann, Z. Physik **126**, 344 (1949). $I \geq 3/2$ reported for both odd isotopes.

A Four-Figure Method of Ray Tracing

W. H. STEEL
National Standards Laboratory, Commonwealth Scientific and Industrial Research Organisation, Sydney, Australia
September 25, 1950

IN the calculation of the aberrations of an optical system by trigonometrical methods using the usual formulas, the aberration is usually found as the difference between two nearly equal quantities; and to obtain the aberrations correct to 2 or 3 significant figures, 6-figure accuracy is generally required in the ray traces. Four-figure accuracy is, however, quite sufficient in the calculations if the aberration is calculated at each surface and carried forward through the system, as in the standard procedure given by Conrady[1] for the calculation of spherical aberration as an optical path difference.

A knowledge of the optical path difference alone does not enable the system to be corrected for spherical aberration, however, for the value of the marginal spherical aberration is also required.

We first outline a method for calculating the marginal spherical aberration at each surface based on ray traces of 4-figure accuracy, and show that the chromatic aberration and coma from the same ray traces may be found. For this purpose a more suitable measure of spherical aberration than the longitudinal spherical aberration is required, as the magnitude of the latter changes greatly at each surface. This is found by defining an angular spherical aberration for the marginal ray by analogy with Conrady's[2] definition of primary angular aberration. In his notation, the angular aberrations AA before a surface, and AA' after the surface, are equal to $(LA/l)\sin U$ and $(LA'/l')\sin U'$ respectively.

For a single surface it can readily be shown that

$$AA' = (NP'/N'P)AA + [(P'/P) - 1]\sin I' \qquad (1)$$

and for the succeeding surface

$$AA_2 = AA'_1 y_1/y_2, \qquad (2)$$

where $P = L\sin U$, $P' = L'\sin U'$ for the marginal ray, and $y = lu$ for the paraxial ray. When a marginal ray trace is carried out by Smith's method,[3] the quantity $P'/P - 1$ is found in the course of the calculations; and the angular aberration can be found, by using Eqs. (1) and (2) at each surface, with very little extra calculation.

For most optical systems a combination of this procedure with the optical path difference formulas gives the axial aberrations from the results of one marginal and one paraxial ray trace. Both traces are carried out to 4-figure accuracy by Smith's method for the marginal ray, and the angular spherical aberration is found as above. The following further aberrations can be calculated from the same ray traces:

(1) The optical path difference ΣW at the marginal focus, where

$$W = -[(1+\cos U)(1+\cos I)(1+\cos I') \times (1+\cos U')]^{-1} N(P'-P)\sin I \qquad (3)$$

for each surface.

(2) Chromatic aberration, which by Conrady's path difference formula[4] is ΣE, where

$$E = (d'-D')(N_F - N_C) \qquad (4)$$

for each component, calculated for a marginal ray of wave-length 5550A.

(3) The coma, which in terms of the quantities of the last surface is given to sufficient accuracy by

$$OSC' \doteq (\sin U'/u') - 1 - (l'/l' - l_{pr}')\cdot(AA'/u'). \qquad (5)$$

[1] A. E. Conrady, M.N.R.A.S. **65**, 594 (1905).
[2] A. E. Conrady, *Applied Optics and Optical Design* (Oxford University Press, 1929).
[3] T. Smith, Proc. Phys. Soc. London **17**, 252 (1922).
[4] A. E. Conrady, M.N.R.A.S. **64**, 182 (1904).

The Refractive Indices of Lithium Fluoride*

D. S. L. DURIE
Division of Physics, National Research Council, Ottawa, Canada
September 25, 1950

TO this date no fifth-place refractive indices for LiF have been published in scientific journals: the only data that are available from these sources are those of Guyulai[1] and Hohls,[2] which are accurate in the third decimal place. However, fifth-place

indices have been determined by Kessler of Zeiss, which are recorded, it appears, only in Merte's *Das photographische Objectiv seit dem Jahre 1929* (Springer-Verlag., Vienna, 1943).

Kessler's values cover the wave-length region from 0.185 to 1.08μ at twenty-nine wave-length points. Some measurements have been taken in this laboratory in the region from 0.3 to 2.5μ, and they are in agreement with his values. Table I lists our data

TABLE I. Indices of LiF at 20°C.

Wave-length (A)	n (NRC)	n (Kessler)
3021 Hg	1.40811	1.40811
3341 Hg	1.40408	1.40408
4046 Hg	1.39845	1.39849
4358 Hg	1.39681	1.39682
5461 Hg	1.39302	1.39305
5875 He	1.39209	1.39211
6678 He	1.3907	...
7065 He	1.3901	...
8408 A	1.3887	...
10830 He	1.3865	1.38650
20581 He	1.3782	...

taken at 20°C together with those of Kessler taken at the same wave-lengths.

Since there was no statement regarding the accuracy of his data, it may be assumed that an error of at least 1×10^{-5} can occur. Such an error, when added to a calculated possible error of 3×10^{-5} in our figures, accounts for the maximum discrepancy, namely, 4×10^{-5}. The indices listed to the fourth place only have an accuracy of 10×10^{-5}.

The measurements were made with the reflecting autocollimating spectrometer shown in the diagram. The virtual image of the entrance slit (N) is at the focal point of the spherical mirror (C). Light illuminating (N) passes under the large mirror (M) and is collimated by (C). The mirror (M) thrusts into the collimated light from above, thus intercepting part of it and directing it toward the 30° prism (P) situated on the prism table (T), the rotations of which can be measured by means of the circle microscopes (A) and (B). An aluminum coating on one of the prism faces directs

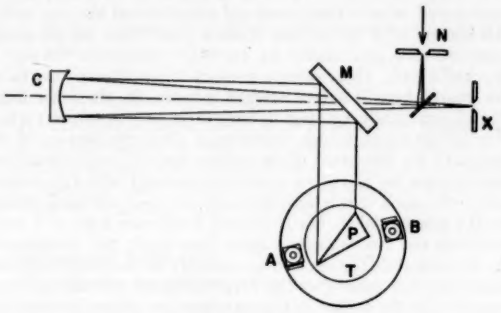

FIG. 1. Reflecting autocollimating spectrometer.

the light back in the direction from which it came; and it is ultimately detected at the exit slit (X) by means of a photo-cell, a PbS cell, or the eye plus a microscope.

The speed and convenience with which minimum deviation settings can be made in the extravisual regions, together with the fact that it is an achromatic system, are the chief advantages of the method. At the same time certain limitations are imposed. The method is inherently less sensitive than that employing minimum deviation in the usual way and the presence of the large mirror (M) results in some degree of vignetting or aperture losses.

* Contribution from National Research Council, Ottawa, Canada, N.R.C. 2249.

[1] Z. Guyulai, Z. Physik **46**, 80 (1928).

[2] H. W. Hohls, Ann. Physik **29**, 433 (1937).

JOURNAL OF THE OPTICAL SOCIETY OF AMERICA VOLUME 40, NUMBER 12 DECEMBER, 1950

Book Reviews

Electron Microscopy: Techniques and Applications

R. W. G. WYCKOFF. Interscience Publishers, Inc., New York, 1949. Pp. 248+vii. Price $5.00.

The Electron Microscope, Its Development, Present Performance and Future Possibilities

D. GABOR. Chemical Publishing Company, Inc., New York, 1948. Pp. 164+viii. Price $4.95.

Elektronenoptik I, Grundzüge der theoretischen Elektronenoptik

ALEXANDER A. RUSTERHOLZ. Verlag Birkhäuser, Basel, 1950. Pp. 249. Price 25 Swiss francs (paperbound); 29 Swiss francs (stiff cover).

The literature of electron optics and of electron microscopy shows curious ups and downs. At the very first there were some really competent books on the subject, such as Brüche and Scherzer's *Geometrische Elektronenoptik* or Maloff and Epstein's *Electron Optics*. Then came a period, mostly during the war years when the books appearing on the subject had a deplorably low quality. In the post-war years, the quality of books on those subjects reverted to a very high standard, and it is a pleasure to report that this trend is still kept up in some of the most recent books on the subjects.

The order in which these three books are reviewed is neither chronological nor alphabetical. First is listed the least theoretical one: Wyckoff's book which, as its title implies, is essentially a treatment of techniques and applications of the electron microscope. The book consists of ten chapters, seven of which make excellent reading. These chapters are the ones in which the author discusses many of the techniques applied in electron microscopy and the conclusions from the results achieved in certain applications. The applications discussed, as well as the techniques applied, are somewhat restricted to biological subjects. While this fact may restrict the book's usefulness, in a sense it enhances the value of the volume because the author is on extremely familiar grounds. It is no wonder that the treatment is always clear and lucid because many of the techniques and applications have been developed by the author himself. Nowhere is the presentation of these subjects as comprehensive as in this book. This reviewer wishes that he could add as much praise for the first three chapters which contain an introductory chapter, a chapter on electron microscopes, and a chapter on the adjustment of the microscope. The first two chapters are rather short and not always quite accurate. The third one leans a little toward the incomplete side by giving the adjustment of one particular type of microscope without giving much help to users of other types of microscopes. On the whole, however, the reader of this book will be essentially interested in the later

chapters and the lower standards applied in the first chapters do not take anything from the value of this excellent book.

In an entirely different vein is the recent, second edition, book by Gabor. The author is a well-known physicist who has repeatedly contributed to both theoretical and experimental electron optics. His treatment of the subject is much more from the physicists' point of view and makes an excellent companion volume to Wyckoff's book. Those aspects in which Wyckoff may have failed are treated here in a very original manner. On the other hand, there is practically nothing, or very little, on the subjects which Wyckoff treats with high competence. The organization of the book and the treatment of its subject make it very stimulating reading even for physicists already acquainted with this subject and at the same time it does not make the book too hard reading for the non-specialist. Mathematical details are kept to a strict minimum and can be easily skipped by a reader not interested in the theoretical side of electron microscopy. All the praise here contained does not mean that this reviewer agrees with all the views expressed by the author but, even where the author's views may be open to discussion, the contents are presented in such a lucid manner that this reviewer, at least, finds it very refreshing.

The third book here reviewed is apparently the first volume of a larger treatise on electron optics. Whereas this first volume (which constitutes at the same time Volume 15 of a collection called *Lehr- und Handbucher der Ingenieurwissenschaften*) is entirely devoted to theoretical electron optics; the preface announces a second volume which has been devoted to questions concerning applied electron optics, particularly problems of cathode-ray tubes and of the electron microscope. The organization of the material in the first volume at hand is excellent. The whole subject of theoretical electron optics is built up in a very logical and straightforward manner with a very good presentation of the work accomplished by the different theoretical schools engaged in this subject. The treatment almost everywhere is reasonably rigorous, yet complete enough for a person to use the book as a compendium of the most important theoretical material published on the subject. At the same time, approximate methods used in field mapping and in ray-tracing are not neglected and where it is needed the relation of the theory to the experiment is clearly outlined, too. In view of the very successful presentation of the subject, this reviewer regrets that the author did not include in his book at least one extensive chapter on the electron optics of time-variable fields. With the growing importance of transit-time devices, a comprehensive treatment of the time-variable fields is still missing in the electron optical literature and a succinct presentation of this subject would be desirable.

The typography of all three books is excellent. Wyckoff's book is very well illustrated, and most of the rather delicate details of electron micrographs come out very well in reproduction.

L. MARTON
National Bureau of Standards
Washington, D. C.

Handbook of Experimental Stress Analysis

M. HETÉNYI, editor. John Wiley and Sons, Inc., New York, 1950. Pp. 1077+xii. Price $15.00.

There are two basic reasons why there should be a growing interest in the application of experimental methods to the solution of practical problems in engineering. In the first place, the experimental methods are frequently the only means of obtaining even an approximate answer to many problems; in the second place, they often provide a sufficiently accurate result much more quickly than available methods of mathematical analysis. The book under review is one which will be of interest to many readers, both to those who are using and developing these methods and to those who may wish to find out what sort of problems can be solved by experimental stress analysis. The eighteen chapters and three appendices in the book have been contributed by different authors. The book was initiated by the Society for Experimental Stress Analysis to provide a unified presentation of all existing methods of determining mechanical strength.

Some of the chapters are descriptions of principal methods of measurement and others deal with major fields of application. The appendices discuss theoretical subjects which are of fundamental importance in the planning and interpretation of experimental stress work. Thus, L. H. Donnell and W. T. Savage wrote a chapter on mechanical gauges and extensometers. Additional chapters on techniques for strain measurement are: optical gauges by J. L. Maulbetsch; electrical-resistance gauges and circuit theory by C. O. Dohrenwend and W. R. Mehaffey; electric-inductance gauges by B. F. Langer; electric-capacitance gauges by B. C. Carter, J. R. Forshaw, and J. F. Shannon; and strain rosettes by J. H. Meier. Measurement of vibratory motion using a variety of techniques is discussed by J. Ormondroyd, R. B. Allnutt, F. Mintz, and R. D. Specht. Testing machines for both static and dynamic loads are reviewed by J. Marin. The use of brittle coatings is treated by the editor, M. Hetényi. The subject of photo-elasticity is discussed in two parts, fundamentals and two-dimensional applications by T. J. Dolan and W. M. Murray, and three-dimensional methods by D. C. Drucker. X-ray analysis techniques are described by C. S. Barrett. Methods of crack detection are presented by C. Lipson.

Six chapters are, separately, surveys of certain topics or aspects of experimental stress analysis. C. W. MacGregor gives an account of mechanical properties of materials. C. R. Soderberg covers the subject of working stresses and C. J. Horger that of residual stresses. The interpretation of service fractures is discussed by R. E. Peterson with many descriptions of typical fractures. The use of structural models is treated by J. B. Wilbur and C. H. Norris. Finally, a complete exposition on the use of analogies is given by R. D. Mindlin and M. G. Salvadori.

The appendices are devoted to the fundamentals of the theory of elasticity by S. P. Timoshenko, dimensional analysis by J. N. Goodier, and the precision of measurements by M. Hetényi.

The book is well produced and clearly printed. The diagrams and pictures are easily interpreted. The book was arranged and edited by M. Hetényi who, in addition, wrote one of the chapters and one of the appendices. This is one of the indispensable books for any engineer concerned with the design and improvement of mechanical structures.

SAMUEL LEVY
National Bureau of Standards
Washington, D. C.

Manual of Standardized Procedures for Spectrophotometric Chemistry.

HAROLD J. FISTER. Standard Scientific Supply Corporation, New York, 1950. Pp. 500. Price $30.00.

This manual which has code-numbered paging is in a loose-leaf binder which has been designed for expansion and change of methods. The methods are for the most part biochemical assay procedures for a clinical laboratory involving colorimetric or spectrophotometric determination of the particular constituent or element. Each procedure is in general given with references, principles, sample procurement, test procedure, and calibration procedure. The methods are varied for different types of spectrophotometric equipment or colorimeters equipped with a narrow band-pass filter. The methods are essentially taken from existing literature and are arranged in a convenient form for the medical or clinical technician.

WALLACE R. BRODE
National Bureau of Standards
Washington, D. C.

International Optical News

International Commission of Optics: Recommendations Concerning Experimental Conditions for Investigations on Visual Sensitivity and Discrimination

At the London meeting of the International Commission of Optics of July, 1950, which was reported in these columns in October, a special *ad hoc* committee was appointed to draw up a set of recommended standard practices applicable to experiments in physiological optics. It was noted that it is very difficult to make the desirable, close comparisons of data taken in various laboratories, since the details of experimental conditions are seldom, if ever, sufficiently similar. In order to correct this unsatisfactory state of affairs, it was suggested that a certain standard set of conditions might be employed at some time during experimental programs on vision and the efficiency of vision through instruments.

It should be emphasized that there is no desire to impose one set of experimental conditions to the exclusion of others. On the contrary, it is hoped that each laboratory will compare results obtained under the "standard conditions" with those obtained under different experimental conditions. For example, an observer might compare results obtained using the standard test with similar results obtained using the Landolt *C*. Comparison between the results obtained using the standard illuminant and others obtained using monochromatic light would also be very useful. The I.C.O., through its national committees, proposes to ask experimenters in this field to include, when appropriate, some experiments carried out under the standard conditions. These experiments will then provide a basis for a quantitative comparison with results obtained in other laboratories.

The working committee that was appointed to study this important subject consists of R. W. Ditchburn and W. S. Stiles of the United Kingdom, J. M. Otero of Spain, and A. Arnulf of France (Chairman). The preliminary draft of its recommendations is given here, in the hope that it will be carefully studied by all workers in experimental physiological optics, and that comments, criticisms, and suggestions will be sent to the undersigned. After their collation and consideration by the U. S. A. National Committee of the International Commission of Optics, these recommendations will be submitted to the I.C.O. working committee as a statement of the opinion of U. S. workers on this proposal for international standardization.

Proposed Standard Conditions

1. Test Object

(*a*) *Shape*

Perception test: (i) Circular or square disk.

(ii) Vertical line whose length subtends an angle of at least 5° at the eye of the observer and whose ratio of length to breadth is at least 20.

Resolution test: A pair of one of the elements just described, with their centers separated by a distance equal to twice the width of one object. The limit of resolution is defined by the distance between centers (or axes of symmetry) when the two objects are just resolved.

(*b*) *Contrast*

Definition: $C=(B-b)/B$, where B=brightness of background, and b=brightness of object.

Contrast>0 and varying from 0 to 1 when the object is darker than the background.

Contrast<0 and varying from 0 to $-\infty$ when the object is brighter than the background.

It is recommended that a logarithmic scale of contrast be used.

2. Spectral Composition of Light

The composition should be the same for object and background. White light should be used: I.C.I. Standard Illuminants *A*, *B*, or *C*. Illuminant *A* is preferred for low brightness experiments. If filters are used to reduce brightness, great care should be taken to obtain accurately neutral filters.

3. Background Brightness

The following brightnesses are recommended:

(i) 10^{-2} stilb.=9.3 candles/ft.^{2}=29 e.f.c.*

(ii) 5×10^{-6} stilb.=4.7×10^{-3} c/ft.^{2}=1.45×10^{-2} e.f.c.

(iii) 10^{-8} stilb.=9.3×10^{-6} c/ft.^{2}=2.9×10^{-5} e.f.c.

All brightnesses are to be measured on the photopic scale.

4. Field of View

The angle subtended by the background, at the eye of the observer, must not be less than

(i) 10° for 10^{-2} stilb.

(ii) 20° for 5×10^{-6} stilb.

(iii) 30° for 10^{-8} stilb.

5. The Observer

Observers with seriously subnormal vision must not be used—see definition of normal observer in Appendix 1.

Adaptation: One hour in artificial light (less than 2 foot-candles) followed by 40 minutes in darkness for adaptation to the lowest brightness (10^{-8} stilb.). Equivalent adaptation may be obtained using red light pre-adaptation, but exact conditions employed should be stated.

Period of an observation: 1 second when background brightness is $>10^{-6}$ stilb.; 5 seconds when brightness is $<10^{-6}$ stilb.

6. Method of Determining the Limit

It is recommended that experimenters determine a number of points on the "probability of seeing" curve. The limit is the point corresponding to 50 percent correct responses after correcting for the correct responses due to chance.

7. Correction of Vision

Day vision is to be corrected where necessary. The correction for night vision should be 1.5 diopters less than that required for day vision. Allowance should be made for loss of light in spectacles if these are not coated with reflection-reducing films. An observer who is emmetropic by day may be tested at low brightness without correction if the object is placed at a distance of 80 cm.

Appendix 1: Definition of Normal Observer

(*a*) *Day Vision.* A normal observer should be able to perceive, against a background of 10^{-2} to 10^{-3} stilb., a black spot whose visual angular diameter is 0.6 minutes of arc. For the same brightness he should be able to perceive a disk of diameter 2° and contrast 0.01.

(*b*) *Night Vision.* The normal observer should be able to detect a black disk of visual angle 10° against a background of 2×10^{-10} stilb. placed at a distance between 15° and 35° from the fovea, provided he is completely dark adapted.

* "Equivalent foot candles"; numerically equal to foot-lamberts.

Appendix 2: Fixation

Experiments may be carried out under conditions in which a trained observer is allowed to use whatever part of his retina he finds to be most sensitive, or a particular part of the retina may be selected by means of a fixation spot. If this is done, the observer must be instructed not to fixate continuously, but to allow his center of vision to traverse the region around the fixation spot. If it is desired to leave no initiative in this matter to the observer, a moving fixation spot may be used. The spot should be made to traverse a closed curve at a known speed. In all cases the exact conditions of fixation should be stated. When a red fixation spot is used, it should be placed at such a distance that the eye is accommodated for the object, allowing for the chromatic aberration of the eye.

STANLEY S. BALLARD
Chairman, U.S.N.C.–I.C.O.
Tufts College
Medford 55, Massachusetts

Minutes of the Thirty-Sixth Meeting of the Board of Directors of the Optical Society of America, Incorporated

HOTEL STATLER, CLEVELAND, OHIO, OCTOBER 25, 1950

IN addition to the transaction of routine business, the following items of general interest to members of the Society were considered.

Announcements by Secretary

Results of letter ballots:

1. Approval of resolutions to elect two honorary members (to be formally announced in this *Journal* in a subsequent issue).
2. Approval of resolution to hold the spring meeting of the Society in New York City on March 20, 21, and 22, 1952.
3. Approval of the appointment of the following Program Committee for the winter meeting to be held in Washington, D. C., on March 1, 2, and 3, 1951:

Wallace R. Brode, *Chairman*

Stanley S. Ballard	Dorothy Nickerson
Burt H. Carroll	Henry O'Bryan
Kasson S. Gibson	Richard Tousey
Archie I. Mahan	Robert A. Woodson

4. Approval of the nomination of Wallace R. Brode as O.S.A. representative on the Division of Physical Sciences of the National Research Council for a term of three years to expire on July 1, 1953.
5. Approval of the reappointment of the following as O.S.A. representatives on the Inter-Society Color Council for a term to expire in October, 1952:

*Deane B. Judd, *Chairman*

E. Q. Adams	*Arthur C. Hardy
Blanche R. Bellamy	Richard S. Hunter
Carl E. Foss	*David L. MacAdam
G. A. Fry	Dorothy Nickerson

J. L. Saunderson

* Voting delegates.

6. Approval of the appointment of the following Committee on Transfer from Associate to Regular Membership.

Wallace R. Brode, *Chairman*
Seibert Q. Duntley
Fred Paul

7. Approval of the resolution to award the Adolph Lomb Medal for 1950 to H. Richard Blackwell.

Appointment of Associate Editors

The large increase in papers submitted to referees prompted the Editor to request approval of additional associate editors to cover the fields of fluorescence and phosphorescence, physiological optics, and geometrical optics. Appointment of the following associate editors was unanimously approved.

For a term to expire on December 31, 1951:

H. W. Leverenz

For a term to expire December 31, 1953:

Glenn A. Fry

For a term to expire on December 31, 1955:

Stanley S. Ballard

Future Meetings of the Society

The next meeting of the Society will be held at the Wardman Park Hotel, Washington, D. C., on March 1, 2, and 3, 1951. The annual meeting in 1951 will be held in Chicago, Illinois, in conjunction with meetings of all the founder societies of the American Institute of Physics, and has been tentatively scheduled for the week of October 22, 1951. A spring meeting of the Society will be held in New York City on March 27, 28, and 29, 1952.

Membership

The Secretary reported informally a net gain of fifty-one members between January 1 and October 1, 1950.

ARTHUR C. HARDY, *Secretary*

Errata*

1949, Vol. 39

Kornfeld, G. "Latent-Image Distribution by X-Ray Exposures."
Page 1020, reference 2 should read "S. E. Sheppard and A. P. H. Trivelli, Phot. J. **66**, 505 (1926); L. Silberstein and A. P. H. Trivelli, Phil. Mag. **9**, 787 (1930).

Rood, Joseph L. "Some Properties of Thin Evaporated Films on Glass."
Page 855, Eq. (1). "x" should read "x_1."
Page 855, reference 1. "Doris L. Cabellero" should read "Doris L. Caballero."
Page 855, Eq. (5) should not be broken up into two terms; the correct form is

$$R=\frac{\left[n_1n_2(1-n_0)-(n_1^2-n_0n_2^2)\tan\frac{x_1}{2}\tan\frac{x_2}{2}\right]^2+\left[n_2(n_0-n_1^2)\tan\frac{x_1}{2}+n_1(n_0-n_2^2)\tan\frac{x_2}{2}\right]^2}{\left[n_1n_2(1+n_0)-(n_1^2+n_0n_2^2)\tan\frac{x_1}{2}\tan\frac{x_2}{2}\right]^2+\left[n_2(n_0+n_1^2)\tan\frac{x_1}{2}+n_1(n_0+n_2^2)\tan\frac{x_2}{2}\right]^2}.$$

1950, Vol. 40

Foster, L. V. "Microscope Optics."
Page 279, lines 18–20, "Fig. 9a" should read "Fig. 9c"; "Fig. 9b" should read: "Fig. 9a"; "Fig. 9c" should read "Fig. 9b." "Figur 9d" reads correctly.
Page 280, Fig. 9, the caption should read "(a) bright phase contrast, (b) dark phase contrast, (c) regular brightfield illumination, and (d) dark field illumination."

Ives, Herbert E. "Extrapolation from the Michelson-Morley Experiment."
Page 188, substitute for the sentence following Eq. (26) the following paragraph:
"Directing attention to the quantity $f_D(W)f_T(W+Y)/f_T(W)f_D(W+Y)$ we note that this must be a constant independent of W for any chosen values of D' and q. It will be invariant for all values of W if the two quotients $f_D(W)/f_T(W)$ and $f_T(W+Y)/f_D(W+Y)$, which are homogeneous in their variables, are each individually invariant. Taking first $f_D(W)/f_T(W)$, if W is put equal to zero, both numerator and denominator become unity, in accordance with the property of $f_D(W)$ noted in Section IV; hence the value of the quotient is unity. Taking next $f_T(W+Y)/f_D(W+Y)$, if W is put equal to $-Y$, the numerator and denominator become unity, and also the quotient. We thus establish that the quantity $f_D(W)f_T(W+Y)/f_T(W)f_D(W+Y)$ has the value unity."

Kubota, Hiroshi. "On the Interference Color of Thin Layers on Glass Surface."
Page 147, X', Y', and Z' of Eq. (4) must be multiplied by $4BC$.
Page 148, section 4, line 3, "$\cos^2\delta$" should read "$\cos^2\delta/2$."
Page 149, section 4, last line, "bluish purple or red pink" should read "purple blue or pink." This nomenclature is based on a diagram of K. L. Kelly, J. Opt. Soc. Am. **33**, 627 (1943).
Page 149, section 5, line 5, " 'sharp cutting' yellow filter" should read " 'sharp cutting' filter"; yellow is an unnecessary restriction.

Middleton, W. E. K. "The Colors of Distant Objects."
Page 374, the second equation of the group numbered (10) should read

$$Y=\int_0^\infty W_\lambda\beta_\lambda[1+(f_\lambda C_W+f_\lambda-1)e^{-\sigma_\lambda r}]d\lambda$$

and differs from the equations for X and Z above and below it only in one factor.

Webb, J. H. "Low Intensity Reciprocity-Law Failure in Photographic Exposure: Energy Depth of Electron Traps in Latent-Image Formation; Number of Quanta Required to Form the Stable Sublatent Image."
Page 3, reference 5 should include "C. H. Evans" as co-author with "J. H. Webb."

* The reverse side of this printed page is blank so that readers may cut out the corrections and attach them to the individual articles.

Author Index to Volume 40

References with (A) are abstracts of papers presented at meetings of the Optical Society of America; (T) designates title only; (L) designates Letters to the Editor.

Adams, Kenneth B. (see Burns, Keivin)—339
Adcock, W. A. (see Hornig, D. F.)—497
Aicher, J. O. Measurement of 1849A radiation by afterglow of manganese-activated calcium silicate—805(A)
Allen, Ralph G. (see Coleman, Howard S.)—261(A)
Alpern, Mathew. Effect of luminance, exposure asynchrony, and spatial separation of stimuli on the magnitude of metacontrast—796(A)
Anderson, Charles H. (see Fassel, Velmer A.)—803(A)/742
Anslow, Gladys A. and Ruth C. Shea. Ultraviolet dissociation spectra of Nylons—262(A)
Arroe, O. H. and J. E. Mack. Hollow-cathode source design for high resolution spectroscopic studies with small samples —386
Archer, James E. (see Harrison, George R.)—259(A)
Aschenbrenner, Claus M. Workshop method of figuring concave mirrors by quantitative Foucault tests—258(A)

Babcock, Horace W. An integrating photometer for low light levels—409
Back, Frank G. Lens tester—257(A)
Baird, Walter S. Recording grating monochromator for the range 180 to 4000 millimicrons—259(A)
Ballard, Stanley S. (see Combes, Lewis S.)—256(A)
—— (see McCarthy, Kathryn A.)—256(A)
——, **Lewis S. Combes, and Kathryn A. McCarthy.** Gross variations in the optical, mechanical, and thermal properties of synthetic crystalline lithium fluoride—798(A)
Barnes, R. Bowling. Book review of *Infrared Determination of Organic Structures* by H. M. Randall, R. G. Fowler, Nelson Fuson, and R. J. Dangl—252
Bass, Arnold M. and H. Sponer. Fluorescence studies of some simple benzene derivatives in the near ultraviolet. I. Fluorobenzene and chlorobenzene—389
Baum, William A. and Lawrence Dunkelman. Ultraviolet radiation of the high pressure xenon arc—782
Bauple, R., A. Gilles, J. Romand, and B. Vodar. Absorption spectra of samples of quartz and corundum in ultraviolet. Electric and thermic treatment of quartz—788(L)
Beasley, John K. (see Harris, Louis)—801(A)
Beeching, R. *Electron Diffraction* (Book). Reviewed by J. Rand McNally, Jr.—477
Belknap, Marion A. (see Gibson, Kasson S.)—435
Benford, James R. and Richard L. Seidenberg. Phase contrast microscopy for opaque specimens—259(A)/314
Benson, Nels C., Georg Hass, and Noel W. Scott. 72-inch high vacuum evaporator and its glow discharge equipment —687
Berl, Walter G. *Physical Methods in Chemical Analysis* (Book) Reviewed by Philip J. Elving—792
Berry, Chester R. Growth of silver filaments and dendrites—615
Bersis, D. S. Two infra-red sensitive SrS phosphors with Zn dominant activator—335(L)
Billings, B. H. Birefringent frustrated total reflection filter—471
——, **S. Sage, and W. Draisin.** One-angstrom pass-band polarization interference filter—262(A)
Bingley, F. J. Application of projective geometry to the theory of color mixture—264(A)
Bird, G. (see Land, E. H.)—61
Bird, George R. (see Blout, Elkan R.)—304
Birren, Faber. *Color Psychology and Color Therapy* (Book). Reviewed by Ralph M. Evans—696
Blank, John M. Interferometric measurements of wavelengths in the spectrum of mercury isotope 198—345
Blout, Elkan R., George R. Bird, and David S. Grey. Infra-red microspectroscopy—304
——, **Richard S. Corley, and Patricia L. Snow.** Infra-red transmitting filters. II. The region 1 to 6μ—415
Bouman, M. A. Peripheral contrast thresholds of the human eye—825
—— **and H. A. van der Velden.** Ricco's law and the quanta-explanation of vision—336(L)
Bowen, John H. (see Harvalic, Zaboj V.)—755
Bozman, W. R. (see Meggers, W. F.)—262(A)
Brauer, Peter. Rise in brightness of infra-red sensitive phosphors—353
Brice, Arthur T. (see Saylor, Charles Proffer)—329
Brice, B. A., M. Halwer, and R. Speiser. Photoelectric light-scattering photometer for determining high molecular weights—768
Britton, William C. (see Watson, John T.)—258(A)
Brode, Wallace R. Book review of *Elementary Photography* by Gilford G. Quarles—620
—— Book review of *Fluorescence and Phosphorescence* by Peter Pringsheim—545
—— Book review of *An Introduction to Luminescence of Solids* by H. W. Leverenz—406
—— Book review of *Introduction to Theoretical and Experimental Optics* by Joseph Valasek—182
—— Book review of *Manual of Spectroscopy* by Theodore A. Cutting—181
—— Book review of *Manual of Standardized Procedures for Spectrophotometric Chemistry* by Harold J. Fister—880
—— Book review of *Optics (Volume III of Principles of Physics Series)* by Francis W. Sears—252
—— Book review of *Quantitative Ultramicroanalysis* by Paul L. Kirk—620
—— Book review of *Spectrochemical Procedures* by Charles E. Harvey—696
Broida, H. P. (see Oldenberg, O.)—381
Brown, F. W. (see Greenfield, M. A.)—643
Brown, W. R. J. Effect of chromatic surrounding fields on color discrimination—797(A)
Brumley, Corwin H. and David Richardson. Electro-optic crystal interferometer—800(A)
Bube, Richard H. Luminescence and trapping in zinc-sulfide-type phosphors—260(A)
Buc, G. L. and E. I. Sterns. Transmittance of interference filters—336(L)
Bullock, B. W. and S. Silverman. Rapid scanning spectrometer for oscillographic presentation in the near infra-red—257(A)/608
Burns, Keivin, Kenneth B. Adams, and Jean Longwell. Interference measurements in the spectra of neon and natural mercury—339

Cady, W. M. (see Gordon, G.)—852
Callahan, Francis P., Jr. Application of Bouguer's law to non-uniform films—263(A)
Camus, Jean (see Harrison, George R.)—800(A)
Carpenter, Robert O'B. Electro-optic effect in uniaxial crystals of the dihydrogen phosphate type. III. Measurement of coefficients—225
—— Induced birefringence of ADP and KDP as a function of temperature—798(A)
Carroll, Burt H. Book review of *Structure et Propriétés des Couches Photographiques* by L. P. Clerc—545

Carswell, W. E. Two methods of determining a recognizable relationship between areas of color, related to both Munsell and Ostwald—265(A)
Catalán, Miguel A. and Rafael Velasco. Changes in g-values, in a spectrum, for different magnetic fields—653
Chalklin, F. C. (see Worsnap, B. L.)—790
Chandler, Alfred B. Spectrographic determination of high hafnium in hafnium-zirconium dioxide—262(A)
Chapman, Marian Holmes (see Middleton, W. E. Knowles)—795(A)
Cheydleur, B. F. (see Oldham, Max S.)—544(L)
Clapper, Franklin R. (see Williams, Franklin C.)—796(A)
Clark, Mason E. (see Fisher, Russell A.)—255(A)
Clerc, L. P. *Structure et Propriétés des Couches Photographiques* (Book). Reviewed by Burt H. Carroll—545
Cleveland, E. Lynn and Richard C. Raymond. Light scattering by layered distributions of small metal spheres—795(A)
Code, A. D. (see Hiltner, W. A.)—149
Coleman, Howard S. and Ralph G. Allen. Optical constants of metallic films—261(A)
—— **and Harold E. Rosenberger.** Attenuation of brightness contrast caused by atmospheric optical haze—507
—— **and Harold E. Rosenberger.** Comparison of visual and photoelectric measurements of the attenuation of brightness contrast by the atmosphere—371
—— **and Harold E. Rosenberger.** Effect of wave-length on the attenuation of brightness contrast by the atmosphere—263(A)
Colthup, N. B. Spectra-structure correlations in the infra-red region—397
Combes, Lewis S. (see Ballard, Stanley S.)—798(A)
—— **and Stanley S. Ballard.** Studies of the inelastic behavior of optical crystals—256(A)
Convey, J. and J. K. Hurwitz. Analysis of the excitation characteristics of spectra emitted by ferrous alloys—803(A)
Corley, Richard S. (see Blout, Elkan R.)—415
Coulston, J. G. (see Guest, P. G.)—787(L)
Covell, William (see O'Brien, Brian)—260(A)
Curcio, J. A., H. S. Stewart, and C. C. Petty. Determination of flame temperature from the OH emission—264(A)
Cutting, Theodore A. *Manual of Spectroscopy* (Book). Reviewed by Wallace R. Brode—181

Dangl, R. J. (see Randall, H. M.)—252
Davidson, H. R. Calculation of subtractive color mixtures—230
—— Visual sensitivity to surface color differences—797(A)
——, **I. H. Godlove, J. M. Lambert, and G. J. Wright.** Illuminant-converting filter for use with the automatic tristimulus integrator—817
de Beauregard, O. Costa. *La Theorié de la Relativité Restreinte* (Book). Reviewed by Max Herzberger—252
deBretteville, A., Jr. Properties of large barium titanate crystals—796(T)
Delaney, J. C. Galvanometer scale for the direct reading of intensities—787(L)
Desvignes, F. (see Terrien, J.)—845
DeVore, J. R. Refractive indices of rutile and sphalerite—266(A)
Dieke, G. H. and A. B. F. Duncan. *Spectroscopic Properties of Uranium Compounds* (Book). Reviewed by D. L. Timma—181
di Francia, G. Toraldo. Parageometrical optics—600
Dimmick, Forrest L. (see Morris, Ailene)—795(A)
Dixon, E. O. (see MacNeille, S. M.)—261(A)
Draisin, W. (see Billings, B. H.)—262(A)
Duncan, A. B. F. (see Dieke, G. H.)—181
Dunkelman, Lawrence (see Baum, William A.)—782
—— **and Charles Lock.** Ultraviolet spectral sensitivity characteristics of photo-multipliers having quartz and glass envelopes—264(A)
Duntley, Seibert Q. Reflectance of submerged objects—795(A)
Durie, D. S. L. Refractive indices of lithium fluoride—878(L)
Dwyer, Robert J. Variable frequency electronic interrupter for the direct current arc—180(L)

Eberhardt, W. H. Slit-width effects in spectrophotometry—172
Eisen, Fred C. (see Wolfe, Robert N.)—143
Elby, F. P. Comatic aberration in infra-red spectrometer design—256(A)/450
Ellis, Joseph W. and Leonard Glatt. Channeled infra-red spectra produced by birefringent crystals—141
Elving, Philip J. Book review of *Physical Methods in Chemical Analysis* by Walter G. Berl—792
Epstein, L. Ivan. Calculation of third-order aberrations with the aid of IBM machines—255(A)
—— Edge-effect in phase contrast—803(A)
—— Extension of Toraldo's theory of phase contrast. I—291
—— **and Donald R. Herriott.** Extension of Toraldo's theory of phase contrast. II—576
Eros, Stephen. Fluorescent lamp spiralling—805(A)
Evans, J. C. and T. A. King. Five-inch molded silver chloride correctors for Kellner-Schmidt system—799(A)
Evans, Ralph M. Book review of *Color Pyschology and Color Therapy* by Faber Birren—696

Fabritus, George. Lamp quality optical inspection equipment—794(T)
Farnsworth, Dean (see Judd, Deane B.)—833
Fassel, Velmer A. and Charles H. Anderson. Quantitative spectrographic analysis of zirconium-hafnium mixtures—803(A)/742
Fastie, William G. Ambient temperature independent thermopiles for radiation pyrometry—805(A)
—— Small plane grating monochromator—800(A)
Feder, Donald P. Method of tracing skew rays—255(A)
Ferguson, W. F. C. (see Greig, J. H.)—504
Fetterley, G. H. and W. M. Hazel. D.c. arc source and automatic controller—76
Feynman, Richard P. Role of quanta in ordinary optical phenomena—261(T)
Finkelstein, N. A. Efficient grating mounting—800(A)
—— Integrating sphere for reflectance measurements in the ultraviolet—178(L)
Fisher, Russell A., William C. Knopf, and Mason E. Clark. Iron arc spectrum between 1.2 and 2.0 microns—255(A)
Fister, Harold J. *Manual of Standardized Procedures for Spectrophotometric Chemistry* (Book). Reviewed by Wallace R. Brode—880
Fleck, Horst (see Haber, Heinz)—459
Fochs, P. D. Method of determining concurrently the thickness and refractive index of a thin film or lamina—623(L)
Fonda, Gorton R. Dependence of emission spectra of phosphors upon activator concentration and temperature—347
Fortmiller, L., T. H. James, R. F. Quirk, and W. Vanselow. Combined effect of infra-red radiation and intensification upon the photographic latent image—487
Foss, Carl E. (see Granville, Walter C.)—265(A)
Foster, L. V. Microscope optics—275
Fowler, R. G. (see Randall, H. M.)—252
Frerichs, Rudolf. On the relations between crystal counters and crystal phosphors—219
Fry, D. L. (see Mansfield, W. O., Jr.)—804(A)
Fry, Glenn A. Effect of chromatic aberration on the blurredness of the retinal image—796(A)
Fuhrmeister, J. C. (see Mansfield, W. O., Jr.)—804(A)
Fuson, Nelson (see Randall, H. M.)—252

Gardner, Irvine C. New resolving power test chart—257(A)
—— Book review of *Die Brechzahlen einiger Halogenidkristalle* (*The Refractive Indices of Halogen Salt Crystals*) by H. Harting—477
—— Book review of *Die Optik in der Feinmesztechnik* by Karl Räntsch—28
—— **and Clarence H. Hahner.** Research and development in applied optics and optical glass at the National Bureau of Standards—251(N)
Garlick, G. F. J. *Luminescent Materials* (Book). Reviewed by Ferd E. Williams—406
——**and A. F. Gibson.** Errata: The luminescence of photoconducting phosphors—79
Gatterer, Alois and Joseph Junkes. *Atlas der Restlinien* (Book). Reviewed by William F. Meggers—695
Geissbuhler, John O. Design consideration for sealed-beam type lamps—805(A)
Gergely, György. Rise and decay of willemite luminescence—356
Gibb, Thomas R. P., Jr. Book review of *Analytical Absorption Spectroscopy* by M. G. Mellon—695
Gibson, A. F. (see Garlick, G. F. J.)—79
Gibson, Kasson S. and Marion A. Belknap. Permanence of glass standards of spectral transmittance—435
Gill, J. F. (see Teago, F. J.)—477
Ginther, Robert J. (see Schulman, James H.)—337(L), 854
Gilles, A. (see Bauple, R.)—788(L)
Givens, M. Parker and Walter P. Siegmund. Absorption of selenium in the extreme ultraviolet—804(A)
Glasser, L. G. (see Troy, D. J., Jr.)—80
Glatt, Leonard (see Ellis, Joseph W.)—141
Gliddon, Gordon H. Book review of *Optique Physiologique: Volume II. Lumière et Couleurs* by Yves Le Grand—620
Godlove, I. H. Color change from daylight to night light, calculated and observed—797(A)
—— (see Davidson, H. R.)—817
—— (see Granville, Walter C.)—265(A)
Golay, Marcel J. E. Panoramic display of far infra-red spectra—801(A)
—— System of static multislit spectrometer—257(A)
Gold, Louis. On the effect of slit dimensions on collimated beam intensity—119(L)
Goldmark, Peter C. Visual aspects of the CBS color television system—263(T)
Goldstein, Emmanuel. Measurement of fluctuating radiation components in the sky and atmosphere—795(A)
Gordon, G. and W. M. Cady. Apparatus for time-resolved spectroscopy—852
Goren, Mayer B. Simple method for evaluation of atomic and ionic ground states—74
Granville, Walter C., Carl E. Foss, and I. H. Godlove. Color harmony manual: colorimetric analysis of third edition—265(A)
Green, Milton. On the equation of the characteristic curve of photographic emulsions—266(A)
—— Three-line method of obtaining characteristic curves for heterochromous photometry—842
—— **and M. Ritter.** Measurement of reciprocity failure with the log$D$ preliminary curve—799(A)
Greenfield, M. A. and F. W. Brown. Calculation of index of refraction of gases from absorption data—643
Greig, J. H. and W. F. C. Ferguson. New mounting for an echelette diffraction grating—504
Grey, David S. New series of microscope objectives. III. Ultraviolet objectives of intermediate numerical aperture—283
—— (see Blout, Elkan R.)—304
Griffin, Paul M. and J. Rand McNally, Jr. Interferometric investigation of Ca and Hg—262(A)
Griffith, Grace E. Position of the bands of Fabry Perot type filters as a function of angle of incidence—261(A)
Grodsky, Vladimir. Bronze glass molds replacing cast iron glass molds—177(L)
Guest, P. G. and J. G. Coulston. Fresnel interference in the Michelson interferometer—787(L)
Guth, S. K. Brightness relationships for comfortable seeing—794(T)

Haber, Heinz. Torus grating—153
—— **and Horst Fleck.** Color saturation threshold meter—459
Hahner, Clarence H. (see Gardner, Irvine C.)—351(N)
Halwer, M. (see Brice, B. A.)—768
Hammond, Harry K., III and Isadore Nimeroff. Measurement of 60° specular gloss—265(A)
Hamsher, D. H. (see Nelson, C. N.)—863
Hanson, W. T., Jr. Color correction with colored couplers—166
Hardy, Arthur C. and F. Mansfield Young. Colorimetry by abridged spectrophotometry—59(L)
Harriman, M. W. and S. B. Williams. Visibility on cathode-ray tube screens: positive *vs.* negative signals on an intensity modulated scope—102
Harris, Clyde W. Optical design by a matrix method—819
Harris, Louis and John K. Beasley. Theory for the infra-red absorption of gold blacks—801(A)
——, **John K. Beasley, and Arthur L. Loeb.** Reflection and transmission of radiation by metal films and the influence of non-absorbing backings—801(A)
Harrison, George R. Retrogression in spectroscopy—127
—— Book review of *Photoelectricity and Its Application* by V. K. Zworykin and E. G. Ramberg—28
—— **and James E. Archer.** Rapid interferometric calibration of precision screws—259(A)
——, **Edward H. Jacobsen, and Jean Camus.** Automatic control of groove straightness in grating ruling—800(A)
Harting, H. *Die Brechzahlen einiger Halogenidkristalle* (*The Refractive Indices of Halogen Salt Crystals*) (Book). Reviewed by Irvine C. Gardner—477
Harvalik, Zaboj V. and John H. Bowen. Subjective spectral band limits under controlled conditions—755
Harvey, Charles E. *Spectrochemical Procedures* (Book). Reviewed by Wallace R. Brode—696
—— (see Hasler, M. F.)—262(A)
Hasler, M. F. Quantometry in 1950—804(A)
—— **and C. E. Harvey.** Spectrochemical methods of brass analysis—262(A)
Hass, Georg (see Benson, Nels C.)—687
Haupt, Geraldine Walker. Potassium chromate standard of spectral transmittancy for the ultraviolet—802(A)
Hazel, W. M. (see Fetterley, G. H.)—76
Herriott, Donald R. (see Epstein, L. Ivan)—576
Herzberger, Max. Optical model of physics—424
—— Book review of *La Theorie de la Reldtivité Restreinte* by O. Costa de Beauregard—252
Hetényi, M. *Handbook of Experimental Stress Analysis* (Book). Reviewed by Samuel Levy—880
Higgins, G. C. (see Jones, L. A.)—799(A)
—— **and K. Stultz.** Variation of visual acuity with various test-object orientations and viewing conditions—135
Hiltner, W. A. and A. D. Code. Compensation for seeing in stellar photoelectric spectrophotometry—149
Hodge, Edwin S. (see Schoen, A. L.)—23
Hoerlin, Herman and F. W. H. Mueller. Gold sensitization of x-ray films—266(A)/246
Holbourn, A. H. S. Production of diffraction gratings—59(L)
Holden, Robert B., William J. Taylor, and Herrick L. Johnston. Variable thickness low temperature infra-red cell—757
Holland, Dan H. (see Peterson, E. W.)—253(L)
Hopkins, Robert E. and Louise Rivoli. Lens for Institute of Optics' high speed camera—256(A)
—— **and Louise Rivoli.** Study of telescope refracting objectives—802(A)

Hornig, D. F., G. E. Hyde, and W. A. Adcock. Ratio-recording double-beam infra-red spectrophotometer with automatic slit-control—497
Hotchkiss, Robert N., Francis E. Washer, and Fred W. Rosberry. Spurious resolution of photographic lenses—802(A)
Hoyt, G. D. and W. W. McCormick. Study of the short duration, high intensity, electric arc as a source of visible light—658
Hughes, Harold K., (see Murphy, Robert W.)—259(A)/779
Humez, David E. Close temperature control of a large room—800(A)
—— New recording comparison microphotometer—802(A)
Humphreys, Curtis J. Extensions to the infra-red emission spectrum of mercury—255(A)
—— Book review of *Infrared Radiation Therapy Sources and Their Analysis with Scanner* by Leopold Rovner—545
—— **and Henry J. Kostkowski.** Infra-red emission spectrum of vanadium—801(A)
Hunt, R. W. G. Effects of daylight and tungsten light-adaptation on color perception—362
Hunter, Richard S. New goniophotometer—265(A)
—— (see Nickerson, Dorothy)—263(A)/446
Hurwitz, J. K. (see Convey, J.)—803(A)
Hyde, G. E. (see Hornig, D. F.)—497

Ishiguro, Kozo. Phase-shift measurement of thin films and its amplification—789(L)
Ives, Herbert E. Extrapolation from the Michelson-Morley experiment—185

Jackson, L. C. *Wave Filters* (Book). Reviewed by J. Rand McNally, Jr.—790
Jacobs, John E. Performance of cadmium sulfide as a detector of x-radiation—798(A)
Jacobsen, Edward H. (see Harrison, George R.)—800(A)
Jaffe, Halina (see Jaffe, Joseph H.)—53
Jaffe, Hans. Optical aspects of piezoelectric crystals—795(T)
Jaffe, Joseph H. and Halina Jaffe. Measurement of thickness of infra-red absorption cells—53
James, R. W. *X-Ray Crystallography* (Book). Reviewed by J. Rand McNally, Jr.—790
James, T. H. (see Fortmiller, L.)—487
Jarrell, Richard F. (see McNally, Fred A.)—800(A)
Johnson, F. S. (see Tousey, R.)—264(A)
—— **and R. Tousey.** Fluorescence sensitized photo-multipliers for the measurement of vacuum ultraviolet radiation—264(A)
Johnson, Peter D. and Frank J. Studer. Reflectance as a measure of absorption in solid crystalline materials—121(L)
Johnson, R. C. *Atomic Spectra* (Book). Reviewed by J. Rand McNally, Jr.—790
Johnston, Herrick L. (see Holden, Robert B.)—757
Jones, L. A. and G. C. Higgins. Photographic granularity and graininess. V. A variable magnification instrument for measuring graininess: structural and performance characteristics—799(A)
Jones, R. Clark. Reversibility and irreversibility of optics, or, is optics possible—798(T)
—— Trapping of light in fluorescent bodies—261(A)
Judd, Deane B. Errata: A comparison of direct colorimetry of titanium pigments with their indirect colorimetry based on spectrophotometry and a standard observer—52
—— Book review of *Language of Drawing and Painting* by Arthur Pope—28
——, **Lorenzo Plaza, and Dean Farnsworth.** Tritanopia with abnormally heavy ocular pigmentation—833
Junkes, Joseph (see Gatterer, Alois)—695
Jurmain, J. and D. E. Williamson. Analog computer for spectrographic analysis of high alloys—804(A)

Kagarise, R. E. (see Rank, D. H.)—89
Keller, Herbert B. (see Keller, Joseph B.)—48
Keller, Joseph B. and Herbert B. Keller. Determination of reflected and transmitted fields by geometrical optics—48
Kessler, Karl G. (see Meggers, William F.)—737
Kiess, C. C. Comment on "Spark spectra of elements 43 and 61"—177(L)
King, T. A. (see Evans, J. C.)—799(A)
Kirk, Paul L. *Quantitative Ultramicroanalysis* (Book). Reviewed by Wallace R. Brode—620
Kivenson, Gilbert. Some considerations in the design of double-beam analyzers for industrial control—112
Kjellgren, Bengt. Some experiences in the production of large clear crystals from solutions—795(T)
Klein, Myron W. (see Smakula, Alexander)—799(A)/748
Klick, Clifford C. (see Schulman, James H.)—337(L), 622(L), 854
—— **and James H. Schulman.** Existence of "sub-bands" in the luminescence emission spectrum of manganese activated zinc silicate—509
Knopf, William C. (see Fisher, Russell A.)—255(A)
Kostkowski, Henry J. (see Humphreys, Curtis J.)—801(A)
Kowalewski, Dora G. and Valdemar J. Kowalewski. On a method for the calibration of photographic emulsions—621(L)
Kowalewski, Valdemar J. (see Kowalewski, Dora G.)—621(L)
Kraushaar, R. Diffraction grating interferometer—480(L)
Kremers, H. C. Growing optical crystals from the fused melt—795(T)
Kubota, Hiroshi. On the interference color of thin layers on glass surface—146
—— On sensitive color—621(L)

Lamb, Mary A. (see Plyler, Earle K.)—255(A)
Lambert, J. M. (see Davidson, H. R.)—817
Land, E. H., G. Bird, and W. A. Shurcliff. Detection of tracks and stars in nuclear track plates—61
Langton, William G. Baird Associates ruling engine—258(A)
Lee, George Hamor. *Introduction to Experimental Stress Analysis* (Book). Reviewed by Walter Ramberg—790
Le Grand, Yves. *Optique Physiologique: Volume II. Lumière et Couleurs* (Book). Reviewed by Gordon H. Gliddon—620
Leibhardt, Edward. Dividing gear for a ruling engine—623(L)
Leverenz, H. W. *An Introduction to Luminescence of Solids* (Book). Reviewed by W. R. Brode—406
Leininger, R. K. Spectrochemical determination of major constituents of limestone—804(A)
Levy, Samuel. Book review of *Handbook of Experimental Stress Analysis* by M. Hetényi—880
Liston, Max D. (see White, John U.)—29, 93
——**and John U. White.** Amplification and electrical systems for a double beam recording infra-red spectrophotometer—36
Lock, Charles (see Dunkelman, Lawrence—264(A)
—— (see Packer, D. M.)—264(A)
Loeb, Arthur L. (see Harris, Louis)—801(A)
Longwell, Jean (see Burns, Keivin)—339
Lonsdale, Kathleen. *Crystals and X-Rays* (Book). Reviewed by A. L. Patterson—181
Loofbourow, John R. Microspectroscopy—317
—— (see Vallee, Bert L.)—803(A)/751
Lord, R. C. and E. Nielsen. Apparatus for low temperature study of the Raman effect—255(A)/655
Luneburg, Rudolf K. Metric of binocular visual space—627
Lyon, Donald W. and E. Louise Poore. Some new infra-red phosphors—179(L)

MacAdam, David L. Loci of constant hue and brightness determined with various surrounding colors—264(A)/589
—— Maximum attainable luminous efficiency of various chromaticities—120(L)

—— Method of colorimetric integration using punched-card accounting machines—138
—— Should an American revision of the ICI colorimetry data be proposed?—798(A)
Macdonald, Duncan E. Criteria for detection and recognition of photographic detail—258(A)
——, **Grant D. Ross, and William W. Tunnicliffe.** Video techniques in aerial reconnaissance—263(A)
Mack, J. E. (see Arroe, O. H.)—386
MacNeille, S. M. and E. O. Dixon. Electrical computer for calculating the optical properties of multilayer interference films—261(A)
Mahan, A. I. and E. E. Price. Diffraction pattern deterioration by roof prisms—664
Mandelker, Jakob. *Principles of a New Energy Mechanics* (Book). Reviewed by Hans Mueller—181
Mansfield, W. O., Jr., J. C. Fuhrmeister, and D. L. Fry. Spectrographic determination of the halogens and sulfur in engine deposits—804(A)
Marcus, Bernard. Lens testing bench—257(A)
Marechal, A. Coherent set of tolerances for geometrical aberrations, including excentration effects—60(L)
Marton, L. Electron *vs.* photons: a comparison of microscopes 269
—— Book review of *Electron Microscopy: Techniques and Applications* by R. W. G. Wyckoff—879
Matossi, F. (see Oldham, Max S.)—544(L)
—— Book review of *Elektronenoptik I, Grundzüge der theoretischen Elektronenoptik* by Alexander A. Rusterholz—879
—— Book review of *The Electron Microscope, its Development, Present Performance and Future Possibilities* by D. Gabor—879
Mayo, Eleanor G. (see Middleton, W. E. Knowles)—805(A)
Mazumder, K. C. Cadmium spectra—120(L)
McCarthy, Kathryn A. (see Ballard, Stanley S.)—798(A)
—— **and Stanley S. Ballard.** Measurements of the thermal conductivity of optical crystals—256(A)
McCormick, W. W. (see Hoyt, G. D.)—658
McCubbin, T. King, Jr. and William M. Sinton. Recent investigations in the far infra-red—254(A)/537
McMahon, H. O. Thermal radiation from partially transparent reflecting bodies—376
McNally, Fred A. and Richard F. Jarrell. Concave replica grating results—800(A)
McNally, J. Rand, Jr. (see Griffin, Paul M.)—262(A)
——(see Smith, D. D.)—803(A), 878(L)
——(see Stukenbroeker, George L.)—262(A), 336(L)
—— Book review of *Applications of Interferometry* by W. E. Williams—790
—— Book review of *Atomic Spectra* by R. C. Johnson—790
—— Book review of *Electron Diffraction* by R. Beeching—477
—— Book review of *Hyperfine Structure in Line Spectra and Nuclear Spin* by S. Tolansky—477
—— Book review of *Mercury Arcs* by F. J. Teago and J. F. Gill—477
—— Book review of *Metre-Kilogram-Second System of Electrical Units* by R. K. Sas and F. B. Pidduck—477
—— Book review of *Wave Filters* by L. C. Jackson—790
—— Book review of *X-Ray Crystallography* by R. W. James —790
—— Book review of *X-Ray Optics* by A. J. C. Wilson—477
—— Book review of *X-Rays* by B. L. Worsnap and F. C. Chalklin—790
—— **and G. L. Stukenbroeker.** Spectrum shifts for thorium isotopes—803(A)
Medveson, L. T. Halftone masking theory from Neugebauer equations—796(A)
Meggers, William F. Book review of *Atlas der Restlinien* by Aldis Gatterer and Joseph Junkes—695
—— **and Karl G. Kessler.** Wave-lengths of mercury 198—801(A)/737
——, **B. F. Scribner, and W. R. Bozman.** Absorption and emission spectra of promethium—262(A)
Mellon, M. G. *Analytical Absorption Spectroscopy* (Book). Reviewed by Thomas R. P. Gibb, Jr.—695
Meltzer, Robert J. Resolving power of infra-red prism spectrometers—257(A)
Menzel, Donald H. Book review of *Stellar Evolution* by Otto Struve—791
Meyer, D. R. (see Mote, F. A.)—584
Middleton, W. E. Knowles. Colors of distant objects—263(A)/373
—— Curve computer—263(A)
—— **and Marian Holmes Chapman.** Investigators on meteorological estimates of the visual range—795(A)
—— **and Eleanor G. Mayo.** Variation in horizontal distribution of light from candlepower standards—805(A)
Millson, Henry E., Jr. (see Millson, Henry E.)—430
Millson, Henry E. and Henry E. Millson, Jr. Observations on exceptional duration of mineral phosphorescence—430
Milne, Gordon G. New reciprocity failure in photographic exposure at high intensity—799(A)
—— (see O'Brien, Brian)—260(A)
Moore, Charlotte E. Book review of *Hydrogen in Chemical Atoms* by William Mayo Venable—696
Morris, Ailene and Forrest L. Dimmick. Visual acuity at very low levels of illumination—795(A)
Moss, T. S. Ultimate limits of sensitivity of lead sulfide and telluride photo-conductive detectors—602
Mote, F. A., A. J. Riopelle, and D. R. Meyer. Effect of intermittent preadapting light upon subsequent dark adaptation in the human eye—584
Mueller, F. W. H. (see Hoerlin, Herman)—266(A)/246
Mueller, Hans. Book review of *Principles of a New Energy Mechanics* by Jakob Mandelker—181
Mundie, L. G. (see Oldham, Max S.)—544(L)
Murphy, Robert W. and Harold K. Hughes. Simultaneous recording of two wave-length ranges with the Littrow spectrograph—259(A)/779
Murray, Allen E. Effect of antireflection films on color in optical instruments—262(A)

Nagel, Max R. Sensitometric effects in motion-blurred negatives—799(A)
Nagy, Elemér. Emission bands of willemite in phosphorescence —407(L)
Nelson, C. N. and D. H. Hamsher. Photography of high altitude aerial objects—863
Nicholls, R. W. Kinetics of excitation of molecular nitrogen —805(A)
Nickerson, Dorothy. Certain color changes under artifiical lighting—797(A)
—— Munsell renotations used to study color space of Hunter and Adams—85
——, **Richard S. Hunter, and Marshall G. Powell.** New automatic colorimeter for cotton—263(A)/446
Nielsen, E. (see Lord, R. C.)—655
Nielsen, J. Rud (see Richards, Charles M.)—255(A), 438, 442
Nierenberg, Richard N. Unique method of obtaining a uniformly bright area—260(A)
Nimeroff, Isadore (see Hammond, Harry K., III)—265(A)

O'Brien, Brian. Local variations of the Stiles and Crawford effect—796(A)
——, **Gordon G. Milne, and William Covell.** Fast closure slit closure with low inertia—260(A)
——, **Gordon G. Milne, and William Covell.** Improved image dissector for very high speed motion photography—260(A)
O'Brien, Brian, Jr. Spectral sensitivity of photo-sensitive acid resists—799(A)

Oldenberg, O. and H. P. Broida. Application of photoelectric multiplier tubes to the sensitive measurement of absorption of changes of relative light intensities—381
Oldham, Max S., L. G. Mundie, F. Matossi, and B. F. Cheydleur. Method for the determination of optical constants of semitransparent films—544(L)
Opler, Ascher. Spectrophotometry in the presence of stray radiation: a table of log $[(100-k)/(T-k)]$—401
Osterberg, Harold. Microscope imagery and interpretations—295
—— **and Gilbert E. Pride.** Effect of particle size on the diffraction image in microscopy with narrow-coned, axial illumination—14
—— **and Gilbert E. Pride.** Measurement of unresolved, single particles of uniform thickness by means of variable phase microscopy—64

Packer, D. M. and C. Lock. Thermocouple measurements of spectra intensities in the vacuum ultraviolet—264(A)
Patterson, A. L. Book review of *Crystals and X-Rays* by Kathleen Lonsdale—181
Perry, J. W. Abridged spectrophotometric colorimetry with photo-cells—119(L)
Peterson, E. W. and Dan H. Holland. On the shape of the sensitive cathode area of electron multiplier photo-tubes—253(L)
Petty, C. C. (see Curcio, J. A.)—264(A)
Pidduck, F. B. (see Sas, R. K.)—477
Plant, W. R. New recording spectroradiometer—805(A)
Plaza, Lorenzo (see Judd, Deane B.)—833
Plyler, Earle K. Infra-red absorption spectra of twelve chlorinated benzenes—801(A)
—— (see Tilton, Leroy W.)—540, 798(A)
—— **and Mary A. Lamb.** Infra-red spectrum of CH_2ClF—255(A)
Poore, E. Louise (see Lyon, Donald W.)—179(L)
Pope, Arthur. *Language of Drawing and Painting* (Book). Reviewed by Deane B. Judd—28
Powell, Marshall G. (see Nickerson, Dorothy)—263(A)/446
Price, E. E. (see Mahan, A. I.)—664
Pride, Gilbert E. (see Osterberg, Harold)—14, 64
Pringsheim, Peter. *Fluorescence and Phosphorescence* (Book). Reviewed by Wallace R. Brode—545
Pryor, Paul L. Military standard on photographic lenses—801(A)

Quarles, Gilford G. *Elementary Photography* (Book). Reviewed by Wallace R. Brode—620
Quirk, R. F. (see Fortmiller, L.)—487

Ramberg, E. G. (see Zworykin, V. K.)—28
Ramberg, Walter. Book review of *Introduction to Experimental Stress Analysis* by George Hamor Lee—790
Randall, H. M., R. G. Fowler, Nelson Fuson, and R. J. Dangl. *Infrared Determination of Organic Structures* (Book). Reviewed by R. Bowling Barnes—252
Rank, D. H. Some high speed spectrograph objectives—256(A)/462
—— **and R. E. Kagarise.** Empirical convergence correction of depolarization measurements—89
Räntsch, Karl. *Die Optik in der Feinmesztechnik* (Book). Reviewed by Irvine C. Gardner—28
Raymond, Richard C. (see Lynn, Cleveland E.)—795(A)
—— (see Walker, Marshall J.)—766
Reimer, Charles B. (see Vallee, Bert L.)—803(A)/751
Rense, William A. Polarization studies of light diffusely reflected from ground and etched glass surfaces—55
Richards, Charles M. and J. Rud Nielsen. Raman spectra of *cis*- and *trans*-2-butene and 1,3-butadiene in the gaseous and liquid states—255(A)
—— **and J. Rud Nielsen.** Raman spectra of *cis*- and *trans*-2-butene in the gaseous and liquid states—442
—— **and J. Rud Nielsen.** Raman spectrum of 1,3-butadiene in the gaseous and liquid states—438
Richardson, David (see Brumley, Corwin H.)—800(A)
——, **R. S. Wiley, and G. J. Sheldon.** Improved diffraction gratings and echelles—259(A)
Richardson, John (see Tousey, R.)—264(A)
Riopelle, A. J. (see Mote, F. A.)—584
Ritter, M. (see Green, M.)—799(A)
Rivoli, Louise (see Hopkins, Robert E.)—256(A), 802(A)
Roberts, Shepard and Ferd E. Williams. Theory of the luminescence of sulfide phosphors—516
Romand, J. (see Bauple, R.)—788(L)
Romer, Alfred, Robert D. Turner, and Irene Comfort Stehli. Wave-lengths of the potassium lines 3446A and 3447A—178(L)
Rosberry, Fred W. (see Hotchkiss, Robert N.)—802(A)
—— (see Washer, Francis E.)—801(A)
Rosenberger, Harold (see Coleman, Howard S.)—263(A), 371, 507
Ross, Grant D. (see Macdonald, Duncan E.)—262(A)
Rouse, Arthur G. New source for spectro-chemical analysis—82
Rovner, Leopold. *Infrared Radiation Therapy Sources and Their Analysis with Scanner* (Book). Reviewed by Curtis J. Humphreys—545
Rozsa, J. T. Spectrochemical analysis of biological leaf material—804(A)
Rupert, C. S. and John Strong. Carbon arc as an infra-red source—455
Russell, Henry Norris. Arc and spark spectra of gadolinium—550
—— Estimation of ionization potentials by comparison with neighboring elements—618
Rusterholz, Alexander A. *Elektronenoptik I, Grundzüge der theoretischen Elektronenoptik* (Book). Reviewed by L. Marton—879

Sage, S. (see Billings, B. H.)—262(A)
Salzberg, Bernard. Propagation of electromagnetic waves through a stratified medium. I.—465
Sas, R. K. and F. B. Pidduck. *Metre-Kilogram-Second System of Electrical Units* (Book). Reviewed by J. Rand McNally Jr.—477
Saunders, James B. Precise topography of optical surfaces—258(A)
Saylor, Charles Proffer, Arthur T. Brice, and F. Zernike. Color phase-contrast microscopy: requirements and applications—329
Scheibner, E. J. (see Schulz, L. G.)—761
Schlegel, Richard. Optical refraction and Fermat's principle at a point—244
Schoen, A. L. and Edwin S. Hodge. Photographing spectra in the vacuum ultraviolet—23
Schulman, James H. Effect of high energy radiation on luminescent properties of crystals and glasses—796(T)
—— (see Klick, Clifford C.)—509
—— **and Clifford C. Klick.** On the fluorescence and phosphoresence emission spectra of manganese-activated zinc silicate—622(L)
——, **Robert J. Ginther, and Clifford C. Klick.** Some optical properties of lead-activated sodium chloride phosphors—854
——, **Clifford C. Klick, and Robert J. Ginther.** Variation of emission spectrum of manganese-activated zinc beryllium silicate with decay time—337(L)
Schulz, L. G. Accurate thickness measurements with a Fabry-Perot interferometer—177(L)
—— Effect of phase changes in white light interferometry—802(A)

—— Interferometric method for accurate thickness measurements of thin evaporated films—690
—— **and E. J. Scheibner.** Experimental study of the change in phase accompanying reflection of light from thin evaporated films—761
Scott, G. D. (see Sennett, R. S.)—203
Scott, Noel W. On increasing the adhesion and durability of optical coatings—804(A)
—— (see Benson, Nels C.)—687
Scribner, B. F. (see Meggers, W. F.)—262(A)
Sears, Francis W. *Optics (Volume III of Principles of Physics Series)* (Book). Reviewed by Wallace R. Brode—252
Seidenberg, Richard L. (see Benford, James R.)—259(A)/314
Sennett, R. S. and G. D. Scott. Structure of evaporated metal films and their optical properties—203
Shankland, R. S. Scientific work of Albert A. Michelson—794(T)
Shea, Ruth C. (see Anslow, Gladys A.)—262(A)
Sheldon, G. J. (see Richardson, David)—259(A)
Shenstone, A. G. Cadmium spectra—121(L)
Shurcliff, W. A. (see Land, E. H.)—61
Siegmund, Walter P. (see Givens, M. Parker)—804(A)
Silverman, S. (see Bullock, B. W.)—257(A)/608
Sinden, R. H. Some consequences of the additivity of luminosities—647
Sinton, William M. (see McCubbin, T. King, Jr.)—254(A)/537
Sloan, Louise L. Comparison of the Nagel anomaloscope and a dichroic filter anomaloscope—41
Smakula, Alexander. Color centers in fused and crystalline quartz—266(A)
—— **and Myron W. Klein.** Influence of optical working on surface structure of plastic crystals—799(A)/748
Smith, D. D. and J. R. McNally, Jr. Isotope shifts for Sm^{144} and Sm^{154}—803(A)
—— **and J. R. McNally, Jr.** Isotope shifts in enhanced samarium isotopes—878(L)
Smith, F. D. and A. F. Turner. Phase shifts in interference filters—261(A)
Smith, Warren J. Comments on "The design of triplet anastigmat lenses of the Taylor type"—406(L)
Snow, Patricia L. (see Blout, Elkan R.)—415
Speiser, R. (see Brice, B. A.)—768
Sponer, H. (see Bass, Arnold M.)—389
Stamm, Robert F. Calibration of differential refractometers 788(L)
Stearns, E. I. (see Buc, G. L.)—336(L)
Steel, W. H. Four-figure method of ray tracing—878(L)
Stehli, Irene Comfort (see Romer, Alfred)—178(L)
Stephens, Robert E. Comments on "The Design of Triplet Anastigmat Lenses of the Taylor Type"—407
——(see Tilton, Leroy W.)—540
Stewart, H. S. (see Curcio, J. A.)—264(A)
Stookey, S. D. Photosensitive glass—265(A)
Strong, John. New Johns Hopkins ruling engine—258(A)
—— (see Rupert, C. S.)—455
Struve, Otto. *Stellar Evolution* (Book). Reviewed by Donald H. Menzel—791
Studer, Frank J. (see Johnson, Peter D.)—121(L)
Stukenbroeker, G. L. (see McNally, J. R., Jr.)—803(A)
—— **and J. R. McNally, Jr.** Hyperfine structure of U^{233}—262(A)
—— **and J. Rand McNally, Jr.** Preliminary results on the spin of U^{235}—336(L)
Stultz, K. (see Higgins, G. C.)—135
Sutherland, G. B. B. M. Recent work on the two forms of diamond—254(T)
Sziklai, George C. Tristimulus photometer—797(A)

Taylor, William J. (see Holden, Robert B.)—577
Teago, F. J. and J. F. Gill, *Mercury Arcs* (Book). Reviewed by J. Rand McNally, Jr.—477
Terrien, J. and F. Desvignes. Photometric separator for precision visual spectrophotometry—845
Thiers, Ralph E. Step-sector for the astigmatic spectrograph—849
Theissing, H. H. Macrodistribution of light scattered by dispersions of spherical dielectric particles—232
Thorington, Luke. Temperature dependence of the emission of an improved manganese-activated magnesium germanate phosphor—260(A)/579
Thorndike, E. M. Wide-angle, underwater camera lens—823
Tilton, Leroy W. and Earle K. Plyler. Refractivity of lithium fluoride with application to the calibration of infra-red spectrometers—798(A)
——, **Earle K. Plyler, and Robert E. Stephens.** Refractive index of silver chloride for visible and infra-red radiant energy—540
Timma, D. L. Book review of *Spectroscopic Properties of Uranium Compounds* by G. H. Dieke and A. B. F. Duncan —181
Tolansky, S. *Hyperfine Structure in Line Spectra and Nuclear Spin* (Book). Reviewed by J. Rand McNally, Jr.—477
Toran, Nestor (see Tousey, R.)—264(A)
Torkington, P. Calibration of infra-red spectrometers—481(L)
Tousey, R. (see Johnson, F. S.)—264(A)
——, **F. S. Johnson, John Richardson, and Nestor Toran.** Monochromator for the vacuum ultraviolet—264(A)
Troy, D. J., Jr. and L. G. Glasser. Reducing stray light errors in the Hunter multipurpose reflectometer—80
Tunnicliffe, William W. (see Macdonald, Duncan E.)—263(A)
Turner, A. F. (see Smith, F. D.)—261(A)
Turner, Robert D. (see Romer, Alfred)—178(L)
Tyler, John E. New photometric device—693

Valasek, Joseph. *Introduction to Theoretical and Experimental Optics* (Book). Reviewed by Wallace R. Brode—182
Vallee, Bert L., Charles B. Reimer, and John R. Loofbourow. Influence of argon, helium, oxygen, and carbon dioxide on emission spectra in the d.c. arc—803(A)/751
van der Velden, H. A. (see Bouman, M. A.)—336(L)
van Heel, A. C. S. High precision measurements with simple equipment—809
Vanselow, W. (see Fortmiller, L.)—487
Velasco, Rafael (see Catalán, Miguel A.)—653
Venable, William Mayo. (*Hydrogen in Chemical Atoms* (Book). Reviewed by Charlotte E. Moore—696
Vodar, B. (see Bauple, R.)—788(L)
von Schelling, Hermann. Method for calculating the effect of filters on color vision—419

Walker, Marshall J. and Richard G. Raymond. Measurement of Faraday effect and Cotton-Mouton effect using transient magnetic and a photo-multiplier-type compensator—266(A)/766
Washer Francis E., (see Hotchkiss, Robert N.)—802(A)
—— **and Fred W. Rosberry.** New resolving power test chart —801(A)
Watson, John T. and William C. Britton. Deterioration of image quality by photographic windows—258(A)
—— **and Vincent Young.** Optical quality in large glass blanks —258(A)
Weaver, K. S. Measurement of photographic transmission density—524
—— On the standard source for low level photometry—60(L)
Webb, J. H. Low intensity reciprocity-law failure in photographic exposure: energy depth of electron traps in latent-image formation; number of quanta required to form the stable sublatent image—3

—— Low intensity reciprocity-law failure in photographic exposure. II. Multiplet-quantum hits in a critical time period—266(A)/197
West, C. D. Polarizer, polarizing beam splitter, and birefringent elements; and some optical systems in which they enter—796(T)
White, John U. Design of a multiple reflection Raman tube—803(A)
—— (see Liston, Max D.)—36
—— **and Max D. Liston.** Construction of a double beam recording infra-red spectrophotometer—29
—— **and Max D. Liston.** Performance of a double-beam recording infra-red spectrophotometer—93
Wiley, R. S. (see Richardson, David)—259(A)
Wilkins, J. Ernest, Jr. Resolving power of a coated objective. II—222
—— Theory of the refractometer—259(A)
Williams, Ferd E. Book review of *Luminescent Materials* by G. F. J. Garlick—406
—— (see Roberts, Shepard)—516
Williams, Franklin C. Objectives and methods of density measurement in sensitometry of color films—104
—— **and Franklin R. Clapper.** Multiple inter-reflections in photographic color prints—796(A)
Williams, H. D. Growing large barium titanate crystals—796(T)
Williams, S. B. (see Harriman, M. W.)—102
Williams, W. E. *Applications of Interferometry* (Book). Reviewed by J. Rand McNally, Jr.—790
Williamson, D. E. (see Jurmain, J.)—804(A)
Wilson, A. J. C. *X-Ray Optics* (Book). Reviewed by J. Rand McNally, Jr.—477
Wolf, Ernst and Michael J. Zigler. Dark adaptation level and size of testfield—211
Wolfe, Robert N. and Fred C. Eisen. Spatial photographic recording of fine interference phenomena—143
Woodruff, J. F. Use of briquetted samples in the spectrochemical analysis of carbon and alloy steels and other metals—192
Woodson, Robert A. Schmidt system aberration investigation—802(A)
Wooters, Glenn. Lens centering in microscope objectives—521
Wormser, Eric M. On the design of wide angle Schmidt optical systems—256(A)/412
Worsnap, B. L. and F. C. Chalklin. *X-Rays* (Book). Reviewed by J. Rand McNally, Jr.—790
Wright, G. J. (see Davidson, H. R.)—817

Young, F. Mansfield (see Hardy, Arthur C.)—59(L)
Young, Vincent (see Watson, John T.)—258(A)
Younkin, S. G. Measurement of small color differences in tomato purees—265(A)/596

Zernike, F. Precision method for measuring small phase differences—326
—— (see Saylor, Charles Proffer)—329
Zigler, Michael (see Wolf, Ernst)—211
Zworykin, V. K. and E. G. Ramberg. *Photoelectricity and Its Application* (Book). Reviewed by George R. Harrison—28

JOURNAL OF THE OPTICAL SOCIETY OF AMERICA VOLUME 40, NUMBER 12 DECEMBER, 1950

Annual Subject Index to Volume 40

Key to Index Use

1. **Subjects,** not titles, have been indexed.

2. **Contents** of papers (and abstracts of papers presented at meetings) have been indexed rather than a word breakdown of the title.

3. Principal subjects are given in **boldface** type. Cross-referenced subjects which should be consulted for a more thorough coverage are given in *italics* after the principal subject.

4. (A), (L), (B), (N), etc. indicate, (A) Abstracts of meeting papers; (L) Letters to the Editor; (B) Book Reviews, and (N) Notes. In the case of abstracts of meeting papers, since several abstracts appear on the same page and often on the same or similar subject, the abstract number is also given. If the paper covered by the abstract has been submitted and published in the same year as the abstract, this has been indicated by a solidus (/) between the abstract notation and the Journal page of the full article, i.e., 264 (A*67*)/589 indicates that the paper described in abstract No. *67* on page 264 has been published in full on page 589.

Book Reviews and Letters to the Editor have not been as thoroughly broken down into subjects but have been confined to principal subjects and separate listings under headings of Book Reviews and Letters to the Editor, which in the former have included authors and reviewers.

5. Subjects have been indexed in subdivisions according to key words with prepositions such as "on," "in," "of," "with," etc. included where essential for euphoneous interpretation, but not affecting the alphabetical arrangement of the principal subject. In many cases, where obvious, these prepositions have been omitted.

Aberration, chromatic, effect on vision—796(A*10*)
comatic, in infra-red spectrometer—256(A*15*)/450
geometrical, coherent set of tolerances for—60(L)
ray tracing calculation of—878(L)
Schmidt system—256(A*10*)/412, 802(A*51*)
third-order, calculated with IBM machines—255(A*9*)
torus grating—153
ultraviolet microscope objectives—283
Absorption (see also *Spectra*)
by free radicals—381
theory of—424
Adaptometers, Hecht-Shlaer, monocular—584
Aerial Reconnaissance, video techniques in—263(A*55*)
Alignment, high precision—809
American Society for Testing Materials, Marburg Lecturer, 1950, Wallace R. Brode—547(N)
meeting, June, 1950—547(N)
Ammonium Dihydrogen Phosphate (ADP), birefringent material in polarization interference filter—262(A*46*)
Anomaloscope, dichroic filter—41
Nagel—41
Applied Optics, research and development at the National Bureau of Standards—251(N)
Astronomy, stellar evolution—791(B)
Atmospheric Optics, attenuation of brightness contrast—263(A*57*)
attenuation of brightness contrast, visual and photoelectric measurements compared—371
color of distant objects—263(A*56*)/373, 883
optical haze—507
radiation fluctuations—795(A*6*)
visual range—795(A*5*)
wave-length effects—263(A*57*)

Atomic Spectra (see *Spectra*)
Attenuation of Contrast, atmospheric—507
visual and photoelectric measurements—371
wave-length effect on—263(A*57*)

Barium Titanate Crystals, production of—796(A*14*)
properties of—796(A*15*)
Beam Interrupters, types of—112
Biological Leaf Material, spectrochemical analysis for—804(A*64*)
Birefringent Layers, in dihydrogen phosphate (ADP and KDP) crystals—798(A*26*)
filter—471
Blackwell, H. Richard
Adolph Lomb Medalist—794
Book Reviews
Analytical Absorption Spectroscopy. Edited by M. G. Mellon. Reviewed by T. R. P. Gibb, Jr.—695(B)
Application of Interferometry. W. E. Williams. Reviewed by J. R. McNally, Jr.—790(B)
Atlas of Spectra (Atlas der Restlinien). A. Gatterer and J. Junkes. Reviewed by W. F. Meggers—695(B)
Atomic Spectra. R. C. Johnson. Reviewed by J. R. McNally, Jr.—790(B)
Color Psychology and Color Therapy. F. Birren. Reviewed by R. M. Evans—696(B)
Crystals and X-Rays. K. Lonsdale. Reviewed by A. L. Patterson—181(B)
Electron Diffraction. R. Beeching. Reviewed by J. R. McNally, Jr.—477(B)
Electron Microscope, Its Development, Present Performance and Future Possibilities. D. Gabor. Reviewed by L. Marton—879(B)
Electron Microscopy: Techniques and Applications. R. W. G. Wyckoff. Reviewed by L. Marton—879(B)
Electron Optics. I. Fundamentals of Theoretical Electron Optics (Electronenoptik. I. Grundzüge der Theoretischen Elektronen-optik). A. A. Rusterholz. Reviewed by L. Marton—879(B)
Elementary Photography. G. Quarles. Reviewed by W. R. Brode—620(B)
Fluorescence and Phosphorescence. P. Pringsheim. Reviewed by W. R. Brode—545(B)
Handbook of Experimental Stress Analysis. M. Hetenyi. Reviewed by S. Levy—880(B)
Hydrogen in Chemical Atoms. W. M. Venable. Reviewed by C. E. Moore—696(B)
Hyperfine Structure in Line Spectra and Nuclear Spin. S. Tolansky. Reviewed by J. R. McNally, Jr.—477(B)
Infrared Determination of Organic Structures. H. M. Randall, R. G. Fowler, N. Fuson, and J. R. Dangl. Reviewed by R. B. Barnes—252(B)
Infrared Radiation Therapy Sources and Their Analysis with Scanner. Leopold Rovner. Reviewed by C. J. Humphreys—545(B)
Introduction to Experimental Stress Analysis. G. H. Lee. Reviewed by W. Ramberg—790(B)
Introduction to Luminescence of Solids. W. Leverenz. Reviewed by W. R. Brode—406(B)
Introduction to Theoretical and Experimental Optics. J. Valasek. Reviewed by W. R. Brode—182(B)
The Language of Drawing and Painting. A. Pope. Reviewed by D. B. Judd—122(B)
Luminescent Materials. G. F. J. Garlick. Reviewed by F. E. Williams—406(B)
Manual of Spectroscopy. T. A. Cutting. Reviewed by W. R. Brode—181(B)
Manual of Standardized Procedures for Spectrophotometric Chemistry. H. J. Fister. Reviewed by W. R. Brode—880(B)
Mercury Arcs. F. J. Teago and J. F. Gill. Reviewed by J. R. McNally, Jr.—477(B)
Metre-Kilogram-Second System of Electrical Units. R. K. Sas and F. B. Pidduck. Reviewed by J. R. McNally, Jr.—477(B)
Optics. F. W. Sears. Reviewed by W. R. Brode—252(B)
Photoelectricity and its Application. V. K. Zworykin and E. G. Ramberg. Reviewed by G. R. Harrison—28(B)
Physical Methods of Chemical Analysis. Vol. I. Edited by W. G. Berl. Reviewed by P. J. Elving—791(B)
Physiological Optics. Volume II. Light and Color (Optique Physiologique. Volume II. Lumiére et Couleurs). Y. Le Grand. Reviewed by G. H. Gliddon—620(B)
Precision Measurements in Optics (Die Optik in der Feinmesztechnik). K. Räntsch. Reviewed by I. C. Gardner—28(B)
Principles of a New Energy Mechanics. J. Mandelker. Reviewed by H. Mueller—181(B)
Quantitative Ultramicroanalysis. P. L. Kirk. Reviewed by W. R. Brode—620(B)
Refractive Indices of Halogen Salt Crystals (Die Brechzahlen einiger Halogenidkristalle). H. Harting. Reviewed by I. C. Gardner—477(B)
Spectrochemical Procedures. C. E. Harvey. Reviewed by W. R. Brode—696(B)
Spectroscopic Properties of Uranium Compounds. G. H. Dieke and A. B. F. Duncan. Reviewed by D. L. Timma—181(B)
Stellar Evolution. O. Struve. Reviewed by D. H. Menzel—791(B)
Structure and Properties of Photographic Emulsions (Structure et Propriétés des Couches Photographiques). L. P. Clerc. Reviewed by B. H. Carroll—545(B)
Theory of Special Relativity (La Théorie de la Relativité Restreinte). O. Costa de Beauregard. Reviewed by M. Herzberger—252(B)
Wave Filters. L. C. Jackson. Reviewed by J. R. McNally, Jr.—790(B)
X-Rays. R. L. Worsnap and F. C. Chalkin. Reviewed by J. R. McNally, Jr.—790(B)
X-Ray Crystallography. R. W. James. Reviewed by J. R. McNally, Jr.—790(B)
X-Ray Optics. A. J. C. Wilson. Reviewed by J. R. McNally, Jr.—477(B)
Bouguer's Law, non-uniform films—263(A*58*)
Brass, spectrochemical analysis of—262(A*53*)
1,3-Butadiene, configuration of, from Raman spectra—255(A*6*)/438

Calcium, isotopes investigated interferometrically—262(A*52*)
Cadmium, spectral analysis of—120(L), 121(L)
Cadmium Sulfate, x-ray detector—798(A*25*)
Carbon Arc (see also *Sources, Light Sources,* and *Spectrochemical Analysis*)
infra-red source—455
Cathode Ray Tube, cathode targets—102
grid targets—102
infra-red spectrometer using—257(A*17*)/608
intensity modulated scope—102
phosphor excitation—336
screens, visibility on—102
Cell, infra-red, for low temperature—757
infra-red absorption, thickness measurement—53
Chemical Analysis (see also *Spectrochemical Analysis*)
physical methods of—791(B)
Chlorobenzene, fluorescence of, in near ultraviolet—389
Chlorofluoromethane, infra-red spectra of—255(A*4*)
Collimation, intensity of beam reduced by—119(L)
Color (see also *Colorimetry*)
antireflection films, effect on—262(A*47*)
band width assignment of color—755

Color (continued)
centers in fused and crystalline quartz—266(A*79*)
changes from daylight to night light, calculated and observed—797(A*21*)
changes under artificial lighting—797(A*20*)
chromaticities, luminous efficiency attainable—120(L)
differences, visual sensitivity to—797(A*18*)
discrimination, chromatic surrounding field, effect on—797 (A*19*)
distant objects—263(A*56*)/373, 000
films, sensitometry of—104
half-tone masking theory in—796(A*17*)
harmony manual, colorimetric analysis of—265(A*69*)
illuminant-stable, vision test—793(N)
interference, thin layers on glass surface—146, 883
luminous efficiency of various chromaticities—120(L)
mixture, theory of, and projective geometry—264(A*66*)
mixtures, tristimulus value of—230
Munsell—265(A*68*)
Munsell renotations and color space of Hunter and Adams—85
Neugebauer's Theory in—796(A*17*)
Nicol prisims with thin crystal plate producing—621(L)
perception—620(B)
affected by daylight and tungsten light-adaptation—362
dichroic filter anomaloscope studies—41
Nagel anomaloscope studies—41
pleochroism, infra-red—141
prints, inter-reflections in—796(A*16*)
psychology—696(B)
reproduction with coupler dyes—166
sensitive—621(L)
space of Hunter and Adams, studied by Munsell renotations—85
surrounding, effect on constant hue and brightness loci—264(A*67*)/589
television, CBS—263(A*54*)
tristimulus values calculated—817
tristimulus values of subtractive color mixtures—230
vision affected by filters—419
Colorimeter, new automatic, for cotton—263(A*60*)/446
Colorimetry (see also *Color*)
abridged spectrophotometry—59(L), 119(L)
additive luminosities—647
automatic tristimulus integrator—817
chemical analysis procedures—880(B)
color harmony manual, analysis of—265(A*69*)
constant hue and brightness loci determinations—264 (A*67*)/589
cotton measurements—263(A*60*)/446
gloss measurements—265(A*71*)
Hunter color-difference meter—265(A*70*)/596
Hunter multipurpose reflectometer measurements—80
International Commission on Illumination (I.C.I.), revision of data—798(A*22*)
recommendations—183(E)
tristimulus system, calculation of interference colors—146
conversion into Hunter's and Adams' data—85
integration with punched cards—138
meter, for determining color saturation threshold—459
micro-quantitative—620(B)
National Bureau of Standards Circular on—479(N)
scales, Adam—85
Hunter—85
spectrophotometric, abridged—119(L)
tomato purees, color differences—265(A*70*)/596
tristimulus values, calculation of, based on illuminant approximating illuminant A—817
Color meter, for determining saturation threshold—459
Coma, aberration in infra-red spectrometer—256(A*15*)/450
central, calculation and verification of—521
microscope objective with eccentric or tilted lens—521
ray tracing—878(L)
torus grating—153
Commensurator, precision screws calibrated with—259(A*30*)
Commerce Department Award, Judd, Deane B., recipient of—441(N)
Computers, aberrations, third-order calculated—255(A*9*)
absorbance values in infra-red corrected for stray radiation—401
analog for spectrochemical analysis—804(A*66*)
Cartesian curves—263(A*59*)
colorimetric integration, I.C.I., tristimulus system—138
electrical, calculation of properties of multilayer interference films—261(A*42*)
infra-red absorbance values corrected for stray radiation—401
Corundum, reflection spectra in extreme uv absorption—788(L)
Cotton, color measured with new automatic colorimeter—263(A*60*)/446
Cotton-Mouton Effect, measurement of—266(A77)/766
Coupler Dyes, correction of color reproduction—166
Crystals, absorption compared with reflectance data of KBr:Tl—121(L)
ammonium dihydrogen phosphate (ADP), for interferometer—800(A*40*)
barium titanate, production of—796(A*14*)
properties of—796(A*15*)
birefringent, dihydrogen phosphate crystals—798(A*26*)
polarization interference filter—262(A*46*)
production of channeled infra-red spectra—141
rutile—266(A*78*)
counters—219
dihydrogen phosphate type, electro-optic effect in—125
electro-optic effect—225
inelastic behavior—256(A*14*)
infra-red optical, thermal conductivity of—256(A*13*)
lithium fluoride, properties of—798(A*28*)
luminescent properties by radiation—796(A*12*)
optical working of surface of—799(A*29*)/748
phosphors—219
photoelectric properties of—219
piezoelectric—225, 795(A*3*)
polarization—225
potassium bromide, thallium activated, absorption and reflectance—121(L)
production of, from fused melt—795(A*2*)
from solutions—795(A*1*)
quartz, color centers in fused and crystalline—266(A*79*)
reflectance compared with absorption data of KBr:Tl—121(L)
rutile, refractive index of—266(A*78*)
silver chloride, molded Schmidt plate—799(A*30*)
sphalerite, refractive index of—266(A*78*)
symposium on, at Cleveland Meeting 1950—795(A)
thallium bromide-iodide—799(A*29*)/748
uniaxial—225
x-ray detection—798(A*25*)
and x-rays—181(B)
Crystallography, x-ray—790(B)

Diamond, properties of—254(A*1*)
Dielectric Particles, light scattering by—232
Diffraction, alignment measurements by—809
echelette grating, new mounting for—504
electron—477(B)
geometrical aberrations—60(L)
grating interferometer—480(L)
image in microscopy—14

pattern and phase contrast—291
pattern deterioration by roof prisms—664
pattern of coated objective—222
phase difference measured—326
phase microscopy—295
torus grating—153
variable phase microscopy—64
x-ray, from crystals—181(B)
Diffraction Gratings (see *Gratings*)
Diffraction Optics, theory of—424
Densitometer, Densitometry
calibration of photographic emulsions—842
color, analytical—104
pot-opal type—524
sensitometry of color films—104
sphere type—524
Double-Beam Analyzer, infra-red, design of—112
ultraviolet, design of—112
Drawing and Painting—122(B)

Echelles—127
interferometer tests for—259(A*29*)
Editorials
Harrison, Dean George R., retirement as editor—1(E)
International Commission on Illumination Recommendations, 1948—183(E)
Optical Society of America, Society finances—549(E)
Physics Today—2(E), 807(E)
Electrical units, law establishing—663(N)
meter-kilogram-second system—477(B)
Electromagnetic Theory, wave propagation in stratified medium—465
Electron Microscopy—269
Electron Multiplier, photo-tube, sensitive cathode area shape—253(L)
Electron Optics, theory of—269, 879(B)
Emission Spectra (see *Spectra* and *Sources*)
Emission, theory of—424
Errata—686(N)
color, of distant objects—883
interference, of thin layers on glass surface—883
colorimetry, direct and indirect compared—52
films, thin evaporated, on glass—883
Michelson-Morley experiment—883
microscope optics—883
phosphors, photo-conducting—79
photographic emulsions
reciprocity law failure—883
x-ray exposure—883
Excitation, of molecular nitrogen, kinetics of—805(A*76*)
Eye (see *Vision*)

Fabry-Perot, filters—261(A*45*)
interferometer—345
Faraday Effect, measurement of—266(A77)/766
Fermat's Principle, parageometrical optics—600
refraction—244
Films, Metal Films, Thin Films
adhesion of—804(A*68*)
antireflection, and their effect on color—262(A*47*)
evaporated—203
index of refraction of—623(L)
interference colors on glass—146, 883
metallic, and their optical constants—261(A*44*)
multilayer interference of—261(A*42*)
non-uniform and Bouguer's Law—263(A*58*)
optical properties of aluminum, antimony, copper, gold, nickel, palladium, silver—203
phase change in reflection from evaporated metal and dielectric—761
phase shift in—789(L)
reflection and transmission of—807(A*44*)
semi-transparent, determination of optical constants of —544(L)
structure of—203
thickness of—623(L)
thickness measurement by interferometer—690
Filters, color vision—419
electrical wave—790(B)
Fabry-Perot type—261(A*45*)
infra-red transmitting—415
interference—261(A*43*)
interference, influence of angle of incidence—336(L)
interference, transmittance of—336(L)
interference, polarization—262(A*46*)
thallium bromide-iodide—799(A*29*)/748
total reflection, birefringent—471
visible absorbing—415
Flame Temperature, hydroxide emission band in uv—264(A*61*)
Fluorescence (see *Luminescence* and *Phosphors*)
Fluorite, microscope, objective using—283
Fluorobenzene, fluorescence of, in near ultraviolet—389
Foucault Tests, concave mirrors figured by quantitative—258(A*23*)
Free Radicals, intensity changes due to absorption by—381

Garnett Theory—203
Geometrical Optics, aberration, set of tolerances for—60(L)
matrices—819
objectives, high speed spectrograph—256(A*11*)/462
reflected and transmitted field intensity determined by—48
Schmidt system, design of wide angle—256(A*10*)/412
theoretical and experimental—182(B)
theory of—424
Geometry, projective, and theory of colors—264(A*66*)
German Glass Technology Society, meeting, Düsseldorf, June, 1950—548(N)
Glass, luminescent properties by radiation—796(A*12*)
molds for—177(L)
photographic windows and resolution—258(A*25*)
photo-sensitive—265(A*73*)
research at National Bureau of Standards—251(N)
standards of spectral transmittance—435
surfaces, polarization studies of light diffusely reflected from —55
Gold Black, infra-red absorption, theory of—801(A*43*)
Goniophotometers—265(A*72*)
Grain, in photographic emulsion—799(A*31*)
Gratings, concave, replica—800(A*37*)
diffraction, interferometer tests for—259(A*29*)
production of—59(L)
ruling engine for—258(A*27*), 258(A*28*)
echelette diffraction, new mounting for—504
mounting of—800(A*38*)
plane, as monochromator—800(A*36*)
replica of concave—800(A*37*)
ruling control, electronic—800(A*41*)
ruling engine's dividing gear—623
ruling, techniques of—127
torus, auto-imagining, theory of—153
Group for the Advancement of Spectrographic Methods (G.A.M.S.)
meetings—191(N), 372(N)
symposium, Strasbourg—543(N)

Hafnium, spectrochemical determination of, in hafnium-zirconium dioxide—262(A*49*)
Halogens, spectrochemical analysis for—804(A*63*)
Harrison, George R.
Ives Medal Address—127
Ives Medalist, 1949—123

Harrison, George R. (continued)
retirement as editor—1(E)
scientific publications—125
Herschel Effect, photographic latent image—487
Hunter Color-Difference Meter, tomato purees—265(A*70*)/596
Hydroxide Radical, emission band in ultraviolet used in flame temperature determinations—264(A*61*)

Illuminating Engineering Society
Gold Medal Award, 1950, William F. Little recipient—793(N)
meeting, 1950—793(N)
new officers, 1951—793(N)
Image, deterioration by photographic plate glass windows—258(A*25*)
Image Dissector, high speed motion photography—260(A*37*)
Infra-Red Absorption Cells, thickness measured—53
Infra-Red (see also *Spectra, Spectrometers*)
absorption of gold black—801(A*43*)
cell, measurement of thickness—53
variable thickness—757
filters, for transmission, region 1 to 6μ—415
heat lamp radiation measured—545(B)
low temperature measurement—757
optical crystals, thermal conductivity of—256(A*13*)
phosphors, sensitive to—335(L)
photo-conductive cells, sensitivity for—603
punch-card committee—547(N)
source, the carbon arc—455
Infra-Red Spectra (see *Spectra*)
Instruments (see also *Colorimeters, Spectrometers,* etc.)
channeled, produced by birefringent crystals—141
differential refractometer—788(L)
galvanometer intensity scale—787(L)
glow discharge arrangement for vacuum evaporator—687
infra-red cells for variable thickness-low temperature—757
monochromatic, with plane grating—800(A*36*)
photometric, flicker—693
photo-multiplier compensator for determination of optical rotation—266(A77)/766
for vacuum evaporated coatings—687
Intensity, measurements in vacuum ultraviolet with thermocouple—264(A*63*)
reduction of beam by collimation—119(L)
Interference, alignment measurements by—809
colors of thin layers on glass surface—146, 883
filters, Fabry-Perot type—261(A*45*)
phase shifts in—261(A*43*)
polarization—262(A*46*)
transmittance of—336(L)
Fresnel, in Michelson interferometer—787(L)
Lloyd mirror, bands produced by—143
Michelson interferometer—787(L)
multilayer, films and their properties calculated by electrical computer—261(A*42*)
phase change on reflection from thin films—761
phase shift measurements of thin films—789(L)
photographic recording of—143
spectra measurements of neon and natural mercury—339
topographic measurements of optical surfaces—258(A*26*)
Interferometer, Interferometry
ammonium dihydrogen phosphate (ADP) crystal for—800(A*40*)
application—790(B)
calcium isotopes studied with—262(A*52*)
diffraction grating—480(L)
electro-optic crystal for—800(A*40*)
Fabry-Perot—345
mercury isotopes studied with—345, 262(A*52*)
Michelson—787(L)
phase changes in white light—802(A*55*)
photometric setting—326
precision screws calibrated by—259(A*30*)
refraction, index of, determined by—623
thickness of infra-red absorption cells measured by—53
thin film, measured by—690
refractive index determined by—623
Inter-Society Color Council, meeting 1950—92(N)
International Commission on Illumination (I.C.I.)
announcement of survey of radiant energy receivers—778(N)
illuminants—797(A*22*), 798(A*23*)
recommendations, 1948—183(E)
revision of colorimetry data, proposal for—798(A*22*)
International Commission of Optics (I.C.O.)
documents available—478(N), 792(N)
London meeting, July, 1950—274(N), 697(N)
proposed standard conditions for experiments in physiological optics—881(N)
report from U.S. National Committee—478(N)
International Optical News
I.C.O. London meeting—697(N)
London Conference on Optical Instruments, July, 1950—698(N)
Iron, arc spectrum of—255(A*3*)
Isotope Shifts—803(A*61*)
in samarium spectrum—803(A*61*)
in thorium spectrum—803(A*62*)
Ives Medal
presentation to George R. Harrison, October, 1949—123
retrogression in spectroscopy, acceptance address by George R. Harrison—127

Jones, Lloyd A., biographical note in PSA Journal—191(N)
Judd, Deane B., receives Commerce Department Medal—441(N)

Kirchhoff's Law extended—376

Lamps, afterglow measurements of ultraviolet radiation from 805(A*75*)
mercury, high pressure, color corrected by magnesium fluorogermanate: manganese activated—260(A*36*)/579
quality, testing of—794
sealed beam, design of—805(A*73*)
spiraling on fluorescent—805(A*74*)
Lenses, blanks tested for optical quality—258(A*24*)
high speed camera of Institute of Optics—256(A*12*)
long focal length, for photography—863
microscope objectives—521
photographic, military, standards for—801(A*48*)
spurious resolution of—802(A*50*)
testing of—257(A*21*)
telescope refracting objectives—802(A*52*)
tester—257(A*21*)
testing bench for photographic objectives—257(A*19*)
triplet anastigmat, of Taylor type—406(L), 407(L)
Letters to the Editor
aberrations, geometrical—60(L)
absorption spectra, quartz and corundum—788(L)
atomic spectra, samarium isotopes—878(L)
chromaticities, luminous efficiency attainable—120(L)
color, sensitive—621(L)
colorimetry, abridged spectrophotometry—59(L), 119(L)
dividing gear for ruling engine—623(L)
electron multiplier photo-tube—253(L)
films, semitransparent, determination of optical constants—544(L)
galvanometer intensity scale—787(L)
glass, bronze molds for—177(L)
gratings, diffraction, production of—59(L)

infra-red spectrometers, calibration of—481(L)
intensity reduction of beam by collimation—119(L)
interference, Fresnel in Michelson interferometer—787(L)
interferometer, diffraction grating—480(L)
lens, triplet anastigmat, of Taylor type—406(L), 407(L)
light source, d.c. intermittent arc—180(L)
luminescence, emission band of willemite—407(L)
emission spectra of manganese-activated zinc silicate—622(L)
infra-red phosphors—179(L)
photographic emulsion, calibration of—621(L)
photometry, standard source for low level—60(L)
ray tracing—878(L)
reflectance, ultraviolet, measurements—178(L)
reflection compared with absorption of solid KBr:Tl—121(L)
refraction, indices of lithium fluoride—878(L)
refractometer, calibration of—788(L)
spectra, cadmium—120(L), 121(L)
potassium, 3446A and 3447A—178(L)
spark, of technetium and promethium—177(L)
spectrophotometry, abridged, colorimetry by—59(L), 119(L)
thin films, determination of thickness and refractive index—623(L)
phase-shift measurement of—789(L)

Light (see also *Radiant Energy* and *Radiation*)
intensity differences measured with photo-multiplier tubes—381
International Commission on Illumination recommendations 1948—183(E)
scattering by small particles—232
speed of—185, 883

Light Sources (see also *Sources* and *Spectra*)
arc, emission spectra—76
d.c. arc, intermittent—180(L)
electric arc—658
flash lamps, gas discharge—648
high pressure xenon arc as ultraviolet source—782
hollow-cathode, for high resolution and small samples—386
mercury arc, for depolarization measurements—89
for photometers—336(L)
short duration, high intensity—658
uniformly bright area—260(A*39*)
variable, in stellar photoelectric spectrophotometry, compensation for—149

Limestone, spectrochemical analysis of—804(A*65*)

Liouville's Theorem, parageometrical optics—600

Lithium Fluoride
calibration of infra-red spectrometers—798(A*27*)
inelastic behavior—256(A*14*)
mechanical properties—798(A*28*)
optical properties—798(A*28*)
refractive index of—798(A*27*), 878(L)
thermal conductivity of—256(A*13*)

Little, William F., I.E.S. Gold Medal Award recipient—793(N)

Lomb, Adolph, Medal (1950)
presented to H. Richard Blackwell—794

Luminance, metacontrast as effected by—796(A*9*)

Luminescence (see also *Phosphors*)
absorption data of KBr:Tl compared with reflectance—121(L)
activator concentration and influence on emission spectra—345
crystal phosphors—219
crystals and glasses, effect of high energy radiation—796(A*12*)
emission spectra, dependence on activator concentration and temperature—345
lead-activated sodium chloride phosphors—854
zinc beryllium silicate, manganese activated and decay time—337(L)
excitation of willemite (zinc silicate) by cathode-ray—356
fluorescence, of fluorobenzene and chlorobenzene vapors in the near ultraviolet—389
and phosphorescence—545(B)
and the trapping of light—261(A*40*)
infra-red sensitive, oxy salts—179(L)
phosphors—353
magnesium activated calicum silicate—805(A*75*)
manganese activated zinc silicate phosphor, emission spectrum—509, 622(L)
phosphorescence, duration of, in minerals—430
zinc silicates (willemite)—407(L)
potassium bromide, thallium activated—121(L)
solids, and theory of phosphor absorption—406(B)
inorganic—406(B)
sulfide phosphors, theory of—516
temperature dependence of manganese-activated magnesium germanate phosphor—260(A*36*)/579
temperature effect on emission spectra—345
zinc sulfide type phosphors—260(A*35*)

Luminosity, definition of—647

Mechanics, principles of a new energy—181(B)

In memoriam
Nutting, Perley G.—404
Worthing, Archie G.—404

Mercury
arcs—477(B)
infra-red spectra—255(A*5*)
isotope 198, spectra of—801(A*45*)/737, 345
isotopes investigated interferometrically—262(A*52*)
natural, standards, secondary—339

Metal Films (see *Films*)

Michelson-Morley Experiment, extrapolation of—185, 883

Microphotometer, recording—802(A*54*)

Microscope (see *Microscopy*)

Microscopy, airy limit of resolution—14
dark-field illumination for nuclear track plates—61
designs—275, 883
diffraction, image in—14
electron, comparison with photon—269
course in at Cornell University, August, 1950—454(N)
history and future—879(B)
metal films, study of—203
techniques and applications—879(B)
illumination, narrow-coned axial—14
infra-red—304
lamps for—275, 883
objectives—275, 283, 883
coated to alter diffraction pattern—222
lens centering in—521
optics of—275, 883
particle size effect on diffraction image in—14
phase, resolving power in—295
phase contrast—275, 883
color—329
color plate of fiber glass, sodium chlorate, protozoan, onion root—330
edge effect in—803(A*56*)
opaque specimens—259(A*34*)/314
Toraldo's theory of—291, 576
phase differences, measurement of—326
photon—269
reflected light in phase contrast—259(A*34*)/314
resolution—222
airy limit—14
limits of—295
tests for—275, 883
spectrometry, micro—317

Microscopy, (continued)
stage micrometer, from photographic record of interference bands—144
ultraviolet—275, 883
objectives for—283
variable phase—64
measurement of unresolved single particle—64
Minerals, duration of phosphorescence—430
Mirrors (see also *Films* and *Reflection*)
adhesion of metal films for—804(A*68*)
concave, figured by quantitative Foucault tests—256(A*23*)
Schwarzschild, for microscopic objectives—283
vacuum evaporator for—687
Monochromator (see also *Spectrometers*)
grating, 180 to 4000 mμ—259(A*32*)
plane grating—800(A*36*)
vacuum ultraviolet grating—264(A*62*)

National Bureau of Standards
colorimetry—479(N)
optics and optical glass research—251(N)
spectrographic standards—741(N)
spectrophotometry—479(N)
Neon, standards, secondary—339
Newtonian Relativity—185
Nitrogen, kinetics of excitation of molecules—805(A*76*)
Nomenclature
International Commission on Illumination Recommendations—183(E)
luminosity terminology—647
Nuclear Tracks, microscopic dark-field illumination of plates for—61
photographic emulsions for—61
Nutting, Perley G., in memoriam—404
Nylon, ultraviolet dissociation spectra of—262(A*50*)

Optical Society of America
alphabetical directory of members—699
geographical directory of members—726
local sections news
Chicago section installed—408
meeting, March, 1950—408
News Letter No. 5, February, 1950—191
officers, 1951–52—545
Rochester section history—625
medals
Adolph Lomb Medal to H. Richard Blackwell—794
Frederic Ives Medal to George R. Harrison—123
meetings
March, 1950 (New York)
abstracts of papers presented—254
minutes of meeting of Board of Directors—482
proceedings—254
October, 1950, thirty-fifth annual (Cleveland)—547, 595
abstracts of papers presented—795
minutes of meeting of Board of Directors—882
proceedings—794
March, 1951
advance announcement—692
annual reports for 1949
editor of publications—482
secretary—483
treasurer—485
society finances—549(E)
Optical Society of America, Journal of
binding announcement—418(N)
Optics—252(B)
London conference on, July, 1950—274(N)
microscope—275, 883
theory of—424
in stratified medium—465

Oscillograph (see *Cathode Ray Tube*)

Paint, gloss measurements of —265(A*71*)
Parageometrical Optics—600
Particle, unresolved, optical properties measured by variable phase microscopy—64
Phase Contrast, color—329
edge effect—803(A*56*)
Phase Contrast Microscopy (see *Microscopy*)
Phase Shifts
interference filters—261(A*43*)
Phosphorescence (see *Luminescence, Phosphors*)
Phosphors, calcium silicate, manganese activated—347
crystal
argon, cadmium sulfide, diamond, silver bromide, silver chloride, thallium chloride, and zinc sulfide—219
duration of phosphorescence in natural minerals—430
infra-red sensitive—179(L), 335(L)
double activated—353
magnesium germanate, manganese-activated—260(A*36*)/579
oxygen-containing—179(L)
sodium chloride, lead activated—854
strontium selenide and sulfide, europium-samarium activated—353
strontium sulfide, with zinc, bismuth, and samarium activation—335(L)
sulfide—516
zinc beryllium silicate, manganese activated—337(L), 347
zinc silicate (willemite)—407(L)
cathode-ray excitation—356
manganese activated—509, 622(L), 347
zinc sulfide—260(A*35*)
Photo-Conductive Cells, lead sulfide and telluride, infra-red sensitivity of—603
Photoelectric, colorimeter—119(L)
spectrophotometric compensating control—149
Photoelectricity, application to optical problems—28(B)
Photographic Emulsions (see also *Photography*)
calibration of—266(A*75*), 621(L), 842
color correction with coupler dyes—166
color films—104
development of, and hair-silver formation—615
exposure of—266(A*74*)/197
granularity and graininess, instrument for measuring—799(A*31*)
high altitude—863
high contrast—863
infra-red irradiation of—487
interference bands in, used as stage micrometer for microscope—143
latent image formation—266(A*76*)/246
energy depth of electron traps—3, 883
and Herschel effect—487
low intensity—266(A*74*)/197
multiple quanta in critical time—266(A*74*)/197
nuclear tracks, detection of—61
performance characteristics—799(A*31*)
properties and structure—545(B)
reciprocity law failure—3, 266(A*74*)/197, 799(A*34*), 799(A*35*), 883
recording of fine interference phenomena by—143
silver filaments and dendrites, growth of—615
sublatent image formation—3, 883
for vacuum ultraviolet spectra—23
x-ray, sensitized by gold—266(A*76*)/246
Photographic Flash Lamps
short duration, high intensity gas discharge—658
Photographic Objectives (see *Lenses*)
Photography (see also *Photographic Emulsion*)
color print, inter-reflections in—796(A*16*)

detail, criteria for 258(A22)
elementary—620(B)
filters, color—863
of high altitude objects—863
image dissector for high speed motions—260(A37)
images and their formation—104
lenses, long-focal-length—863
photo-sensitive glass for recording images—265(A73)
shutter for, fast closure slit—260(A38)
Photometer, Photometry
galvanometer intensity scale—787(L)
heterochromous—842
integrating for low light levels—409
interference measurements—326
light source for, used to evaluate slope of absorption curve—336(L)
modulated filament circuit for—693
photoelectric, for turbidimetry—768
recording micro—802(A54)
separator for visual spectrophotometry—845
standard sources for low level—60(L)
tristimulus—797(A22)
Photometric Units established by law—663(N)
Photo-Multipliers, envelopes of, in quartz—264(A54)
fluorescence sensitized—264(A65)
light intensity differences measured by—381
sensitivity to ultraviolet light—264(A64)
vacuum ultraviolet radiation measured by—264(A65)
Photo-Sensitive Receivers, aerial reconnaissance—263(A55)
Photo-Sensitivity, of acid resists—799(A33)
Physical Optics (see also *Geometrical Optics, Optics, Physiological Optics*)
reversibility and irreversibility in—798(A24)
theoretical and experimental—182(B)
Physics Abstracts, 229(N), 646(N)
Physics Today—2(E), 807(E), 765(N)
Physiological Optics (see *Vision*)
Pittsburgh Conference on analytical chemistry and applied spectroscopy—47(N), 844(N)
Plexiglas, inelastic behavior—256(A14)
Polarization, birefringent frustrated total reflection filter—471
crystals, measurements—304
depolarization measurements—89
infrared spectroscopy—141
interference filter—262(A46)
magnetic effects on—266(A77)/766
optical properties entering into—796(A13)
photo-multiplier observation of—266(A77)/766
reflection from dielectric surfaces—55
Potassium, arc spectra of—178(L)
Potassium Chloride, inelastic behavior—256(A14)
Precision Measurements in optics—28(B)
Prisms
Amici roof—664
infra-red spectrometers and resolution—257(A16)
roof, diffraction pattern deterioration by—664
silver chloride, index of refraction for visible and infra-red—540
Promethium (Element 61)
absorption spectra of—262(A48)
emission spectra of—262(A48)
spark spectra of—177(L)

Quanta, optical phenomena—261(A41)
Quantometer—804(A67)
Quartz
absorption spectra of—788(L)
microscope objectives of—283

Radar
cathode-ray tube screens for—102
Radiant Energy, Radiation (see also *Light*)
distribution from candlepower standard—805(A72)
matter and—185
reflection and transmission of metal films and non-absorbing backings—801(A44)
thermal and reflection—376
Radiometry, thermopiles for—805(A71)
Raman Spectra, atlas of—816(N)
1,3-butadiene—255(A6)/438
cis- and *trans-*2-butenes—255(A6)/442
depolarization values of—89
excitation unit for—255(A7)/655
low temperature observations—255(A7)/655
reflection tube for—803(A57)
spectrograph objectives for—462
Ray Tracing, marginal spherical aberration calculated by—878(L)
Reciprocity Law Failure, high intensity photographic exposure—799(A34)
low intensity—3, 266(A74)/197, 883
measurement of—799(A35)
Reflection, absorption of solid KBr:Tl crystals measured by—121(L)
antireflections—262(A47)
electromagnetic theory of—761
filter, total, birefringent—471
geometrical optics method of determining reflected and transmitted field intensity—48
gloss, specular measured—265(A71)
goniophotometer for measurement of—265(A72)
integrating sphere for, in ultraviolet—178(L)
interference filters, Fabry-Perot type—261(A45)
metal-spacer-metal type—261(A43)
metal films—801(A44)
and calculation of their optical constants—261(A44)
multilayer interference films—261(A42)
phase change by thin films—761
polarization studies—55
Raman tube—803(A57)
submerged objects—795(A7)
thermal radiation—376
trapping light in fluorescent materials—261(A40)
Reflectometer, Hunter multipurpose, reduction of stray light in—80
Refraction, birefringent ammonium dihydrogen phosphate in polarization interference filter—262(A46)
birefringent crystals—141
of carbon dioxide—643
of Fermat's principle—244
of halogen salt crystals—477(B)
of lithium fluoride—798(A27), 878(L)
parageometrical—600
refractometer calibration—788(L)
of rutile—266(A78)
of silver chloride—540
skew rays traced by vector method—255(A8)
of sphalerite—266(A78)
of thin films—623(L)
of water vapor—643
Refractometer, differential, calibration of—788(L)
theory of—259(A33)
Relativity, Newtonian—185, 883
physics and—424
special theory of—185, 252(B), 883
Resolution, infra-red microspectrometer—304
measurement of, with test chart—257(A20)
microscopy, limits of—295
objective coated—222
photographic detail detected and recognized—258(A22)
photographic plate glass windows affecting—258(A25)
prism infra-red spectrometers—257(A16)

Resolution, (continued)
spurious, of photographic lenses—802(A*50*)
test chart for—801(A*49*)
Ricco's Law, in vision—336(L)
Röntgen Rays (see *X-Rays*)
Ruling Engine
Baird Associates—258(A*28*)
dividing gear for—623
new Johns Hopkins—258(A*27*)

Samarium (Element 43)
isotope spectral shifts—803(A*61*)
Scattering, of light by small metal spheres—795(A*4*)
Schmidt Optical System, aberration of—802(A*51*)
in astronomy—794
corrector plates of silver chloride—799(A*30*)
Schwarzchild Mirrors, infra-red microspectrometers—304
microscope objectives—283
Screws, precision, interferometric calibration of—259(A*30*)
Selenium, absorption in extreme ultraviolet—804(A*69*)
Sensitometry, effects in motion-blurred negatives—799(A*32*)
Shutter, slit, fast closure with low inertia—260(A*38*)
Silver Chloride, thermal conductivity of—256(A*13*)
Silver Filaments, growth of—615
Skew Rays, tracing of—255(A*8*)
Slit, collimated beam intensity effected by—119(L)
shutter for photography—260(A*38*)
static multislit spectrometer—257(A*18*)
width effects in spectrophotometry—172
Society for Applied Spectroscopy, meeting announcements—73(N), 224(N), 617(N), 816(N)
Sources (see also *Light Sources*)
induction heating, for spectrochemical analysis—82
standard for low level photometry—60(L)
Spectra (see also *Raman Spectra, X-Rays*)
Theory (see also *Atomic* and *Molecular Spectra*)
atomic states, evaluation of—74
g-value change in magnetic fields—653
hyperfine structure—477(B)
ionic ground states, evaluation of—74
ionization potential, estimation of—618
theoretical and experimental—182(B)
torus grating, production by—153
Atomic and Emission
atlas of spectra—695(B)
atomic spectra—790(B)
cadmium, analysis of—120(L), 121(L)
gadolinium, arc and spark—550
hydrogen in chemical atoms—696(B)
hydroxide radical—264(A*61*)
iron arc, 1.2 and 2.0μ—255(A*3*)
mercury, infra-red—255(A*5*)
mercury, natural—339
mercury isotope 198—345, 801(A*45*)/737
neon—339
noble gases, influence on emission spectra—803(A*58*)/751
potassium lines, 3446A and 3447A—178(L)
promethium (element 61)—177(L)
promethium, emission and absorption of—262(A*48*)
samarium isotopes—803(A*61*), 878(L)
technetium (element 43)—177(L)
thorium, isotope shifts of—803(A*62*)
uranium 235, spin in—262(A*51*), 363(L)
vanadium, infra-red emission—801(A*46*)
Molecular, Infra-Red Absorption
ammonia—93, 254(A*2*)/537
androsterone—304
atomsphere—254(A*2*)/537
benzene—93
benzylamine—93
carbon dioxide in breath—93
chlorinated benzenes, absorption of—801(A*42*)
chlorofluoromethane—255(A*4*)
correlated with structure—397
ethylene—93
gold blacks—801(A*43*)
hydrogen chloride—254(A*2*)/537
iso-octane—93
organic structures determined by—252(B)
penicillin in Nujol—93
phenyl alanine—304
polyvinyl alcohol—304
punch card—547(N)
ramie fiber—304
solid substances—254(A*2*)/537
solvent compensation—93
structure correlations—397
thymine—304
tissues, micro-spectra—304
toluene in Nujol—93
Molecular, Ultraviolet, and Visible
corundum absorption—788(L)
Nylon, ultraviolet dissociation—262(A*50*)
quartz absorption, in extreme uv—788(L)
selenium in ultraviolet, absorption of—804(A*69*)
uranium compounds—181(B)
vacuum ultraviolet photography—23
Spectral Sensitivity, photo-sensitive acid resists—799(A*33*)
Spectral Transmission Standards
permanence of—435
potassium chromate as—802(A*53*)
Spectrochemical Analysis, analog computer for—804(A*66*)
analytical absorption spectra—695(B)
biological leaf material—804(A*64*)
brass—262(A*53*)
direct reading "Quantometer"—804(A*67*)
ferrous alloys, influence of excitation characteristics on—803(A*59*)
hafnium in hafnium-zirconium dioxide—262(A*49*)
halogens in engine deposits—804(A*63*)
heterochromous photometry—842
limestone—804(A*65*)
Littrow spectrograph with dual range recording—259(A*31*)/779
metals—192
procedures—696(B)
samples, briquetted—192
sources
d.c. arc, influence of argon, carbon dioxide, helium, and oxygen on—803(A*58*)/751
source for, induction heating—82
standards for, from National Bureau of Standards—741(N)
steel—192
trace impurities—82
zinc base alloys—192
zirconium-hafnium mixtures—803(A*60*)/742
Spectrographs, astigmatic, step-sector for—849
dual range recording with Littrow spectrograph—259(A*31*)/779
modern industrial, course at Boston College, July, 1950—405(N)
objective, high speed—256(A*11*)/462
Spectrometry, Spectrophotometry (see also **Photometry**)
abridged—59(L), 119(L)
chemical analysis procedures—880(B)
color control—119(L)
colorimetry, by abridged—59(L)
filter, illuminant converting—817
infra-red, absorbance values corrected for stray radiation—401
calibration of—481(L)
calibration with lithium fluoride—798(A*27*)

comatic aberration in—256(A*15*)/450
detector: a pin-type thermocouple for amplification system for—36
double-beam recording—93
amplification and electrical systems of—36
construction of—29
micro—304
multislit—801(A*47*)
static—257(A*18*)
noise level in—93
oscillographic recording in near infra-red—257(A*17*)/608
prism, resolving power—257(A*16*)
ratio-recording double-beam—497
stray radiation—401
reduction of, with thallium bromo-iodide—799(A*29*)/748
wave-length calibration in infra-red—93
integrating sphere for reflectance measurements in ultraviolet—178(L)
light source, variable compensation of—149
micro-, quantitative—620(B)
photoelectric, stellar—149
Photoelectric, Group, London Summer School, July, 1950—754(N)
slit-width effects—172
spectral transmittance standards—435
visual, photometric separator for
Spectroradiometer, recording—805(A*70*)
Spectroscopy, astronomical, integrating photometer for—409
d.c. intermittent arc—180(L)
hyperfine structure measurements—386
infra-red source, the carbon arc—455
isotope shift measurements—386
manual of—181(B)
micro—317
resolution increased with hollow cathode source design—386
Standards, candlepower, distribution from—805(A*72*)
mercury 198 as—801(A*45*)/737
military, on photographic lenses—801(A*48*)
potassium chromate as spectral transmission—802(A*53*)
secondary spectral, mercury and neon—339
spectral transmittance, permanence of—435
spectrochemical analysis, National Bureau of Standards—741(N)
Step Sector, astigmatic spectrograph—849
Stray Light, Stray Radiation
absorbance values in infra-red corrected for—401
infra-red absorbance values corrected for—401
reduction of, in Hunter multipurpose reflectometer—80
in infra-red spectrophotometers by thallium bromoiodide—799(A*29*)/748
Stress Analysis, handbook of experimental—880(B)
introduction to experimental—790(B)
Surfaces (Optical)
quality of—258(A*26*)
concave, quality of—258(A*23*)
Symposia, electromagnetic wave propagation, June, 1950—328(N)
molecular structure and spectroscopy (Ohio State University) June, 1950—282(N)

Technetium (Element 43), spark spectra of—177(L)
Technical Publications
Beckman Bulletin—750(N)
Better Analysis—548(N)
Colorimetry—479(N)
absorption analysis—361(N)
Educational Focus—361(N)
Infrared Spectrograms, catalog of—361(N), 750(N)
Illuminant-Stable Color Vision Test—793(N)
Instrument News—361(N)
Optical, glass and optical research at the National Bureau of Standards—251(N)
images, theory of (La Theorie des Images Optiques)—506(N)
Opticians, assembly of (Reunions d'Opticiens)—506(N)
Sensitized materials for scientific and industrial laboratory—548(N)
Spectrographer's News Letter—361(N)
Spectrophotometry—479(N)
Telescopes, refracting objectives for—802(A*52*)
Television, color, CBS—263(A*54*)
Temperature, control for test room—800(A*39*)
Test Chart, for resolving power—801(A*49*)
Thallium Bromide-Chloride, inelastic behavior—256(A*14*)
Thallium Bromide-Iodide, filter for reduction of stray light in infra-red spectrophotometer—799(A*29*)/748
inelastic behavior—256(A*14*)
Thermal Conductivity, crystals used in infra-red optical systems—256(A*13*)
Thin Films (see *Films*)
Thermocouple, vacuum ultraviolet spectral intensities measured by—264(A*63*)
Thermopiles, for radiometry—805(A*71*)
Thorium, isotope spectral shifts—803(A*62*)
Topography, optical surfaces—258(A*26*)
Toraldo's phase contrast theory—291, 576
Transmission, potassium chromate as spectral standard for—802(A*53*)
standards, permanence of—435
Tristimulus, integrator, automatic photometer for—797(A*22*)
Twinkle, fluctuating radiation in sky and atmosphere—795(A*6*)
Turbidimetry, theory and instrumentation—768

Ultraviolet (see also *Spectra* and *Spectrometer*)
measurement of reflectance in—178(L)
microscopy—275
microspectra—317
vacuum, spectra, emulsion for photographing—23
xenon arc as high pressure radiation source—782
Uranium, spectroscopic properties of—181(B)
spin of U^{235}—262(A*51*), 336(L)

Vacuum Ultraviolet, monochromator—264(A*62*)
photographic emulsion for—23
spectral intensities measured with thermocouples—264(A*63*)
Vector, method for tracing skew rays—255(A*8*)
Vision, acuity at low illumination levels.—795(A*8*)
acuity variation with test-object orientation and viewing conditions—135
adaptation and its effect on color perception—362
Alley experiment in—627
binocular space in—627
brightness relationships—794
chromatic aberration effect on—796(A*10*)
color, absorption by intraocular media and macular pigment—419
discrimination affected by chromatic surrounding fields—797(A*19*)
effect of filters on—419
test—793(N)
perception, daylight and tungsten light-adaptation—362
dichroic filter anomaloscope studies—41
Nagel anomaloscope studies—41
cone—825
contrast threshold of the eye—825
dark adaptation level—211
preceded by intermittent preadapting light—584
Fechner's Law, sensation-intensity ratio—647

Vision (continued)
International Commission on Illumination, recommendations, 1948—183(E)
light and color—620(B)
metacontrast—796(A*9*)
multiple stimuli effect on—796(A*9*)
myopia, night—336(L)
non-Euclidian metric for—627
perception of color affected by daylight and tungsten light-adaptation—362
photopic—211
quanta explanation of —336(L)
retired image blurredness—796(A*10*)
retinal properties in—796(A*11*)
rod—825
scotopic—795(A*8*), 211
sensitivity to surface color differences—797(A*18*)
spectral band limits—755
standard conditions, I.C.O. recommendations—881(N)
Stiles and Crawford effect—796(A*11*)
television, CBS color—263(A*54*)
testfield size—211
theories of—620(B)
visibility curve—647
visual range, meteorological estimates of—795(A*5*)
Video, devices in aerial reconnaissance—263(A*55*)
Vanadium, emission spectra in infra-red—801(A*46*)

Worthing, A. G.
in memoriam—404
memorial award—355(N)

X-Rays (Röntgen Rays)—790(B)
cadmium sulfide, detection of—798(A*25*)
crystallography—790(B)
diffraction from crystals—181(B)
optics—477(B)
X-Ray Films, gold sensitization of—266(A*76*)/246

Zeeman Pattern, recording of—127
Zirconium-Hafnium Mixtures, spectrochemical analysis of—803(A*60*)/742